UNIVERSITY OF OKLAHOMA

GRADUATE COLLEGE

METAL-LIGAND COVALENCY IN URANIUM, THORIUM, AND CERIUM COORINDATION CHEMISTRY: ELUCIDATING THE NATURE OF CHEMICAL BONDING IN F-ELEMENT COMPLEXES USING PHOSPHORUS LIGANDS

A DISSERTATION

SUBMITTED TO THE GRADUATE FACULTY

in partial fulfillment of the requirements for the

Degree of

DOCTOR OF PHILOSOPHY

By

STEWART BRAGG YOUNGER-MERTZ

Norman, Oklahoma

2022

METAL-LIGAND COVALENCY IN URANIUM, THORIUM, AND CERIUM COORINDATION CHEMISTRY: ELUCIDATING THE NATURE OF CHEMICAL BONDING IN F-ELEMENT COMPLEXES USING PHOSPHORUS LIGANDS

A THESIS APPROVED FOR THE

DEPARTMENT OF CHEMISTRY AND BIOCHEMISTRY

BY THE COMMITTEE CONSISTING OF

Dr. Donna Nelson, Chair

Dr. Shanteri Singh

Dr. Yihan Shao

Dr. Andrew Madden

Abstract

Herein the syntheses and characterization of model actinide and lanthanide complexes bearing phosphorus-based ligands are reported. High-symmetry molecular models featuring phosphorus-based ligands are very advantageous for experimental metal-ligand covalency studies because phosphorus-31 nuclear magnetic resonance spectroscopy and phosphorus-Kβ X-ray emission spectrometry can be used to study the electronic structure and orbital interactions of metal-phosphorus bonds. Furthermore, high-symmetry models simplify spectral interpretation, and reduce the complexity of computational studies of the actinides. The quantum chemistry of the actinides is very complex because relativistic effects and spin-orbit coupling are very important influences on the electronic structures of these elements. Low-symmetry and high coordination numbers are very common in actinide coordination chemistry, which further complicates actinide computational chemistry. The creation of molecular models with high-symmetry and low coordination numbers greatly reduces the complexity of empirical electronic structure studies. Using a combination of advanced spectroscopy and advanced computational methods, details about the metal-ligand orbital interactions in actinide and lanthanide complexes can be obtained. Herein reactions of advanced *f*-element amide complexes with phosphorus-based compounds are reported, with the intention of creating high-symmetry, low-coordinate *f*-metal complexes for empirical electronic structure investigations.

Dedication

First and foremost, I dedicate this work to my grandparents, DeWayne and John Louis "Jack" Younger (Moe and Papa), and to my children, John Louis "Jack" Younger-Mertz and William Stewart Younger-Mertz.

I also dedicate this work to my parents, Michele and Michael Mertz. I also dedicate this work to my great-aunt and great-uncle, Barbara and Jerry Ware, and my great-grandmother, Dorothy Bragg. I also dedicate this work to my uncles, Michael Younger and Patrick Younger, and my aunts, Patricia Younger, Karen Younger, and Fe Younger. I also dedicate this work to my cousins, John Lawrence Younger, Carlotta Younger, Tiffany Younger and her son Christopher, Michael P. Younger, Victor Younger, and Sophia Younger.

I also dedicate this work to the mother of my children, Shannon Elizabeth Donoghue. I also dedicate this work to my friends: Jimmy, Sean, Noni, Kevin, Raley, Lacy, Garrett, Jeremy, Christina, Kelly, Johnny, Tanner, Oz, Lauren, Drue, Shawn, Jesse, Joe, Oscar, Lopez, Twon, Delores, Ken, Jenn, Kristen, and Dan.

Acknowledgments

I would like to thank my adviser, Dr. Donna Nelson, for all her help and support during my time at the University of Oklahoma. I appreciate all of the time and effort she has put into helping me complete my doctoral degree, and I am grateful for everything she has done for me. I thank her for teaching me Advanced Organic Chemistry, and for serving as my research adviser and helping me complete my degree. I am very lucky to have met Dr. Nelson, and I could not have asked for a more supportive Ph.D. adviser. I would also like to thank the member of my committee, Dr. Andrew Madden, Dr. Yihan Shao, and Dr. Shanteri Singh, for all their help and support during my time at the University of Oklahoma.

I would also like to thank my undergraduate adviser, Dr. Elizabeth Nalley, for recognizing my potential, and encouraging me to pursue a career in chemistry. I appreciate her unwavering support. She has provided superb chemical education to my family for three generations. Before me, both my uncle and my grandfather attended her classes. I appreciate all that she has done for me and my family.

I would also like to thank Dr. RKT for recognizing my potential and introducing me to the exciting world of Inorganic Chemistry and Actinide Chemistry. None of this work would have been possible without him. Thank you for this life-changing opportunity to work with uranium and thorium.

I would like to thank Dr. Susan Nimmo for her unwavering support over the years. I am very grateful for all of her assistance in the NMR lab. I would also like to thank Dr. Doug Powell for his assistance with X-ray diffraction analyses, and for teaching the X-ray crystallography course. I would also like to thank Dee Stone for all her support and assistance in the chemistry stockroom.

I would like to thank Dr. Jerome Duggan, Dr. Gary Glass, and Dr. Barney Doyle for recognizing my potential, and introducing me to the world of Ion Beam Analysis. I would also like to thank Dr. Claire Pacheco and Dr. Thomas Calligaro for allowing me the opportunity to use the accelerator at C2RMF at the Louvre Museum in Paris, and I would like to thank Quentin, Brice, and Laurent for their help with the analyses.

Table of Contents

List of Figures

List of Schemes

List of Abbreviations

α	alpha	mg	milligram
Å	angstrom	N*	bis(trimethylsilyl)amido
β	beta	NMR	nuclear magnetic resonance
t-Bu	*tert*-butyl	*p*	para
Cy	cyclohexyl	Ph	phenyl
Cp	cyclopentadienyl	PIXE	particle-induced x-ray emission
Cp*	pentamethylcyclopentadienyl	PIGE	particle-induced gamma emission
DME	dimethoxyethane	σ	sigma
γ	gamma	THF	tetrahydrofuran
g	gram	XES	X-ray emission spectroscopy
κ	kappa	XRD	X-ray diffraction
Me	methyl		
MeV	mega electron volt		
mmol	millimole		
mL	milliliter		

Introduction

The art of sublimation is central to nuclear science and technology. Volatile uranium compounds are essential for enrichment processes based on gaseous diffusion or centrifugation, and the synthesis of volatile uranium hexafluoride for enrichment is vital to the nuclear power industry [1-6]. Uranium-235 is needed for the operation of nuclear reactors and nuclear weapons, and our energy security and national security [7] depend on the enrichment of uranium-235 using volatile uranium hexafluoride. Uranium hexafluoride can be conveniently purified via sublimation [3] (the compound sublimes at 56.5°C at atmospheric pressure). Once pure, it can be used in gas centrifuges for the enrichment of uranium-235. In addition to uranium hexafluoride, plutonium hexafluoride and neptunium hexafluoride are also very volatile [8]. The tetravalent uranium halides are much less volatile (UCl_4 sublimes between 500-650°C), and trivalent uranium halides are essentially non-volatile (UCl_3 boils at about 1410°C) [8]. Uranium tetraborohydride is a highly volatile tetravalent uranium compound (sublimes at about 60°C under vacuum) [9], and numerous organometallic *f*-element compounds are volatile [10]. Trivalent actinide and lanthanide amides, like $U[N(SiMe_3)_2]_3$, $Np[N(SiMe_3)_2]_3$, $Pu[N(SiMe_3)_2]_3$, $Ce[N(SiMe_3)_2]_3$, $Pr[N(SiMe_3)_2]_3$, $Nd[N(SiMe_3)_2]_3$, $Sm[N(SiMe_3)_2]_3$, and $Yb[N(SiMe_3)_2]_3$, are also volatile [11-15]. The tris[bis(trimethylsilyl)]amido compounds of uranium (sublimes at about 80°C under vacuum), neptunium (sublimes at about 60°C under vacuum), plutonium (sublimes at about 60°C under vacuum), and all lanthanides (sublime between 80-100°C under vacuum) can be purified by sublimation, and these

compounds have become very important molecular precursors for actinide and lanthanide coordination chemistry and materials science [11-15].

Figure 0.1: Oxide-Free Depleted Uranium Metal Turnings (^{238}U)

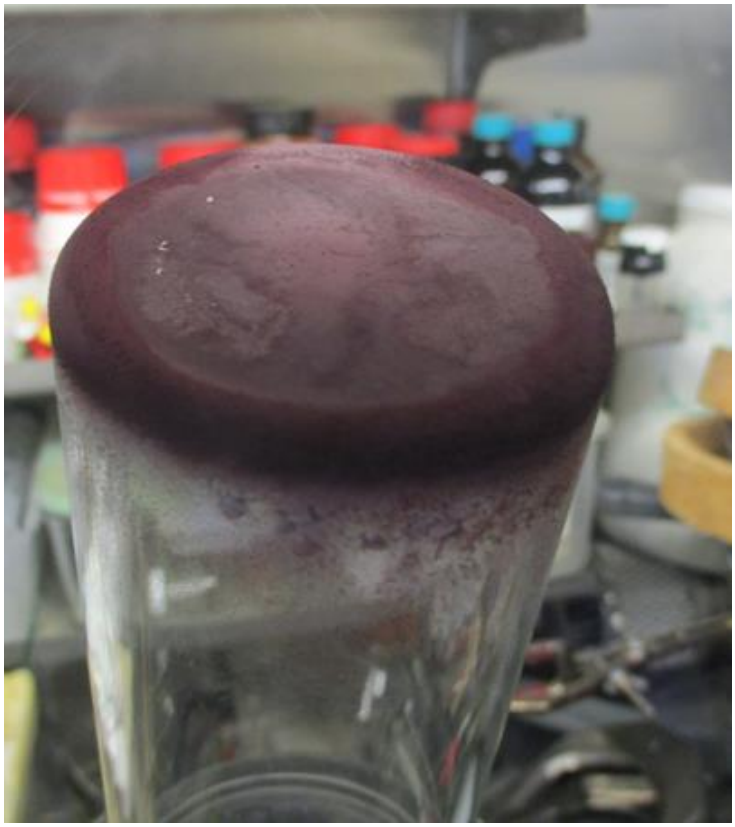

Figure 0.2: Tris[bis(trimethylsilyl)amido]uranium(III), $U[N(SiMe_3)_2]_3$, deposited on sublimation apparatus. Sublimed by Stewart Younger-Mertz (Spring 2018).

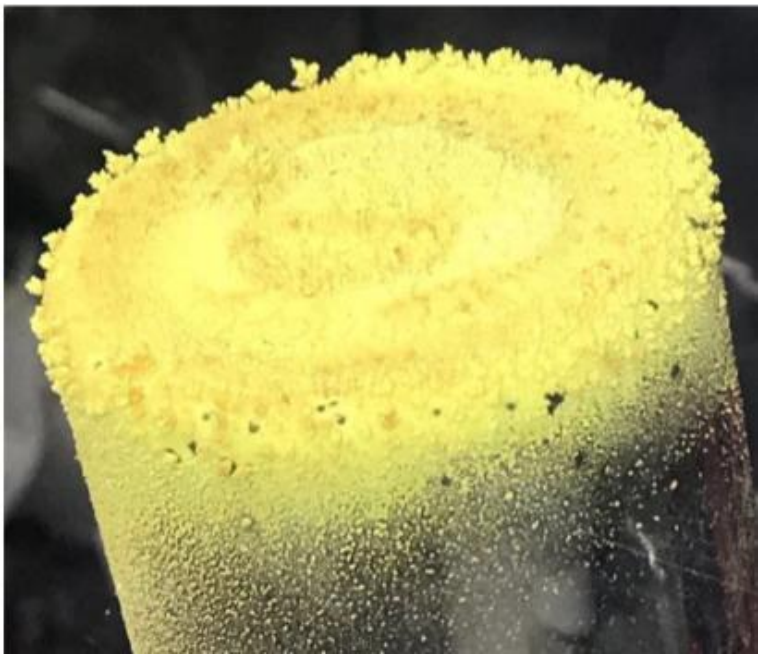

Figure 0.3: Tris[bis(trimethylsilyl)amido]cerium(III), $Ce[N(SiMe_3)_2]_3$, deposited on sublimation apparatus. Sublimed by Stewart Younger-Mertz (Spring 2018).

The *f*-elements play a central role in high-energy industrial societies. Despite their vital importance, the fundamental nature that governs the behavior of *f*-elements has eluded chemists and physicists since the Manhattan Project [16]. Theoreticians continue to struggle to predict the properties of *f*-element compounds, and these difficulties have major ramifications for industries that revolve around *f*-elements [16]. This gap in knowledge is especially problematic in the nuclear industry, particularly with respect to the science of *f*-element separations [16]. *f*-element separation processes occur throughout the nuclear fuel cycle [17-19]. For example, *f*-elements are often co-located in ore deposits, and they must be separated to be useful in the numerous industries that involve *f*-elements [4]. *f*-element separations also occur during the production and isolation of plutonium [20-22]. Once plutonium is created in fuel rods in nuclear reactors, it is

separated from uranium and *f*-element fission products [20-22]. The production of uranium and thorium from their ores, and plutonium from nuclear fuel rods, are well-developed processes [4, 23-28]. These processes depend on simple redox chemistry and take advantage of the higher oxidation states of plutonium, uranium, and thorium. Most *f*-elements exist in the trivalent oxidation state [4]. However, thorium exists exclusively in the tetravalent oxidation state in nature [29], and uranium and plutonium prefer the hexavalent and tetravalent oxidations states, respectively [30, 31]. This makes the separation of thorium, uranium, and plutonium from their trivalent counterparts a relatively straightforward task. The separation of the lanthanide elements from each other, though extremely demanding industrially, are theoretically straightforward processes that either take advantage of subtle differences in the ionic radii of lanthanide elements, or take advantage of the stable divalent oxidation states of some lanthanides, or the stable tetravalent oxidation state in the case of cerium [4, 32].

One of the most critical problems facing the nuclear industry is the separation of the trivalent minor actinides from trivalent lanthanide fission products in spent nuclear fuel and high-level nuclear waste [16-19]. The minor actinides prefer the trivalent oxidation state like the lanthanide elements, and their ionic radii are very similar to the lanthanide fission products found in nuclear fuel rods [4, 16]. As a result, conventional *f*-element separation processes based on simple redox chemistry or differences in ionic radii are ineffective for the separation of minor actinides from lanthanide fission products [17-19]. The extremely radioactive minor actinide isotopes found in high-level nuclear

waste, and our current inability to effectively manage and dispose of them, creates the necessity to store these isotopes deep underground in geological deposits for thousands, or even millions of years [2, 6]. This problem has ramifications that extend well beyond the nuclear industry. Our inability to effectively manage and dispose of high-level nuclear waste has many political, economic, social, and environmental ramifications that every high-energy society must face. Through the lens of global climate science, one could argue that every single human being on Earth is affected by the problems created by high-level nuclear waste. The reliance of high-energy societies on fossil fuels as their primary source of energy is now considered a major economic, social, and environmental problem by people on both sides of the political spectrum. Nuclear power is currently the only viable alternative to fossil fuels that can supply high-energy industrial societies with cheap, reliable, and abundant energy. Solar and wind power are intermittent technologies that require enormous amounts of land to produce energy on a very large scale. Utilization of nuclear power based on nuclear fission is the most practical solution to our current energy and environmental crises. Nuclear power based on nuclear fusion will also become a practical solution in the coming decades. However, in order to take decisive action to solve our current energy and environmental crises as quickly as possible, the problem of high-level nuclear waste must be resolved. This problem must be resolved before the nuclear fission industry can take the reins from the fossil fuel industry and become the primary source of energy for high-energy industrial societies. The nuclear fuel cycle must become a closed cycle before this evolutionary transition can take place.

One of the leading strategies for addressing the problem of high-level nuclear waste is the proposed *partition and transmutation* method of disposing of high-level nuclear waste [33-38]. This method involves the transmutation of transuranic minor actinides into short-lived radioactive isotopes or stable isotopes, with the aim of reducing the volume of high-level nuclear waste that needs to be stored long-term in geological deposits by over 90% [33-38]. These transmutations can be achieved by bombarding minor actinide targets with high-energy neutron beams [34, 35]. However, for this strategy to work, the minor actinides must first be partitioned from lanthanide fission products [33-38]. According to Stacey, studies indicate "that it is practical to achieve >90% transuranics (TRU) burnup with a neutron source strength P_{fus} < 400 MW by repeatedly burning ≈25% of the TRU fuel, then recycling and reprocessing the TRU fuel to remove neutron absorbing fission products and adding fresh TRU" [35]. Lanthanides have large neutron capture cross-sections and poison the transmutation process [33-38]. For the partition and transmutation method to become a viable strategy for ameliorating the problem of high-level nuclear waste, our methods for separating trivalent lanthanide fission products from the trivalent minor actinides must be improved. Advances in trivalent *f*-element separation science proceed slowly on a largely empirical basis [16]. To drastically improve our ability to partition the minor actinides from trivalent lanthanides, a vertical leap in our theoretical understanding of the chemical behavior of the *f*-elements must occur.

The separation of trivalent lanthanides from trivalent actinides is based on the empirical observation that soft-donor extractants have a slight preference for actinides over lanthanides, presumably due to the increased ability of actinides to engage in covalent bonding interactions due to the greater radial extent of the 5*f* and *6d* orbitals compared to the 4*f* and 5*d* orbitals of the lanthanides [16]. We currently do not have a solid theoretical foundation for understanding how these covalent metal-ligand interactions work, and we do not fully understand the conditions that facilitate and optimize covalency in actinide-ligand interactions [16]. As a result, our ability to improve trivalent *f*-element separations is drastically hindered [16]. In order for a vertical leap in our understanding of the nature of covalency in *f*-element systems to occur, we must create and study model actinide and lanthanide systems that are amenable to experimental and theoretical quantum chemical investigations. That is the subject of this dissertation. Herein the syntheses and characterization of model actinide and lanthanide complexes bearing phosphorus-based ligands are reported. High symmetry molecular models featuring phosphorus-based ligands are very advantageous for experimental metal-ligand covalency studies because phosphorus-31 nuclear magnetic resonance spectroscopy and phosphorus-Kβ X-ray emission spectrometry can be used to study the electronic structure and orbital interactions of metal-phosphorus bonds. Furthermore, high symmetry models simplify spectral interpretation, and reduce the complexity of computational studies of the actinides. The quantum chemistry of the actinides is very complex because relativistic effects and spin-orbit coupling are very important influences on the electronic structures of these elements [16]. Low symmetry and high coordination

numbers are very common in actinide coordination chemistry [4], which further complicates actinide computational chemistry. The creation of molecular models with high symmetry and low-coordination numbers greatly reduces the complexity of empirical electronic structure studies. Using a combination of advanced spectroscopy and advanced computational methods, details about the metal-ligand orbital interactions in actinide and lanthanide complexes can be obtained. Herein reactions of advanced *f*-element amide complexes with phosphorus-based compounds are reported, with the intention of creating high symmetry, low-coordinate *f*-metal complexes for empirical electronic structure studies.

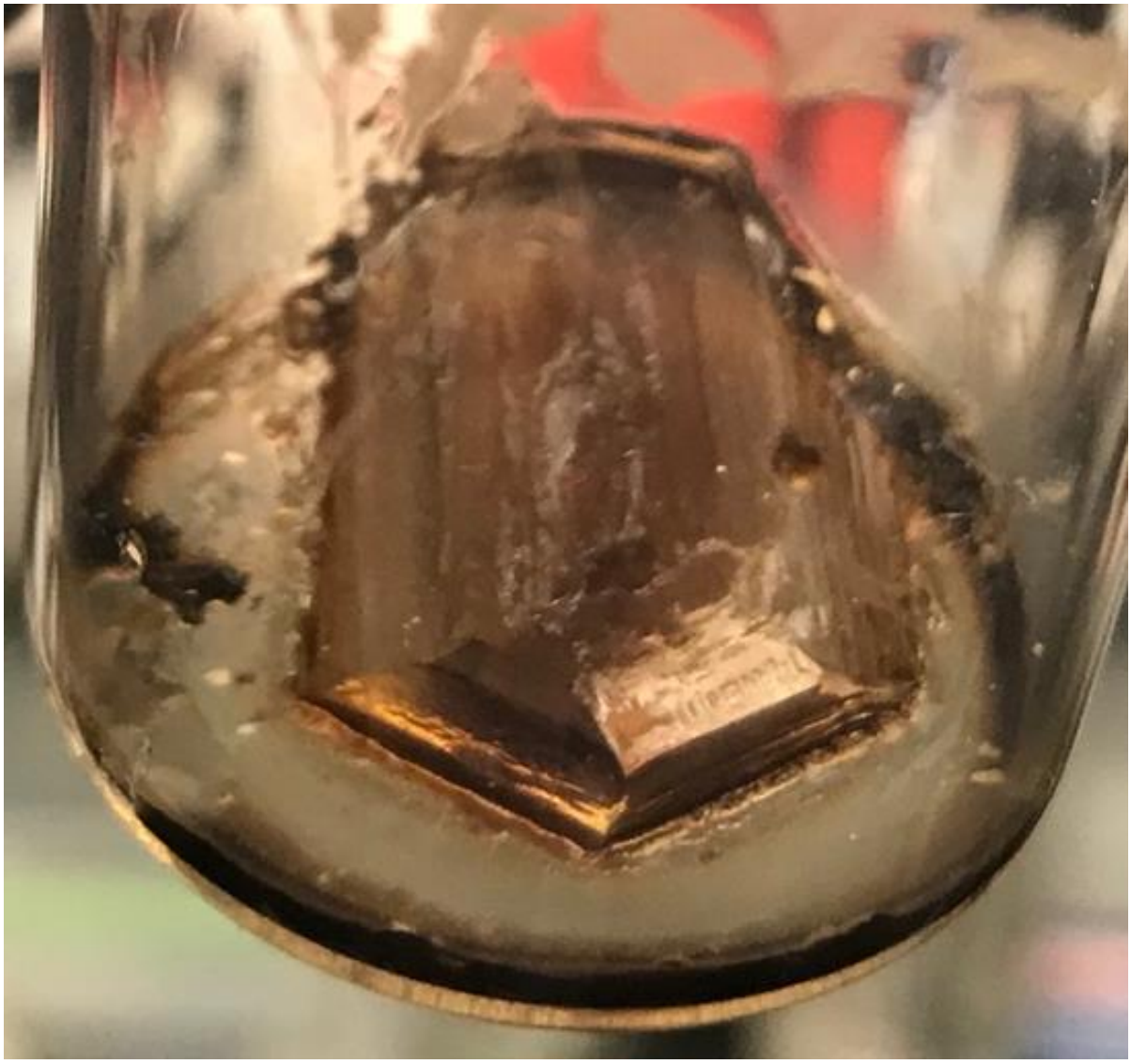

Figure 0.4: Large Crystal (~0.5g) of $Ce[OPPh_3][N(SiMe_3)_2]_3$

Tris[bis(trimethylsilyl)amido][triphenylphosphine oxide]cerium(III),

synthesized and characterized by Stewart Younger-Mertz (Spring 2018).

References

[1] Lide, David R. 2008. Properties of the Elements and Inorganic Compounds. Section 4 in *CRC Handbook of Chemistry and Physics*, edited by David R. Lide, 88th edition. CRC Press, Boca Raton.

[2] Schultis, J. Kenneth and Richard E. Faw. 2008. *Fundamentals of Nuclear Science and Engineering*. CRC Press, Boca Raton.

[3] Klapötke, Thomas M. 2013. Laboratory-Scale Synthesis of Gold Trifluoride and Uranium Hexafluoride. Chapter 17 in *Efficient Preparations of Fluorine Compounds*, edited by Herbert W. Roesky, First Edition. John Wiley & Sons, Inc., Hoboken.

[4] Cotton, Simon. 2006. *Lanthanide and Actinide Chemistry*. John Wiley & Sons Ltd, Chichester.

[5] Krane, Kenneth S. 1988. *Introductory Nuclear Physics*. John Wiley & Sons.

[6] Masterson, Robert E. 2017. *Nuclear Engineering Fundamentals: A Practical Perspective*. CRC Press, Boca Raton.

[7] Kroenig, Matthew. 2018. *The Logic of American Nuclear Strategy: Why Strategic Superiority Matters*. Oxford University Press, New York.

[8] Brown, D. 1968. *Halides of the Lanthanides and Actinides.* John Wiley & Sons, Bath.

[9] Schlesinger, H. I. and Herbert C. Brown. 1953. Uranium(IV) Borohydride. *Journal of the American Chemical Society* 75: 219-221.

[10] Edelmann, F. T. 1997. *Lanthanides and Actinides*. Volume 6 in Synthetic Methods of Organometallic and Inorganic Chemistry, edited by W. A. Herrmann. Georg Thieme, Stuttgart.

[11] Avens, L., S.G. Bott, D.L. Clark, A.P. Sattelberger, J.G. Watkin, and B.D. Zwick. 1994. A Convenient Entry into Trivalent Actinide Chemistry: Synthesis and Characterization of $AnI_3(THF)_4$ and $An[N(SiMe_3)_2]_3$ (An = U, Np, Pu) *Inorganic Chemistry* 33: 2248-2256.

[12] Bradley, Donald C., Joginder S. Ghotra, and F. Alan Hart. "Low Co-ordination Numbers in Lanthanide and Actinide Compounds. Part I. The Preparation and Characterization of Tris{bis(trimethylsilyl)-amido}lanthanides." *Journal of the Chemical Society Dalton Transactions* 1973: 1021.

[13] Andersen, Richard A. 1979. "Tris((hexamethyldisilyl)amido)uranium(III): Preparation and Coordination Chemistry. *Inorganic Chemistry* 18(6): 1507.

[14] Anwander, Reiner. 1996. "Lanthanide Amides." *Topics in Current Chemistry* 179: 33-112.

[15] Emslie, David J. H. 2018. "Actinides: Amido Complexes." *Encyclopedia of Inorganic and Bioinorganic Chemistry*, John Wiley & Sons, Ltd., pp. 1-18.

[16] Kaltsoyannis, N. and A. Kerridge. 2014. "Chemical Bonding of Lanthanides and Actinide." In *The Chemical Bond*, edited by G. Frenking and S. Shaik, pp. 337-355. Wiley-VCH, Marburg.

[17] Nash, Kenneth L. and Gregory R. Chopin. 1995. *Separations of f-Elements*. Plenum Press, New York.

[18] Nash, Kenneth L., Charles Madic, Jagdish N. Mathur, and Jérôme Lacquement. 2006. Actinide Separation Science and Technology. In *Chemistry of the Actinide and Transactinide Elements,* edited by Morss, L., N.M. Edelstein, and J. Fuger. Springer, Berlin.

[19] Nash, Kenneth L. and Gregg J. Lumetta. 2011. *Advanced separation techniques for nuclear fuel reprocessing and radioactive waste treatment.* Woodhead Publishing Limited, Cambridge.

[20] Wilkinson, W. D. 1960. *Extractive and Physical Metallurgy of Plutonium and Its Alloys.* Interscience Publishers, Inc., New York.

[21] Coffinberry, A. S. and W. N. Miner. 1961. *The Metal Plutonium*. The University of Chicago Press, Chicago.

[22] Cleveland, J. M. 1970. *The Chemistry of Plutonium*. Gordon and Breach Science Publishers.

[23] Katz, Joseph J. and Glenn T. Seaborg. 1957. *The Chemistry of the Actinide and Transactinide Elements*. Methuen & Co. Ltd., London.

[24] Clegg, John W. and Dennis D. Foley. 1958. *Uranium Ore Processing*. Addison-Wesley Publishing Company, Inc., Reading.

[25] Harrington, Charles D. and Archie E. Ruehle. 1959. *Uranium Production Technology*. D. Van Nostrand Company, Inc., Princeton.

[26] Wilkinson, W. D. 1962. *Uranium Metallurgy Volume 1: Uranium Process Metallurgy*. Interscience Publishers, New York.

[27] Gittus, J. H. 1963. *Uranium*. Metallurgy of the Rarer Metals-8. Butterworth Inc., Washington, D. C.

[28] Merritt, Robert C. 1971. *The Extractive Metallurgy of Uranium*. Colorado School of Mines Research Institute, Golden.

[29] Wickleder, Mathias S., Blandine Fouresy, and Peter K. Dorhout. 2006. Thorium. Chapter 3 in *Chemistry of the Actinide and Transactinide Elements*, edited by L. Morss, N.M. Edelstein, J. Fuger . Springer, Berlin.

[30] Grenthe, Ingmar, Janusz Drożdżyński, Takeo Fujino, Edgar C. Buck, Thomas E. Albrecht-Schmitt, and Stephen F. Wolf. 2006. Uranium. Chapter 5 in *Chemistry of the Actinide and Transactinide Elements*, edited by L. Morss, N.M. Edelstein, J. Fuger. Springer, Berlin.

[31] Clark, David L., Siegfried S. Hecker, Gordon D. Jarvinen, and Mary P. Neu. 2006. Plutonium. Chapter 7 in *Chemistry of the Actinide and Transactinide Elements*, edited by L. Morss, N.M. Edelstein, J. Fuger . Springer, Berlin.

[32] Sastri, V.S., J.-C. Bünzli, V. Ramachandra Rao, G.V.S. Rayudu, and J.R. Perumareddi. 2003. *Modern Aspects of Rare Earths and their Complexes.* Elsevier, Amsterdam.

[33] Warib, D.M. 2011. Developments in the partitioning and transmutation of radioactive waste. Chapter 12 in *Advanced separation techniques for nuclear fuel reprocessing and radioactive waste treatment*, edited by Kenneth L. Nash and Gregg J. Lumetta.. Woodhead Publishing Limited, Cambridge.

[34] Stacey, Weston M. 2007. Tokamak D-T fusion neutron source requirements for closing the nuclear fuel cycle. *Nuclear Fusion* 47: 217-221.

[35] Stacey, Weston M. 2010. *Fusion: An Introduction to the Physics and Technology of Magnetic Confinement Fusion*. Wiley-VCH Verlag GmbH & Co., Weinheim.

[36] Ryzhkov, S. V. and A. Yu. Chirkov. 2019. *Alternative Fusion Fuels and Systems*. CRC Press, Boca Raton.

[37] Burakov, B. E., M. L. Ojovan, and W. E. Lee. 2011. *Crystalline Materials for Actinide Immobilisation*. Imperial College Press, London.

[38] Kislik, Vladimir S. 2012. *Solvent Extraction: Classical and Novel Approaches.* Elsevier, Oxford.

Chapter 1

Synthesis of Uranium-Phosphido Complexes

Introduction

In this chapter, the synthesis of a uranium(IV) amido-phosphido complex, U[PHPh][$N(SiMe_3)_2$]$_3$, is reported. Uranium-phosphorus bonds are rare phenomena that have the potential to offer new insights into the nature of chemical bonding in uranium complexes. Uranium is considered a hard Lewis acid that has a high affinity for hard Lewis bases (fluoride, oxide, etc.) [1]. The stable uranyl dication (UO_2^{2+}) is ubiquitous in nature [1], and UO_2 and UF_6 are stable forms of uranium that are at the heart of the nuclear industry. UO_2 is used as nuclear fuel, and UF_6 is used for the enrichment of ^{235}U used for nuclear power and nuclear weapons [2, 3]. On the other hand, uranium and phosphorus are a frustrated couple (a hard acid, soft base mismatch). Bonds formed between uranium and phosphorus are highly unstable and are not found in nature. These bonds can be formed under special laboratory conditions in the absence of air and moisture. Uranium-*phosphate* interactions are very common, and are ubiquitous in nature and the nuclear fuel cycle [4]; however, there is an oxygen between the uranium and phosphorus in these systems. Direct uranium-phosphorus bonds are quite rare and very understudied [5-11].

The insight that can be gained from the study of uranium-phosphorus bonds is fundamental in nature and can be used to address long standing questions revolving

around the nature and degree of covalency in uranium-ligand bonds. If significant orbital mixing is possible in actinide and lanthanide systems, it will most likely be maximized through the use of soft-donor atoms like phosphorus, sulfur, and heavier pnictogens and chalcogens [12, 13]. Metal-ligand covalency has been a reoccurring theme in actinide chemistry since chemists began making volatile organometallic uranium compounds as part of the Manhattan project during World War II [14-65]. The advantages of using phosphorus to study chemical bonding in uranium are twofold. First, from a theoretical standpoint, anionic phosphide ligands are soft Lewis bases with polarizable valence shells that can delocalize to some degree into the uranium 5*f* and/or 6*d* orbital manifolds. Second, from a practical standpoint, the bonding interactions between uranium and phosphorus can be studied conveniently through a combination of ^{31}P-NMR spectroscopy and phosphorus Kβ X-ray emission spectroscopy.

The history of actinide-phosphido chemistry begins in the 1980's. In 1984, Marks and co-workers reported the syntheses of bridging phosphinidenes of uranium and thorium [5]. In 1985, the syntheses of the first thorium bis(phosphido) complexes, $Cp^*_2Th(PR_2)_2$ (R = Ph, Cy, Et), were reported [66]. $Cp^*_2Th(PPh_2)_2$ was used to synthesize heterobimetallic thorium phosphido complexes, $Cp^*_2Th(PPh_2)_2Ni(CO)_2$ and $Cp^*_2Th(PPh_2)_2PtPMe_3$ [67, 68]. In 1993, the syntheses of uranium and thorium bis(trimethylsilyl)phosphido complexes, $Cp^*_2An(Cl)[P(SiMe_3)_2]$ and $Cp^*_2An(Me)[P(SiMe_3)_2]$ (An = U, Th), were reported [6]. Both the uranium and thorium forms of $Cp^*_2An(Me)[P(SiMe_3)_2]$ undergo cyclometallation to form $Cp^*_2An[\kappa^2(P,C)$-

$P(SiMe_3)CH_2$] [6]. More recently, the Walensky group synthesized the first primary bis(phosphido) complexes of the actinides with the formula $Cp^*_2Th(PHR)_2$ (R = Tipp or Mes) [69]. The Arnold group reported a similar compound, $Th(Bc^{Mes})_2(HPMes)_2$ [70,71]. Homoleptic chelating complexes $Th(PPP)_4$ and $U(PPP)_4$ have also been reported, which feature both neutral and monoanionic metal-phosphorus interactions [72]. Liddle and co-workers have recently synthesized a series of parent actinide phosphido and arsenido complexes, $(Tren^{TIPS})An(PH_2)$ and $(Tren^{TIPS})An(AsH_2)$ (An = U, Th) [9, 73]. The phosphido complexes synthesized by the Walensky and Liddle groups were subsequently used to synthesize actinide phosphinidene (An=P) complexes [9, 74].

The history of lanthanide-phosphido chemistry begins in the 1970's [8, 75]. The lanthanide phosphido complexes reported in the 1970's and 1980's were bridged complexes with multiple metal centers [8, 75]. The first terminally bound lanthanide complexes were not reported until the late 1980's and 1990's, when Aspinall reported $[Ln\{N(SiMe_3)_2\}_3(PPh_2)]$ (Ln = La, Eu) and $[Ln\{N(SiMe_3)_2\}_3(PPh_2)(Ph_3PO)]]$ (Ln = La, Eu, Y) [12], and when Rabe and coworkers reported homoleptic lanthanide tris(phosphido) complexes $Ln[P(SiMe_3)_2]_3$ (Ln = Nd, Tm) [76, 13]. Much progress has been made in synthesis and characterization of rare earth complexes with anionic phosphorus ligands since these initial advances, and this area was reviewed by Nief in 1998 [8], and Kaercher and Roesky in 2014 [75]. To date, no terminally bound lanthanide phosphinidenes have been synthesized [75]. However, Kiplinger and coworkers synthesized the first bridged lanthanide phosphinidene, $[(PNP^{iPr})Lu]_2(\mu\text{-}PMes)_2$ [77]. Walter and co-workers also

reported the synthesis of an alkali-metal halide bridged phosphinidiide thorium metallocene complex in 2019 [10].

Our explorations into actinide-phosphorus chemistry involved attempts to generate homoleptic and heteroleptic actinide-phosphido (PR_2^-) complexes, with the intention of studying these complexes spectroscopically and computationally, and also with the intention of using these complexes as precursors to phosphinidene (PR^{2-}) and phosphide (P^{3-}) complexes. These reactions included salt metathesis or protonolysis reactions using $PhPH_2$ or LiPHPh reacting with UCl_4, $ThCl_4(DME)_2$, $[((H_3C)_3Si)_2N]_2U[\kappa^2$-$(C,N)$-$CH_2Si(CH_3)_2N(Si(CH_3))]$, $UCl[N(SiMe_3)_2]_3$, $ThCl[N(SiMe_3)_2]_3$, $UCl_2[N(SiMe_3)_2]_2$, or $U[N(SiMe_3)_2]_3$. The most promising results were obtained through the reaction of $PhPH_2$ with $[((H_3C)_3Si)_2N]_2U[\kappa^2$-$(C,N)$-$CH_2Si(CH_3)_2N(Si(CH_3))]$. NMR data suggest the synthesis of $U[PHPh][N(SiMe_3)_2]_3$. Work in the area was discontinued soon after these initial results were obtained, and further studies and characterization of the product of this reaction are highly desirable.

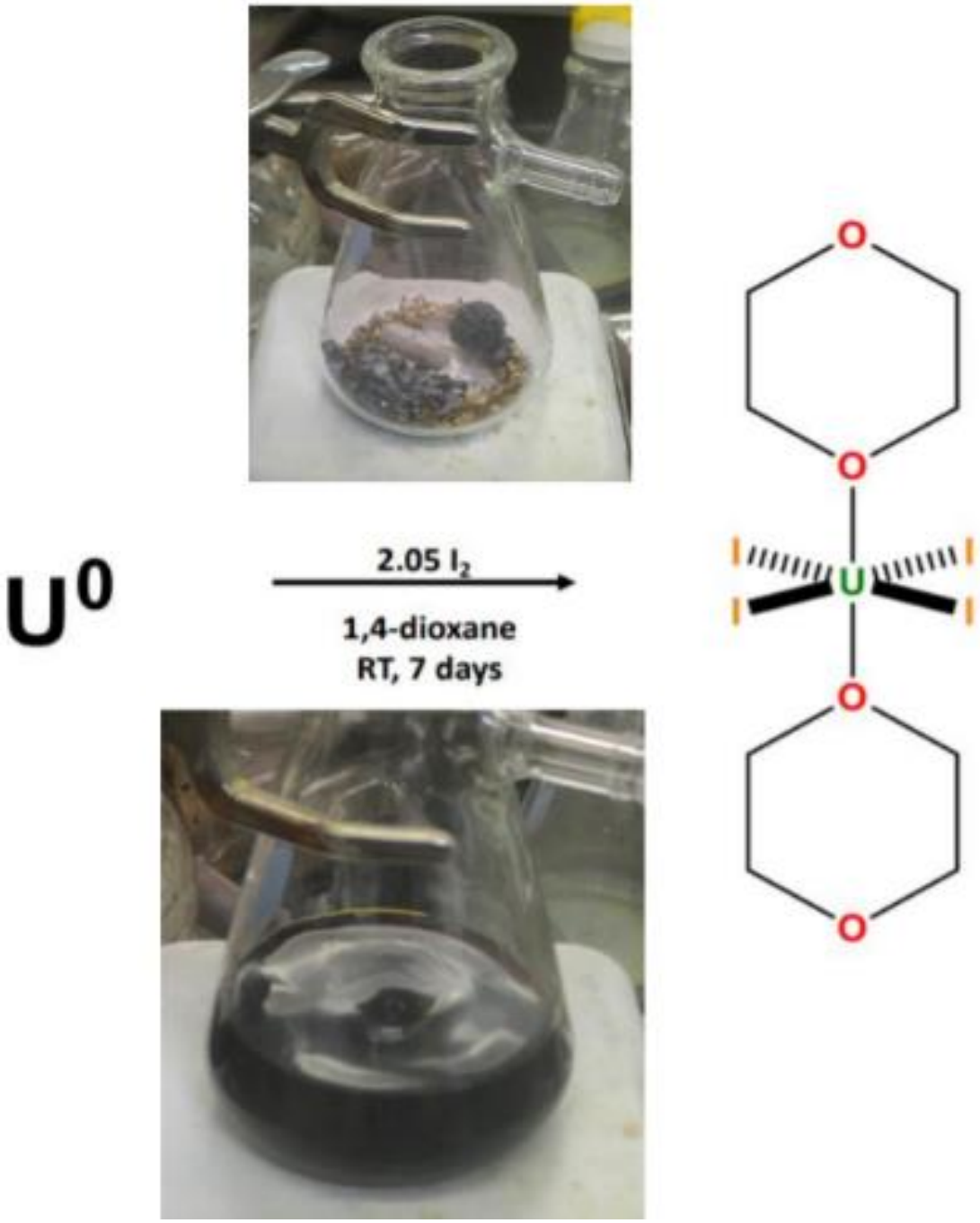

Scheme 1.1: Synthesis of $UI_4(1,4\text{-dioxane})_2$ using uranium metal and elemental iodine, and 1,4-dioxane.

Figure 1.1: $UI_4(1,4\text{-dioxane})_2$

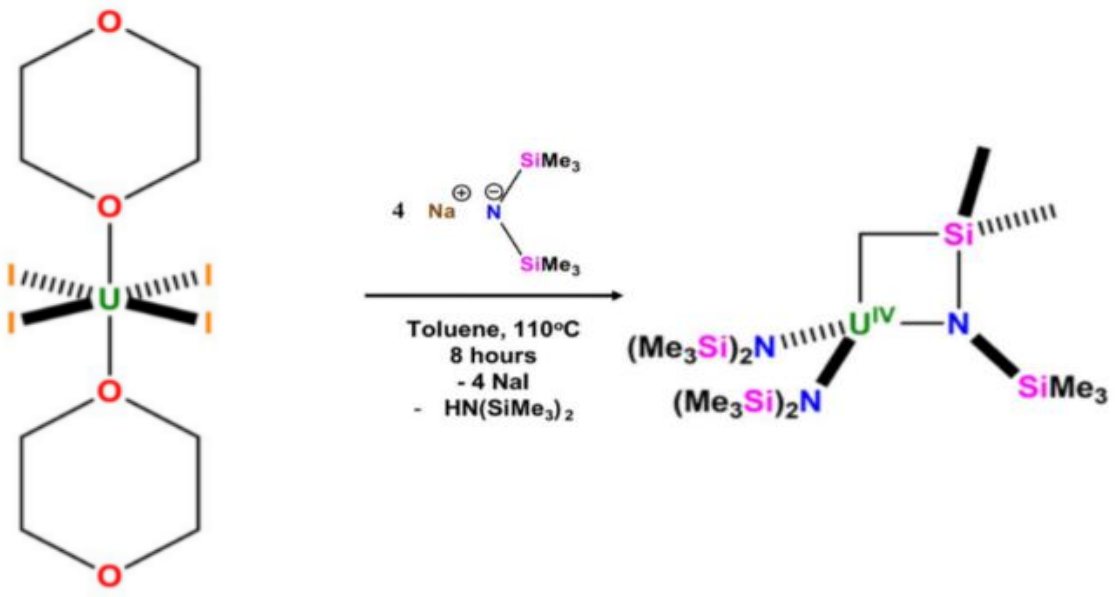

Scheme 1.2: Synthesis of $[((H_3C)_3Si)_2N]_2U[\kappa\text{-}2\text{-}(C,N)\text{-}CH_2Si(CH_3)_2N(Si(CH_3))]$

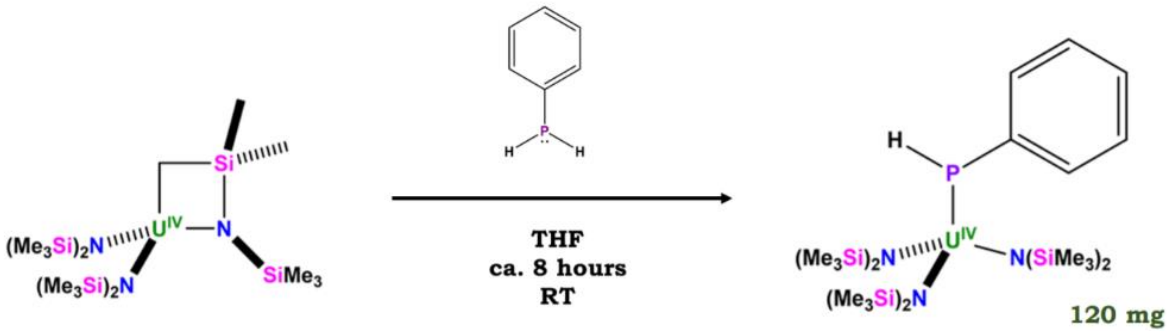

Scheme 1.3: Reaction of cyclo-metalated uranium amide with phenyl phosphine.

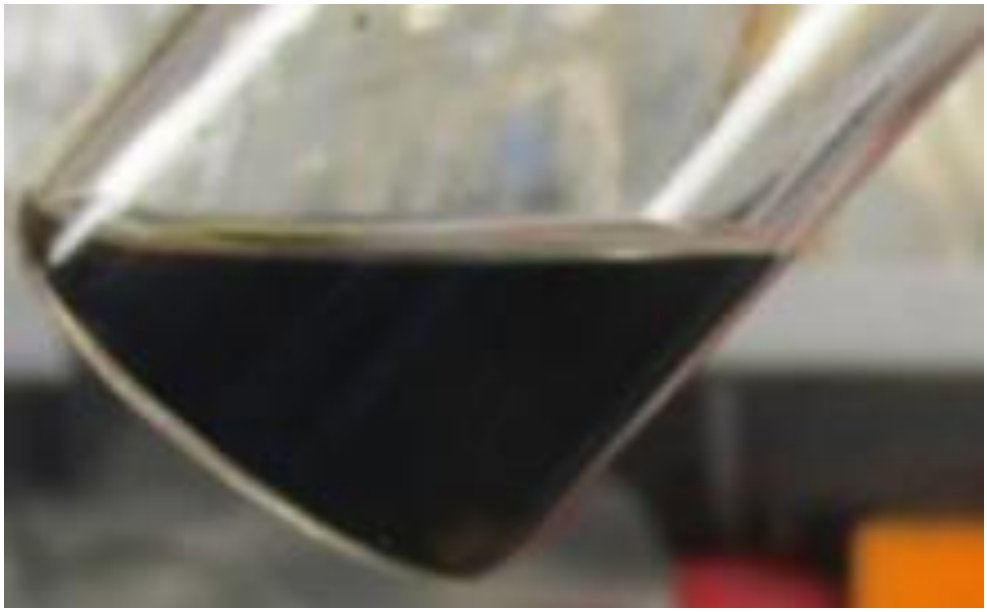

Figure 1.2: $[((H_3C)_3Si)_2N]_2U[\kappa\text{-}2\text{-}(C,N)\text{-}CH_2Si(CH_3)_2N(Si(CH_3))]$ in THF

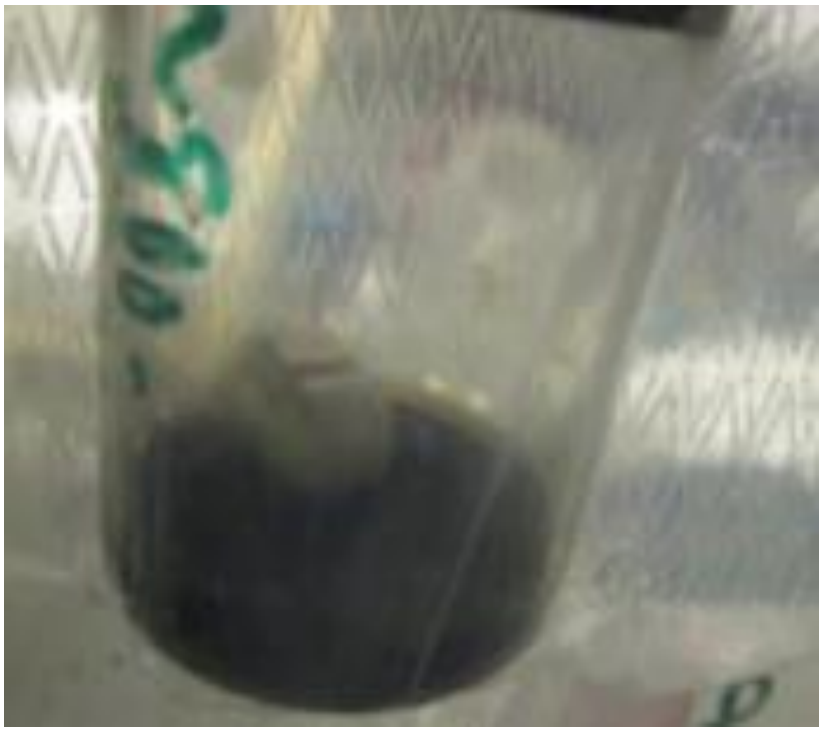

Figure 1.3: Residue generated from the reaction of H_2PPh with $[((H_3C)_3Si)_2N]_2U[\kappa\text{-}2\text{-}(C,N)\text{-}CH_2Si(CH_3)_2N(Si(CH_3))]$ (^{31}P δ -48.2 ppm)

Experimental

All experimental operations were conducted with rigorous exclusion of air and moisture using Schlenk techniques [78, 79] and standard glove-box methods [80] using a Vacuum Atmospheres glovebox with a recirculating dinitrogen atmosphere. Solvents were bought anhydrous or HPLC-grade (pentane, hexane, toluene, acetonitrile) and further purified using a Vacuum Atmospheres Solvent Purifier System. 1,4-dioxane, tetrahydrofuran, and diethyl ether were dried over sodium benzophenone ketyl, and degassed using three freeze-pump-thaw cycles prior to use. All solvents were stored under dinitrogen in a glove-box, and stored over 4 Å molecular sieves for at least 24 hours prior to use. Glassware was dried at 150°C before use. ^{1}H and ^{31}P NMR spectra were recorded using a Bruker 400 MHz spectrometer at 298 K. Deuterated benzene (Cambridge Isotopes) was stored over 4 Å molecular sieves for at least 24 hours prior to use.

Oxide encrustations were removed from the uranium metal using concentrated nitric acid [34]. Once the turnings achieved a brilliant lustre, the nitric acid was decanted, and the turnings were rinsed with acetone and stored in a dinitrogen atmosphere glovebox. These operations are reported in the literature [34, 81]. Utmost care must be taken to minimize exposure of the cleaned turnings to air by immediately covering the turnings with acetone once the nitric acid is decanted; uranium metal is pyrophoric, and thick orange fumes will start billowing off the turnings if they are exposed to air for too long. Iodine (sublimed) was used as purchased (Aldrich). $KN(SiMe_3)_2$ was used as purchased (Aldrich). Phenylphosphine was used as purchased or synthesized according

to the literature [82]. [((H$_3$C)$_3$Si)$_2$N]$_2$U[κ^2-(*C,N*)-CH$_2$Si(CH$_3$)$_2$N(Si(CH$_3$))] was prepared as previously reported [34]. ThCl$_4$(DME)$_2$, UCl$_4$, UI$_4$(1,4-dioxane)$_2$, UI$_3$(1,4-dioxane)$_{1.5}$, UCl[N(SiMe$_3$)$_2$]$_3$, ThCl[N(SiMe$_3$)$_2$]$_3$, UCl$_2$[N(SiMe$_3$)$_2$]$_2$, and U[N(SiMe$_3$)$_2$]$_3$ were prepared according to published methods [34, 50, 83-86].

Caution! *Depleted uranium (primary isotope ^{238}U) is a weak* α*-emitter (4.197 MeV) with a half-life of 4.47 x 10^9 years, and natural thorium (primary isotope ^{232}Th) is a weak* α*-emitter (4.012 MeV) with a half-life of 1.41 x 10^{10} years; manipulations and reactions should be carried out in monitored fume hoods or in an inert atmosphere drybox in a radiation laboratory equipped with* α*-counting equipment*.

Synthesis of U[PHPh][N(SiMe$_3$)$_2$]$_3$

0.138 grams (0.192 mmol) of [((H$_3$C)$_3$Si)$_2$N]$_2$U[κ-2-(*C,N*)-CH$_2$Si(CH$_3$)$_2$N(Si(CH$_3$))] was dissolved in 10 mL of THF. 0.021 grams (0.192 mmol) of H$_2$PPh was dissolved in 5 mL of THF and added to the [((H$_3$C)$_3$Si)$_2$N]$_2$U[κ-2-(*C,N*)-CH$_2$Si(CH$_3$)$_2$N(Si(CH$_3$))] solution dropwise at room temperature. A slight color change was observed from dark brown to burgundy brown, and the solution was stirred for 6 hours at room temperature. The THF was removed *in vacuo*, and the residue was dissolved in pentane and filtered. The pentane was removed *in vacuo* and a dark brown solid was afforded in 75% yield (0.119 grams).

^{31}P *NMR Data* (C$_6$D$_6$, 298 K): δ -48.2 ppm.

Alternate. 0.803 grams (1.12 mmol) of [((H$_3$C)$_3$Si)$_2$N]$_2$U[κ-2-(C,N)-CH$_2$Si(CH$_3$)$_2$N(Si(CH$_3$))] was dissolved in 10 mL of THF. 0.123 grams (1.12 mmol) of H$_2$PPh was dissolved in 5 mL of THF and added to the [((H$_3$C)$_3$Si)$_2$N]$_2$U[κ-2-(C,N)-CH$_2$Si(CH$_3$)$_2$N(Si(CH$_3$))] solution

dropwise at room temperature. A slight color change was observed from dark brown to burgundy brown, and the solution was stirred for 6 hours at room temperature. The THF was removed *in vacuo*, and the residue was dissolved in pentane and filtered. The pentane was removed *in vacuo* and the dark brown product was sealed and stored for further characterization via NMR and X-ray emission spectrometry.

Attempted Synthesis of U[PHPh][$N(SiMe_3)_2]_3$ via Salt Metathesis

0.025 grams (0.033 mmol) of U$Cl[N(SiMe_3)_2]_3$ was dissolved in 3 mL of THF. 0.004 grams (0.033 mmol) of LiHPPh [87] was dissolved in 3 mL of THF and added to the U$Cl[N(SiMe_3)_2]_3$ solution dropwise at room temperature. An immediate color change was observed from brown to dark red, and the solution was stirred for 6 hours at room temperature. The solution was filtered, THF was removed *in vacuo*, and dark brown solid was afforded in quantitative yield (0.027 grams). The residue was dissolved in C_6D_6 for NMR analysis.

^{31}P *NMR Data* (C_6D_6, 298 K): δ -48.19 ppm.

Attempted Synthesis of Th[PHPh][$N(SiMe_3)_2]_3$ via Salt Metathesis

0.029 grams (0.039 mmol) of Th$Cl[N(SiMe_3)_2]_3$ was dissolved in 5 mL of THF. 0.005 grams (0.039 mmol) of LiHPPh was dissolved in 5 mL of THF and added to the Th$Cl[N(SiMe_3)_2]_3$ solution dropwise at room temperature. A fast color change was observed from colorless to dark yellow, and the solution was stirred for 24 hours at room temperature. The solution became a dark red-orange. The solution was filtered, the THF was removed *in*

vacuo, and a dark red solid was afforded in quantitative yield (0.032 grams). NMR and XRD analyses were inconclusive.

Attempted Synthesis of $U[PHPh]_2[N(SiMe_3)_2]_2$ via Salt Metathesis

0.005 grams (0.0073 mmol) of $UCl_2[N(SiMe_3)_2]_2$ was dissolved in 3 mL of THF. 0.002 grams (0.0146 mmol) of LiHPPh was dissolved in 3 mL of THF and added to the $UCl_2[N(SiMe_3)_2]_2$ solution dropwise at room temperature. A drastic color change was observed from light green-yellow to a dark brown-purple, and the solution was stirred overnight at room temperature. The solution was filtered, and THF was removed *in vacuo*. The products were intractable, and NMR analysis was inconclusive.

Attempted Synthesis of $U[PHPh]_4$

0.038 grams (0.1 mmol) of UCl_4 was dissolved in 10 mL of THF. 0.046 grams (0.399 mmol) of LiPHPh was dissolved in 5 mL of THF and added to the UCl_4 solution dropwise at room temperature. A strong color change was immediately observed from light green to dark brown/black. The solution was stirred for 6 hours at room temperature. The THF was removed *in vacuo*. The residue was dissolved in C_6D_6 and analyzed via NMR.

^{31}P *NMR Data* (C_6D_6, 298 K): δ -40.7 ppm.

Attempted Synthesis of $Th[PHPh]_4$

0.019 grams (0.34 mmol) of $ThCl_4(DME)_2$ was dissolved in 10 mL of THF. 0.016 grams (1.37 mmol) of LiPHPh was dissolved in 5 mL of THF and added to the $ThCl_4$(DME) solution dropwise at room temperature. A strong color change was immediately

observed from colorless to dark blood red. The solution was stirred for 6 hours at room temperature. The THF was removed *in vacuo*. The residue was dissolved in C_6D_6 and analyzed via NMR. NMR results were inconclusive.

Attempted Synthesis of $Ce[PHPh]_3$

0.021 grams (0.852 mmol) of $CeCl_3$ was dissolved in 10 mL of THF. 0.030 grams (2.55 mmol) of LiPHPh was dissolved in 5 mL of THF and added to the $CeCl_3$ solution dropwise at room temperature. A strong color change was immediately observed from colorless to deep-orange. The solution was stirred for 6 hours at room temperature. The THF was removed *in vacuo*. The residue was dissolved in C_6D_6 and analyzed via NMR.

^{31}P *NMR Data* (C_6D_6, 298 K): δ -134.84 ppm.

Attempted Synthesis of $[Li][U[PPh][N(SiMe_3)_2]_3]$

0.235 grams (0.33 mmol) of $[((H_3C)_3Si)_2N]_2U[\kappa\text{-}2\text{-}(C,N)\text{-}CH_2Si(CH_3)_2N(Si(CH_3))]$ was dissolved in 10 mL of THF. 0.038 grams (0.33 mmol) of LiPHPh was dissolved in 5 mL of THF and added to the $[((H_3C)_3Si)_2N]_2U[\kappa\text{-}2\text{-}(C,N)\text{-}CH_2Si(CH_3)_2N(Si(CH_3))]$ solution dropwise at room temperature. No major color change was observed, and the solution was stirred for 10 hours at room temperature. The THF was removed *in vacuo*. The residue was extracted in toluene, filtered, and isolated *in vacuo*. The residue was extracted again with pentane, filtered, and isolated *in vacuo*. A dark brown residue was afforded (0.035 grams; 66% yield). No conclusive NMR data was obtained.

Attempted Synthesis of $[Li][U[PHPh][N(SiMe_3)_2]_3]$

0.026 grams (0.036 mmol) of $U[N(SiMe_3)_2]_3$ was dissolved in 5 mL of THF. 0.004 grams (0.036 mmol) of LiPHPh was dissolved in 5 mL of THF and added to the $U[N(SiMe_3)_2]_3$ solution dropwise at room temperature. A color change from purple to dark brown was observed, and the solution was stirred for 9 hours at room temperature. The THF was removed *in vacuo*. The residue was extracted in toluene, filtered, and isolated *in vacuo*. The residue was extracted again with pentane, filtered, and isolated *in vacuo*. A dark brown residue was afforded (0.022 grams; 66.6% yield). No conclusive NMR data was obtained.

Results and Discussion

Our quest to synthesize direct actinide-phosphorus bonds began with zealous attempts to synthesize complexes featuring metal-phosphorus multiple bonds. Very few actinide phosphinidene complexes have been previously reported, and no monomeric actinide phosphide (An≡P) complexes have been reported [5, 7-11, 45, 69, 74, 75, 77]. A uranium-phosphorus triple-bond would be a holy grail in actinide chemistry, and much of our synthetic efforts were focused on the generation of a uranium phosphide complex. An equal amount of zeal was directed towards the synthesis of actinide phosphinidene (An=P) complexes. Our initial efforts to synthesize actinide-phosphorus multiple bonds focused on installing anionic phosphorus ligands via salt metathesis, however, difficulties were encountered with this synthetic strategy. This could possibly be due to the reducing nature of lithium phosphide salts. Sattelberger and co-workers experienced unexpected redox reactions when attempting to install bis(trimethylsilyl)phosphide

ligands on U(IV) via salt metathesis with $LiP(SiMe_3)_2$ [6]. Instead of the expected substitution of chloro ligands with phosphide ligands, the lithium phosphide salt reduced the metal center to U(III) without the installation of the phosphide ligand [6]. The ability of $LiP(SiMe_3)_2$ to reduce U(IV) was demonstrated by Blake et al. in 1988 [88].

Our initial efforts focused on the use of LiPHPh in salt metathesis reactions with $UCl[N(SiMe_3)_2]_3$ to synthesize $U[PHPh][N(SiMe_3)_2]_3$. It is possible that the use of NaPHPh, Na_2PPh, KPHPh, or K_2PPh in reactions with $UCl[N(SiMe_3)_2]_3$, $UBr[N(SiMe_3)_2]_3$, or $UI[N(SiMe_3)_2]_3$ could yield better results. However, unfortunate administrative constraints prevented these reaction pathways from being explored. These reaction pathways should be explored by someone in the future.

Instead of continuing a strategy based on salt metathesis, we explored a more atom-efficient strategy based on protonolysis of the U(IV) metallacycle $[((H_3C)_3Si)_2N]_2U[\kappa^2\text{-}(C,N)\text{-}CH_2Si(CH_3)_2N(Si(CH_3))]$. Karmel et al. recently reported several catalysis studies involving protonolysis reactions of this U(IV) metallacycle [89], and Arnold and co-workers synthesized a thorium-imido complex via protonolysis of the analogous Th(IV) metallacycle, $[((H_3C)_3Si)_2N]_2Th[\kappa^2\text{-}(C,N)\text{-}CH_2Si(CH_3)_2N(Si(CH_3))]$ [90]. This synthetic strategy yielded positive results, and NMR data suggest the possible synthesis of a tetravalent uranium phosphido-amido complex, $U[PHPh][N(SiMe_3)_2]_3$. If the identity of the product is indeed $U[PHPh][N(SiMe_3)_2]_3$, this complex could potentially be deprotonated to form a phosphinidene.

This protonolysis strategy produced promising initial NMR results, warranting further studies; however, due to unfortunate admininstrative circumstances, this research came to an abrupt halt soon after these initial results were achieved. This initial work lays the groundwork for future projects that hold enormous potential to advance our understanding of orbital interactions in molecular uranium complexes. One can envision reacting a library of primary and secondary phosphines with $[((H_3C)_3Si)_2N]_2U[\kappa^2\text{-}(C,N)\text{-}CH_2Si(CH_3)_2N(Si(CH_3))]$ to yield complexes with the general formulas $U^{IV}[PHR][N(SiMe_3)_2]_3$ and $U^{IV}[PR_2][N(SiMe_3)_2]_3$. A series of complexes with these general formulas can provide unprecedented insight into the nature of the orbital interactions involved in U-P functionalities, and how the ionicity/covalency of the U-P bond is modulated by the identity of the organic substituents (R) bound to phosphorus. These orbital interactions could possibly be studied in detail using a combination of ^{31}P NMR spectroscopy coupled with Quantum Theory of Atoms in Molecules (QTAIM) calculations, and phosphorus-Kβ X-ray emission spectroscopy coupled with Time-Dependent Density Functional Theory (TD-DFT) calculations.

The uranium(IV) silyl-amide metallacycle, $[((H_3C)_3Si)_2N]_2U[\kappa\text{-}2\text{-}(C,N)\text{-}CH_2Si(CH_3)_2N(Si(CH_3))]$, is a strong Brønsted base, and deprotonates phenylphosphine, H_2PPh, to form $U[PHPh][N^*]_3$ ($N^* = N(SiMe_3)_2$. The U-C bond in the metallacycle is highly polar and exhibits highly selective reactivity and catalytic activity. The U(IV) metallacycle easily deprotonates aromatic and aliphatic alcohols and thiols to form aryloxides, alkoxides, and thiolates. Phenylphosphine is much less acidic (pKa = 24.5) [118], and its

reaction with $[((H_3C)_3Si)_2N]_2U[\kappa\text{-}2\text{-}(C,N)\text{-}CH_2Si(CH_3)_2N(Si(CH_3))]$ to form a uranium-phosphido complex further demonstrates the strength of this silyl-amide Brønsted base. Direct anionic uranium-phosphorus bonds are extremely rare and present a unique opportunity to study uranium orbital interactions with soft-donor ligands.

The residue formed through the reaction of phenylphosphine with the U(IV) silyl-amide metallacycle is highly soluble in pentane and benzene, and ^{31}P NMR analysis yielded a resonance at δ -48.2 ppm. The phosphorus nucleus of phenylphosphine, H_2PPh, resonates at δ-123.8 ppm. The following empirical formula can be used to predict the ^{31}P NMR shifts of primary phosphines, RPH_2:

$$\delta_P = -163.5 + 2.5\ \sigma^c$$

When R = phenyl, the shift constant (σ^c) is equal to 18. Solving for δ_P yields an NMR resonance of -118.5 ppm. Empirical ^{31}P NMR data for phenylphosphine, H_2PPh, ranges from -118.7 ppm to -125.7 ppm in the literature, which agrees well with the value of -118.5 ppm obtained from the empirical formula above.

The NMR chemical shift observed for a given compound upon coordination to a metal can be used to calculate the *coordination chemical shift* (Δδ), using the following formula:

$$\Delta\delta = \delta_P\ (\text{complex}) - \delta_P\ (\text{ligand})$$

Coordination of the phenyphosphide ligand (^-PHPh) results in a downfield shift from -123.8 pm to -48.2 ppm, giving coordination chemical shift (Δδ) of +75.6 ppm. This

result indicates that the uranium metal center withdraws electron density from the phosphorus nucleus. The ^{1}H NMR for the residue was quite complex. Three broad roughly equivalent peaks were observed in the typical paramagentic $SiMe_3$ region, at δ -2.93 ppm, δ -2.4 ppm, and δ -4.0 ppm. Another large resonance was also observed at δ -10.07 ppm. Three smaller, very deshielded resonances were also observed at δ -14.93 ppm, δ -15.55 ppm, and δ -16.19 ppm. These could potentially correspond to aromatic protons of the coordinated phosphido ligand. Lastly, a sharp resonance was observed at δ 4.35 ppm. This resonance likely corresponds to the P-H proton. This agrees well with the analogous zirconium-phenylphosphido complex, where the P-H proton was observed at δ 3.97 ppm.

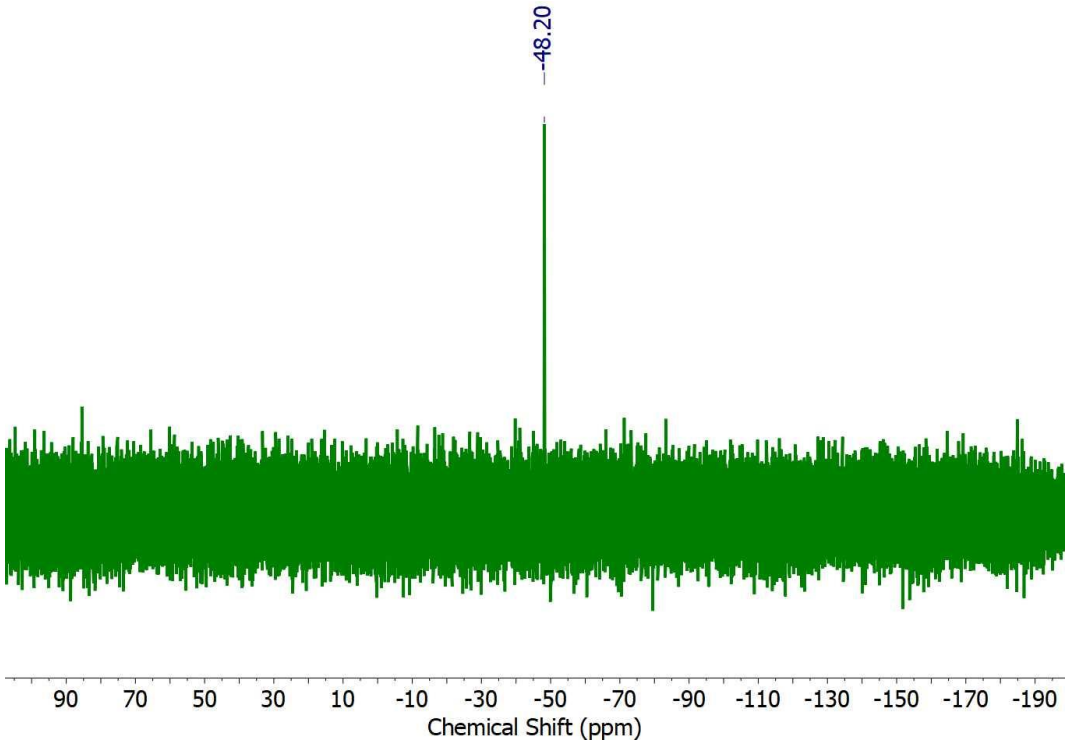

Figure 1.4: ^{31}P NMR spectrum for U[PHPh][N*]$_3$.

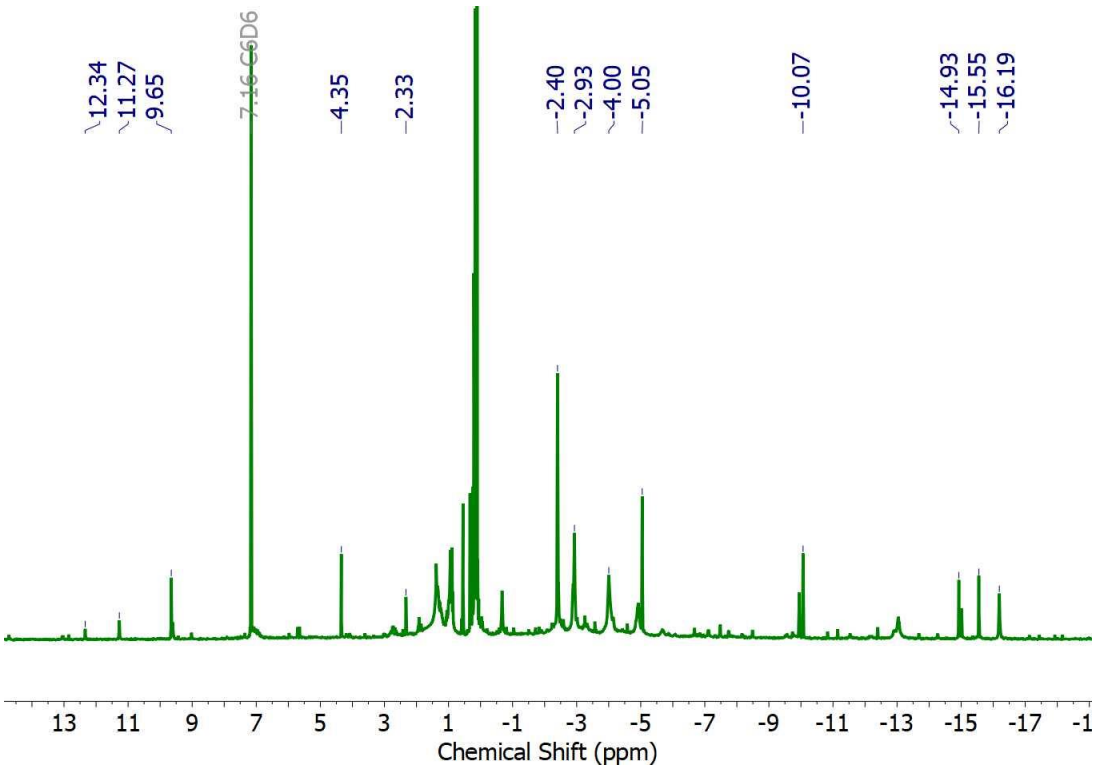

Figure 1.5: ^{1}H NMR spectrum for U[PHPh][N*]$_3$.

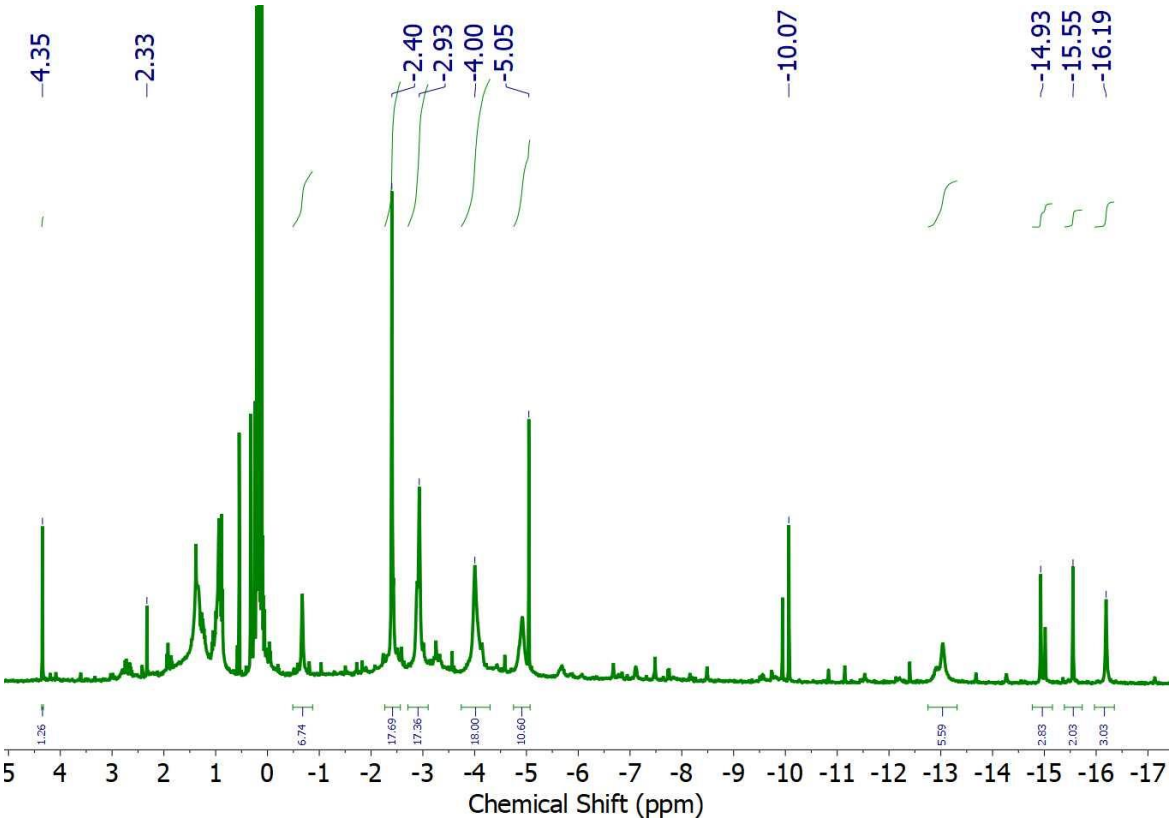

Figure 1.6: ^{1}H NMR spectrum for U[PHPh][N*]$_3$ (zoomed in).

Initially, the negative value of this chemical shift generated a degree of skepticism, since metal-phosphides often yield very deshielded, positive NMR resonances, often much greater than +100 ppm. For example, $Cp^*_2ThCl[P(SiMe_3)_2]$ resonates at δ_P = 109 ppm and $(Tren^{TIPS})UPH_2$ resonates at δ_P = 595 ppm. This called the identity of the product into question. It was contemplated that perhaps the phenyphosphine was not deprotonated, and instead formed a Lewis-base adduct using the lone electron pair on the phosphorus. However, reexamination of the metal-phosphide ^{31}P NMR literature made us aware of a zirconium complex, $(N_3N)Zr[PHPh]$ ($N_3N = N(CH_2CH_2NSiMe_3)_3^{3-}$), which has a similar structure to the target U(IV) complex, $U[PHPh][N^*]_3$. The phosphorus nucleus in this zirconium complex resonates at -48.16 [115], which is essentially identical to the resonance obtained from the residue formed by the reaction of phenylphosphine with the U(IV) metallacycle in this work. The similar zirconium(IV) phosphido complex was generated in an identical manner to our U(IV) phosphido complex, via protonolysis of a tetravalent silyl-amide metallacycle (shown below). It does not seem coincidental that a nearly isostructural Zr(IV) complex would have an essentially identical ^{31}P NMR chemical shift as the uranium(IV) analogue. It is indeed surprising that that the zirconium and uranium complexes would have identical chemical shifts, especially since Zr(IV) is diamagnetic (d^0) and U(IV) is paramagnetic (f^2). However, the realization that a nearly isostructural Zr complex has an identical phosphorus NMR resonance increased our confidence that the product was most likely the intended uranium amido-phosphido complex, $U[PHPh][N^*]_3$. Furthermore, $(Tren^{TIPS})ThPH_2$ resonates at -144.1 ppm. This clarified in our minds that negative phosphorus NMR shifts are not without precedent in

metal-phosphide NMR literature, as the above mentioned zirconium- and thorium-phosphido complexes show. Further structural, spectroscopic, and magnetic characterization will be necessary to unambiguously confirm the identity of the product. Nevertheless, the extraordinary agreement of the phosphorus NMR with an analogous zirconium phenylphosphide complex suggests the successful synthesis of a previously unreported uranium phenylphosphide complex, U[PHPh][N*]$_3$.

Given that uranium(IV) is paramagnetic (f^2), with two unpaired f-electrons, it is surprising that a phosphorus signal was observed; direct metal-phosphorus bonds in paramagnetic complexes are often ^{31}P NMR silent. However, Liddle and co-workers observed a phosphorus resonance for (Tren^{TIPS})UPH$_2$, so such an observation is not unprecedented. The observation of this signal provides further evidence that ^{31}P NMR can be a useful tool for studying uranium(IV)-ligand covalency. A series of *pseudo*-isostructural compounds with different aryl and alkyl groups attached to the phosphorus could shed light on how the identity of the phosphorus substituent influences the nature of the uranium-phosphorus bond. Phosphide ligands that result in a larger coordination chemical shift (Δδ) are expected to have larger degrees of metal-ligand covalency, and aliphatic phosphide ligands, like $^-$PH(*t*-butyl), with greater electron donation ability, are likely to yield a large coordination chemical shift (Δδ).

The ^{31}P NMR literature for terminal metal-phosphido complexes can be divided into two main categories: 1) complexes with planar phosphido ligands (Σ<P ≈ 360°) and 2) complexes with pyramidal phosphido ligands (Σ<P less than 360°). Pyramidal

phosphido ligands are sp^3 hybridized, with the phosphorus lone pair relatively localized on the phosphorus, resulting in a relatively shielded phosphorus nucleus compared to planar carbene-like phosphido ligands. Planar phosphido ligands generate much more deshielded resonances. The phosphorus atom in planar phosphido ligands is sp^2 hybridized, and the lone pair residing in an unhybridized p-orbital can engage in π-interactions with a metal cation, thereby deshielding the phosphorus nucleus. Some zirconium and hafnium complexes have been reported that possess both planar *and* pyramidal phosphido ligands, resulting in two distinct ^{31}P NMR resonances [116]. For example, in $Cp_2Hf(PCy_2)_2$, the pyramidal σ-donating phosphido ligand resonates at δ_P -15.3 ppm, and the planar π-donating phosphido ligand resonates at δ_P +270.2 ppm [116]. With these results in mind, one would expect the phosphido ligand in $U[PHPh][N^*]_3$ to be pyramidal, since the phosphorous nucleus resonates at δ -48.2 ppm. Indeed, the analogous zirconium-phosphido complex mentioned above has a pyramidal geometry, as shown by X-ray diffraction in previous work [x]. The Th-PH_2 complex reported by Liddle and coworkers is also pyramidal, and resonates at δ -144.1 ppm. The isostructural U-PH_2 complex also appears to have a pyramidal phosphide moiety just by looking at the published crystal structure; however, the sum of the bonds angles around phosphorus was not reported, and it is hard to say definitively how the geometry of the U-PH_2 unit compares to the Th-PH_2 unit. Indeed, the uranium analogue resonates at δ 595 ppm, and one would expect such a deshielded phosphorus nucleus to be relatively planar, with significant π-interactions. Given the ^{31}P NMR resonance of δ -48.2 ppm, it is likely that the U-PHPh unit in N^*_3U-PHPh is pyramidal like the Zr-PHPh unit in (N_3N)Zr-PHPh.

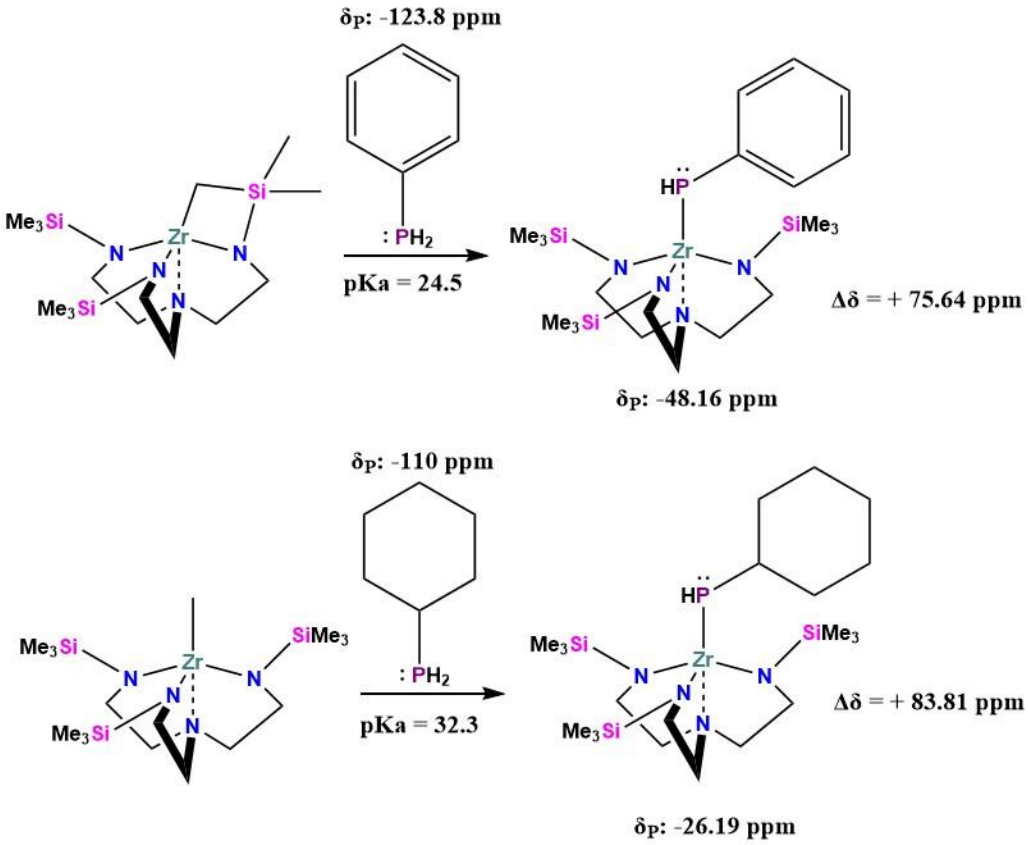

Figure 1.7: Zirconium-phosphido syntheses and ^{31}P NMR chemical shifts [115].

$U[PHPh][N(SiMe_3)_2]_3$ can also be synthesize via salt metathesis using $UCl[N(SiMe_3)_2]_3$ and LiPHPh. Our initial efforts to generate $U[PHPh][N(SiMe_3)_2]_3$ started with this strategy; however, it was initially thought that this reaction was unsuccessful. However, after reviewing the data again in light of the positive results obtained via protonolysis of the metallacycle, it appears that the salt metathesis synthesis of $U[PHPh][N(SiMe_3)_2]_3$ was successful. A ^{31}P NMR resonance was observed at δ -48.2 ppm, identical to the result obtained via protonolysis.

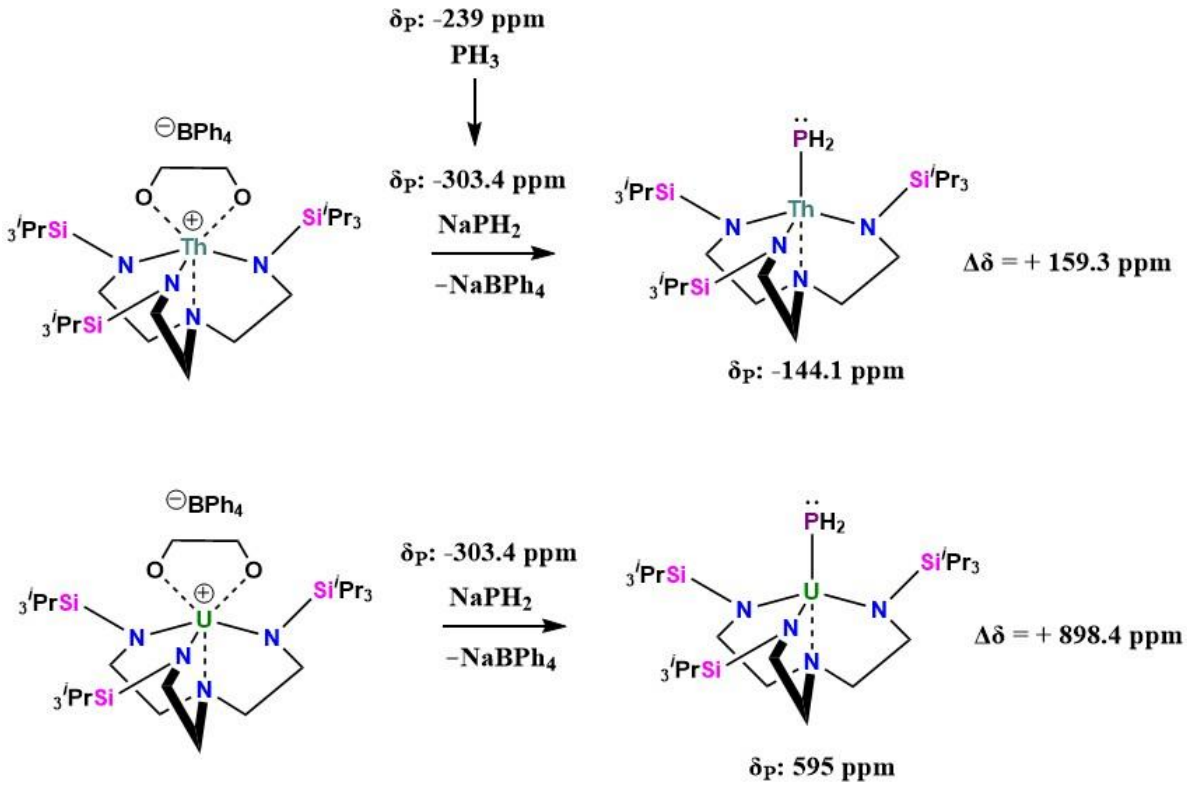

Figure 1.8: Thorium- and Uranium-phosphido syntheses and ^{31}P NMR chemical shifts [9, 117].

Lithium phenylphosphide, LiPHPh, was dissolved in THF and added to a stirring THF solution of Cl-U[N*]$_3$. The solution turned from brown to dark blood-red. The solution was evaporated to dryness, extracted with toluene, filtered, evaporated to dryness, extracted with pentane, filtered, and recrystallized in pentane. The masses obtained suggest the product was obtained in essentially quantitative yield, however, this reaction was conducted on a very small scale. X-ray diffraction analysis of a crystal with an exceedingly foul stench yielded the structure of a complex lithium phenylphosphide cluster that has not been previously reported. Efforts then shifted to a strategy based on

protonolysis of the U(IV) amide-metallacycle with H_2PPh. Though the salt metathesis strategy starting from Cl-U[N*]$_3$ yielded the same ^{31}P NMR resonance as the protonlysis strategy starting from the metallacycle (δ_P = -48.2 ppm), important differences in the ^1H NMR were observed. The P-H proton was not observed for the residue obtained via salt metathesis, and several of the broad paramagnetically shifted peaks observed for the residue obtain via reaction with the metallacycle were not observed, with the exception of the resonance at δ -10.1 ppm. The fact that the resonance at δ -10.1 ppm was observed using both strategies (along with the identical ^{31}P NMR resonance) suggests that this could in fact be the $SiMe_3$ resonance of the amide ligands. The ^1H NMR for the residue obtained from reaction with the metallacycle might show *both* symmetrized and desymmetrized amide ligands in equilibrium.

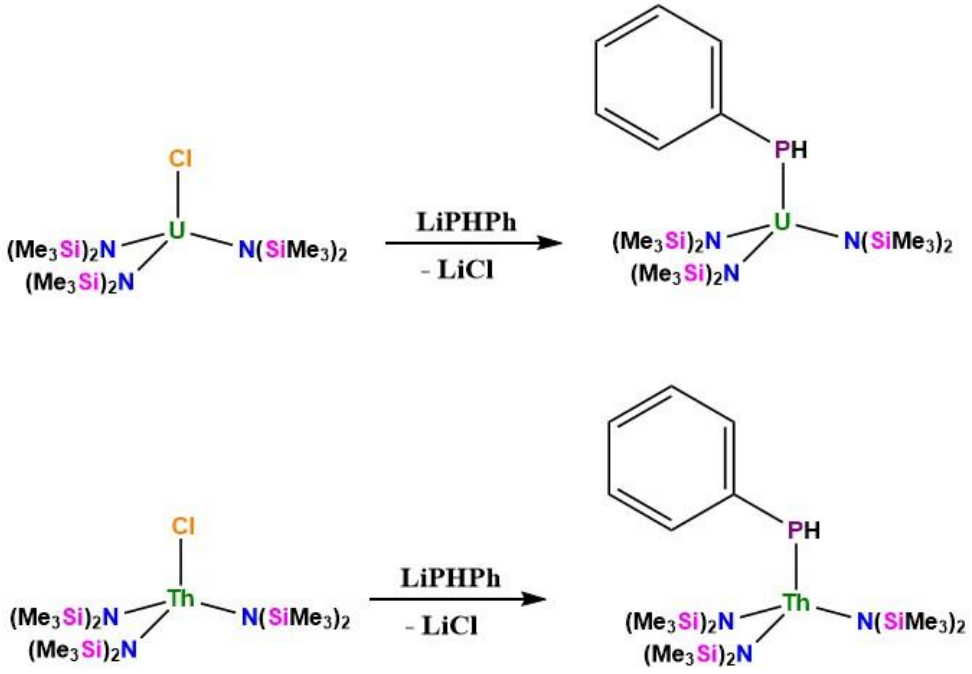

Scheme 1.4: Salt metathesis reaction using MCl[N*]$_3$ (M = U, Th).

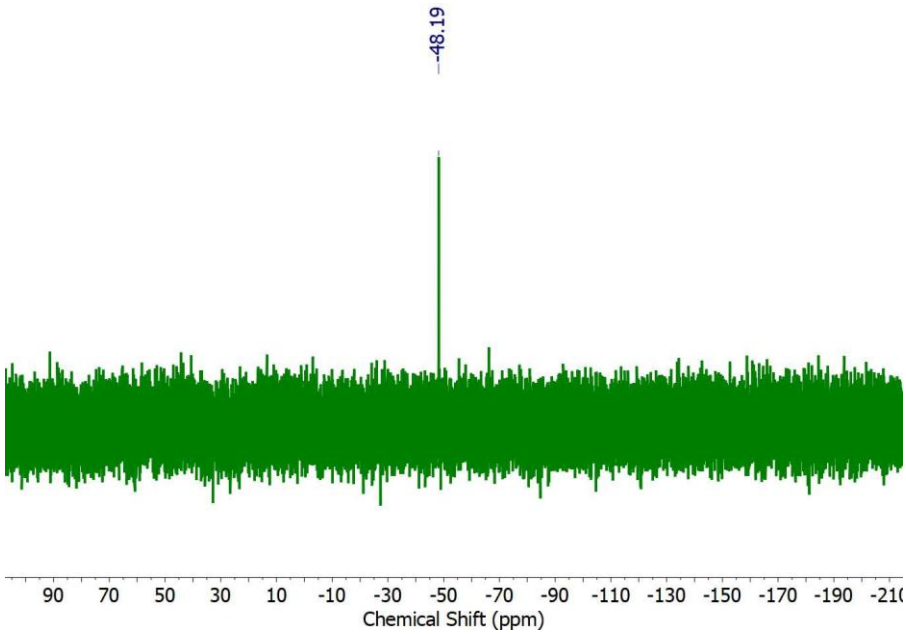

Figure 1.9: ^{31}P NMR spectrum for U[PHPh][N*]$_3$ made via salt metathesis.

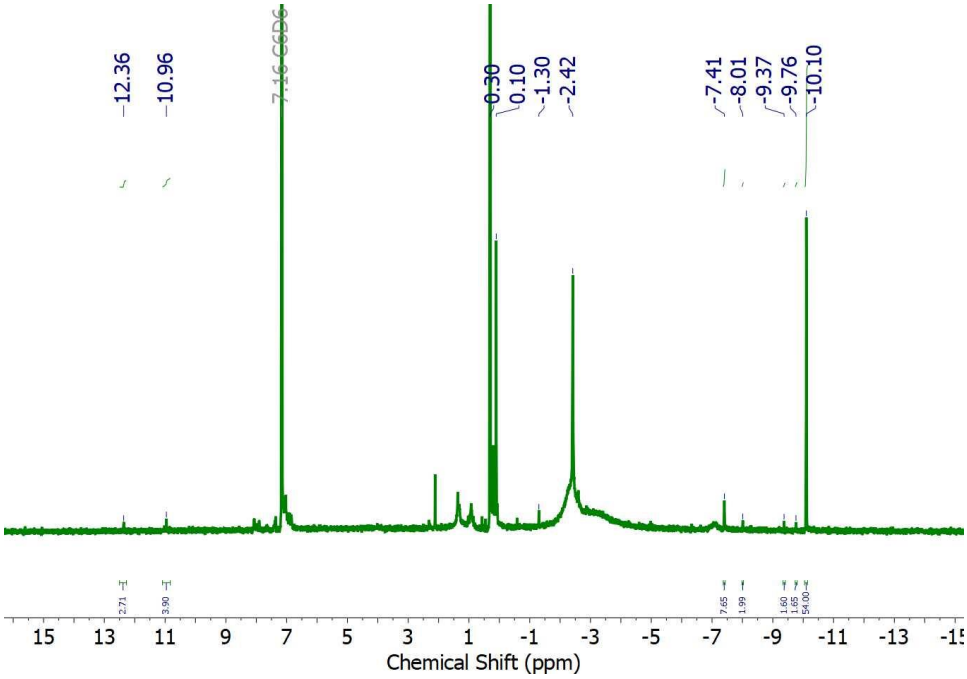

Figure 1.10: ^{1}H NMR spectrum for U[PHPh][N*]$_3$ made via salt metathesis.

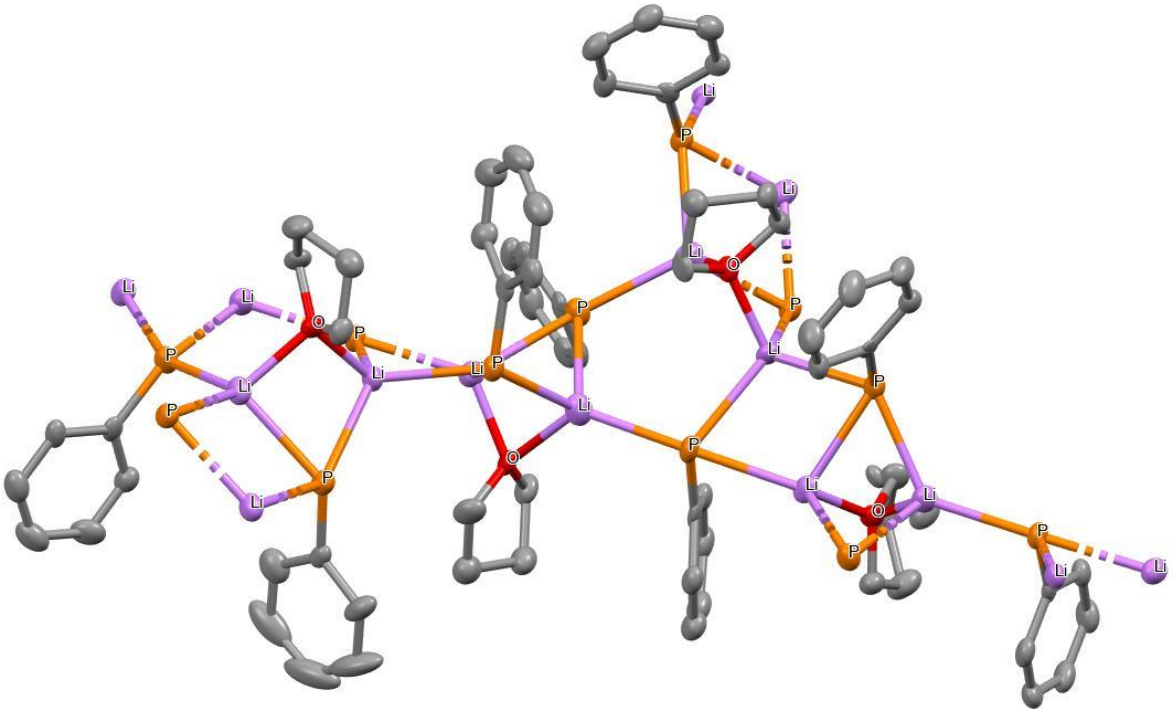

Figure 1.11: Single-crystal X-ray diffraction structure of previously unreported lithium phenylphosphide cluster, $C_{64}H_{80}Li_8O_4P_8 \cdot 2\ C_6H_6$.

The salt metathesis strategy was used to attempt the synthesis of the thorium(IV) analogue, Th[PHPh][N*]$_3$. LiPHPh was dissolved in THF and added to a stirring solution of Cl-Th[N(SiMe$_3$)$_2$]$_3$. There was an immediate color change from colorless to dark yellow, and then eventually to a dark red-orange. No resonances were observed in the ^{31}P NMR results, possibly due to low sample concentration. No peaks associated with LiPHPh or H_2PPh were observed. X-ray diffraction analysis of a crystal obtained from this reaction yielded the starting material, Cl-Th[N*]$_3$. Evidence that partial reaction occurred can be seen in the ^{1}H NMR data. The SiMe$_3$ resonance is split in two. The resonance at δ 0.41 ppm corresponds to the starting material, Cl-Th[N(SiMe$_3$)$_2$]$_3$. However, another roughly equivalent peak was observed at δ 0.39 ppm, potentially corresponding to the target thorium complex, Th[PHPh][N(SiMe$_3$)$_2$]$_3$. Furthermore, small, sharp resonances at δ 4.31, δ 3.86, δ 3.37, and δ 3.11, all with an approximate 1:54 ratio with respect to the peak at δ 0.39 ppm. The P-H proton could be assigned to any of these resonances, with δ 4.31 ppm and δ 3.86 ppm being the most likely candidates, when comparable Zr and U analogues are considered. Additionally, the splitting of these small peaks seem to provide evidence of P-H coupling. Aside from the SiMe$_3$ signal, the phosphido ligand should generate four resonances. The four small resonances could correspond to the three aromatic resonances and the P-H resonance.

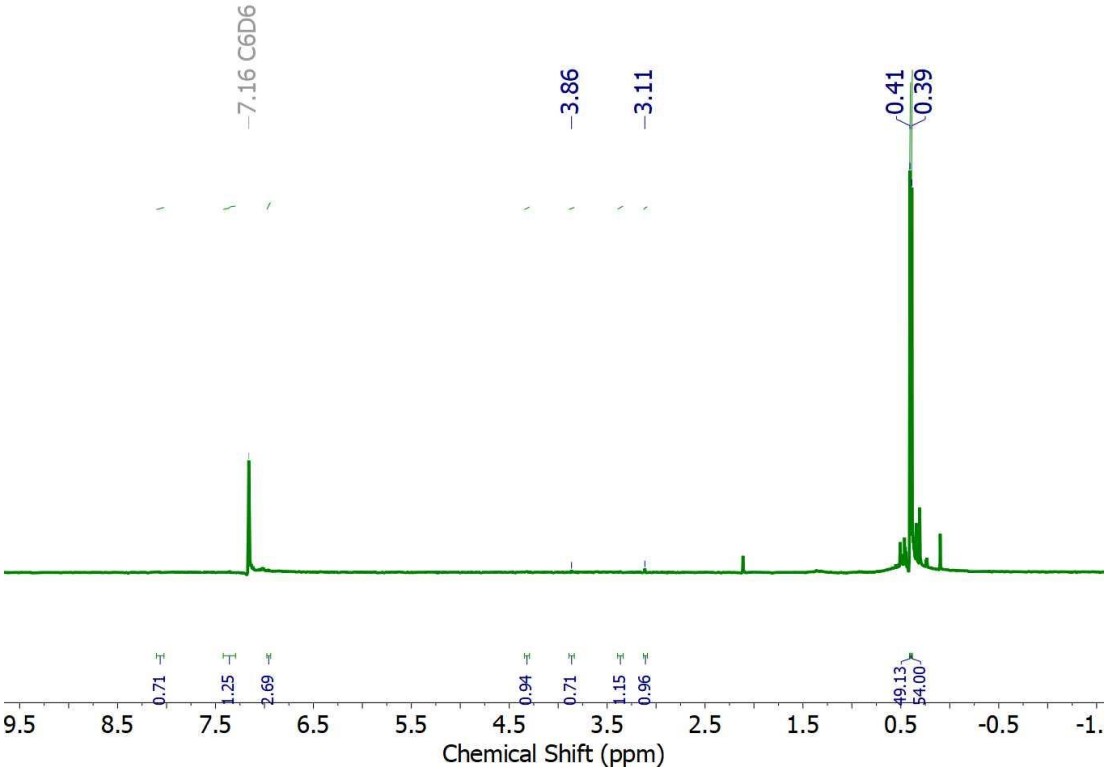

Figure 1.12: ^{1}H NMR spectrum for Th[PHPh][N*]$_3$ made via salt metathesis.

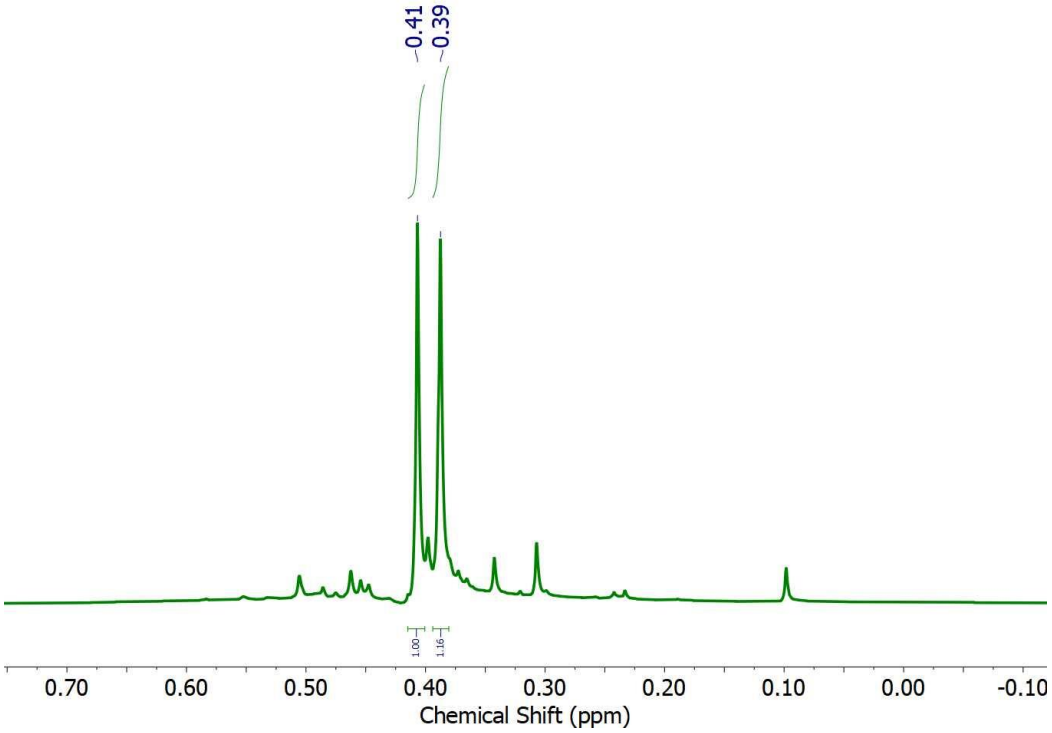

Figure 1.13: ^{1}H NMR spectrum for Th[PHPh][N*]$_3$ ($SiMe_3$ region).

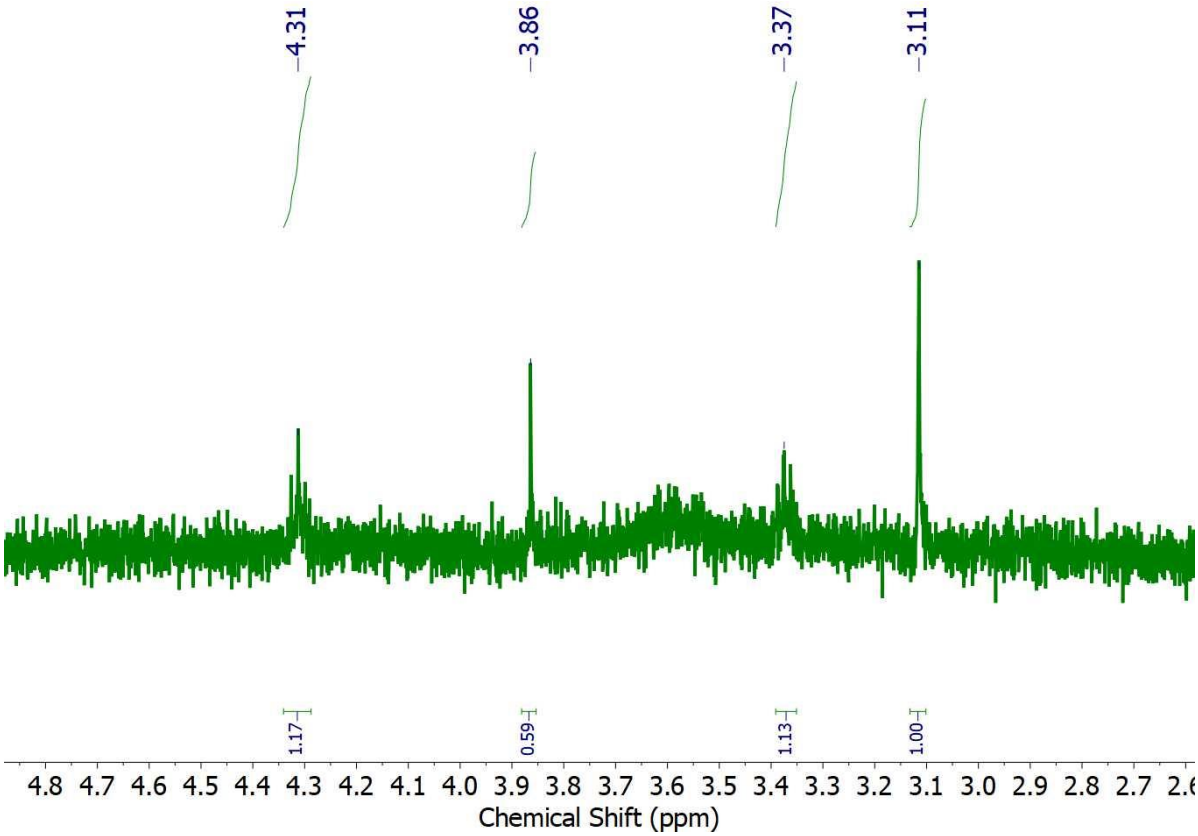

Figure 1.14: ^{1}H NMR spectrum for Th[PHPh][N*]$_3$ (P-H region).

The synthesis of a bis-phosphido bis-amide uranium(IV) complex was also attempted via salt metathesis using $UCl_2[N^*]_2$ and two equivalents of LiPHPh. A THF solution of LiPHPh was added to a stirring THF solution of $UCl_2[N^*]_2$. A drastic color change was immediately observed from light greenish-yellow to dark brownish-purple, suggesting a reaction took place. However, the reaction was conducted on a very small scale, and no conclusive NMR results were obtained. However, this reaction should be investigated further in the future.

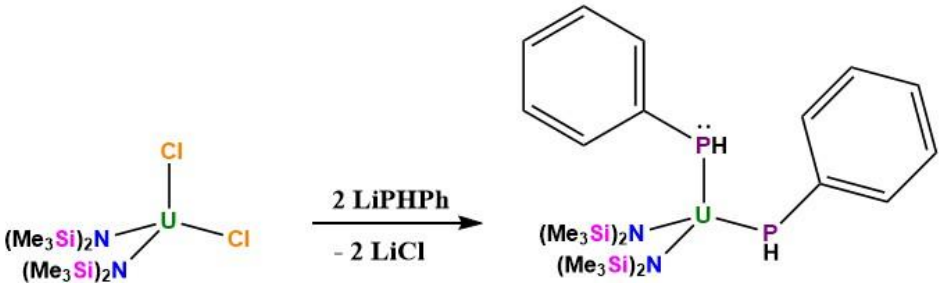

Scheme 1.5: Salt metathesis reaction using $UCl_2[N^*]_2$.

Attempted were also made to generate an anionic uranium(IV) phosphinidene complex via protonolysis using the U(IV) silylamide metallacycle and LiPHPh. Arnold and coworkers generated a Th(IV) imido complex in a similar fashion, using the Th(IV) silylamide metallacycle and KNHDipp. A THF solution of LiPHPh was added to a stirring THF solution of the U(IV) metallacycle. The solution turned form light brown to dark brown. The solution was evaporated to dryness, extracted with toluene, filtered, evaporated to dryness, extracted with pentane, filtered, evaporated to dryness, and analyzed via NMR. The residue was ^{31}P NMR-silent. However, an extremely shielded signal was observed in the ^{1}H results at δ -37.51 ppm, suggesting potential phosphinidene formation. More work should be done to investigate this reaction pathway, and structural characterization is needed to confirm the identity of the compound generating the resonance δ -37.51 ppm, if it is not simply a spectral artifact.

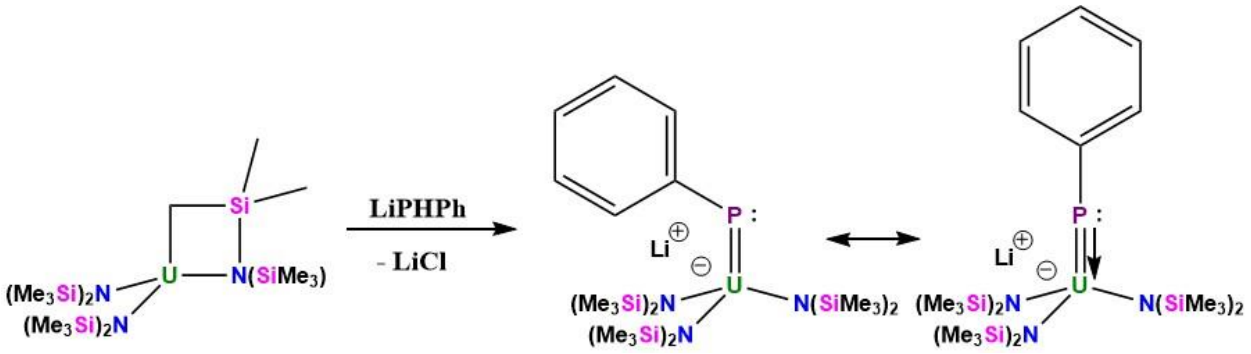

Scheme 1.6: Attempted phosphinidene synthesis.

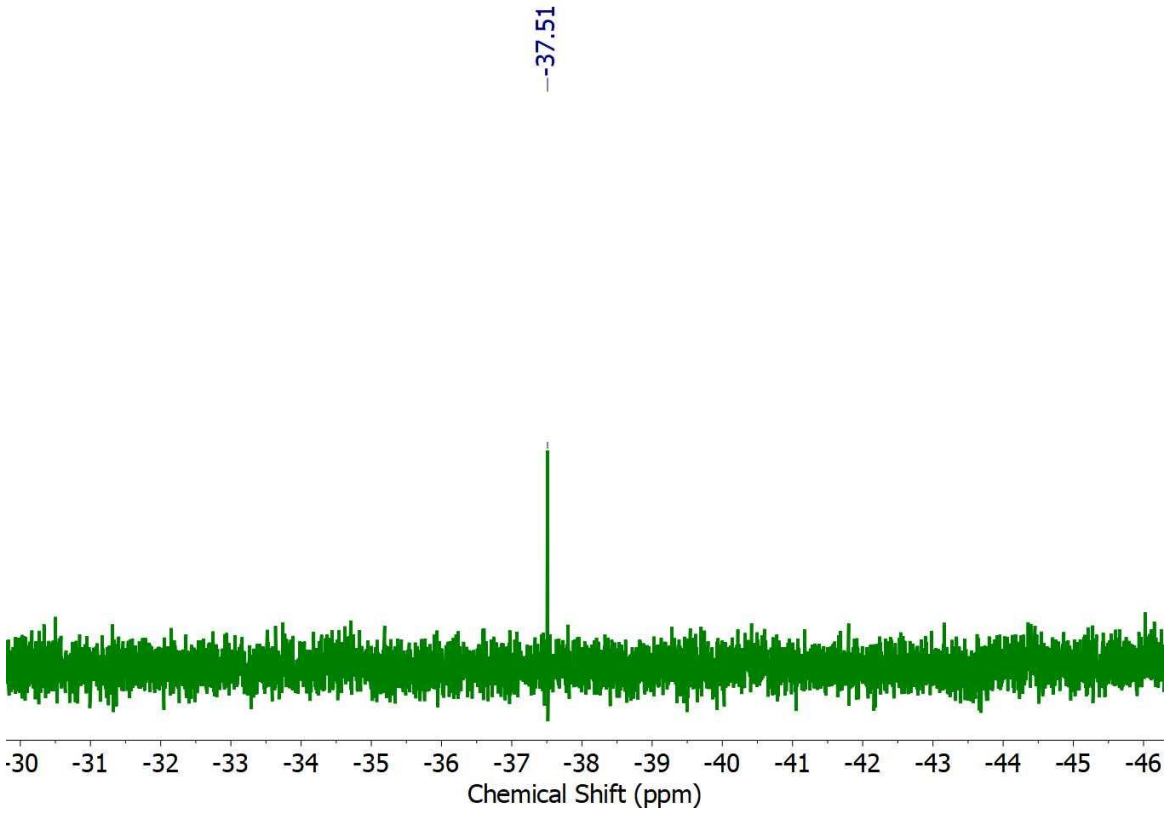

Figure 1.15: ^{1}H NMR spectrum for attempted synthesis of $[Li][U[PPh][N^*]_3]$.

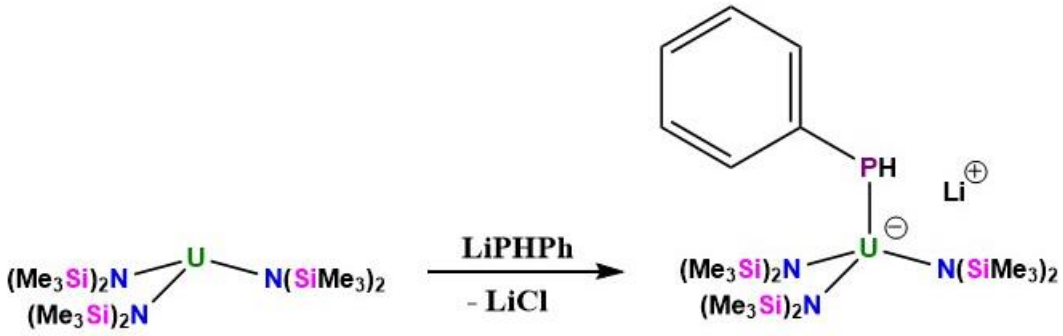

Scheme 1.7: Simple addition reaction with $U[N^*]_3$.

An attempt was made to generate an anionic uranium(III) phosphido-tris(amido) complex via simple addition of LiPHPh to $U[N(SiMe_3)_2]_3$. A THF solution of LiPHPh was added to a stirring THF solution of $U[N(SiMe_3)_2]_3$. The purple solution immediately turned brown. The solution was evaporated to dryness, extracted with toluene, filtered, evaporated to dryness, extracted with pentane, filtered, evaporated to dryness, and dissolved in C_6D_6 for NMR analysis. The residue was ^{31}P NMR silent. However, a noteworthy ^1H NMR spectrum was obtained. The target complex should generate at least five resonances (three aromatic, one P-H, and one $SiMe_3$). Indeed, five paramagnetically broadened peaks were observed at δ 3.25 ppm, δ 1.02 ppm, δ -2.41, δ -2.94 ppm, and δ -5.82 ppm. More work will be necessary to make definitive assignments for these resonances, and this reaction pathway should be investigated further in the future.

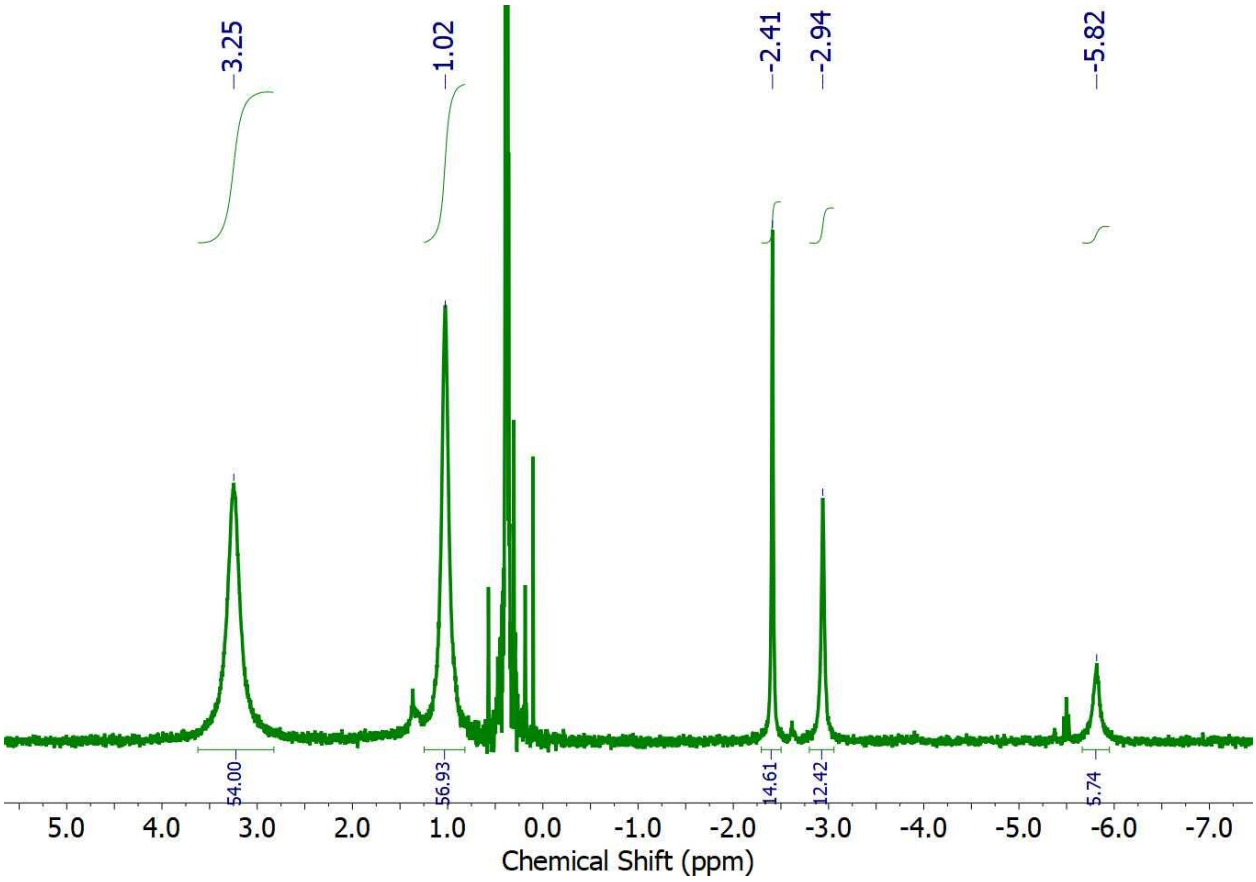

Figure 1.16: ^{1}H NMR spectrum for attempted synthesis of [Li][U[PHPh][N*]$_3$].

Efforts were made to generate homloleptic phenylphosphido complexes of uranium, thorium, and cerium. A THF solution of LiPHPh was added to a stirring THF solution of UCl_4. An immediate color change from light green to dark brown/black was observed. After work-up and NMR analysis, this residue generated a ^{31}P NMR resonance at δ -40.7 ppm. This chemical shift is very similar to the resonance observed for the mono-phenylphosphido complex U[PHPh][N*]$_3$ (δ_P = -48.2 ppm). The similarity of the resonances suggests the synthesis of a homoleptic phenylphosphido complex, U[PHPh]$_4$. Broad resonances were observed in the ^{1}H NMR spectrum, however, it was difficult to

interpret, possibly due to low sample concentration. Aromatic resonances in paramagnetic systems are often problematic.

Scheme 1.8: Salt metathesis reaction using UCl_4.

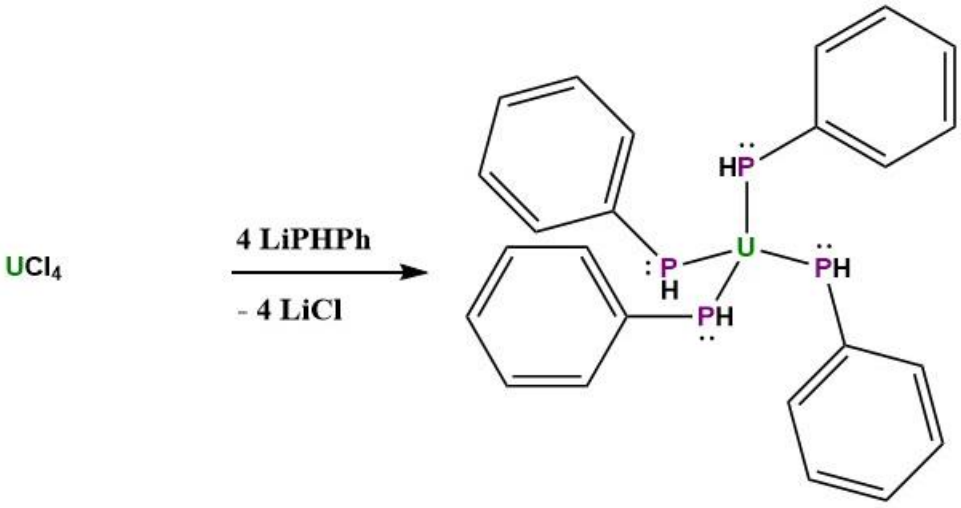

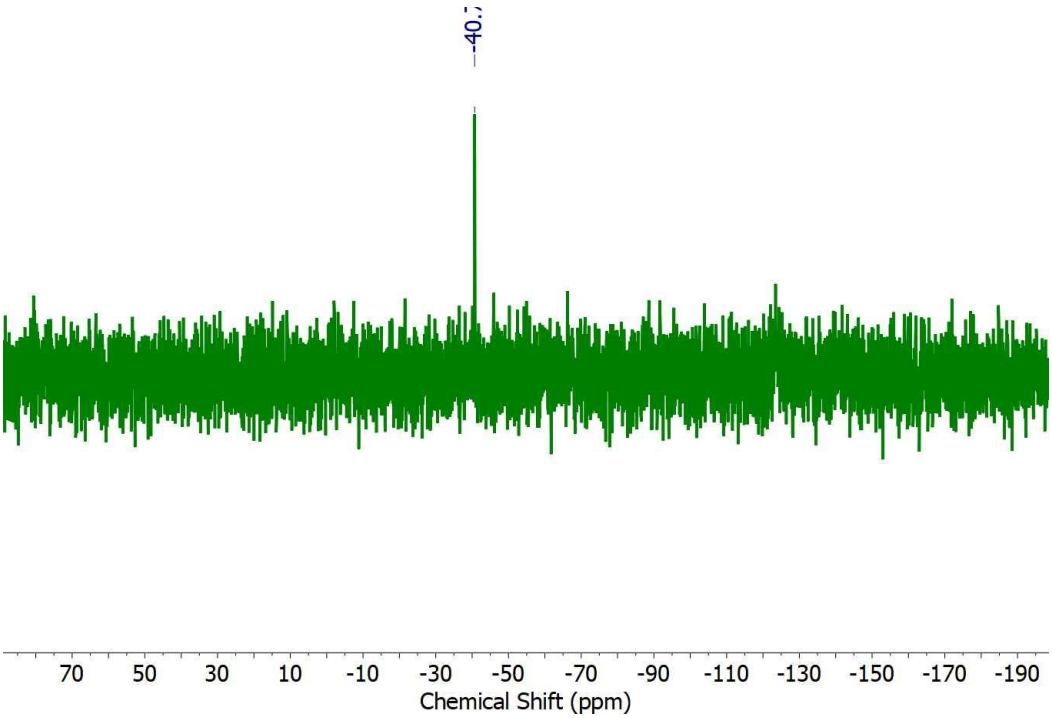

Figure 1.17: ^{31}P NMR spectrum for attempted synthesis of $U[PHPh]_4$.

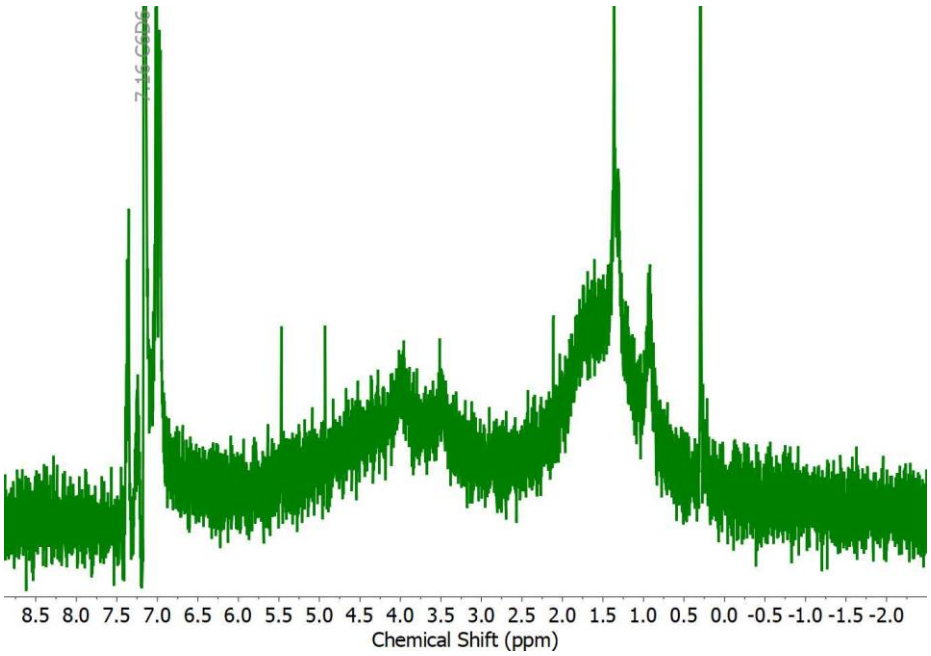

Figure 1.18: ^{1}H NMR spectrum for attempted synthesis of $U[PHPh]_4$.

A similar reaction was attempted with $ThCl_4(DME)_2$, with the intention of synthesizing $Th[PHPh]_4$. A THF solution of LiPHPh was added to a stirring colorless THF solution of $ThCl_4(DME)_2$. An immediate color change was observed from clear to dark blood-red. After work-up and NMR analysis, the only ^{31}P NMR resonance observed was at δ -123 ppm, which corresponds to H_2PPh. However, some interesting peaks were also observed between δ 3-5 ppm, which might correspond to the P-H protons of coordinated phosphido ligands, especially the resonance at δ 4.47 ppm. This reaction warrants further investigation in the future.

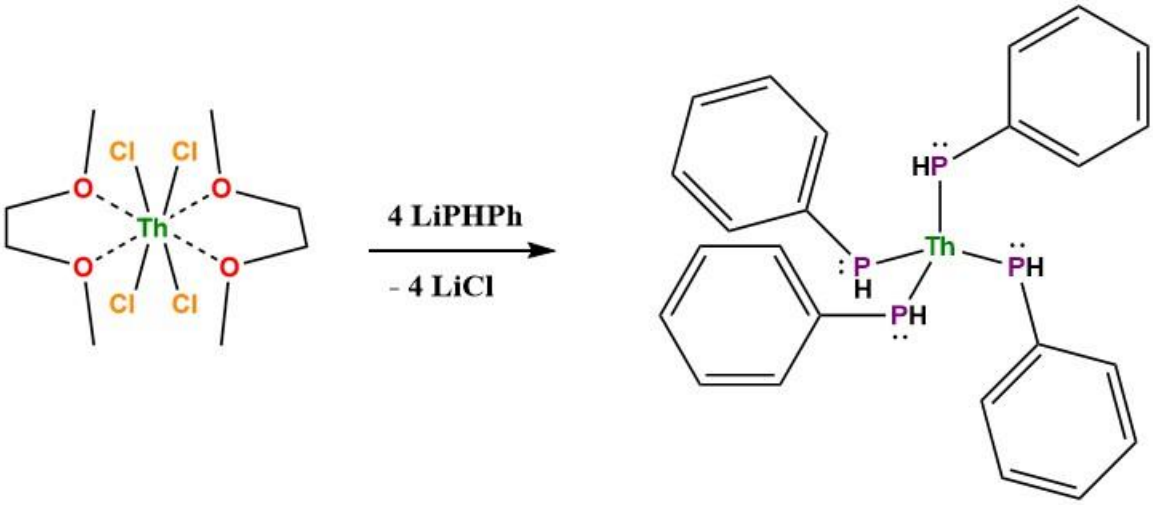

Scheme 1.9: Salt metathesis reaction using $ThCl_4(DME)_2$.

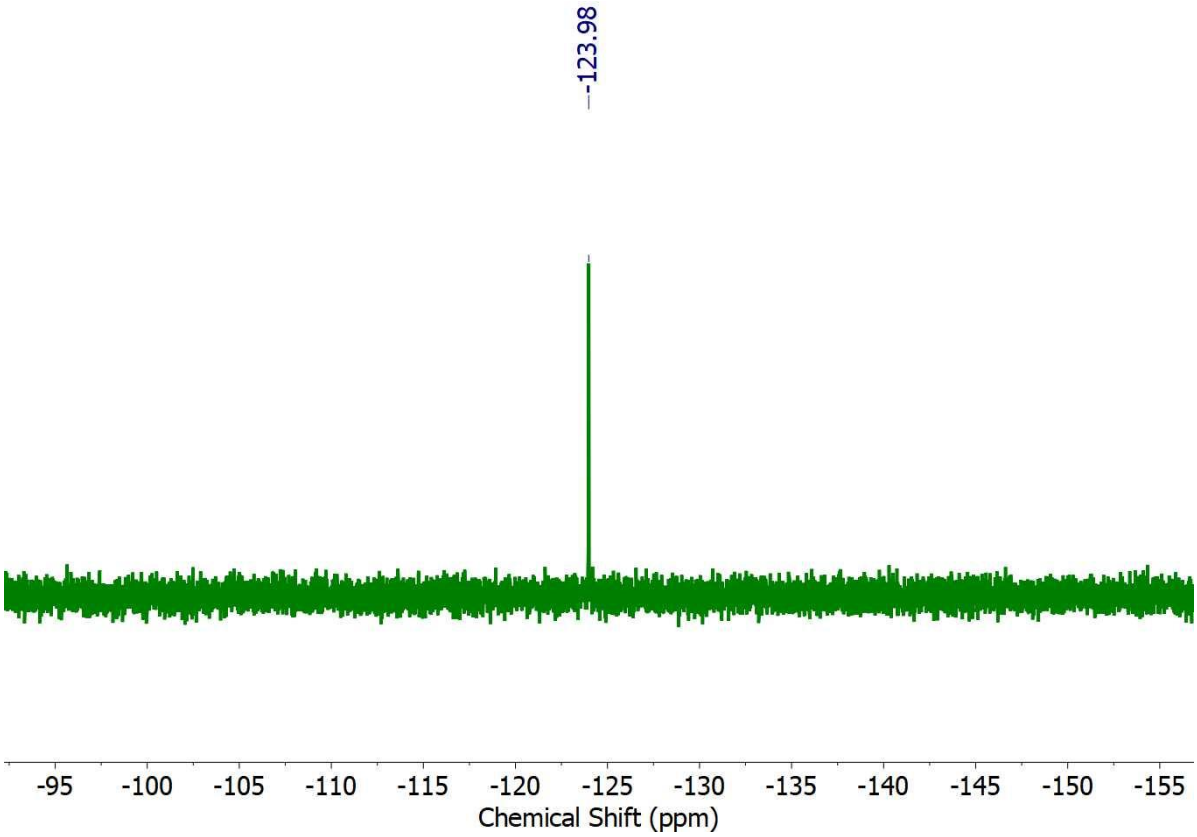

Figure 1.19: ^{31}P NMR spectrum for attempted synthesis of $Th[PHPh]_4$.

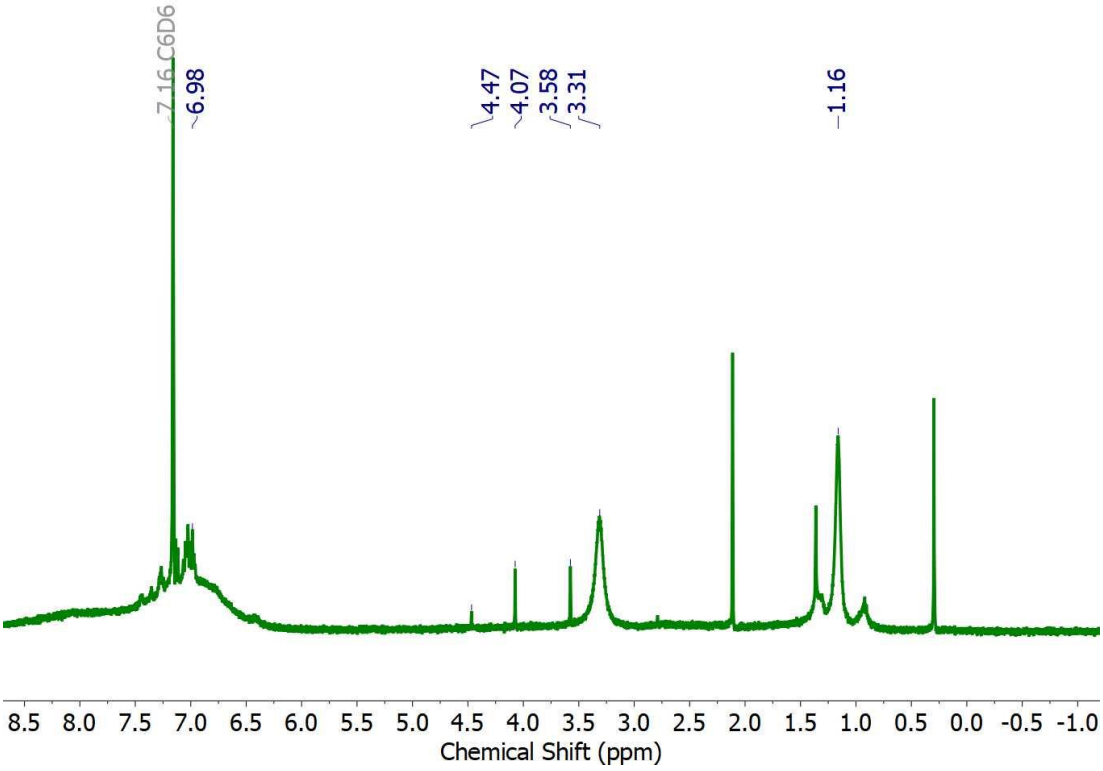

Figure 1.20: ^{1}H NMR spectrum for attempted synthesis of $Th[PHPh]_4$.

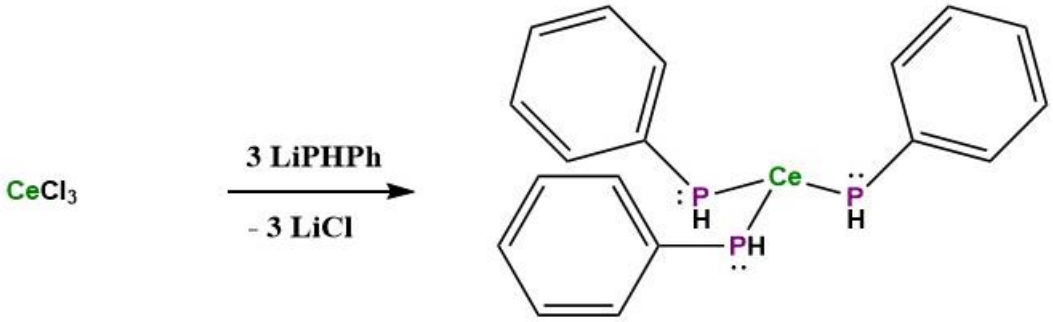

Scheme 1.10: Salt metathesis reaction using $CeCl_3$.

An attempt to generate a homoleptic Ce(III) phenylphosphido complex, $Ce[PHPh]_3$, was made using $CeCl_3$ and LiPHPh. Three equivalents of LiPHPh in THF was added to a stirring THF solution of $CeCl_3$. An immediate color change from colorless to deep-orange was observed. After work-up and NMR analysis, an extremely broad ^{31}P NMR resonance was observed at δ -134.84 ppm. This compares well to alkali-metal phenylphosphido complexes [96] and also the terminal $Th[PH_2]$ phosphide complex δ -144 ppm [117]. Extremely broad resonances were also observed in the ^{1}H spectrum at δ 7.61 ppm, δ 7.02 ppm, δ6.8 ppm, and δ 1.09 ppm. Furthermore, a resonance was also observed at δ 4.07 that could correspond to P-H protons. These are promising initial NMR results, and this exploratory reaction certainly warrants further investigation. High-symmetry, low coordinate models help simplify the complex problems encountered in studies of *f*-element electronic structures, and complexes with direct metal-phosphorus bonds can be used to study metal-ligand covalency using a dual ^{31}P NMR-PKβ XES approach, thereby allowing one to view the electronic structures of f-block metals through the eyes of phosphorus.

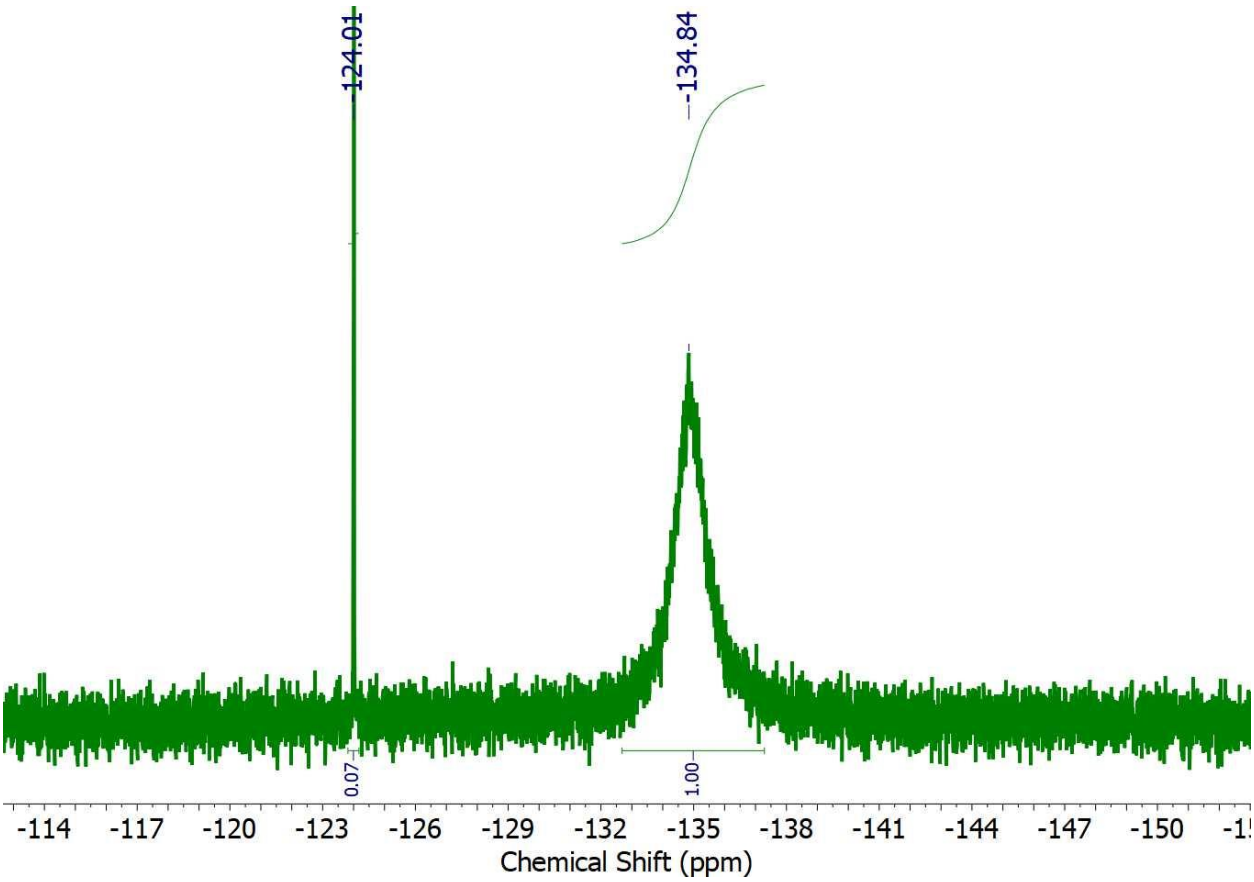

Figure 1.21: ^{31}P NMR spectrum for attempted synthesis of $Ce[PHPh]_3$.

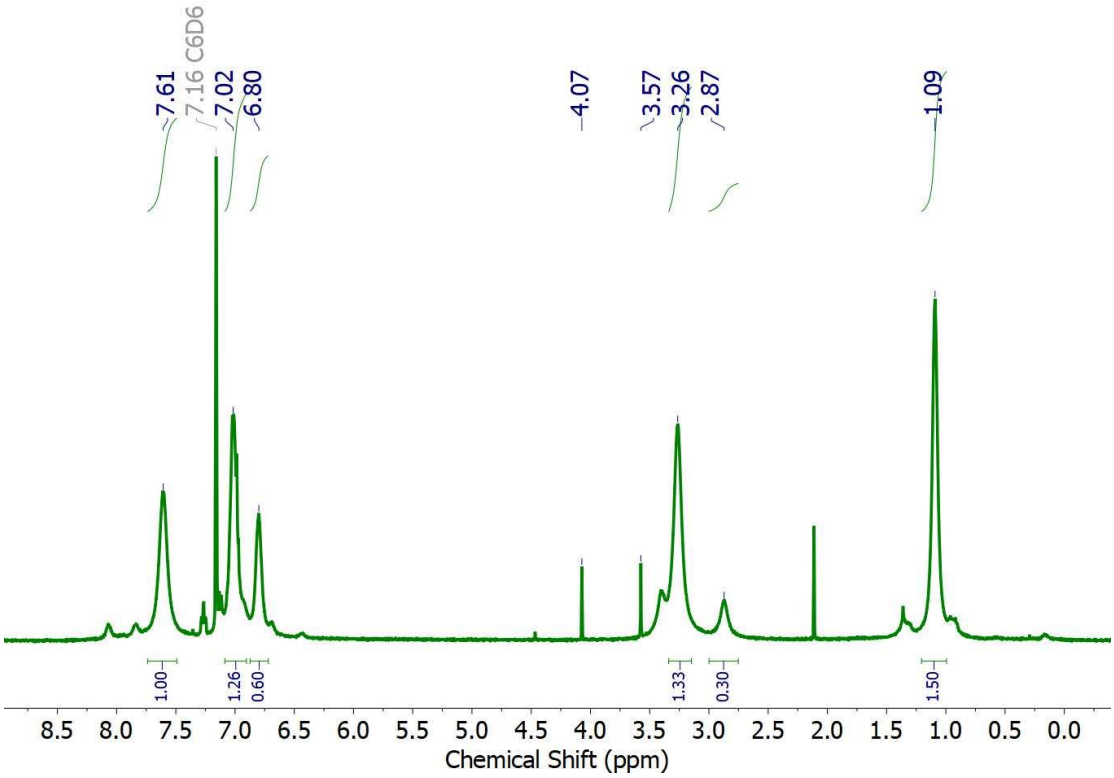

Figure 1.22: ^{1}H NMR spectrum for attempted synthesis of $Ce[PHPh]_3$.

Concluding Remarks and Future Opportunities

Our quest to synthesize uranium-phosphorus bonds began using salt metathesis as our initial synthetic strategy. Our primary goal was to synthesize uranium phosphido functionalities that could then be transformed into molecular phosphinidene and

phosphide functionalities. To date, a molecular complex featuring a terminal uranium-phosphide functionality (U≡P) continues to elude synthetic chemists. Actinide-pnictogenide chemistry remains in a very rudimentary stage of development, and an enormous amount of work remains to be done in order to attain the level of advancement that has been achieved in the chemistry of transition metals with anionic pnictogen-based ligands [91-113].

U[PHR][$N(SiMe_3)_2$]$_3$ and U[PR_2][$N(SiMe_3)_2$]$_3$ type complexes hold great potential for the synthesis of novel functionalities and likely will exhibit rich reactivity. U[PHR][$N(SiMe_3)_2$]$_3$ type complexes could be transformed to phosphinidenes with the formula U[PR][$N(SiMe_3)_2$]$_3$, which can provide unprecedented insight into the nature of the esoteric pentavalent oxidation state of uranium, as well as the paradigmatic inverse-trans influence [20, 114]. U[PR][$N(SiMe_3)_2$]$_3$-type complexes could ultimately yield U[P][$N(SiMe_3)_2$]$_3$. The synthesis and characterization of U[P][$N(SiMe_3)_2$]$_3$ would be considered a monumental achievement in molecular *f*-block chemistry, and would inspire chemists to synthesize isostructural complexes with neptunium, plutonium, and americium. The synthesis of molecular actinide complexes with direct bonds to phosphorus, coupled with the analysis of these bonds by NMR and X-ray spectroscopies, and QTAIM/TD-DFT calculations, could yield incredible insight into the fundamental nature of actinide-ligand orbital interactions. Such insight is vital for the optimization of *f*-element separations in the nuclear fuel cycle and for the implementation of the partition and transmutation strategy for the disposal of high-level nuclear waste.

References

[1] Morss, L., N.M. Edelstein, J. Fuger. 2006. *Chemistry of the Actinide and Transactinide Elements*. Springer, Berlin.

[2] Masterson, Robert E. 2017. *Nuclear Engineering Fundamentals: A Practical Perspective*. CRC Press, Boca Raton.

[3] Krane, Kenneth. 1988. *Introductory Nuclear Physics*. John Wiley & Sons, Inc., New Dehli.

[4] Cotton, Simon. 2006. *Lanthanide and Actinide Chemistry*. John Wiley & Sons, Inc., Chichester.

[5] Duttera, Michael R., Victor W. Day, and Tobin J. Marks. 1984. Organoactinide Phosphine/Phosphite Coordination Chemistry. Facile Hydride-Induced Dealkoxylation and the Formation of Actinide Phosphinidene Complexes. *Journal of the American Chemical Society* 106: 2907-2912.

[6] Hall, S. W., J. C. Huffman, M. M. Miller, L. R. Avens, C. J. Burns, D. S. J. Arney, A. F. England, and A. P. Sattelberger. 1993. Synthesis and Characterization of Bis(pentamethylcyclopentadienyl)uranium(IV) and -thorium(IV) Compounds Containing the Bis(trimethylsilyl)phosphide Ligand. *Organometallics* 12: 752-758.

[7] Arney, David S. J., R. Chris Schnabel, Brian C. Scott, and Carol J. Burns. 1996. Preparation of Actinide Phosphinidene Complexes: Steric Control of Reactivity. *Journal of the American Chemical Society* 118: 6780-6781.

[8] Nief, François. 1998. Complexes containing bonds between group 3, lanthanide or actinide metals and non-first-row main group elements (excluding halogens). *Coordination Chemistry Reviews* 178-180: 13-81.

[9] Gardner, Benedict M., Gábor Balázs, Manfred Scheer, Floriana Tuna, Eric J. L. McInnes, Jonathan McMaster, William Lewis, Alexander J. Blake, and Stephen T. Liddle. 2014. Triamidoamine-Uranium(IV)-Stabilized Terminal Parent Phosphide and Phosphinidene Complexes. *Angewandte Chemie International Edition* 53: 4484-4488.

[10] Zhang, Congcong, Guohua Hou, Guofu Zi, Wanjian Ding, and Marc D. Walter. 2019. An Alkali-Metal Halide Bridged Actinide Phosphinidiide Complex. *Inorganic Chemistry* 58: 1571-1590.

[11] Vilanova, Sean P. and Justin R. Walensky. 2018. Actinides: Pnictogen Complexes. *Encyclopedia of Inorganic and Bioinorganic Chemistry*. John Wiley & Sons, Ltd.

[12] Aspinall, Helen C., Donald C. Bradley, and Keith D. Sales. 1988. Diphenylphosphido Complexes of the Lanthanides: Reactions of Compounds $[Ln\{N(SiMe_3)_2\}_3]$ (Ln = La or Eu) or $[Ln\{N(SiMe_3)_2\}_3(Ph_3PO)]$ (Ln = La, Eu, or Y) with Ph_2PH to give $[Ln\{N(SiMe_3)_2\}_3(PPh_2)]$ or $[Ln\{N(SiMe_3)_2\}_3(PPh_2)(Ph_3PO)]]$. *Journal of the Chemical Society Dalton Transactions* 1988, 2211.

[13] Rabe, Gerd W., Jürgen Riede, and Annette Schier. 1995. Synthesis and Structural Characterization of the First Lanthanide Tris(phosphido) Complex:

Tm[P(SiMe$_3$)$_2$]$_3$(thf)$_2$. *Journal of the Chemical Society, Chemical Communications* 1995, 577.

[14] Katz, J.J. and E. Rabinowitch. 1951. *The Chemistry of Uranium*. McGraw-Hill Book Company, New York.

[15] Reynolds, L.T. and G. Wilkinson. 1956. π-Cyclopentadienyl Compounds of Uranium-IV and Thorium-IV. *Journal of Inorganic and Nuclear Chemistry* 2: 246-253.

[16] Karraker, D.G., J.A. Stone, E.R. Jones, Jr., and N. Edelstein. 1970. Bis(cyclooctatetraenyl)neptunium(IV) and Bis(cyclooctatetraenyl)plutonium(IV). *Journal of the American Chemical Society* 92:4841.

[17] Cleveland, J.M. 1970. *The Chemistry of Plutonium*. Gordon and Breach, Science Publishers, Inc., New York.

[18] Andersen, R.A. 1979. Tris((hexamethyldisilyl)amido)uranium(III): Preparation and Coordination Chemistry. *Inorganic Chemistry* 18:1507.

[19] Green, Jennifer C., Martin Payne, and Elaine A Seddon. 1982. He-I and He-II Photoelectron Studies of Bonding in Metal Silylamido-complexes. M[N(SiMe$_3$)$_2$]$_n$ (n = 1, 2, 3). *Journal of the Chemical Society Dalton Transactions* 1982: 887-892.

[20] Denning, R.G. 1992. Electronic Structure and Bonding in Actinyl Ions. *Structure and Bonding* 79:215.

[21] Edelmann, F.T. 1996. "Lanthanides and Actinides." Volume 6 In *Synthetic Methods of Organometallics and Inorganic Chemistry*, edited by W.A. Herrmann. Thieme, Stuttgart.

[22] Gourier, Didier, Daniel Caurant, Jean Claude Berthey, Christophe Boisson, and Michel Ephritikhine. 1997. Influence of the Nature of the Ligands on the Electronic Ground State of Organouranium(V) Compounds, Studied by Electron Paramagnetic Resonance. *Inorganic Chemistry* 36: 5931-5936.

[23] Denning, R.G., J.C. Green, T.E. Hutchings, C. Dallera, A. Tagliaferri, K. Giarda, N.B. Brookes, and L. Braicovich. 2002. Covalency in the uranyl ion: A polarized x-ray spectroscopic study. *Journal of Chemical Physics* 117(17): 8008-8020.

[24] Hayton, Trevor W., James M. Boncella, Brian L. Scott, Philip D. Palmer, Enrique R. Batista, and P. Jeffrey Hay. 2005. Synthesis of Imido Analogs of the Uranyl Ion. *Science* 310: 1941-1943.

[25] Kaltsoyannis, N., P. J. Hay, J. Li, J.-P. Blaudeau, B.E. Bursten. 2006. "Theoretical Studies of the Electronic Structure of Compounds of the Actinide Elements." In *The Chemistry of the Actinide and Transactinide Elements*, edited by L.R. Morss, N.M. Edlestein, J. Fuger, pp. 1893-2012. Springer, Berlin.

[26] Denning, Robert G. 2007. Electronic Structure and Bonding in Actinyl Ions and their Analogs. *Journal of Physical Chemistry A* 111: 4125-4143.

[27] Liddle, Stephen T. 2009. Non-traditional ligands in f-block chemistry. *Proceedings of the Royal Society A* 465(2106): 1673-1700.

[28] Kozimor S. A., P. Yang, E. R. Batista, K. S. Boland, C. J. Burns, D. L. Clark, S. D. Conradson, R. L. Martin, M. P. Wilkerson, and L. E. Wolfsberg. 2009. Trends in Covalency for d- and f-Element Metallocene Dichlorides Identified Using Chlorine K-Edge X-ray Absorption Spectroscopy and Time-Dependent Density Functional Theory *Journal of the American Chemical Society* 131:12125.

[29] Tassell, M.J. and N. Kaltsoyannis. 2010. Covalency in AnCp4 (An = Th–Cm): a comparison of molecular orbital, natural population and atoms-in-molecules analyses. *Dalton Transactions* 39: 6719.

[30] Thomson, Robert K., Thibault Cantat, Brian L. Scott, David E. Morris, Enrique R. Batista, and Jaqueline L. Kiplinger. 2010. Uranium azide photolysis results in C-H bond activation and provides evidence for a terminal uranium nitride. *Nature Chemistry* 2: 723-729.

[31] Hayton, Trevor W. 2010. Metal-ligand multiple bonding in uranium: structure and reactivity. *Dalton Transactions* 39: 1145-1158.

[32] Fortier, Skye, Guang Wu, and Tevor Hayton. 2010. Synthesis of a Nitrido-Substiuted Analogue of the Uranyl Ion, $[N{=}U{=}O]^{+}$. *Journal of the American Chemical Society* 132: 6888-6889.

[33] Kirker, I. and N. Kaltsoyannis. 2011. Does covalency really increase across the 5f series? A comparison of molecular orbital, natural population, spin and electron density analyses of AnCp3 (An = Th–Cm; Cp = η5-C5H5). *Dalton Transactions* 40: 124.

[34] Monreal, M.J., R.K. Thomson, T. Cantat, N.E. Travia, B.L. Scott, J.L. Kiplinger. 2011. $UI_4(1,4\text{-dioxane})_2$, $[UCl_4(1,4\text{-dioxane})]_2$, and $UI_3(1,4\text{-dioxane})_{1.5}$: Stable and Versatile Starting Materials for Low- and High-Valent Uranium Chemistry. *Organometallics* 30:2031.

[35] Fortier, Skye, Justin R. Walensky, Guang Wu, and Trevor Hayton. 2011. Synthesis of a Phosphorano-Stabilized U(IV)-Carbene via One-Electron Oxidation of a U(III)-Ylide Adduct. *Journal of the American Chemical Society* 133: 6894-6897.

[36] Kaltsoyannis, Nikolas. 2012. Does Covalency Increase or Decrease across the Actinide Series? Implications for Minor Actinide Partitioning. *Inorganic Chemistry* 52: 3407-3413.

[37] Minasian S. G., J. M. Keith, E. R. Batista, K. S. Boland, D. L. Clark, S. D. Conradson, S. A. Kozimor, R. L. Martin, D. E. Schwarz, D. K. Shuh, G. L. Wagner, M. P. Wilkerson, L. E. Wolfsberg, and P. Yang. 2012. Determining Relative f and d Orbital Contributions to M–Cl Covalency in MCl_6^{2-} (M = Ti, Zr, Hf, U) and UOCl5– Using Cl K-Edge X-ray Absorption Spectroscopy and Time-Dependent Density Functional Theory. *Journal of the American Chemical Society* 134:5586.

[38] Fortier, S., J.L. Bown, N. Kaltsoyannis, G. Wu, T.W. Hayton. 2012. Synthesis, Molecular and Electronic Structure of $U^{V}(O)[N(SiMe_3)_2]_3$. *Inorganic Chemistry* 51: 1625.

[39] Brown, Jessie L., Skye Fortier, Richard A. Lewis, Guang Wu, and Revor W. Hayton. 2012. A Complete Family of Terminal Uranium Chalcogenides, $[U(E)(N\{SiMe_3\}_2)_3]^-$ (E = O, S, Se, Te). *Journal of the American Chemical Society* 134: 15468-15475.

[40] Jones, M.B. and A.J. Gaunt. 2012. Recent Developments in Synthesis and Structural Chemistry of Nonaqueous Actinide Complexes. *Chemical Reviews* 113:1137.

[41] Neidig, Michael L., David L. Clark, and Richard L. Martin. 2013. Covalency in f-element complexes. *Coordination Chemistry Reviews* 257: 394-406.

[42] King, D.M., F. Tuna, E.J.L. McInnes, J. McMaster, W. Lewis, A.J. Blake, S.T. Liddle. 2013. Isolation and characterization of a uranium (VI)-nitride triple bond. *Nature Chemistry* 5:482.

[43] Lewis, Andrew J., Patrick J. Carroll, and Eric J. Schelter. 2013. Reductive Cleavage of Nitrite to Form Terminal Uranium Mono-Oxo Complexes. *Journal of the American Chemical Society* 135: 511-518.

[44] Lukens, Wayne W., Norman M. Edelstein, Nicola Magnani, Trevor W. Hayton, Skye Fortier, and Lani A. Seaman. 2013. Quantifying the σ and π Interactions

between U(V) f Orbitals and Halide, Alkyl, Alkoxide, Amide, and Ketimide Ligands. *Journal of the American Chemical Society* 135: 10742-10754.

[45] Hayton, Trevor W. 2013. Recent Developments in actinide-ligand multiple bonding. *Chemical Communications* 49: 2956-2973.

[46] Smiles, Danil E., Guang Wu, and Trevor W. Hayton. 2014. Synthesis of Terminal Monochalcogenide and Dichalcogenide Complexes of Uranium Using Polychalcogenides, $[E_n]^{2-}$ (E = Te, n = 2; E = Se, n = 4), as Chalcogen Atom Transfer Reagents. *Inorganic Chemistry* 53: 10240-10247.

[47] Smiles, Danil E., Guang Wu, and Trevor W. Hayton. 2014. Reversible Chalcogen-Atom Transfer to a Terminal Uranium Sulfide. *Inorganic Chemistry* 53: 12683-12685.

[48] Anderson, Nickolas H., Samuel O. Odoh, Yiyi Yao, Ursula J. Williams, Brian A Schaefer, John J. Kiernicki, Andrew J. Lewis, Mitchell D. Goshert, Phillip E. Fanwick, Eric J. Schelter, Justin R. Walensky, Laura Gagliardi, and Suzanne C. Bart. 2014. Harnessing redox activity for the formation of uranium tris(imido) compounds. *Nature Chemistry* 6: 919-926.

[49] Kaltsoyannis, N. and A. Kerridge. 2014. "Chemical Bonding of Lanthanides and Actinide." In *The Chemical Bond*, edited by G. Frenking and S. Shaik, pp. 337-355. Wiley-VCH, Marburg.

[50] Smiles, Danil E., Guang Wu, and Trevor W. Hayton. 2014. Synthesis of Uranium-Ligand Multiple Bonds by Cleavage of a Trityl Protecting Group. *Journal of the American Chemical Society* 136: 96-99.

[51] Tobin, J. G., S.-W. Yu, R. Qiao, W.L. Yang, C.H. Booth, D.K. Shuh, A.M. Duffin, D. Sokaras, D. Nordlund, and T.-C. Weng. 2015. Covalency in oxidized uranium. *Physical Review B* 92: 045130.

[52] Smiles, Danil E., Guang Wu, and Trevor Hayton. 2015. Reactivity of $[U(CH_2SiMe_2NSiMe_3)(NR_2)_2]$ (R = $SiMe_3$) with elemental chalcogens: towards a better understanding of chalcogen atom transfer in the actinides. *New Journal of Chemistry* 39: 7563-7566.

[53] Wu, Qun-Yan, Jian-Hui Lan, Cong-Zhi Wang, Yu-Liang Zhao, Zhi-Fang Chai, and Wei-Qun Shi. 2015. Terminal U≡E (E = N, P, As, Sb, and Bi) Bonds in Uranium Complexes: A Theoretical Perspective. *Journal of Physical Chemistry A*: 119: 922-930.

[54] Dolg, M. 2015. *Computational Methods in Lanthanide and Actinide Chemistry*. Wiley, West Sussex.

[55] Brown, Jessie L., Enrique R. Batista, James M. Boncella, Andrew J. Gaunt, Sean D. Reilly, Brian L. Scott, and Neil C. Tomson. 2015. A Linear *trans*-Bis(imido) Neptunium(V) Actinyl Analog: $Np^{V}(NDipp)_2(^{t}Bu_2bipy)_2Cl$ (Dipp = 2,6-$^{i}Pr_2C_6H_3$). *Journal of the American Chemical Society* 137: 9583-9586.

[56] Anderson, Nickolas H., Haolin Yin, John J. Kiernicki, Phillip E. Fanwick, Eric J. Schelter, and Suzanne C. Bart. 2015. Investigation of Uranium Tris(imido) Complexes: Synthesis, Characterization, and Reduction Chemistry of $[U(NDIPP)_3(thf)_3]$. *Angewandte Chemie International Edition* 54: 9386-9389.

[57] Smiles, Danil E., Guang Wu, Peter Hrobárik, and Trevor W. Hayton. 2016. Use of ^{77}Se and NMR Spectroscopy to Probe Covalency of the Actinide-Chalcogen Bonding in $[Th(E_n)\{N(SiMe_3)_2\}_3]^-$ (E = Se, Te; *n* = 1, 2) and Their Oxo-Uranium(VI) Congeners. *Journal of the American Chemical Society* 138: 814-825.

[58] Kerridge, Andrew. 2017. Quantification of f-element covalency through analysis of the electron density: insights from simulation. *Chemical Communication* 53: 6685-6695.

[59] Vitova, T., I Pidchenko, D. Fellhauer, P.S. Bagus, Y. Joly, T. Pruessmann, S. Bahl, E. Gonzalez-Robles, J. Rothe, M. Altmaier, M.A. Denecke, and H. Geckeis. 2017. The role of the 5f valence orbitals of early actinides in chemical bonding. *Nature Communications* 8: 16053.

[60] Dognon, Jean-Pierre. 2017. Electronic structure theory to decipher the chemical bonding in actinide systems. *Coordination Chemistry Reviews* 344: 150-162.

[61] Bart, Suzanne and Eric J. Schelter. 2017. The Vibrancy and Variety of Modern f-Element Organometallic Chemistry. *Organometallics* 36: 4507-4510.

[62] Formanuik, Alasdair, Ana-Maria Ariciu, Fabrizio Ortu, Reece Beekmeyer, Andrew Kerridge, Floriana Tuna, Eric J. L. McInnes, and David P. Mills. 2017. Actinide covalency measured by pulsed electron paramagnetic resonance spectroscopy. *Nature Chemistry* 9: 578-583.

[63] Tobin, J. G., S.-W. Yu, R. Qiao, W.L. Yang, and D.K. Shuh. 2018. Probing covalency with oxidant K edge x-ray absorption spectroscopy of UF_4 and UO_2. *Journal of Vacuum Science & Technology A* 36: 061403.

[64] Lu, Erli, Saira Sajjad, Victoria E.J. Berryman, Ashley J. Wooles, Nikolas Kaltsoyannis, and Stephen Liddle. 2019. Emergence of the structure-directing role of f-orbital overlap-driven covalency. *Nature Communications* 10: 634.

[65] Mullane, Kimberly C., Peter Hrobárik, Thibault Cheisson, Brian C. Manor, Patrick J. Carroll, and Eric J. Schelter. 2019. ^{13}C NMR Shifts as an Indicator of U-C Bond Covalency in Uranium(VI) Acetylide Complexes: An Experimental and Computational Study. *Inorganic Chemstry* 58: 4152-4163.

[66] Wrobleski, Debra A., Robert R. Ryan, Harvey J. Wasserman, Kenneth V. Salazar, Robert T. Paine, and David C. Moody. 1986. Synthesis and Characterization of Bis(diphenylphosphido)bis(pentamethylcyclopentadienyl)-thorium(IV), $[(\eta^5\text{-}C_5(CH_3)_5]_2Th(PPh_2)_2$.

[67] Ritchey, J.M., A.J. Zozulin, D.A. Wrobleski, R.R. Ryan, H.J. Wasserman, D.C. Moody, and R.T. Painei. 1985. An Organothorium-Nickel Phosphido Complex

with a Short Th-Ni Distance. The Structure of $Th(\eta^5\text{-}C_5(CH_3)_5)_2(\mu\text{-}PPh_2)_2Ni(CO)_2$. *Journal of the American Chemical Society* 107: 501.

[68] Hay, P.J., R.R. Ryan, K.V. Salazar, D.A. Wrobleski, and A.P. Sattleberger. 1986. Synthesis and X-ray Structure of $(C_5Me_5)_2Th(\mu\text{-}PPh_2)_2Pt(PMe_3)$: A Complex with a Thorium-Platinum Bond. *Journal of the American Chemical Society* 108: 313.

[69] Behrle, Andrew C., Ludovic Castro, Laurent Maron, and Justin R. Walensky. 2015. Formation of a Bridging Phosphinidene Thorium Complex. *Journal of the American Chemical Society* 137: 14846-14849.

[70] Garner, Mary E. and John Arnold. 2017. Reductive Elimination of Diphosphine from a Thorium-NHC-Bis(phosphide) Complex. *Organometallics* 36: 4511.

[71] Garner, Mary E., Bernard F. Parker, Stephan Hohloch, Robert G. Bergman, and John Arnold. 2017. Thorium Metallacycle Facilitates Catalytic Alkyne Hydrophosphination. *Journal of the American Chemical Society* 139: 12935.

[72] Edwards, P.G, M Harman, M.B. Hursthouse, and J.S. Parry. 1992. The synthesis and crystal structure of the thorium tetraphosphido complex, $Th[P(CH_2CH_2PMe_2)_2]_4$, and actinide complex with only metal-phosphorus ligand bonds. *Journal of the Chemical Society*, *Chemical Communications* 1992: 1469.

[73] Gardner, Benedict M., Gábor Balázs, Manfred Scheer, Floriana Tuna, Eric J. L. McInnes, Jonathan McMaster, William Lewis, Alexander J. Blake, and Stephen T.

Liddle. 2015. Triamidoamine uranium(IV)-arsenic complexes containing one-, two- and threefold U-As bonding interactions. *Nature Chemistry* 7: 582-590.

[74] Vilanova, Sean P., Michael L. Tarlton, Charles L. Barnes, and Justin R. Walensky. 2018. Double insertion of benzophenone into thorium-phosphorus bonds. *Journal of Organometallic Chemistry* 857: 159-163.

[75] Li, Tianshu, Sabrina Kaercher, and Peter W. Roesky. 2014. Synthesis, structure and reactivity of rare-earth metal complexes containing anionic phosphorus ligands. *Chemical Society Reviews* 43: 42-57.

[76] Rabe, Gerd W. and Joseph W. Ziller. 1995. Phosphido Complexes of the Lanthanides. Synthesis and X-ray Crystal Structure Determination of a Tris(phosphido) Species of Neodymium: $Nd[P(SiMe_3)_2]_3(thf)_2$. *Inorganic Chemistry* 34: 5378-5379.

[77] Masuda, Jason D., Kimberly C. Jantunen, Oleg V. Ozerov, Kevin J. T. Noonan, Derek P. Gates, Brian L. Scott, and Jaqueline L. Kiplinger. 2008. A Lanthanide Phosphinidene Complex: Synthesis, Structure, and Phospha-Wittig Reactivity. *Journal of the American Chemical Society* 130: 2408-2409.

[78] Shriver, D.F. 1969. *The Manipulation of Air-sensitive Compounds*. Robert E. Krieger Publishing Company, Malabar.

[79] Jolly, William L. 1970. *The Synthesis and Characterization of Inorganic Compounds*. Prentice-Hall, Inc., Englewood Cliffs.

[80] Barton, Charles J. 1963. Glove Box Techniques. Chapter 4 in *Technique of Inorganic Chemistry* by C.J. Barton, W.W. Brandt, J.F. Hamilton, and D.C. Stewart, edited by Hans B. Jonassen and Arnold Weissberger. Interscience Publishers, New York.

[81] Avens, L., S.G. Bott, D.L. Clark, A.P. Sattelberger, J.G. Watkin, and B.D. Zwick. 1994. A Convenient Entry into Trivalent Actinide Chemistry: Synthesis and Characterization of $AnI_3(THF)_4$ and $An[N(SiMe_3)_2]_3$ (An = U, Np, Pu) *Inorganic Chemistry* 33: 2248-2256.

[82] Taylor, R.C., R. Kolodny, and D.B. Walters. 1973. An Improved Method for the Preparation of Phenylphosphine and a Procedure for the Removal of the Toxic Vapors Produced. *Synthesis and Reactivity in Inorganic and Metal-Organic Chemistry* 3(2): 175-179.

[83] Cantat, Thibault, Brian L. Scott, and Jaqueline L. Kiplinger. 2010. Convenient access to the anhydrous thorium tetrachloride complexes $ThCl_4(DME)_2$, $ThCl_4(1,4\text{-dioxane})_2$ and $ThCl_4(THF)_{3.5}$ using commercially available and inexpensive starting materials. *Chemical Communications* 46: 919-921.

[84] Kiplinger, Jaqueline L., David E. Morris, Brian L. Scott, and Carol J. Burns. 2002. Convenient Synthesis, Structure, and Reactivity of $(C_5Me_5)U(CH_2C_6H_5)_3$: A Simple Strategy for the Preparation of Monopentamethylcyclopentadienyl Uranium(IV) Complexes. *Organometallics* 21(26): 5978-5982.

[85] Turner, Howard W., Richard A. Andersen, Allan Zalkin, and David H. Templeton. 1979. Chloro-, Methyl-, and (Tetrahydroborato)tris((hexamethyldisilyl)amido)thorium(IV) and -uranium(IV). Crystal Structure of (Tetrahydroborato)tris((hexamethyldisilyl)amido)thorium(IV). *Inorganic Chemistry* 18(5): 1221.

[86] McCullough, Laughlin G., Howard W. Turner, Richard A. Andersen, Allan Zalkin, and David H. Templeton. 1981. Preparation and Crystal Structure of the 1,2-Dimethoxyethane Complex of Bis[bis(trimethylsilyl)amido]dichlorouranium(IV). *Inorganic Chemistry* 20: 2869-2871.

[87] Colquhoun, I. J., B.C.E. McFarlane and W. McFarlane. 1983. Structures in Solution of Organophosphorus – Lithium Compounds. *Phosphorus and Sulfur* 18: 61-64.

[88] Blake, P.C., E. Hey, M.F. Lappert, J.L. Atwood, and H.J. Zhang. 1988. Bis(trimethylsilyl)phosphide complexes. *Journal of Organometallic Chemistry* 353: 307-314.

[89] Karmel, Isabell S.R., Natalia Fridman, Matthias Tamm, and Moris S. Eisen. 2014. Mono(imidazoline-2-iminato) Actinide Complexes: Synthesis and Application in the Catalytic Dimerization of Aldehydes. *Journal of the American Chemical Society* 136: 17180-17192.

[90] Bell, Nicola L., Laurent Maron, and Polly L. Arnold. 2015. Thorium Mono- and Bis(imido) Complexes Made by Reprotonation of *cyclo*-Metalated Amides. *Journal of the American Chemical Society* 137: 10492-10495.

[91] Wildman, Elizabeth P., Gábor Balázs, Ashley J. Wooles, Manfred Scheer, and Stephen T. Liddle. 2016. Thorium-Phosphorus triamidoamine complexes containing Th-P single- and multiple-bond interactions. *Nature Communications* 7: 12884.

[92] Rookes, Thomas M., Elizabeth P. Wildman, Gábor Balázs, Benedict M. Gardner, Ashley J. Wooles, Matthew Gregson, Floriana Tuna, Manfred Scheer, and Stephen T. Liddle. 2018. Actinide-Pnictide (An-Pn) Bonds Spanning Non-Metal, Metalloid, and Metal Combination (An = U, TH; Pn = P, As, Sb, Bi). *Angewandte Chemie International Edition* 57: 1332-1336.

[93] Lammertsma, Koop. 2003. Phosphinidenes. *Topics in Current Chemistry* 229: 95-119.

[94] Johnson, Brian P., Gábor Balázs, and Manfred Scheer. 2004. Complexes with a Metal-Phosphorus Triple Bond. *Topics in Current Chemistry* 232: 1-23.

[95] Johnson, Brian P., Gábor Balázs, and Manfred Scheer. 2005. Low-coordinate E_1 ligand complexes of Group 15 elements – A developing area. *Coordination Chemistry Reviews* 250: 1178-1195.

[96] Uhlig, F., S. Gremler, M. Dargatz, M. Scheer, and E. Herrmann. 1991. Bis(trimethylsilyl)phosphide der Alkalimetalle. *Zeitschrift für Anorganische und Allgemeine Chemie* 606: 105-108.

[97] Cowley, Alan H. 1997. Terminal Phosphinidene and Heavier Congeneric Complexes. The Quest is Over. *Accounts of Chemical Research* 30: 445-451.

[98] Masuda, Jason D., Kimberly C. Jantunen, Oleg V. Ozerov, Kevin J. T. Noonan, Derek P. Gates, Brian L. Scott, and Jaqueline L. Kiplinger. 2008. A Lanthanide Phosphinidene Complex: Synthesis, Structure, and Phospha-Wittig Reactivity. *Journal of the American Chemical Society* 130: 2408-2409.

[99] Goel, Subhash C., Michael A. Matchett, Dokun Cha, Michael Y. Chiang, and William E. Buhro. 1993. Homoleptic Disilylphosphido Complexes $\{M[P(SiR_3)_2]_x\}_n$ and their Use as Precursors to Phosphide Semiconductor Nanoclusters. *Phosphorus, Sulfur, and Silicon* 76: 289-292.

[100] Schumann, Herbert, Lutz Rösch, and Walter Schmidt-Fritsche. 1977. Tetrakis(trimethylgermanyl)diphosphin. *Journal of Organometallic Chemistry* 140: C21-C22.

[101] Schumann, Herbert and Heinz-Jürgen Kroth. 1971. Organometallphosphin-substituierte Übergangsmetallkomplexe XIII. Zweikernige Tetracarbonylmangan-organometallphosphin-komplexe. *Journal of Organometallic Chemistry* 32: C47-C48.

[102] Cummins, Christopher C. 2006. Terminal, Anionic Carbide, Nitride, and Phosphide Transition-Metal Complexes as Synthetic Entries to Low-Coordinate Phosphorus Derivatives. *Angewandte Chemie International Edition* 45: 862-870.

[103] Rankin, Matthew A. and Christopher C. Cummins. 2012. Terminal phosphinidene formation *via* tantalaziridine complexes. *Dalton Transactions* 41: 9615.

[104] Waterman, Rory, and T. Don Tilley. 2011. Terminal hafnium phosphinidene complexes and phosphinidene ligand exchange. *Chemical Science* 2: 1320-1325.

[105] Waterman, Rory, and T. Don Tilley. 2006. Terminal stibinidene ligands. Generation of CpCp*Hf=Sb(dmp) and trapping reactions with PMe_3 and 2-butyne. *Chemical Communications* 2006, 4030-4032.

[106] Blaurock, Steffen, and Evamarie Hey-Hawkins. 2002. Syntheses, Crystal Structures and Reactivity of Organometallic Tantalum(IV) Phosphinidene Complexes: *trans*-[{Cp*TaCl(μ-PR)}$_2$] (Cp* = C_5Me_5, R = Cy, *t*Bu, Ph), *cis*- and *trans*-[{Cp*TaCl(μ-PMes)}$_2$] (Mes = =2,4,6-$Me_3C_6H_2$) and *cis*-[{Cp'TaCl(μ-PMes)}$_2$] (Cp' = C_5H_4Me). *European Journal of Inorganic Chemistry* 2002, 2975.

[107] Balázs, Gábor, Marek Sierka, and Manfred Scheer. 2005. Antimony-Tungsten Triple Bond: A Stable Complex with a Terminal Antimony Ligand. *Angewandte Chemie International Edition* 44: 4920-4924.

[108] Scheer, Manfred, Jan Müller, and Marco Häser. 1996. Complexes Containing Phosphorus and Arsenic as Terminal Ligands. *Angewandte Chemie International Edition* 35(21): 2492-2496.

[109] Bredeau, Stéphane, Gereon Altenhoff, Klaus Kunz, Steve Döring, Stefan Grimme, Gerald Kehr, and Gerhard Erker. 2004. Synthesis of Alkylidene-Bridged Cp/Phosphido Group 4 Metal Complexes – Precursors of the "(CpCPR)M – Constrained-Geometry" Catalyst Family. *Organometallics* 23(8): 1836-1844.

[110] Legzdins, Peter, Kevin J. Ross, Stephan F. Sayers, and Steven J. Rettig. 1997. Different Modes of Reaction of Lithium Phosphides with Cp*M(NO)(X)Cl Complexes of Molybdenum and Tungsten. *Organometallics* 16(2): 190-196.

[111] Laplaza, Catalina E., William M. Davis, and Christopher C. Cummins. 1995. A Molybdenum – Phosphorus Triple Bond: Synthesis, Structure, and Reactivity of the Terminal Phosphido (P^{3-}) Complex [Mo(P)$(NRAr)_3$]. *Angewandte Chemie International Edition* 34(18): 2042-2044.

[112] Zanetti, Nadia C., Richard R. Schrock, and William M. Davis. 1995. Monomeric Molybdenum and Tungsten Complexes That Contain a Metal – Phosphorus Triple Bond. *Angewandte Chemie International Edition* 34(18): 2044-2046.

[113] Mösch-Zanetti, Nadia C., Richard R. Schrock, William M. Davis, Klaus Wanninger, Scott W. Seidel, and Myra B. O'Donoghue. 1997. Triamidoamine Complexes of

Molybdenum and Tungsten That Contain Metal – E (E = N, P, and As) Single, Double, or Triple Bonds. *Journal of the American Chemical Society* 119: 11037-11048.

[114] Gregson, Matthew, Erli Lu, David P. Mills, Floriana Tuna, Eric J.L. McInnes, Christoph Hennig, Andreas C. Scheinost, Jonathan McMaster, William Lewis, Alexander J. Blake, Andrew Kerridge, and Stephen T. Liddle. 2017. The inverse-*trans*-influence in tetravalent lanthanide and actinide *bis*(carbene) complexes. *Nature Communications* 8: 14137.

[115] Waterman, Rory. 2007. Selective Dehydrocoupling of Phosphines by Triamidoamine Zirconium Catalysts. *Organometallics* 26: 2492-2494.

[116] Kühl, Olaf. 2008. *Phosphorus-31 NMR Spectroscopy: A Concise Introduction for the Synthetic Organic and Organometallic Chemist.* Springer, Berlin.

[117] Wildman, Elizabeth P., Gábor Balázs, Ashley J. Wooles, Manfred Scheer, and Stephen T. Liddle. 2016. Thorium-phosphorus triamidoamine complexes containing Th-P single- and multiple-bond interactions. *Nature Communications* 7: 12884.

[118] Issleib, K. and R. Kümmel. 1965. Zur P-H- und As-H-Acidität Primärer und Sekundärer Phosphine bzw. Arsine. *Journal of Organometallic Chemistry* 3: 84-91.

Chapter 2

Synthesis of Uranium-, Thorium, and Cerium Phosphinimide Complexes

Introduction

In this chapter, the synthesis and NMR spectroscopy of a uranium phosphinimide complex, $U[NPR_3][N(SiMe_3)_2]_3$ (R = *t*-butyl) is reported. Since the advent of organoactinide chemistry in the mid-twentieth century [1, 2], a great amount of knowledge has been attained regarding the chemical behavior of uranium [3-10]. However, there remains a considerable gap in knowledge concerning the bonding interactions in inorganic and organometallic uranium complexes [11]. This is especially true with respect to the fundamental, underlying principles governing separation processes in the nuclear fuel cycle [10]. A reoccurring theme in organoactinide chemistry is the study of the degree of *f*-orbital participation in uranium-element bonding [1-11]. A greater understanding of the nature of bonding interactions in uranium complexes will facilitate further exploitation of the properties of uranium, and lead to the successful application of this knowledge in the fields of *f*-element separation science [12-14] and catalysis [15,16].

A fruitful approach for studying actinide orbital mixing (covalency) is through the synthesis and characterization of metal-ligand multiple bonds [17-41], since these bonds

are expected to have significant π-interactions. In order to synthesize complexes with metal-element multiple bonds, precursor complexes with bulky ancillary ligands are often synthesized to limit access to the metal center to a localized region. Over the past several decades, cyclopentadienyl (Cp) ligands have been the workhorse for accessing uranium-element multiple bonds [25, 31]. This work focuses on the synthesis and characterization of uranium complexes bearing bulky phosphinimide ligands. Phosphinimide ligands which have steric and electronic properties that are comparable to Cp ligands. However, the steric bulk of phosphinimide ligands is farther removed from the metal center, compared to Cp ligands [42-65], and they have been shown to stabilize metal-element multiple bonds, including the [Mo≡N] fragment [66].

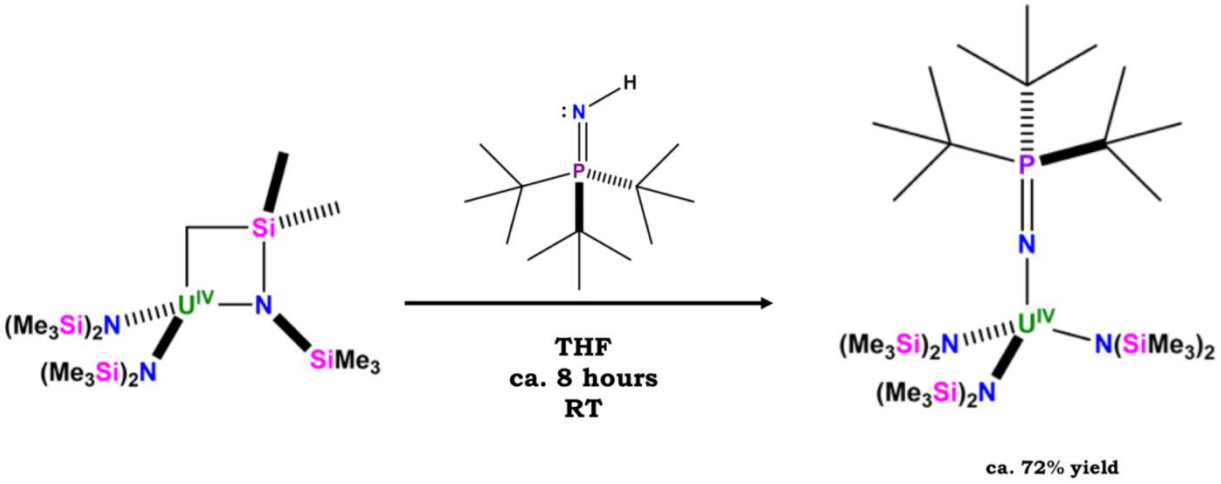

Scheme 2.1: Synthesis of U[NP(*t*-butyl)$_3$][N(SiMe$_3$)$_2$]$_3$

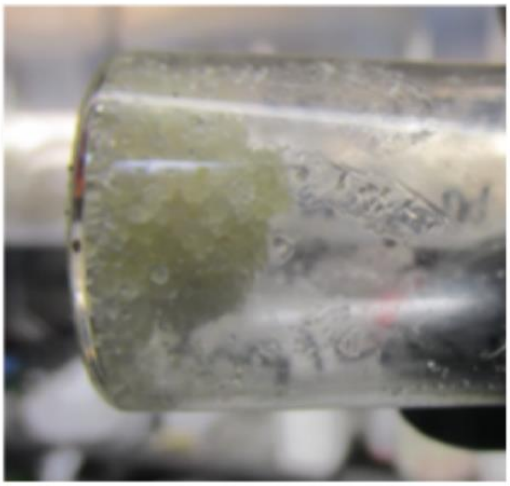

Figure 2.1: HNP(*t*-butyl)$_3$

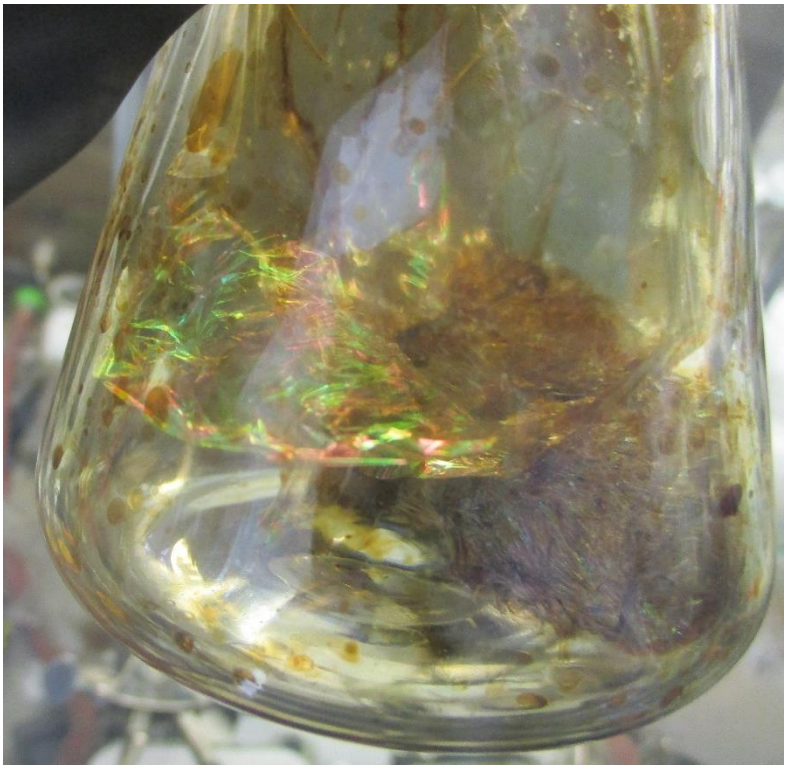

Figure 2.2: U[NP(*t*-butyl)$_3$][N(SiMe$_3$)$_2$]$_3$

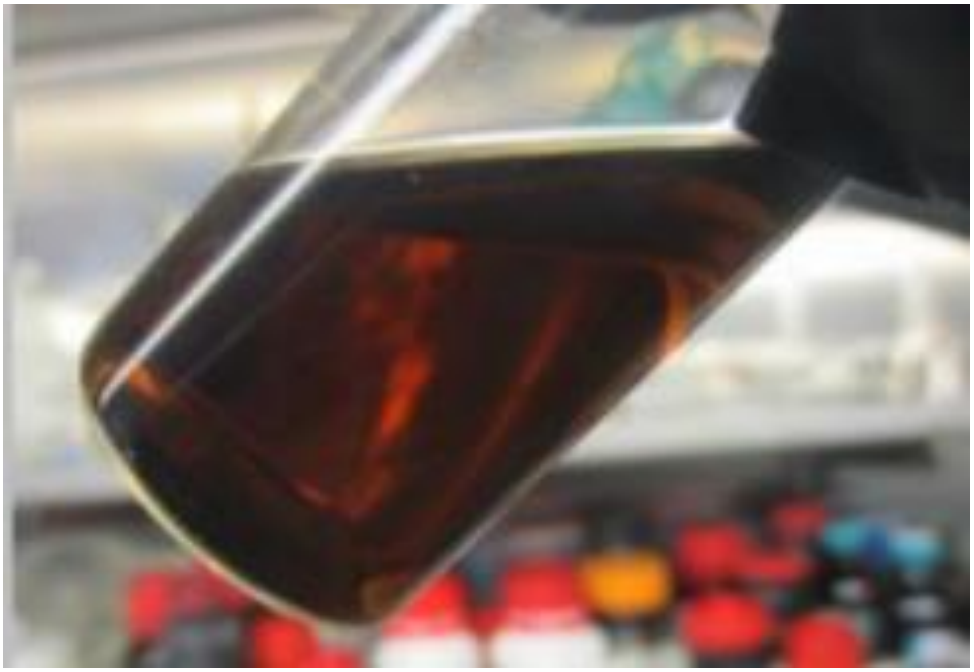

Figure 2.3: U[NP(*t*-butyl)$_3$][N(SiMe$_3$)$_2$]$_3$ in pentane

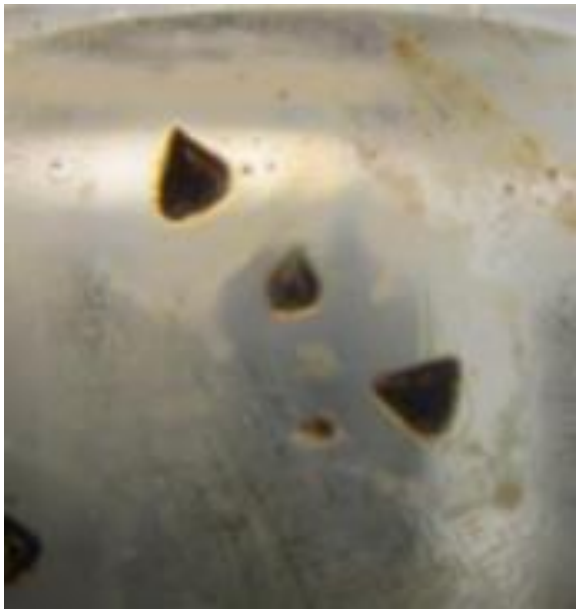

Figure 2.4: Crystals of U[NP(*t*-butyl)$_3$][N(SiMe$_3$)$_2$]$_3$

Phosphinimide ligands are well established in transition metal chemistry and main group chemistry [44-65]; however, phosphinimide-actinide chemistry is in a very poor stage of development [20, 21, 43, 44, 51, 55]. Phosphinimide ligands have highly tunable electronic and steric properties. This feature, coupled with the presence of the highly useful NMR-active ^{31}P nucleus, gives these ligands great potential for facilitating the elucidation of uranium-element orbital interactions.

Phosphinimide complexes of the *s*-, *p*-, and *d*-block metals are more numerous than *f*-block phosphinimide complexes [44, 48, 51, 62]. Several lanthanide phosphinimide complexes are known [44, 51, 62]; however, actinide phosphinimide complexes are extremely rare [20, 21, 43, 44, 48, 51, 55]. The only examples that have been structurally characterized via X-ray diffraction are a tetravalent uranium complex [43] and two hexavalent uranium complexes [20, 21].

Kurt Dehnicke has written multiple reviews on phosphinimide chemistry [44, 48, 51, 62]. He reviewed phosphinimide complexes of transition metals first in 1989 [44], and again in 1999 [51]. He reviewed phosphinimide complexes of main group elements in 1997 [48]. Most recently, he reviewed phosphinimide complexes of rare earth elements in 2003 [62]. Transition metal phosphinimide complexes are known for osmium(VIII), rhenium(VII, VI), molybdenum (VI, V, II), tungsten(VI), vanadium(V, IV), niobium(V), tantalum(V), titanium(IV, III), zirconium(IV), hafnium(IV), ruthenium(IV), iron(III, II), manganese(II), cobalt(II), nickel(II), copper(II, I), zinc(II), cadmium(II), silver(I), and gold(I) [44, 51]. Phosphinimide derivatives of main group elements are known for

hydrogen, lithium, boron, aluminum, gallium, indium, silicon, germanium, tin, nitrogen, phosphorus, arsenic, antimony, sulfur, selenium, tellurium, chlorine, bromine, and iodine [48]. Phosphinimide complexes of rare earth elements are known for yttrium, cerium, dysprosium, erbium, ytterbium, and samarium [44, 51, 62]. A small number of actinide phosphinimide complexes have been reported for thorium(IV) and uranium(IV, VI) [20, 21, 43].

Phosphinimide ligands can be synthesized from substituted and unsubstituted phosphinimine precursors [47, 67-106]. The most convenient and straightforward method for synthesizing phosphinimines is through the Staudinger reaction [67-75, 89, 99]. Azidotrimethylsilane readily reacts with tertiary phosphines via the Staudinger mechanism to afford *N*-trimethylsilyl substituted phosphinimines. In comparison to Cp ligands, the steric bulk of phosphinimide ligands is farther removed from the metal center. This leads to alternate reactivity by leaving the first coordination sphere more open, with a second coordination sphere highly analogous to that of cyclopentadienyl derivatives [44, 47, 48, 51, 62]. As an illustration, the cone angle of the tri(*tert*-butyl)phosphinimide ligand is 87^{o}, compared to 83^{o} for the Cp ligand [63].

Cramer and coworkers reported the syntheses of tetravalent tris-cyclopentadienyl phosphinimide complexes of thorium and uranium in 1988 [43]. They synthesized these complexes via salt metathesis using $LiNPPh_3$ and $AnCp_3Cl$ (An = U or Th) [43]. Only the uranium derivative (UCp_3NPPh_3) was structurally characterized [43]. The U-N-P moiety in this complex was nearly linear (172°) and featured a very short U-N bond (207 pm)

[43]. The U-N bond in this complex is interpreted as a triple bond with p_π- p_π, d_π- p_π, and/or f_π- p_π bonding overlap [43]. This interpretation is supported by extended Hückel molecular orbital calculations using $Cp_3U[NPH_3]$ as a simplified model [43]. These bonding overlaps are optimized as the M-N-P angle approaches linearity [43]. A detailed description of the valence orbital of the U-N bond in $Cp_3U[NPH_3]$ was given [43]. An interaction diagram was provided, showing the interaction of the Cp_3U^+ and NPH_3^- fragments [43]. The upper five orbitals of the Cp_3U^+ fragment were described as having primarily uranium 6d character. The highest energy molecular orbitals are composed of the degenerate x^2-y^2 and xy atomic orbitals (9e). The 8e set of molecular orbitals is composed of xz and yz atomic orbitals, and also has some 7p character. Below these is the $6a_1$ molecular orbital, which is described as the z^2 atomic orbital hybridized with the 7s and 7p atomic orbitals. Below these orbitals in energy are the seven uranium 5f orbitals. Tetravalent uranium has a f^2 configuration, and therefore, two unpaired f-electrons reside in this block of orbitals. $2a_2$ is composed almost entirely of the $y(3x^2-y^2)$ orbital. However, because of the C_{3v} symmetry of this complex, the f_σ orbital (z^3) splits into $3a_1$ and $4a_1$, and the f_π orbitals xz^2 and yz^2 appear in 4e and 5e [43].

The two π and one σ frontier orbitals of the NPH_3^- fragment are fully occupied by electrons. The π orbitals have 91% nitrogen p_x and p_y character, and as a result, this ligand has significant charge separation, with -2.2 e on nitrogen, and +1.0 e on phosphorus. The π orbitals of the phosphinimide ligand interact with the 8e, 5e, and 4e orbitals of the Cp_3U^+ fragment. The 5e and 4e orbitals have f-orbital character, and these bonding

interactions can be described as N x-U xz^2 and N y-U yz^2 overlaps. The U-N σ bond can be described as the interaction between the phosphinimide n orbital and the $6a_1$, $4a_1$, and $3a_1$ orbitals of the Cp_3U^+ fragment. The U-N σ orbital splits in two due to mixing with the Cp_3U bonding orbital. The large π component of the U-N bond supports the idea of multiple bonding in this uranium-phosphinimide system [43]. The $6d_\pi$ orbitals contribute the most to the π interactions, followed by the $5f_\pi$ orbitals. The uranium $7p_\sigma$ and $6d_\sigma$ orbitals contribute most to the σ interaction, while the $5f_\sigma$ orbital contribution is comparatively small [43].

Hexavalent uranium tetra(chloro)oxophosphinimide complexes were synthesized and structurally characterized by Denning and coworkers in the 1990's. These uranyl analogues were synthesized via chlorotrimethylsilane elimination [20, 21]. However, there have been no reports of actinide phosphinimindes since these initial publications.

Experimental

All experimental operations were conducted with rigorous exclusion of air and moisture using Schlenk techniques [107, 108, 110] and standard glove-box methods [109, 110] using a Vacuum Atmospheres glovebox with a recirculating dinitrogen atmosphere. Solvents were bought anhydrous or HPLC-grade (pentane, hexane, toluene, acetonitrile) and further purified using a Vacuum Atmospheres Solvent Purifier System. 1,4-dioxane, tetrahydrofuran, and diethyl ether were dried over sodium benzophenone ketyl, and degassed using three freeze-pump-thaw cycles prior to use. All solvents were stored under dinitrogen in a glove-box, and stored over 4 Å molecular sieves for at least 24 hours

prior to use. Glassware was dried at 150°C before use. ^{1}H and ^{31}P NMR spectra were recorded using a Bruker 400 MHz spectrometer at 298 K. Deuterated benzene (Cambridge Isotopes) was stored over 4 Å molecular sieves for at least 24 hours prior to use.

Oxide encrustations were removed from the uranium metal using concentrated nitric acid [111]. Once the turnings achieved a brilliant luster, the nitric acid was decanted, and the turnings were rinsed with acetone and stored in a dinitrogen atmosphere glovebox. These operations are reported in the literature [111]. Iodine (sublimed) was used as purchased (Aldrich). $CeCl_3$ and $KN(SiMe_3)_2$ was used as purchased (Aldrich). CuF_2 (Aldrich) was used as purchased. *N*-trimethylsilyl phosphinimines were synthesized using literature methods [63, 72, 74-76] from commercially available tertiary phosphines and azidotrimethylsilane (Aldrich). Unsubstituted phosphinimines were prepared from *N*-trimethylsilyl phosphinimines via alcoholysis using literature methods [53, 84]. $KNPPh_3$ was prepared as previously reported [52]. $[((H_3C)_3Si)_2N]_2U[\kappa\text{-}2\text{-}(C,N)\text{-}CH_2Si(CH_3)_2N(Si(CH_3))]$ was prepared according to the literature [110]. $ThCl_4(DME)_2$, UCl_4, $UI_4(1,4\text{-dioxane})_2$, and $UI_3(1,4\text{-dioxane})_{1.5}$ were prepared according to published methods [111-113].

Caution! *Depleted uranium (primary isotope ^{238}U) is a weak* α*-emitter (4.197 MeV) with a half-life of 4.47 x 10^9 years, and natural thorium (primary isotope ^{232}Th) is a weak* α*-emitter (4.012 MeV) with a half-life of 1.41 x 10^{10} years; manipulations and reactions should be carried out in monitored fume hoods or in an inert atmosphere drybox in a radiation laboratory equipped with* α*-counting equipment.*

Synthesis of $U[N=P(t\text{-butyl})_3][N(SiMe_3)_2]_3$

0.485 grams (0.675 mmol) of $[((H_3C)_3Si)_2N]_2U[\kappa\text{-}2\text{-}(C,N)\text{-}CH_2Si(CH_3)_2N(Si(CH_3))]$ was dissolved in 10 mL of THF. 0.148 grams (0.682 mmol) of $HNP(t\text{-butyl})_3$ was dissolved in 10 mL of THF and added to the $[((H_3C)_3Si)_2N]_2U[\kappa\text{-}2\text{-}(C,N)\text{-}CH_2Si(CH_3)_2N(Si(CH_3))]$ solution dropwise at room temperature. A slight color change was observed from dark brown to burgundy-brown, and the solution was stirred for 6 hours at room temperature. The THF was removed *in vacuo*, and the residue was dissolved in pentane and filtered. The pentane was removed *in vacuo* and a dark iridescent solid was afforded in 72% yield (0.455 grams).

^1H *NMR Data* (C_6D_6, 298 K): δ -12.33 ppm (s, 54H, $SiMe_3$), δ 22.96 ppm (s, 27H, $C(CH_3)_3$). ^{31}P *NMR Data* (C_6D_6, 298 K): δ 689.23 ppm.

Synthesis of $U[N=PPh_3][N(SiMe_3)_2]_3$

0.310 grams (0.43 mmol) of $[((H_3C)_3Si)_2N]_2U[\kappa\text{-}2\text{-}(C,N)\text{-}CH_2Si(CH_3)_2N(Si(CH_3))]$ was dissolved in 10 mL of THF. 0.135 grams (0.488 mmol) of $HNPPh_3$ was dissolved in 10 mL of THF and added to the $[((H_3C)_3Si)_2N]_2U[\kappa\text{-}2\text{-}(C,N)\text{-}CH_2Si(CH_3)_2N(Si(CH_3))]$ solution dropwise at room temperature. A slight color change was observed from dark brown to burgundy-brown, and the solution was stirred for 6 hours. The THF was removed *in vacuo*, and the residue was dissolved in pentane and filtered. The pentane was removed *in vacuo* and a dark solid was afforded in 40% yield (0.170 grams). The product was sealed and stored for NMR and elemental analysis.

Synthesis of $UF[N=P(t\text{-butyl})_3][N(SiMe_3)_2]_3$

0.069 grams (0.073 mmol) of $U[N=P(t\text{-butyl})_3][N(SiMe_3)_2]_3$was dissolved in 5 mL of THF. To this solution, 0.036 grams (0.359 mmol) of CuF_2 was added. The solution was stirred at room temperature for 3 hours. The solution was filtered, the THF was removed *in vacuo*, and a brown solid was afforded in 90% yield (0.063 grams). The product was sealed and stored for NMR and elemental analysis.

Attempted Synthesis of $U[N=PPh_3]_3$

0.046 grams (0.06 mmol) of $UI_3(1,4\text{-dioxane})_{1.5}$ was dissolved in 10 mL of THF. 0.057 grams (0.18 mmol) of $KNPPh_3$ was dissolved in 5 mL of THF and added to the $UI_3(1,4\text{-dioxane})_{1.5}$ solution dropwise at room temperature. An immediate color change was observed from dark blue to purple-brown, and the solution became cloudy, indicative of salt formation (KI). The solution was stirred for 2 hours at room temperature. The solution was filtered to remove a light gray salt that formed, and the THF was removed *in vacuo*. A dark brown solid was afforded (0.068 grams). The residue was dissolved in C_6D_6 for NMR analysis.

^{31}P *NMR Data* (C_6D_6, 298 K): δ -1.65 ppm.

Attempted Synthesis of $Ce[N=PPh_3]_3$

0.028 grams (0.11 mmol) of $CeCl_3$ was dissolved in 10 mL of THF/toluene (50/50). 0.107 grams (0.34 mmol) of $KNPPh_3$ was dissolved in 5 mL of THF and added to the $CeCl_3$

solution dropwise at room temperature. An immediate color change was observed from white to yellow. The solution became cloudy, indicative of salt formation (KCl). The solution was stirred for 12 hours at room temperature. The solution was filtered to remove a light gray salt that formed, and the THF was removed *in vacuo*. A colorless solid was afforded (0.098 grams; 89% yield). The residue was dissolved in C_6D_6 for NMR analysis. NMR analysis of the residue was inconclusive.

Attempted Synthesis of $U[N=PPh_3]_4$

0.058 grams (0.06 mmol) of $UI_4(1,4\text{-dioxane})_2$ was dissolved in 10 mL of THF. 0.079 grams (0.25 mmol) of $KNPPh_3$ was dissolved in 5 mL of THF and added to the $UI_4(1,4\text{-dioxane})_2$ solution dropwise at room temperature. The solution immediately turned to a burnt orange color, and the solution became cloudy, indicative of salt formation (KI). The solution was stirred for 8 hours at room temperature. The solution was filtered to remove a light gray salt that formed, and the THF was removed *in vacuo*. The residue was extracted with toluene, filtered, and isolated *in* vacuo. A brown solid was afforded (0.066 grams; 78% yield). The residue was dissolved in C_6D_6 for NMR analysis.

^{31}P *NMR Data* (C_6D_6, 298 K): δ 35.34 ppm.

Attempted Synthesis of $Th[N=PPh_3]_4$

0.018 grams (0.03 mmol) of $ThCl_4(DME)_2$ was dissolved in 10 mL of THF. 0.041 grams (0.13 mmol) of $KNPPh_3$ was dissolved in 5 mL of THF and added to the $ThCl_4(DME)_2$ solution dropwise at room temperature. No color change was observed. The solution became cloudy, indicative of salt formation (KCl). The solution was stirred for 8 hours at

room temperature. The solution was filtered to remove a light gray salt that formed, and the THF was removed *in vacuo*. The residue was extracted with toluene, filtered, and isolated *in vacuo*. A colorless solid was afforded (0.031 grams; 71% yield). The residue was dissolved in C_6D_6 for NMR analysis. NMR analysis of the residue was inconclusive.

Attempted Synthesis of U[N=P(*p*-MeOPh)$_3$]$_4$

0.055 grams (0.145 mmol) of UCl_4 was dissolved in 10 mL of THF. 0.255 grams (0.579 mmol) of Me_3Si-N=P(*p*-MeOPh)$_3$ was dissolved in 5 mL of THF and added to the UCl_4 solution dropwise at room temperature. No color change was observed. The solution was stirred for 24 hours at room temperature. The THF was removed *in vacuo*. The residue was extracted with toluene, filtered, and isolated *in* vacuo. A green solid was afforded (0.165 grams; 67% yield). The residue was dissolved in C_6D_6 for NMR analysis. NMR analysis of the residue was inconclusive.

Attempted Synthesis of Th[N=P(*p*-MeOPh)$_3$]$_4$

0.013 grams (0.023 mmol) of $ThCl_4(DME)_2$ was dissolved in 10 mL of THF. 0.041 grams (0.094 mmol) of Me_3Si-N=P(*p*-MeOPh)$_3$ was dissolved in 5 mL of THF and added to the $ThCl_4(DME)_2$ solution dropwise at room temperature. No color change was observed. The solution was stirred for 24 hours at room temperature. The THF was removed *in vacuo*. A colorless solid was afforded (0.018 grams; 45% yield). The residue was dissolved in C_6D_6 for NMR analysis. NMR analysis of the residue was inconclusive.

Results and Discussion

Our explorations into actinide phosphinimide chemistry began with the intent to synthesize homoleptic phosphinimide complexes via salt metathesis, however, significant difficulties were encountered with this synthetic route. We also attempted to generate homoleptic phosphinimide complexes via chlorotrimethylsilane elimination using thorium, uranium, and cerium chlorides and *N*-trimethylsilyl substituted phosphinimines. These attempted syntheses via chlorotrimethylsilane elimination were unsuccessful. Our efforts then turned to the synthesis of heteroleptic amide-phosphinimide complexes. Our initial attempts to install a singular phosphinimide ligand to uranium and thorium amide complexes via salt metathesis were unsuccessful. After numerous attempts to synthesize actinide phosphinimide complexes via salt metathesis, we shifted our synthetic strategy to protonolysis. Actinide amides and amide-metallacycles are strong Brønsted bases and are ideally suited for protonolysis reactions. This strategy yielded positive results, and the NMR data suggest the successful synthesis of a tetravalent uranium phosphinimide complex, U[NP(*t*-butyl)$_3$][N(SiMe$_3$)$_2$].

Our efforts to synthesize high-symmetry homoleptic phosphinimide complexes were motivated by the intent to use phosphinimide ligands to study actinide covalency using ^{31}P NMR spectroscopy and X-ray spectroscopy. Additionally, we intended to use bulky phosphinimide ligands as ancillary ligands to limit access to the actinide metal center to a localized region where metal-ligand multiple bonds could potentially be installed. Significant progress was made towards our goal of using phosphinimide

ligands to study actinide covalency using ^{31}P spectroscopy. We have developed a strategy for the synthesis of mono-phosphinimide tris-amido complexes via protonolysis of the well-known U^{IV} amide metallacycle. We have also acquired paramagnetic NMR data for the tri(*tert*-butyl) phosphinimide derivative, U[NP(*t*-butyl) $_3$][$N(SiMe_3)_2$]$_3$. This strategy should be extended to other alkyl and aryl phosphinimide derivatives, and the thorium analogues should be synthesized from the Th^{IV} amide metallacycle. A series of isostructural uranium and thorium complexes featuring a variety of alkyl and aryl phosphinimide derivatives can yield valuable insight into the nature of orbital interactions in tetravalent actinide complexes.

The ^{31}P NMR resonance for U[NP(*t*-butyl)$_3$][$N(SiMe_3)_2$] is very deshielded (δ 689.23 ppm). This suggests a considerable degree of covalency in the uranium(IV)-phosphinimide system. The electron density is delocalized over the entire U-N-P system, and the phosphorus nuclear magnetic shielding tensor is very sensitive to the orbital interactions in the metal-phosphinimide bond. A single ^1H NMR signal for the bis(trimethylsilyl)amide ligands was observed (δ -12.33), and this agrees well with a similar U(IV) tris[bis(trimethylsilyl)amido] mono(imidazoline-2-iminato) compound that has recently been reported in the literature by Eisen and co-workers (δ -13.17 ppm) [114]. The *t*-butyl ^1H NMR resonance is very deshielded (δ 22.96 ppm). This large paramagnetic shift suggests a considerable degree of uranium-phosphinimide orbital mixing and electron delocalization in the U-N-P system. This compound easily formed trigonal crystals from pentane (see FIGURE 2.4). X-ray diffractometry was attempted for this

compound; however, a series of bad timely instrument failures, followed by administrative problems, prevented this compound from being fully characterized. This compound, and isostructural analogues with different alkyl and aryl substituents on phosphorus, should be the subject of future work.

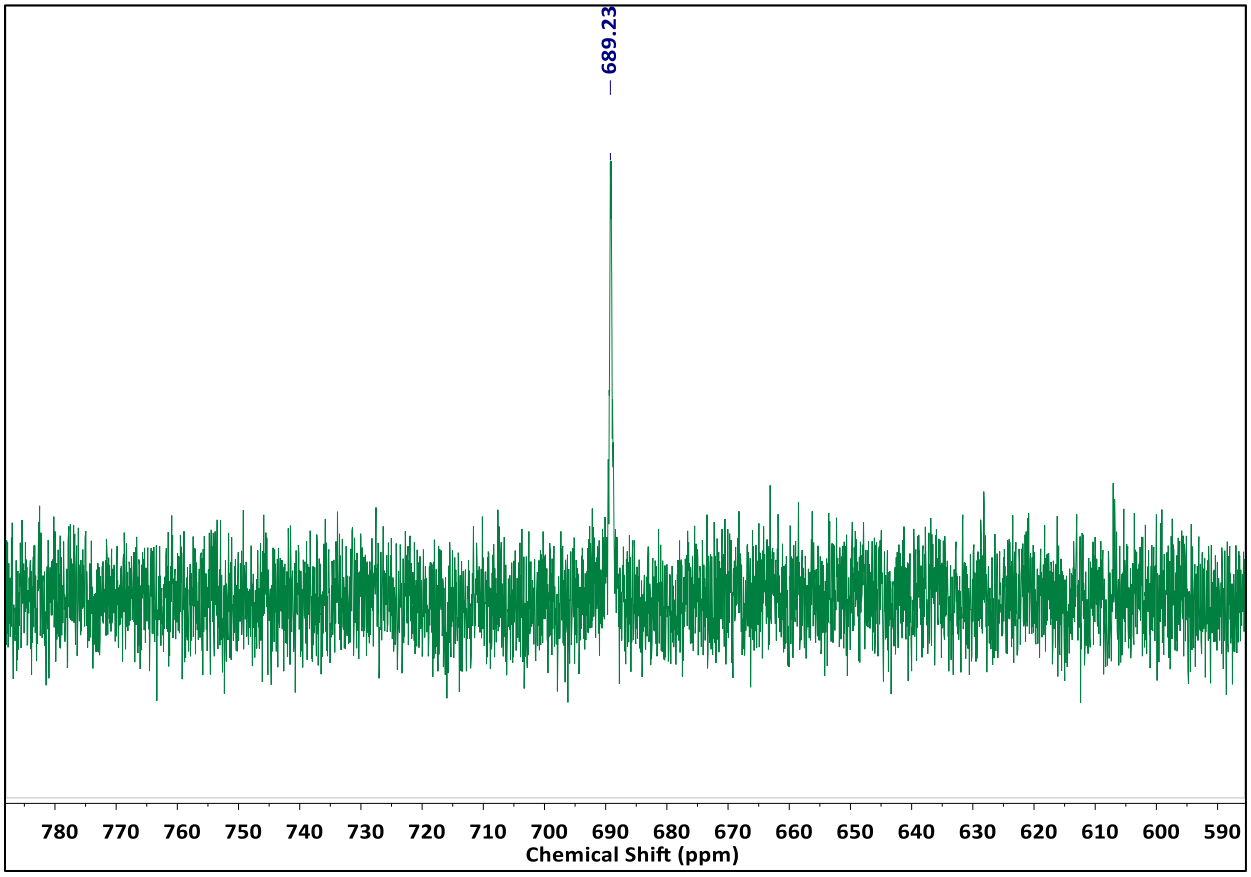

Figure 2.5: ^{31}P NMR spectrum of U[NP(*t*-butyl)$_3$][N(SiMe$_3$)$_2$]$_3$

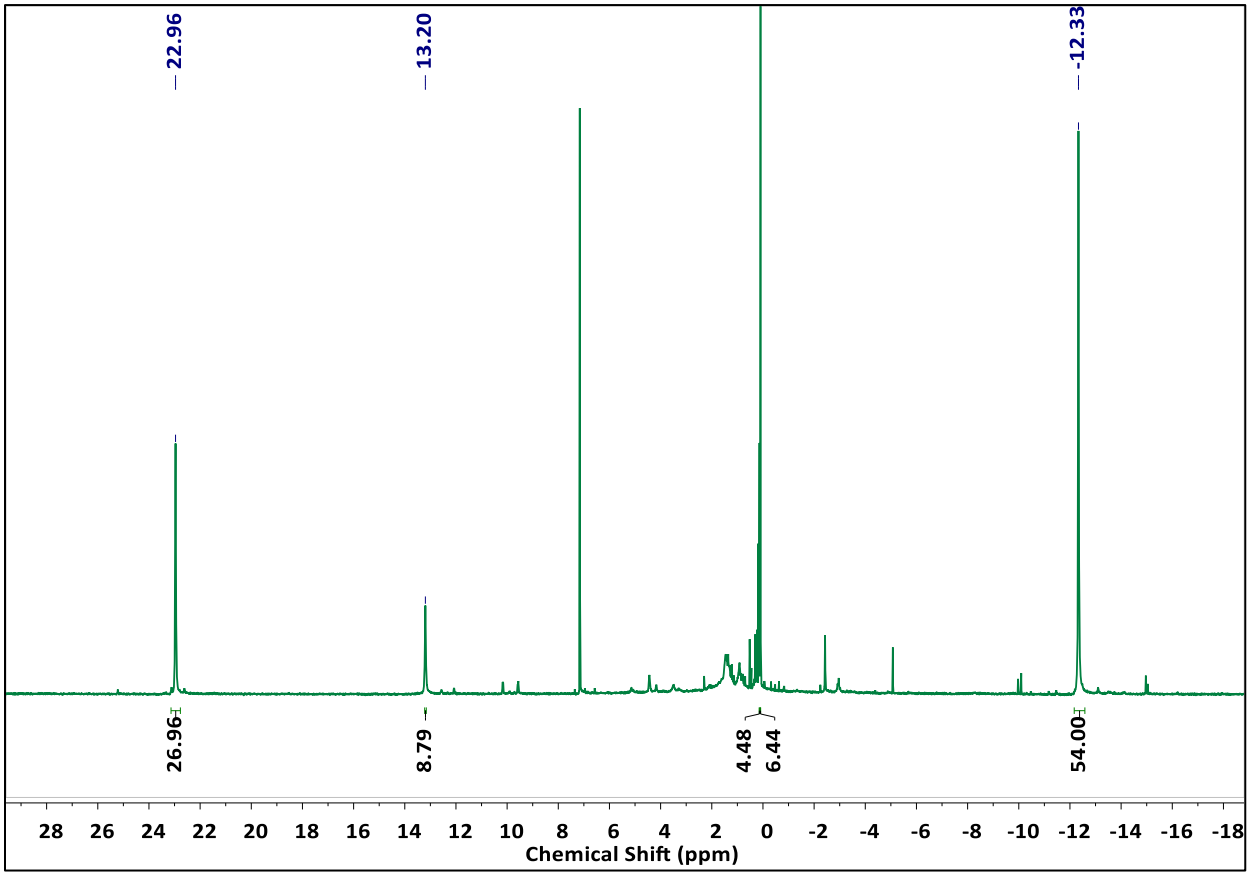

Figure 2.6: ^{1}H NMR spectrum of U[NP(*t*-butyl)$_3$][N(SiMe$_3$)$_2$]$_3$

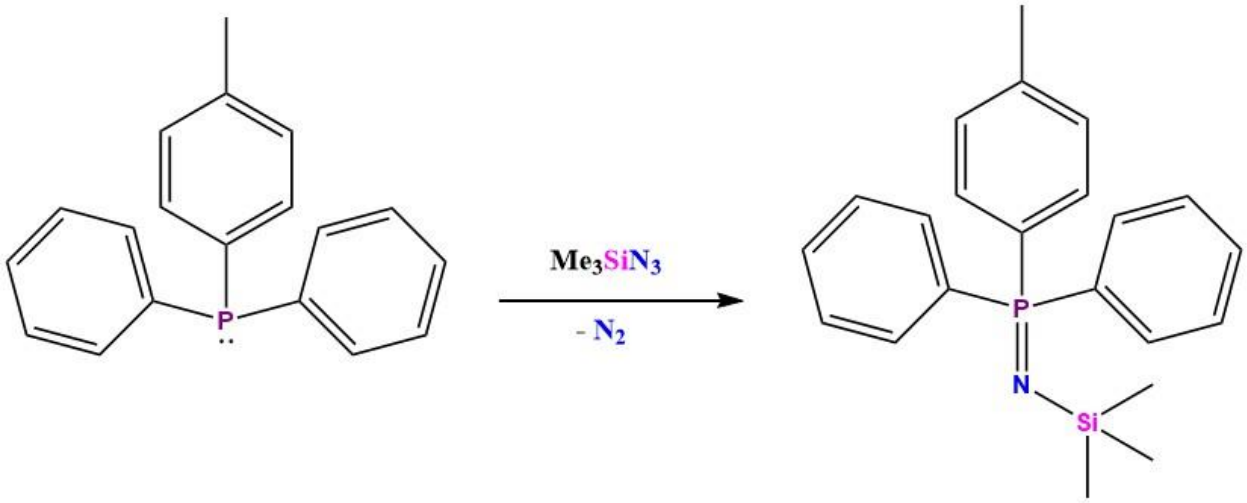

Scheme 2.2: Synthesis of *N*-silyl phosphinimines via Staudinger reaction.

Unsubstituted phosphinimines, R_3PNH (R = *t*-butyl, Ph), react via protonolysis with uranium(IV) silyl-amide metallacycle, $[((H_3C)_3Si)_2N]_2U[\kappa\text{-}2\text{-}(C,N)\text{-}CH_2Si(CH_3)_2N(Si(CH_3))]$, to form amido-phosphinimide complexes $U[NPR_3][N^*]_3$ (R = *t*-butyl, Ph; N* = $^-N(SiMe_3)_2$. R_3PNH compounds are strong neutral bases, and easily react with acids to form ionic compounds with the general formula $[R_3PNH_2][X]$. Therefore, the N-H proton in R_3PNH is relatively non-acidic. Ph_3PNH has a pKa of 28.1 [104], and alkyl derivatives are less acidic. This makes unsubstituted phosphinimines more basic than hexamethdisilazane (pKa = 26). This implies that the amide ligands on the uranium will not deprotonate R_3PNH, and also implies that phosphinimide-metal bonds will be more susceptible to protonolysis than amide-metal bonds. The bonding interactions in these phosphinimide complexes are complex; in addition to the inherently complex nature of the electronic structure of actinide ions, the nature of N-P interaction in phosphinimines and phosphinimide ligands has been debated for decades, as part of the

larger debate concerning the role of d-orbitals (and their ability to accept electron density) in the orbital interactions of phosphorus and other non-first row main groups elements. Phosphinimines and phosphinimide ligands are often drawn with a double-bond between the nitrogen and phosphorus, $R_3P{=}NR$. However, it is evident that these bonding interactions are quite polar, and $R_3P^+\text{-}N^-\text{-}R$, with significant charge separation between the phosphorus and nitrogen, is likely a more realistic depiction of the phosphinimine system. Likewise, the phosphinimide ligand system, often depicted as $R_3P{=}N^-$, is likely more accurately represented by $R_3P^+\text{-}N^{2-}$. The dianionic description of phosphinimides, with three electron pairs available to interact with the metal center, gives a better illustration of how these ligands are able to engage in multiple-bond interactions.

Phosphinimines can be synthesized using a variety of methods. In this work, we used the Staudinger reaction to synthesize trimethylsilyl-substituted phosphinimines, $R_3PNSiMe_3$ (R = *t*-butyl, ethyl, methyl, phenyl, *p*-anisyl, *p*-tolyl). In these Staudinger reactions, an excess of azidotrimethylsilane is added to the tertiary phosphine precursor, and heated at 80˚C for about 5 hours. These substituted phosphinimines can be converted to unsubstituted phosphinimines, R_3PNH, via alcoholysis. Alcoholysis of *N*-$SiMe_3$ substituted alkyl-phosphinimes can be achieved using methanol. However, the aryl-phosphinimes, $Ar_3PNSiMe_3$, are much more moisture sensitive than the alkyl derivates,

and *absolute* isopropanol must be used instead of methanol to avoid hydrolysis of Ph_3PNR to form Ph_3PO.

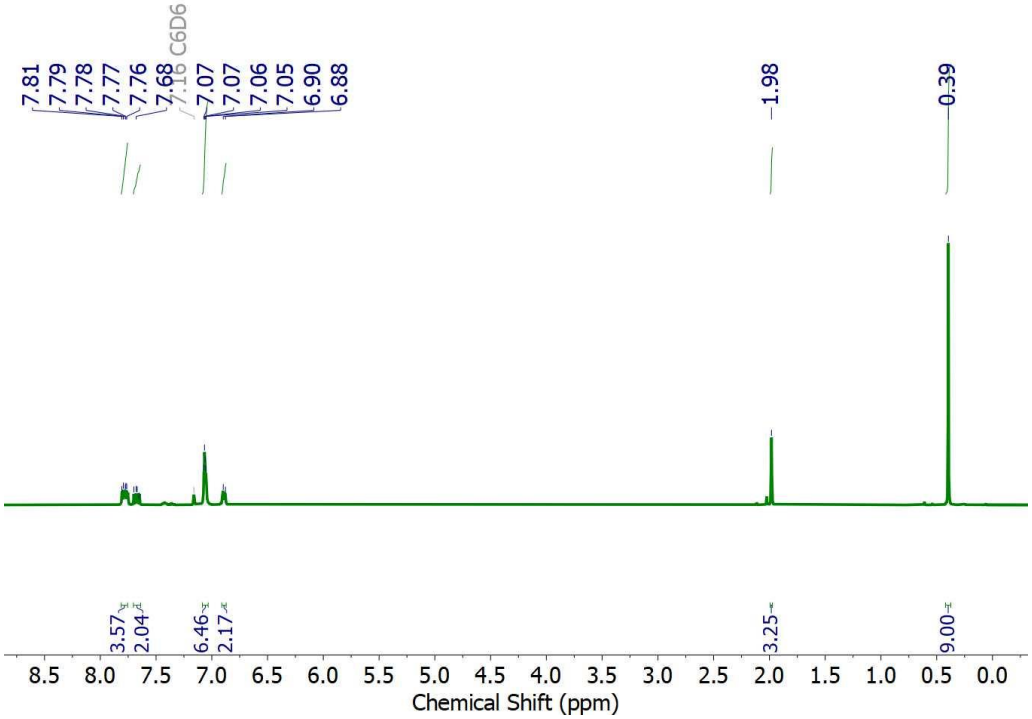

Figure 2.7: ^1H NMR spectrum for $Me_3Si\text{-}NPPh_2$(*p*-tolyl), previously unreported.

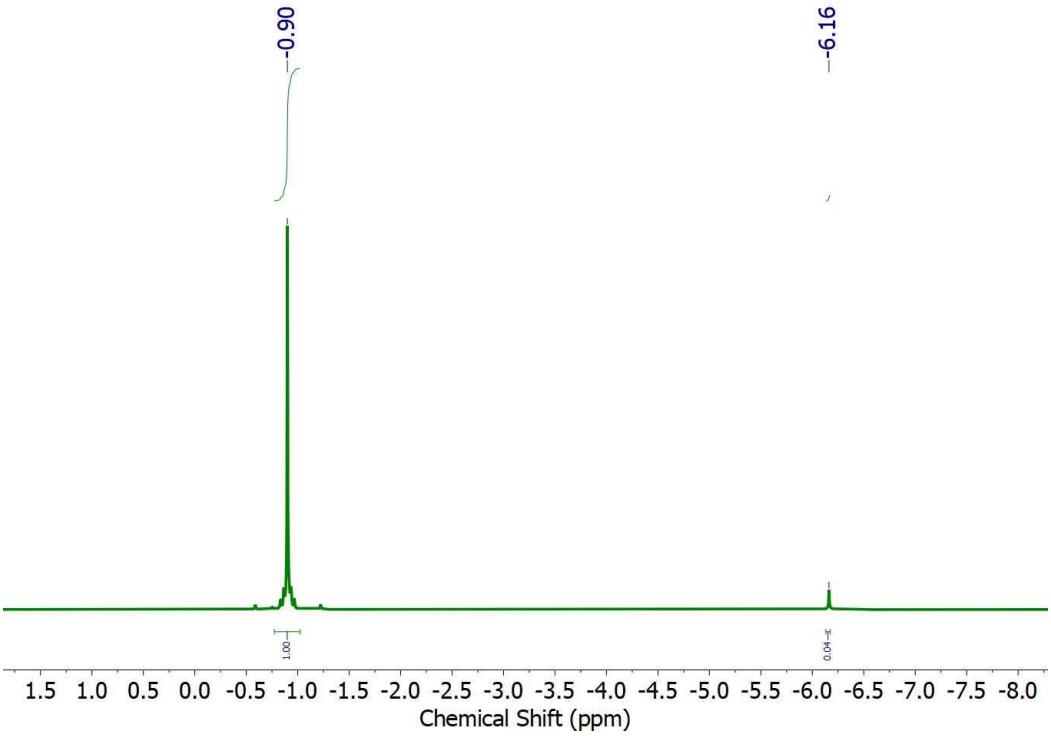

Figure 2.8: ^{31}P NMR spectrum for $Me_3Si\text{-}NPPh_2$(*p*-tolyl), previously unreported.

The phosphorus nucleus in tBu_3PNH resonates at δ 55.8 ppm, whereas Ph_3PNH resonates at δ 18.1 ppm (in C_6D_6). This indicates that the phosphorus nucleus in tBu_3PNH is more deshielded, has greater charge separation between the nitrogen and phosphorus, and also more electron density on nitrogen to donate to the metal center. As a result, it is expected that coordination of the tBu_3PN^- ligand to uranium will result in a greater coordination chemical shift than Ar_3PN^- ligands. However, we were not able to characterize the aryl-phosphinimide uranium complex, $U[NPPh_3][N^*]_3$ ($N^* = {}^-N(SiMe_3)_2$), so we were not able to verify this hypothesis in this work. A ^{31}P NMR chemical shift of δ 689.23 ppm was observed for $U[NP(t\text{-butyl})_3][N(SiMe_3)_2]_3$. This corresponds to a large coordination chemical shift (Δδ) of 633.43 ppm. The coordination chemical shift is much larger than those observed for transition metal phosphinimide complexes; typically phosphinimide ^{31}P resonances are observed from -5 ppm to 50 ppm.

Efforts were made to oxidize the presumed $U[NPR_3][N^*]_3$ complex (R = *t*-butyl) to generate a trigonal bipyramidal pentavalent uranium-fluoride complex of the form $F\text{-}U[NPR_3][N^*]_3$. $U[NPR_3][N^*]_3$ was dissolved in pentane, and an excess of CuF_2 was added to the solution. However, work on this reaction was abruptly discontinued before the residue could be characterized.

Unsubstituted phosphinimines, R_3PNH, can be deprotonated with very strong bases like methyllithium, *n*-butyllithium, sodium amide, and potassium hydride. Following the work of Dehnicke and coworkers, we used potassium hydride, KH, to deprotonate triphenylphosphinimine, $HNPPh_3$, to form potassium

triphenylphosphinimide, $KNPPh_3$. Potassium triphenylphosphinimide has a hexameric structure, and a ^{31}P NMR chemical shift of δ -15.7 ppm in THF (-13.2 ppm in toluene; -14.8 in DME). Similarly, $KNPCy_3$ resonates at -7.8 ppm. When comparing the ^{31}P NMR resonances of phosphinimide salts, $MNPPh_3$ (M = Li, Na, K, Rb, Cs), the ^{31}P resonances becomes progressively more shielded as one moves down the alkali metal series: $LiNPPh_3$, -4.6 ppm; $NaNPPh_3$, -11.2 ppm; $KNPPh_3$, -15.7 ppm; $RbNPPh_3$, -24.0 ppm; $CsNPPh_3$, -24.1 ppm.

In 2001, Dehnicke reported the synthesis of a homoleptic hafnium(IV) complex, $Hf[NPPh_3]_4$. They reacted 4 equivalents of $CsNPPh_3$ with $HfCl_4$ to generate $Hf[NPPh_3]_4$ via salt metathesis. The ^{31}P NMR signal was reported as δ – 5.2 ppm. It is not surprising that the hafnium derivative is most similar to the lithium derivative, since the electronegativity of hafnium (1.3) is more similar to lithium (1.0) than the more electropositive alkali metals. However, compared to $HNPPh_3$ (18.1 ppm) and $Me_3SiNPPh_3$ (-0.5 ppm), the value of -5.2 ppm is quite surprising; often the phosphinimide ligand in a metal complex is more deshielded compared to the free ligand. However, in the case of $Hf[NPPh_3]_4$, it appears the phosphorus nuclei are more shielded in the metal complex compared to the nuclei in the free ligands. $Hf[NPPh_3]_4$ is more deshielded than the alkali-metal phosphinimide salts, with the exception of the lithium derivative, and this implies that the hafnium complex is less ionic (i.e. more covalent) than the heavier alkali-metal analogues. Inspired by these results, we attempted to extend this chemistry to uranium, thorium, and cerium.

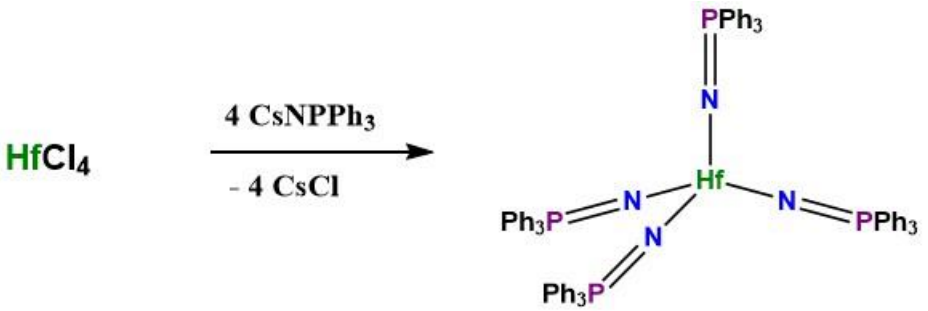

Scheme 2.3: Synthesis of homoleptic hafnium tetrakis(phosphinimide) complex [57].

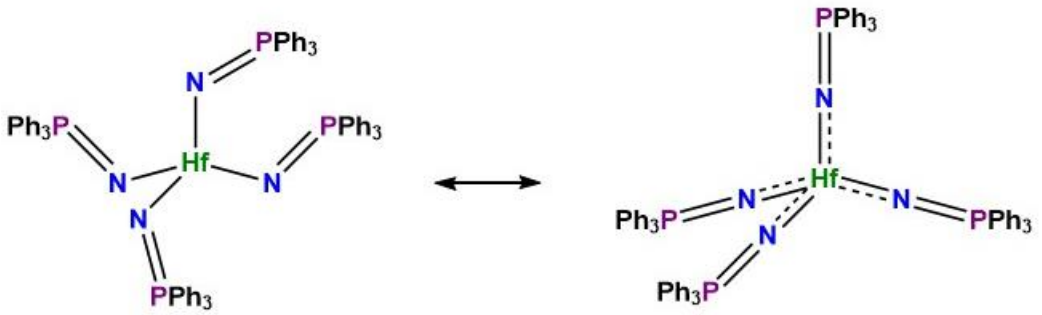

Scheme 2.4: Bent and linear coordination modes of phosphinimide ligands.

$UI_4(1,4\text{-dioxane})_2$ was synthesized as reported by Kiplinger and co-workers in 2011. Uranium metal turnings were allowed to react with 2.05 equivalents of elemental iodine in anhydrous 1,4-dioxane for seven days at room temperature. $UI_4(1,4\text{-dioxane})_2$ is a robust red-orange synthon for non-aqueous uranium chemistry. $UI_4(1,4\text{-dioxane})_2$ was dissolved in THF, and four equivalents of $KNPPh_3$ was added at room temperature and stirred for 8 hours. A cloudy, burnt-orange solution formed after addition of the

potassium phosphinimide salt. The solution was filtered, extracted with toluene, and filtered again, and then analyzed via NMR in d_6-benzene.

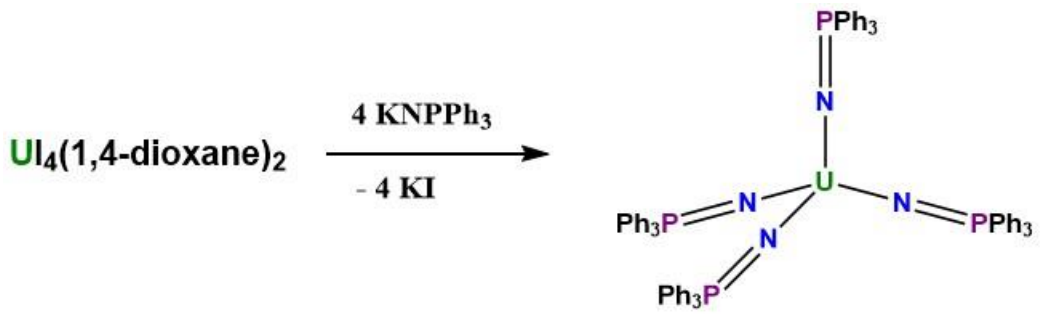

Scheme 2.5: Synthesis of homoleptic uranium tetrakis(phosphinimide) complex.

Four broad, paramagnetically-shifted resonances were observed in the ^{1}H NMR spectrum for this residue at δ 52.06 ppm, 13.55 ppm, 12.9 ppm, and -5.68 ppm, in an approximate 1:2:1:2 ratio. These likely correspond to the aromatic protons of the uranium(IV)-coordinated triphenylphosphinimide ligands. Other signals corresponding to $KNPPh_3$ and/or $HNPPh_3$ were also observed, in addition to residual solvents. The strong paramagnetic deshielding of protons, as far downfield as δ 52.06 ppm is highly indicative of the formation of a U(IV) phosphinimide product. Previous researchers have attributed strong paramagnetic deshielding in the ^{1}H NMR of organometallic U(IV) complexes to elevated levels of metal-ligand covalency (orbital mixing). Given that the

protons are so many atoms away from the paramagnetic ion, such profound paramagnetic shifts indeed suggest a large amount of electron delocalization.

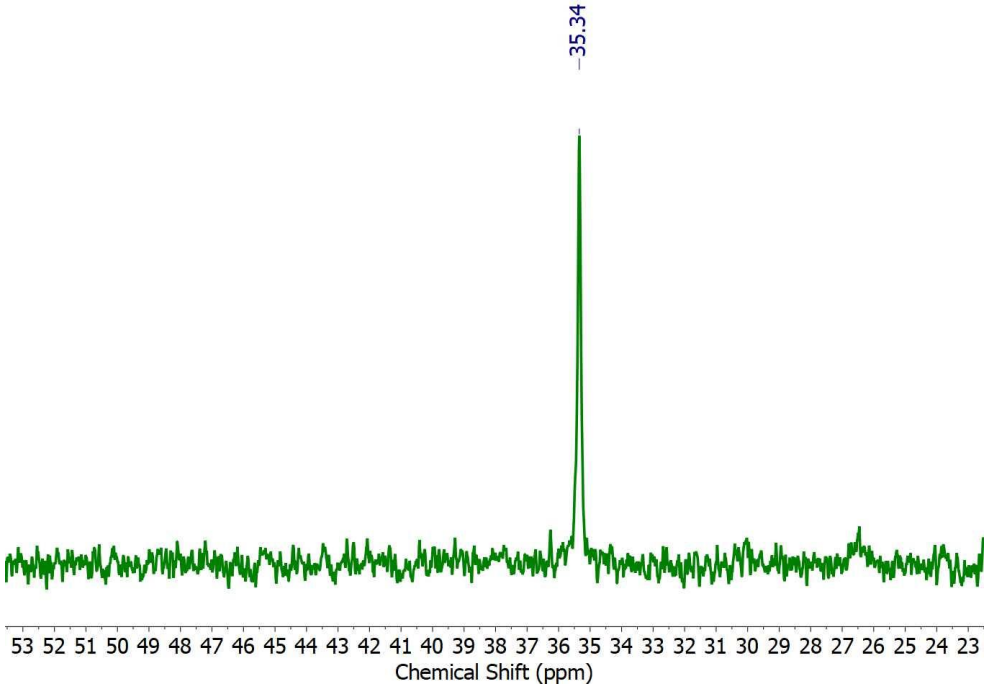

Figure 2.9: ^{31}P NMR spectrum for reaction of $UI_4(1,4\text{-dioxane})_2$ and $KNPPh_3$.

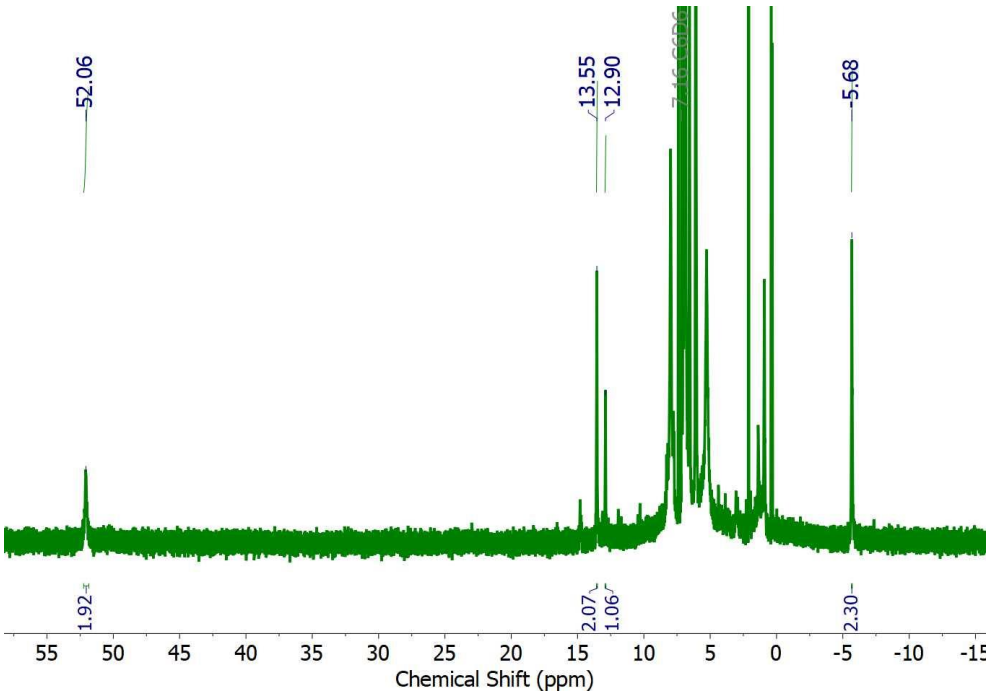

Figure 2.10: ^{1}H NMR spectrum for reaction of $UI_4(1,4\text{-dioxane})_2$ and $KNPPh_3$.

A deshielded ^{31}P NMR resonance was observed at δ 35.34. This is a very typical ^{31}P NMR value for a metal-phosphinimide complex, and is further indicative of U(IV)-phosphinimide formation. This resonance corresponds to a coordination chemical shift (Δδ) equal to 17.24 ppm, with respect to $HNPPH_3$ (δ_P = 18.1 ppm). Dehnicke has previously attributed the observed deshielding of coordinated phosphinimide ligands to π-donation of electron density to electron-withdrawing metal ions.

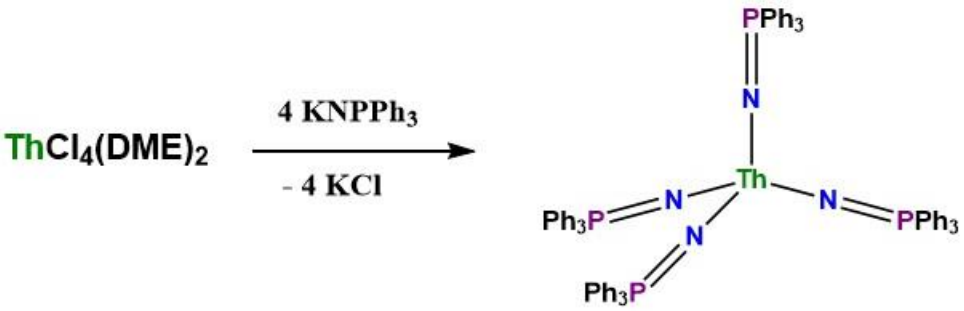

Scheme 2.6: Synthesis of homoleptic thorium tetrakis(phosphinimide) complex.

This methodology above was also applied to thorium(IV). $ThCl_4(DME)_2$ was synthesized from thorium nitrate as described in the literature. This highly soluble non-aqueous synthon was dissolved in THF, and stirred with four equivalents of $KNPPh_3$ at room temperature for 8 hours. No major color change was observed; however, a suspension formed, indicative of salt formation. The reaction mixture was filtered, evaporated to dryness, extracted with toluene, filtered again, and isolated in about 71% yield.

The ^1H NMR features signals in the normal range from 0-10 ppm indicating that the residue is diamagnetic, as expected for residues containing the Th(IV), which has a

closed-shell, f^0 configuration. The ^1H spectrum features sharp, non-shifted signals, corresponding to the uncoordinated ligand, as well as broad, downfield shifted resonances, presumably corresponding to Th(IV)-phosphinimide complexation. The ^{31}P NMR spectrum features two signals at δ -14.71 ppm and δ -15.08 ppm, potentially corresponding to a Th(IV)-phosphinimide complex, and also the unreacted potassium phosphinimide. If this is indeed the case, the peak at δ -15.08 ppm corresponds to $KNPPh_3$, and the peak at δ -14.71 ppm would correspond to the less electropositive thorium(IV)-phosphinimide complex. A negative value for the Th(IV) complex compares well with the isostructural hafnium tetrakis-phosphinimide complex, which resonates at δ_P -5.2. When comparing the ^{31}P NMR resonances of hafnium-, alkali-metal, and the (presumed) thorium-phosphinimide complexes, at first inspection, it qualitatively seems that the electronic structure of Th(IV) is more akin to heavier alkali-metals than group IV transition metals. More work needs to be done to optimize the reaction conditions to generate pure metal-phosphinimide products, and the products of these reactions need to be structurally characterized for any conclusive statements to be made.

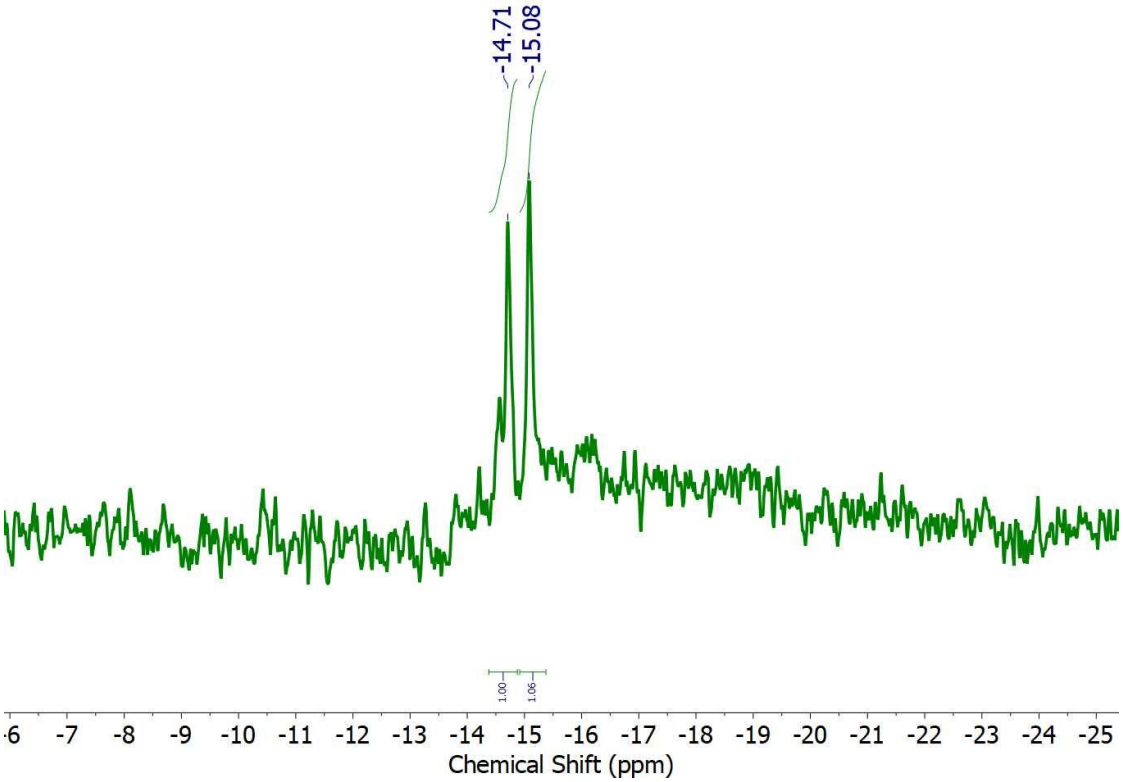

Figure 2.11 ^{31}P NMR spectrum for reaction of $ThCl_4(DME)_2$ and $KNPPh_3$.

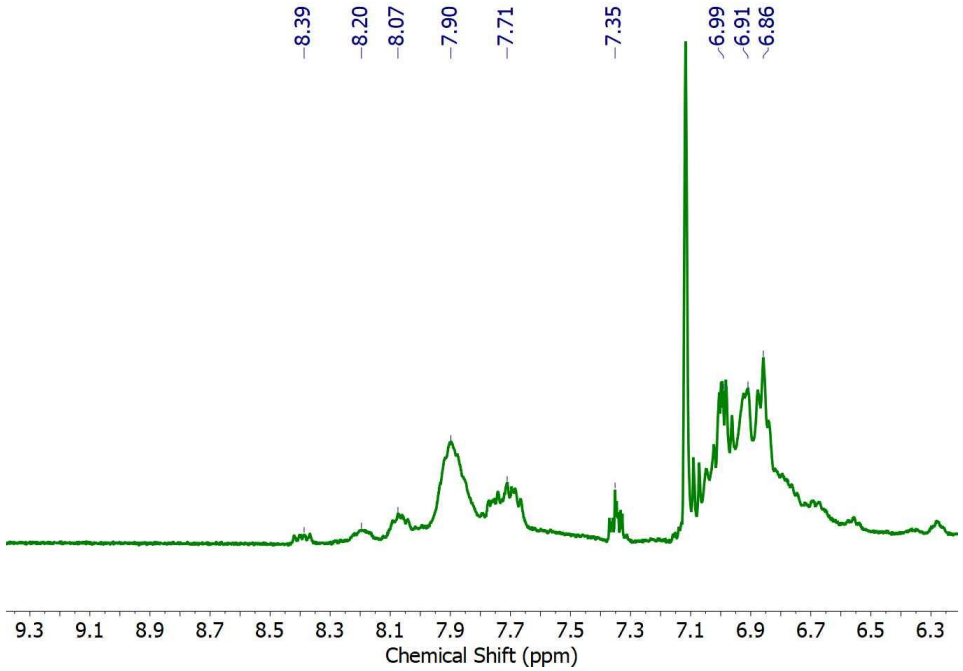

Figure 2.12: ^{1}H NMR spectrum for reaction of $ThCl_4(DME)_2$ and $KNPPh_3$.

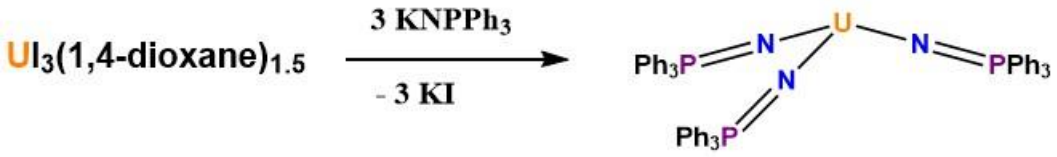

Scheme 2.7: Synthesis of homoleptic uranium tris(phosphinimide) complex.

The synthesis of trivalent homoleptic phosphinimide complexes via salt metathesis was also attempted. $UI_3(1,4\text{-dioxane})_{1.5}$ was synthesized in a manner similar to that described by Kiplinger and co-workers in 2011. Uranium metal turnings were allowed to react with 0.75 equivalents of elemental iodine in anhydrous 1,4-dioxane at room temperature for a week. The dark blue solid was dissolved in THF, and stirred with three equivalents of $KNPPh_3$ for three hours. The solution turned from blue to purple-brown, and became cloudy due to apparent salt formation. The solution was filtered, evaporated to dryness, extracted with toluene, filtered, and isolated in approximately quantitative yield.

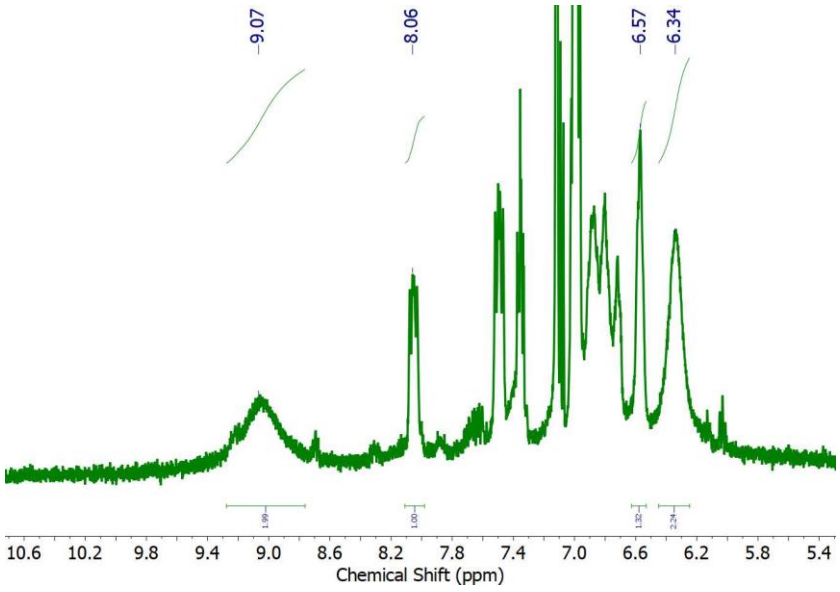

Figure 2.13: ^1H NMR spectrum for reaction of $UI_3(1,4\text{-dioxane})_{1.5}$ and $KNPPh_3$.

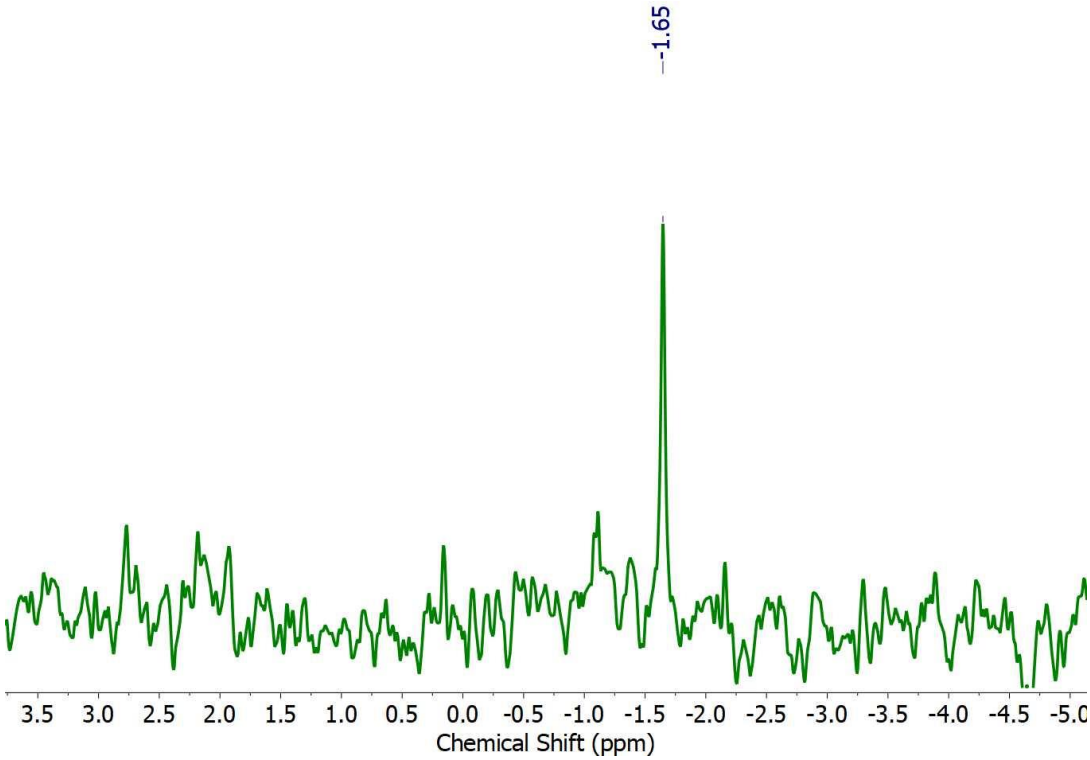

Figure 2.14: ^{31}P NMR spectrum for reaction of $UI_3(1,4\text{-dioxane})_{1.5}$ and $KNPPh_3$.

The ^{1}H NMR was difficult to interpret, with broad deshielded peaks at δ 9.07 ppm and δ 8.06 ppm, as well as broad upfield-shifted peaks at δ 6.57 ppm and δ 6.34 ppm. Aromatic peaks associated with uncoordinated ligands were also observed. The broad peaks observed likely correspond to paramagnetically shifted aromatic protons of U(III)-coordinated phosphinimide ligands. Trivalent uranium is strongly paramagnetic with a f^3 configuration, and the intrinsic single-molecule magnet behavior of uranium(III) has been the subject of a flurry of recent research interest, motivated by potential applications in quantum technologies. The aromatic signals of the target complex are expected to be

extremely broad, and likely correspond to the ones observed near the aromatic region of the spectrum.

A ^{31}P NMR resonance was observed at δ -1.65 ppm that could potentially correspond to a trivalent uranium-phosphinimide complex. However, few comparative examples exist, and this signal cannot be unambiguously assigned without further characterization. Efforts to further investigate and optimize this reaction were abruptly discontinued shortly after these initial results were obtained. If the trivalent homoleptic tris(triphenyl)phosphinimide complex was formed, this new compound could serve as a potent non-aqueous precursor to new trivalent, tetravalent, and pentavalent uranium chemistry. One- and two-electron oxidations of $U[NPPh_3]_3$ could be used to install halide and pseudohalides ligands to generate complexes of the form $[Ph_3PN]_3UX$ and $[Ph_3PN]_3UX_2$. Such low-coordinate, sterically congested phosphinimide complexs could be used to install terminal oxo-, nitride-, and phosphide ligands, and various other metal-ligand multiple bonds.

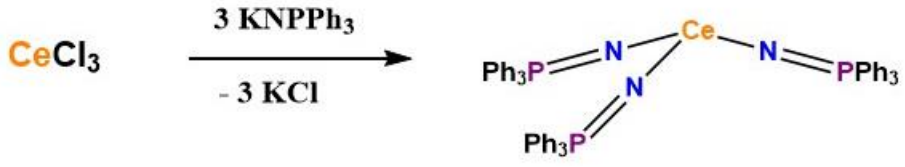

Scheme 2.8: Synthesis of homoleptic cerium tris(phosphinimide) complex.

This chemistry was also extended to cerium(III). Anhydrous $CeCl_3$ was used and purchased, and stirred with three equivalents of $KNPPh_3$ in THF/toluene for a day. An

immediate color change was observed from white to yellow, and the solution became cloudy, indicative of salt formation. The solution was filtered, evaporated to dryness, extracted with toluene, filtered, evaporated to dryness, and dissolved in C_6D_6 for NMR spectroscopy.

Similar to results obtained for uranium(III), the cerium(III) residue also generated broad, paramagnetically shifted peaks near the aromatic region. The extremely broad feature at δ 7.56 ppm is very similar to the broad feature observed for uranium(III) at δ 9.07 ppm. Other signals potentially corresponding to the aromatic protons of a cerium(III) phosphinimide complex were observed at δ 8.23 ppm, δ 7.80 ppm, and δ 7.05 ppm, and signals corresponding to uncoordinated ligand were observed. Cerium(III) is paramagnetic with a f^1 configuration, and paramagnetically-broadened aromatic signals are expected for the target complex. As observed, the magnitude of the dipolar shifts are expected to be less for cerium(III) than uranium(III), since cerium(III) only has one unpaired f-electron, while uranium(III) has three unpaired f-electrons. A deshielded ^{31}P NMR resonance was observed at δ 44.39 ppm, which compares well with the signal at δ 35.34 ppm for the residue obtained via reaction with UCl_4. Both of these resonances fall within the typical rang for transition metal-phosphinimide complexes. Two peaks half the size of the resonance at δ 35.34 were observed at δ 8.62 ppm and δ 5.07 ppm. The peaks observed could be indicative of a mix of products, including bridging and non-bridging species, or the resonances could potentially correspond to different phosphinimide bonding modes. Phosphinimide ligands with an approximately linear

binding mode with strong π-donation of electron density to the metal center are expected to yield more deshielded ^{31}P NMR resonances than bent phosphinimide ligands with little to no π-interactions. Further structural characterization is necessary in order to make any definitive conclusions about the ^{31}P resonances observed.

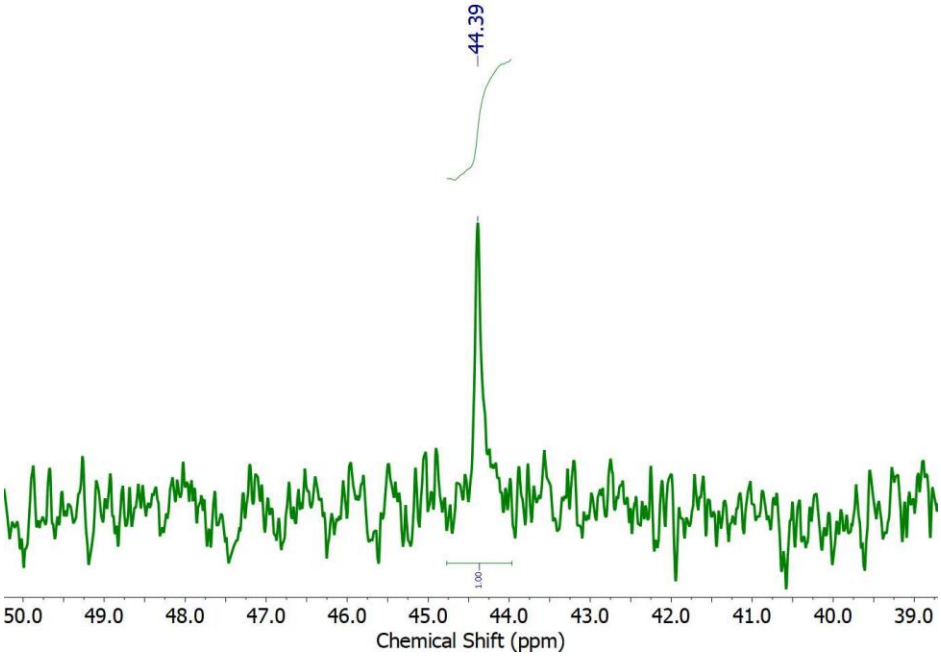

Figure 2.15: ^{31}P NMR spectrum for reaction of $CeCl_3$ and $KNPPh_3$.

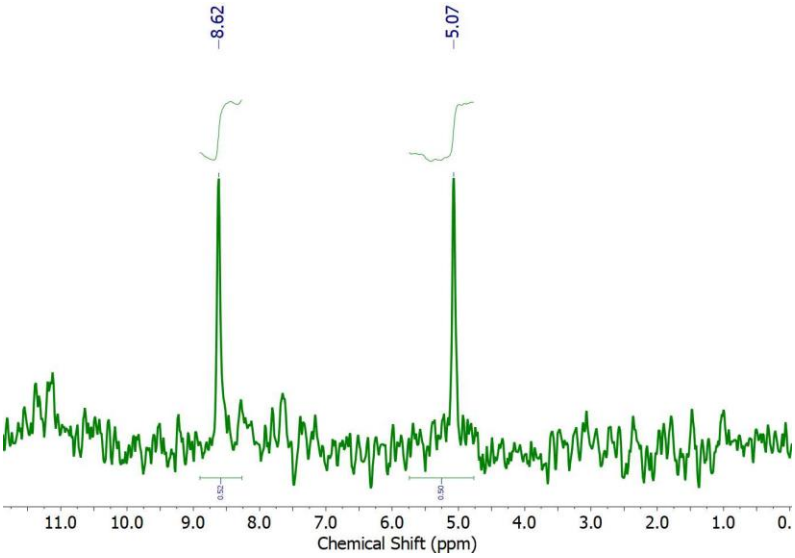

Figure 2.16: ^{31}P NMR spectrum for reaction of $CeCl_3$ and $KNPPh_3$.

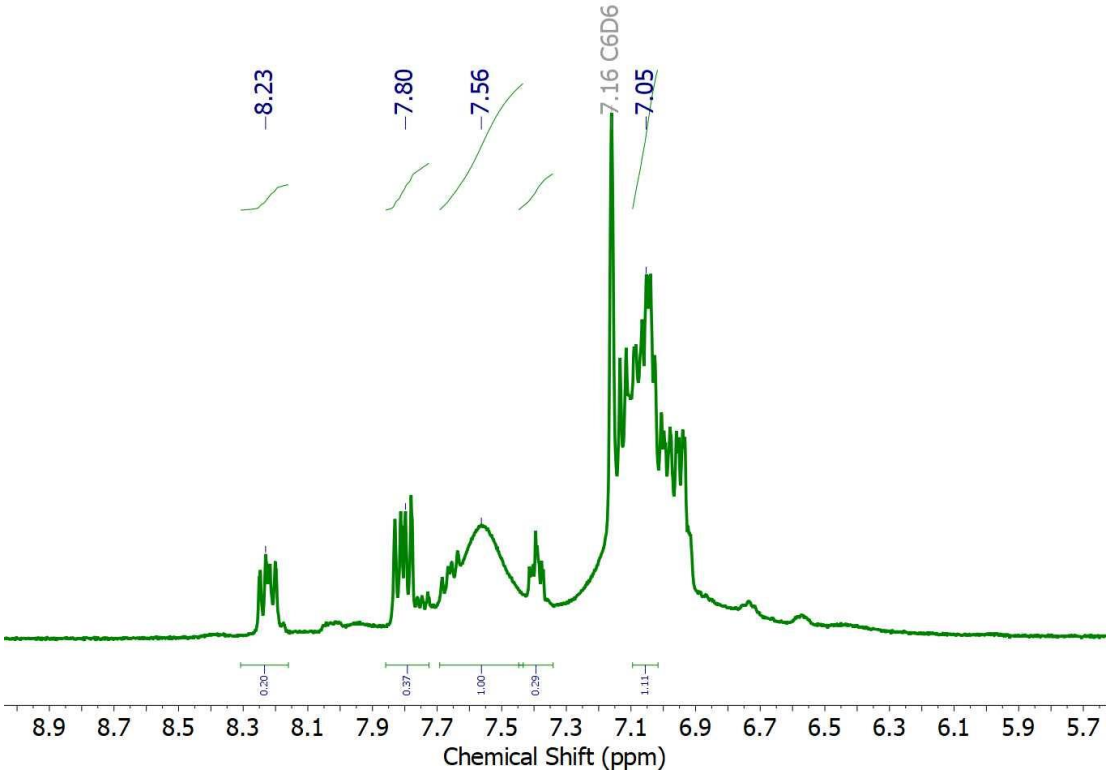

Figure 2.17: ^{1}H NMR spectrum for reaction of $CeCl_3$ and $KNPPh_3$

Concluding Remarks and Future Opportunities

Coordination of a phosphinimide ligand to uranium(IV) results in a large paramagnetic shift as observed in the ^{1}H and ^{31}P NMR spectra of U[N=P(*t*-butyl)$_3$][N(SiMe$_3$)$_2$]$_3$. At first inspection, the shift observed seems much larger than what would be expected due to the pseudocontact contribution alone. The large paramagnetic shift of this complex, 689.23 ppm, suggests a significant contact contribution, presumably due to significant levels of metal-ligand covalency (orbital mixing). Additionally, progress was made toward the synthesis and characterization of homoleptic *f*-element

phosphinimide complexes. This work has yielded promising initial results that indicate ^{31}P NMR spectroscopy and phosphinimide ligands can be useful tools for studying *f*-block electronic structure and metal-ligand covalency.

References

[1] Katz, J.J. and E. Rabinowitch. 1951. *The Chemistry of Uranium*. McGraw-Hill Book Company, New York.

[2] Reynolds, L.T. and G. Wilkinson. 1956. π-Cyclopentadienyl Compounds of Uranium-IV and Thorium-IV. *Journal of Inorganic and Nuclear Chemistry* 2: 246-253.

[3] Morss, L., N.M. Edelstein, J. Fuger. 2006. *Chemistry of the Actinide and Transactinide Elements*. Springer, Berlin.

[4] Tassell, M.J. and N. Kaltsoyannis. 2010. Covalency in AnCp4 (An = Th–Cm): a comparison of molecular orbital, natural population and atoms-in-molecules analyses. *Dalton Transactions* 39: 6719.

[5] Kirker, I. and N. Kaltsoyannis. 2011. Does covalency really increase across the 5f series? A comparison of molecular orbital, natural population, spin and electron density analyses of AnCp3 (An = Th–Cm; Cp = η5-C5H5). *Dalton Transactions* 40: 124.

[6] Kaltsoyannis, Nikolas. 2012. Does Covalency Increase or Decrease across the Actinide Series? Implications for Minor Actinide Partitioning. *Inorganic Chemistry* 52: 3407-3413.

[7] Dognon, Jean-Pierre. 2017. Electronic structure theory to decipher the chemical bonding in actinide systems. *Coordination Chemistry Reviews* 344: 150-162.

[8] Kerridge, Andrew. 2017. Quantification of f-element covalency through analysis of the electron density: insights from simulation. *Chemical Communication* 53: 6685-6695.

[9] Gibson, John K. and Wibe A. de Jong. 2018. *Experimental and Theoretical Approaches to Actinide Chemistry*. John Wiley & Sons, Hoboken.

[10] Lu, Erli, Saira Sajjad, Victoria E.J. Berryman, Ashley J. Wooles, Nikolas Kaltsoyannis, and Stephen Liddle. 2019. Emergence of the structure-directing role of f-orbital overlap-driven covalency. *Nature Communications* 10: 634.

[11] Kaltsoyannis, Nikolas and Andrew Kerridge. 2014. "Chemical Bonding of Lanthanides and Actinides." In *The Chemical Bond: Chemical Bonding Across the Periodic Table*, pp.337-355, edited by Gernot Frenking and Sason Shaik. Wiley-VCH, Weinheim.

[12] Nash, Kenneth L. and Gregory R. Chopin. 1995. *Separations of f-Elements*. Plenum Press, New York.

[13] Nash, Kenneth L., Charles Madic, Jagdish N. Mathur, and Jérôme Lacquement. 2006. Actinide Separation Science and Technology. In *Chemistry of the Actinide and Transactinide Elements,* edited by Morss, L., N.M. Edelstein, and J. Fuger. Springer, Berlin.

[14] Nash, Kenneth L. and Gregg J. Lumetta. 2011. *Advanced separation techniques for nuclear fuel reprocessing and radioactive waste treatment.* Woodhead Publishing Limited, Cambridge.

[15] Barnea, Eyal and Moris S. Eisen. 2006. Organoactinides in Catalysis. *Coordination Chemistry Reviews* 250: 855-899.

[16] Burns, Carol J. and Moris S. Eisen. 2006. Homogenous and Heterogeneous Catalytic Processes Promoted by Organoactinides. In *Chemistry of the Actinide and Transactinide Elements,* edited by Morss, L., N.M. Edelstein, and J. Fuger. Springer, Berlin.

[17] Templeton, David H. and Lieselotte K. Templeton. 1982. X-ray Dichroism and Polarized Anomalous Scattering of the Uranyl Ion. *Acta Crystallographica A* 38: 62-67.

[18] Nugent, W.A. and J. M. Mayer. 1988. *Metal-Ligand Multiple Bonds*. Wiley, New York.

[19] Lin, Zhenyang and Michael B. Hall. 1993. A group theoretical analysis on transition-metal complexes with metal-ligand multiple bonds. *Coordination Chemistry Reviews* 123: 149-167.

[20] Brown, Dean R., Robert G. Denning, and Richard H. Jones. 1994. Synthesis and Crystal Structure of an Analogue of the Uranyl(VI) Ion, containing a Linear O=U=N- Group. *Journal of the Chemical Society*: 2601-2602.

[21] Brown, Dean R. and Robert G. Denning. 1996. Stable Analogs of the Uranyl Ion Containing the -N=U=N= Group. *Inorganic Chemistry* 35: 6158-6163.

[22] Williams, V. Cliff, Matthias Müller, Michael A. Leech, Robert G. Denning, and Malcolm L.H. Green. 2000. Uranium(VI) Sulfilimine Complexes: A New Class of Nitrogen Analogues of the Uranyl Ion. *Inorganic Chemistry* 39: 2538-2541.

[23] Hayton, Trevor W., James M. Boncella, Brian L. Scott, Philip D. Palmer, Enrique R. Batista, and P. Jeffrey Hay. 2005. Synthesis of Imido Analogs of the Uranyl Ion. *Science* 310: 1941-1943.

[24] Denning, Robert G. 2007. Electronic Structure and Bonding in Actinyl Ions and their Analogs. *Journal of Physical Chemistry A* 111: 4125-4143.

[25] Hayton, Trevor W. 2010. Metal-ligand multiple bonding in uranium: structure and reactivity. *Dalton Transactions* 39: 1145-1158.

[26] Fortier, Skye, Guang Wu, and Tevor Hayton. 2010. Synthesis of a Nitrido-Substiuted Analogue of the Uranyl Ion, $[N=U=O]^+$. *Journal of the American Chemical Society* 132: 6888-6889.

[27] Thomson, Robert K., Thibault Cantat, Brian L. Scott, David E. Morris, Enrique R. Batista, and Jaqueline L. Kiplinger. 2010. Uranium azide photolysis results in C-H bond activation and provides evidence for a terminal uranium nitride. *Nature Chemistry* 2: 723-729.

[28] Lu, Erli, Yuxue Li, and Yaofeng Chen. 2010. A scandium terminal imido complex: synthesis, structure and DFT studies. *Chemical Communications* 46: 4469-4471.

[29] Fortier, Skye, Justin R. Walensky, Guang Wu, and Trevor Hayton. 2011. Synthesis of a Phosphorano-Stabilized U(IV)-Carbene via One-Electron Oxidation of a U(III)-Ylide Adduct. *Journal of the American Chemical Society* 133: 6894-6897.

[30] Brown, Jessie L., Skye Fortier, Richard A. Lewis, Guang Wu, and Revor W. Hayton. 2012. A Complete Family of Terminal Uranium Chalcogenides, $[U(E)(N\{SiMe_3\}_2)_3]^-$ (E = O, S, Se, Te). *Journal of the American Chemical Society* 134: 15468-15475.

[31] Hayton, Trevor W. 2013. Recent Developments in actinide-ligand multiple bonding. *Chemical Communications* 49: 2956-2973.

[32] Lewis, Andrew J., Patrick J. Carroll, and Eric J. Schelter. 2013. Reductive Cleavage of Nitrite to Form Terminal Uranium Mono-Oxo Complexes. *Journal of the American Chemical Society* 135: 511-518.

[33] King, D.M., F. Tuna, E.J.L. McInnes, J. McMaster, W. Lewis, A.J. Blake, S.T. Liddle. 2013. Isolation and characterization of a uranium (VI)-nitride triple bond. *Nature Chemistry* 5:482.

[34] Smiles, Danil E., Guang Wu, and Trevor W. Hayton. 2014. Synthesis of Terminal Monochalcogenide and Dichalcogenide Complexes of Uranium Using Polychalcogenides, $[E_n]^{2-}$ (E = Te, n = 2; E = Se, n = 4), as Chalcogen Atom Transfer Reagents. *Inorganic Chemistry* 53: 10240-10247.

[35] Smiles, Danil E., Guang Wu, and Trevor W. Hayton. 2014. Reversible Chalcogen-Atom Transfer to a Terminal Uranium Sulfide. *Inorganic Chemistry* 53: 12683-12685.

[36] Smiles, Danil E., Guang Wu, and Trevor W. Hayton. 2014. Synthesis of Uranium-Ligand Multiple Bonds by Cleavage of a Trityl Protecting Group. *Journal of the American Chemical Society* 136: 96-99.

[37] Anderson, Nickolas H., Samuel O. Odoh, Yiyi Yao, Ursula J. Williams, Brian A Schaefer, John J. Kiernicki, Andrew J. Lewis, Mitchell D. Goshert, Phillip E. Fanwick, Eric J. Schelter, Justin R. Walensky, Laura Gagliardi, and Suzanne C. Bart. 2014. Harnessing redox activity for the formation of uranium tris(imido) compounds. *Nature Chemistry* 6: 919-926.

[38] Bell, Nicola L., Laurent Maron, and Polly L. Arnold. 2015. Thorium Mono- and Bis(imido) Complexes Made by Reprotonation of *cyclo*-Metalated Amides. *Journal of the American Chemical Society* 137: 10492-10495.

[39] Wu, Qun-Yan, Jian-Hui Lan, Cong-Zhi Wang, Yu-Liang Zhao, Zhi-Fang Chai, and Wei-Qun Shi. 2015. Terminal U≡E (E = N, P, As, Sb, and Bi) Bonds in Uranium Complexes: A Theoretical Perspective. *Journal of Physical Chemistry A* 119: 922-930.

[40] Smiles, Danil E., Guang Wu, and Trevor Hayton. 2015. Reactivity of $[U(CH_2SiMe_2NSiMe_3)(NR_2)_2]$ (R = $SiMe_3$) with elemental chalcogens: towards a better understanding of chalcogen atom transfer in the actinides. *New Journal of Chemistry* 39: 7563-7566.

[41] Anderson, Nickolas H., Haolin Yin, John J. Kiernicki, Phillip E. Fanwick, Eric J. Schelter, and Suzanne C. Bart. 2015. Investigation of Uranium Tris(imido) Complexes: Synthesis, Characterization, and Reduction Chemistry of $[U(NDIPP)_3(thf)_3]$. *Angewandte Chemie International Edition* 54: 9386-9389.

[42] Roesky, Herbert W., Kattesh V. Katti, Ulrich Seseke, Uwe Scholz, Regine Herbst, Ernst Egert, and George M. Scheldrick. 1986. Reacktionen von Wolframhexafluorid mit N-Trimethylsilyliminotriphosphoranen – Kristallstruktur von $(Me_3P=N)_2WF_4$. *Zeitschrift für Naturforschungen* 41b: 1509-1512.

[43] Cramer, Roger E., Frank Edelmann, Arthur L. Mori, Steven Roth, John W. Gilje, Kazuyuki Tatsumi, and Akira Nakamura. 1988. Preparation, structure and bonding in an organoactinide imide, $Cp_3AnNPPh_3$ (An = uranium, thorium): a comparison of the bonding of uranium to nitrogen- and oxygen-donor ligands. *Organometallics* 7(4): 841-849.

[44] Dehnicke, Kurt and Joachim Strähle. 1989. Phosphorane Iminato Complexes of Transition Metals. *Polyhedron* 8(6): 707-726.

[45] Nußhär, D., F. Weller, A Neuhaus, G. Frenking, and K. Dehnicke. 1992. Tetrakis(triphenylphosphaniminato)tantalonium-hexachlorotantalat, $[Ta(NPPh_3)_4]TaCl_6$. Synthese, IR-Spektruym, Kristallstruktur und Ab-initio-Rechnungen am $[Ta(NPH_3)_4]^+$-Ion. *Zeitschrift für anorganishe und allgemeine Chemie* 615: 86-92.

[46] Rentschler, Eva, Dirk Nußhär, Frank Weller, and Kurt Dehnicke. 1993. $[W(NPPh_3)_4]Cl_2$ – ein Phosphaniminato-Komplex mit einem Wolfram-Dikation. *Zeitschrift für anorganishe und allgemeine Chemie* 619: 999-1003.

[47] Johnson, A. William. 1993. *Ylides and Imines of Phosphorus*. John Wiley & Sons, Inc. New York.

[48] Dehnicke, Kurt and Frank Weller. 1997. Phosphorane iminato complexes of main group elements. *Coordination Chemistry Reviews* 158: 103-169.

[49] Anfang, S., G. Seybert, K. Harms, G. Geiseler, W. Massa, and K. Dehnicke. 1998. Reacktionen von $LiNPPh_3$ mit den Cyclooctatetraenid-Komplexen $[Ln(C_8H_8)Cl(THF)_2]_2$ von Cer und Samarium. Die Kristallstrukturen von $[LiNPPh_3]_6$, $[Ln(C_8H_8)Li_3Cl_2(NPPh_3)_2(THF)_3]$ (Ln = Ce, Sm) und $[Li(THF)_4][Sm(C_8H_8)_2]$. *Zeitschrift für anorganishe und allgemeine Chemie* 624: 1187-1192.

[50] Anfang, S., K. Harms, F. Weller, O. Borgmeier, H. Lueken, H. Schilder, and K. Dehnicke. 1998. Phosphaniminato-Komplexe Seltener Erden. Synthese und Kristallstrukturen von $[M_2(C_5H_5)_3(NPPh_3)_3 \cdot 3\ C_7H_8$ mit M = Y, Dy und Er. Magnetische Eigenschaften von $[Dy_2(C_5H_5)_3(NPPh_3)_3 \cdot 3\ C_7H_8$. *Zeitschrift für anorganishe und allgemeine Chemie* 624: 159-166.

[51] Dehnicke, Kurt, Matthais Krieger, and Werner Massa. 1999. Phosphoraneiminato complexes of transition metals. *Coordination Chemistry Reviews* 182: 19-65.

[52] Chitsaz, Soheila, Bernhard Neumüller, and Kurt Dehnicke. 1999. Synthese und Kristallstruktur von $[KNPPh_3]_6 \cdot 4\ C_7H_8$. *Zeitschrift für anorganishe und allgemeine Chemie* 625: 9-10.

[53] Stewart, Jeffrey Charles. 2000. *Phosphinimide Complexes of Titanium: Synthesis and Reactivity Studies of a New Family of Organometallic Compounds*. Ph.D. Dissertation, University of Windsor, Windsor, Canada.

[54] Gröb, Thorsten, Gert Seybert, Werner Massa, Frank Weller, Ravi Palaniswami, Andreas Geiner, and Kurt Dehnicke. 2000. Homoleptic Phosphoraniminato Complexes of Rare Earth Elements as Initiators for Ring-Opening Polymerization of Lactones. *Angewandte Chemie International Edition* 39(23): 4373-4375.

[55] Kaltsoyannis, Nikolas. 2000. Computational Study of Analogues of the Uranyl Ion Containing the -N=U=N- Unit: Density Functional Theory Calculations on UO_2^{2+}, UON^+, UN_2, $UO(NPH_3)^{3+}$, $U(NPH_3)_2^{4+}$, $[UCl_4\{NPR_3\}_2]$ (R = H, Me), and $[UOCl_4\{NP(C_6H_5)_3\}]^-$. *Inorganic Chemistry* 39: 6009-6017.

[56] Gröb, Thorsten, Klaus Harms, and Kurt Dehnicke. 2000. Alkalimetall-Phosphaniminate. Neue Synthesen und die Kristallstrukturen von $[RbNPPh_3]_6$ und $[CsNPPh_3]_4$. *Zeitschrift für anorganishe und allgemeine Chemie* 626: 1065-1072.

[57] Gröb, Thorsten, Klaus Harms, and Kurt Dehnicke. 2001. Phosphaniminato-Komplexe des Hafniums. Die Kristallstrukturen von $[Hf(NPPh_3)_4] \cdot 3$ THF und $[Hf(NPPh_3)_2Cl_2(HNPPh_3)_2]$. *Zeitschrift für anorganishe und allgemeine Chemie* 627: 1801-1806.

[58] Ravi, Palaniswamy, Thorsten Gröb, Kurt Dehnicke, and Andreas Greiner. 2001. Ring-Opening Polymeriztion of ε-Caprolactone by Phosphorane Iminato and Cyclopentadienyl Complexes of Rare Earth Elements. *Macromolecular Chemistry and Physics* 202: 2641-2647.

[59] Gröb, Thorsten, Gert Seybert, Werner Massa, and Kurt Dehnicke. 2001. $Cs[Yb(NPPh_3)_4]$ – ein homoleptischer Phosphaniminato-Komplex des Ytterbiums. *Zeitschrift für anorganishe und allgemeine Chemie* 627: 304-306.

[60] Gröb, Thorsten, Christoph Müller, W. Massa, Thomas Miekisch, Gert Seybert, Klaus Harms, and Kurt Dehnicke. 2001. Die Kritallstruckturen der Phosphinimin-Komplexe $[NaI(HNPPh_3)_3]$ und $[SrI_2(HNPPh_3)_2(THF)_2]$ sowie des Natrium-triphenylphosphaniminats $[NaNPPh_3]_6$. *Zeitschrift für anorganishe und allgemeine Chemie* 627: 2191-2197.

[61] Gröb, Thorsten, Soheila Chitsaz, Klaus, and Kurt Dehnicke. 2002. Phospaniminate von Alkalimetallen: Die Kristallstrukturen von $[KNPCy_3]_4$, $[KNPCy_3]_4 \cdot 2OPCy_3$, $[CsNPCy_3]_4 \cdot 4OPCy_3$ and $[Li_4(NPPh_3)(OSiMe_2NPPh_3)_3(DME)]$. *Zeitschrift für anorganishe und allgemeine Chemie* 628: 473-479.

[62] Dehnicke, Kurt and Andreas Greiner. 2003. Unusual Complex Chemistry of Rare Earth Elements: Large Ionic Radii-Small Coordination Numbers. *Angewandte Chemie International Edition* 42: 1340-1354.

[63] Stephan, Douglas W., Jeffrey C. Stewart, Frédéric Guérin, Silke Courtenay, James Kickham, Emily Hollink, Chad Beddie Aaron Hoskin, Todd Graham, Pingrong Wei, Rupert E. v.H. Spence, Wei Xu, Linda Koch, Xiaoliang Gao, and Daryll G. Harrison. 2003. An Approach to Catalyst Design: Cyclopentadienyl-Titanium Phosphinimide Complexes in Ethylene Polymerization. *Organometallics* 22: 1937-1947.

[64] Gauthier, Jeremy Michael Anthony. 2012. *Titanacyclobutene and Cobalt(II) Phosphimide Complexes*. Ph.D. Dissertation, University of Alberta, Edmonton.

[65] Robinson, Thomas P., Richard D. Price, Matthew Davidson, Mark A. Fox, and Andrew L. Johnson. 2015. Why are the $\{Cu_4N_4\}$ rings in copper(I) phosphinimide clusters $[Cu\{\mu\text{-}N{=}PR_3\}]_4$ (R = NMe_3 or Ph) planar? *Dalton Transactions* 44: 5611-5619.

[66] Corbridge, D.E.C. 2013. Metallophosphorus Compounds. Chapter 8 in *Phosphorus: Chemistry, Biochemistry, and Technology*. CRC Press, Boca, Raton.

[67] Staudinger, H. and Jules Meyer. 1919. Über neue organische Phosphorverbindungen III. Phosphinmethylenderivate und Phosphinimine. *Helvetica Chimica Acta* 2: 635-46.

[68] Staudinger, H. and Ernst Hauser. 1921. Über neue organische Phosphorverbindungen IV. Phosphinimine. *Helvetica Chimica Acta* 4: 861-86.

[69] Appel, Rolf and Alfred Hauss. 1960. Phosphin-iminium-chloride and Triphenylphosphin-imin. *Chemische Berichte* 93: 405-411.

[70] Claydon, Ann P., P.A. Fowell, and C.T. Mortimer. 1960. Heats of Formation and Bond Energies. Part III. Trimethylphosphine Oxid, N-ethyltrimthylphosphinimine, and N-ethyltriphenylphosphine Imine. *Journal of the Chemical Society* 1960, 3284-3287.

[71] Appel, Rolf and Alfred Hauss. 1961. Zur Kenntis nichtmetallischer Imin-Verbindungen. VII. Über einige Reaktionen des Triphenylphosphinimins und des Triphenylphosphin-bromimins. *Zeitschrift für anorganische und allgemeine Chemie* 311: 290-301.

[72] Birkofer, Leonhard, Alfred Ritter and Paul Richter. 1963. Thermolyse silylierter Tetrazole. *Chemische Berichte* 96(10): 2750-2757.

[73] Appel, Rolf and Günter Büchler. 1963. Zur Kenntnis nichtmetallischer Imin-Verbinungen. XV. Über Triphenylphosphin-N-halogenimine. *Zeitschrift für anorganische und allgemine Chemie* 320: 3-10.

[74] Birkofer, Leonhard and Sung Man Kim. 1964. Notiz zur Darstellung von Trialkylphosphin-iminen. *Chemische Berichte* 97: 2100-2101.

[75] Birkofer, L. and A. Ritter. 1965. New Methods of Preparative Organic Chemistry IV. The Use of Silylation in Organic Synthesis. *Angewandte Chemie International Edition* 4(5): 417-429.

[76] Schmidbaur, Hubert and Werner Wolfsberger. 1967. Alkylmetallkomplexe von *N*-Silyl-phosphiniminen. *Chemische Berichte* 100: 1000-1015.

[77] Schmidbaur, Hubert and Gerhard Jonas. 1967. Lithium-triorganophosphinimide. *Chemische Berichte* 100: 1120-1128.

[78] Lutskii, A.E., Z.A. Shevchenko, L.I. Smarai, and A.M. Pinchuk. 1967. The Participation of Phosphorus d-Orbitals in the Formation of π-Bonds and in

Conjugation with π-Electron Systems. 1. Vibrational-Electronic Spectra of Compounds with P=O and P=N Bonds. *Zhurnal Obshchei Khimii* 37(9): 2034-2042.

[79] Schmidbaur, Hubert and Gerhard Jonas. 1968. Beiträge zur Chemie der Iminotrialkylphosphorane. *Chemische Berichte* 101: 1271-1285.

[80] Stepanov, B.I. and T.G. Edel'man. 1969. Electronic Absorption Spectra of Aryldiethylphosphazoaryls. The Participation of the P=N Group in Conjugation. *Zhurnal Obshchei Khimii* 39(7): 1549-1551.

[81] Zhmurova, I.N., R.I. Yurchenko, and A.V. Kirsanov. 1971. Auxochromic Action of the Phosphoranylideneamino Group. V. *Zhurnal Obshchei Khimii* 41(4): 778-781.

[82] Ross, Bernd and Klaus-Peter Reetz. 1974. Die Ammonolyse von Organykphosphoranen. *Chemische Berichte* 107: 2720-2729.

[83] Buchner, Wolfgang and Werner Wolfsberger. 1974. ^{31}P- und ^{13}C-Kernresonanzunterschungen an N-Trimethylsilyl-triorganophosphiniminen. *Zeitschrift für Naturforschung* 29b: 328-334.

[84] Shtepanek, A.S., L.M. Tochilkina, and A.V. Kirsanov. 1975. N-Unsubstituted Phosphine Imides. *Zhurnal Obshchei Khimii* 45(10): 2117-2119.

[85] Buder, W. and A Schmidt. 1975. Infrarot-Spektren von Carbamoyl-triphenylphosphiniminen. *Spectrochimica Acta* 31A: 1813-1818.

[86] Shtepanek, A.S., V.A. Zasorina, I.N. Zhmurova, and A.P. Martynyuk. 1975. Phosphorylation of P, P, P-Triphenylphosphine Imide. *Zhurnal Obshchei Khimii* 45(5): 1012-1015.

[87] Wolfsberger, Werner. 1978. Tri(*tert*-butyl)phosphinimin. *Zeitschrift für Naturforschung* 33b: 1452-1456.

[88] Abel, E.W. and S.A. Mucklejohn. 1981. The Chemistry of Phosphinimines. *Phosphorus and Sulfur and the Related Elements* 9(3): 235-266.

[89] Gololobov, Yu.G., I.N. Zhmurova, and L.F. Kasukhin. 1981. Sixty Years of Staudinger Reaction. *Tetrahedron* 37: 437-472.

[90] Egorov, Yu. P., A. A. Kudryavtsev, A. M. Pinchuk, A. P. Marchenko, and V. A. Kovenya. 1982. The Structure and δ^{31}P Chemical Shifts of Phosphazoalkanes [Alykliminophosphoranes]. *Teoreticheskaya I Éksperimental'naya Khimiya* 18(1): 58-65.

[91] Egorov, Yu. P. and I. V. Tsymbal. 1982. Electronic Interactions of Substituents in Phosphazo Compounds and their Electron-Donor Capacity. *Teoreticheskaya I Éksperimental'naya Khimiya* 18(5): 558-564.

[92] Koidan, G.N., A.P. Marchenko, A.A. Kudryavtsev, and A.M. Pinchuk. 1982. Some Properties of Phosphorimidic Triamides. *Zhurnal Obshchei Khimii* 52(9): 2001-2011.

[93] Egorov, Yu. P., A.A. Kudryavtsev, V.P. Prokopenko, and G.N. Koidan. 1983. Effect of Substituents at Phosphorus Atoms on Basicity of Phosphazo Compounds. *Teoreticheskaya I Éksperimental'naya Khimiya* 19(3): 312-318.

[94] Egorov, Yu. P. and A. A. Kudryavtsev. 1983. Structures, δ^{31}P Chemical Shifts, and ν(P=N) Frequencies. *Zhurnal Obshchei Khimii* 53(10): 2222-2228.

[95] Gonbeau, Danielle, Geneviève Pfister-Guillouzo, Marie-Rose Mazières, and Michel Sanchez. 1985. La liaison phosphore – azote. Étude quantochimique de modèles neutres et ioniques H_3PNH, $H_3PNH_2^+$, $H_2PNH_3^+$, H_2PNH^- et $HPNH_2^-$. *Canadian Journal of Chemistry* 63: 3242-3248.

[96] Cristau, H.J., L. Chiche, J. Kadoura, and E. Torreilles. 1988. L'aza-Ylure N-Lithue $(C_6H_5)_3P{=}NLi$. Reactif D'Amination. *Tetrahedron Letters* 29(32): 3931-3934.

[97] Power, William P., Roderick E. Wasylishen, and Ronald D. Curtis. 1989. Phosphorus-31 solid-state nuclear magnetic resonance study of monophosphazenes. *Canadian Journal of Chemistry* 67: 454-459.

[98] Gudat, D., H.M. Schiffner, M. Nieger, D. Stalke, A.J. Blake, H. Grondey, and E. Niecke. 1992. Coordination Isomerism in Pentamethylcyclopentadienyl-Substituted Iminophosphanes: From Classical Structures to a π-Complexed Iminophosphenium Ion. *Journal of the American Chemical Society* 114: 8857-8862.

[99] Gololobov, Yuri G. and Leonid F. Kasukhin. 1992. Recent Advances in the Staudinger Reaction. *Tetrahedron* 48(8): 1353-1406.

[100] Bricklebank, Neil, Stephan M. Godfrey, Anthony G. Mackie, Charles A. McAuliffe, Robin G. Pritchard, and Peter J. Kobryn. 1993. Diiodophorphoranes. Synthesis and Structure in the Solid State and in Solution. *Journal of the Chemical Society Dalton Transactions* 1993: 101-103.

[101] Goumri, Stéphanie, Francis Lacassin, Antoine Baceiredo, and Guy Bertrand. 1996. Synthesis and Multinuclear NMR Characterization of Iminophosphoranyl Phosphines and Silanes. *Heteroatom Chemistry* 7(6): 403-407.

[102] Steiner, Alexander, Stefano Zacchini, Philip I. Richards. 2002. From neutral iminophosphoranes to multanionic phosphazenates. The coordination chemistry of imino-aza-P(V) ligands. *Coordination Chemistry Reviews* 227: 193-216.

[103] Lu, Wen Cai and Chia Chung Sun. 2002. The substituent effect upon the iminophosphorane X_3PNH for X = F, Cl, Br, H, CH_3, C_6H_5, CH_3CH_2, and $(CH_3)_3C$. *Journal of Molecular Structure* 593: 1-7.

[104] Kolomeitsev, Alexander A., Iimas A Kppel, Toomas Rodima, Jan Barten, Enno Lork, Gerd-Volker Röschenthaler, Ivari Kaljurand, Agnes Kütt, Ivar Koppel, Vahur Mäemets and Ivo Leito. 2005. Guanidinophosphazenes: Design, Synthesis, and Basicity in THF and in the Gas Phase. *Journal of the American Chemical Society* 127: 17656-17666.

[105] Rahier, Nicolas J., Jean-Noël Volle, Marie Agnès Lacour, and Marc Taillefer. 2008. Reactivity of Ph_3PNLi towards P^{III} and P^{V} electrophiles. *Tetrahedron* 64: 6645-6650.

[106] Gorlov, Mikhail V., Nikolay S. Bredov, Andrey S. Esin, and Vyacheslav V. Kireev. 2016. A direct synthesis of $Cl_3P{=}NSiMe_3$ from PCl_5 and hexamethyldisilazane. *Journal of Organometallic Chemistry* 818: 82-84.

[107] Shriver, D.F. 1969. *The Manipulation of Air-sensitive Compounds*. Robert E. Krieger Publishing Company, Malabar.

[108] Jolly, William L. 1970. *The Synthesis and Characterization of Inorganic Compounds*. Prentice-Hall, Inc., Englewood Cliffs.

[109] Barton, Charles J. 1963. Glove Box Techniques. Chapter 4 in *Technique of Inorganic Chemistry* by C.J. Barton, W.W. Brandt, J.F. Hamilton, and D.C. Stewart, edited by Hans B. Jonassen and Arnold Weissberger. Interscience Publishers, New York.

[110] Errington, R. J. 1997. *Advanced Practical Inorganic and Metalorganic Chemistry*. Blackie Academic & Professional, London.

[111] Monreal, M.J., R.K. Thomson, T. Cantat, N.E. Travia, B.L. Scott, J.L. Kiplinger. 2011. UI_4(1,4-dioxane)$_2$, [UCl_4(1,4-dioxane)]$_2$, and UI_3(1,4-dioxane)$_{1.5}$: Stable and Versatile Starting Materials for Low- and High-Valent Uranium Chemistry. *Organometallics* 30:2031.

[112] Cantat, Thibault, Brian L. Scott, and Jaqueline L. Kiplinger. 2010. Convenient access to the anhydrous thorium tetrachloride complexes $ThCl_4(DME)_2$, $ThCl_4$(1,4-dioxane)$_2$ and $ThCl_4(THF)_{3.5}$ using commercially available and inexpensive starting materials. *Chemical Communications* 46: 919-921.

[113] Kiplinger, Jaqueline L., David E. Morris, Brian L. Scott, and Carol J. Burns. 2002. Convenient Synthesis, Structure, and Reactivity of $(C_5Me_5)U(CH_2C_6H_5)_3$: A Simple Strategy for the Preparation of Monopentamethylcyclopentadienyl Uranium(IV) Complexes. *Organometallics* 21(26): 5978-5982.

[114] Karmel, Isabell S.R., Natalia Fridman, Matthias Tamm, and Moris S. Eisen. 2014. Mono(imidazoline-2-iminato) Actinide Complexes: Synthesis and Application in the Catalytic Dimerization of Aldehydes. *Journal of the American Chemical Society* 136: 17180-17192.

Chapter 3

Explorations in Tetravalent Cerium Chemistry

Introduction

In this chapter, reactions of *N*-trimethylsilyl phosphinimines with $CeF[N(SiMe_3)_2]_3$ are reported. $CeF[N(SiMe_3)_2]_3$ has great potential to expand molecular Ce(IV) chemistry. However, this potential has yet to be realized. First reported in 2014 [1], the nucleophilicity of the fluoride ligand in $CeF[N(SiMe_3)_2]_3$ was demonstrated using halide exchange reactions via fluorotrimethylsilane elimination [2]. Virtually no progress has been reported on the reactivity of $CeF[N(SiMe_3)_2]_3$ since 2014. In this work, we took the logical next step of exploring other fluorotrimethylsilane elimination reactions in an effort to expand the chemistry of $CeF[N(SiMe_3)_2]_3$. Specifically, we investigated the reactivity of $CeF[N(SiMe_3)_2]_3$ with *N*-trimethylsilyl phosphinimines, $R_3PNSiMe_3$, with the intention of synthesizing Ce(IV) phosphinimide complexes via fluorotrimethylsilane elimination. The installation of phosphinimide ligands to Ce(IV) provides a unique opportunity to study the uranium-like covalency that has been observed in molecular Ce(IV) complexes [3,4]. The presence of the phosphorus atom in phosphinimide ligands provides the opportunity to study metal-ligand covalency using phosphorus nuclear magnetic resonance spectroscopy (^{31}P NMR). In this chapter, the synthesis and NMR spectroscopy of molecular Ce(IV) phosphinimide complexes are reported.

Fluorotrimethylsilane elimination has been used previously to install phosphinimide ligands on hexavalent tungsten [5] and has also been used to install metal-ligand multiple bonds [6]. Phosphinimide ligands exhibit multiple bond character due to π-interactions, and these monoanionic ligands can engage in three-fold bonding interactions, particularly when the metal-nitrogen-phosphorus angle is approximately linear [7]. Dehnicke and co-workers have reported cerium metallocene-phosphinimide complexes [8], and Dehnicke has reviewed phosphinimide chemistry on multiple occasions [7, 9-11]. Cerium amide-phosphinimide complexes have not been reported, and no homoleptic cerium phosphinimide complexes have been reported. Homoleptic phosphinimide complexes of other rare earth elements and transition metals have been reported [10,11].

Halide exchange reactions via fluorotrimethylsilane elimination have been reported for $CeF[N(SiMe_3)_2]_3$ [2]. The syntheses of $CeCl[N(SiMe_3)_2]_3$, $CeBr[N(SiMe_3)_2]_3$, and $CeI[N(SiMe_3)_2]_3$ using fluorotrimethylsilane elimination reactions of $ClSiMe_3$, $BrSiMe_3$, and $ISiMe_3$ with $CeF[N(SiMe_3)_2]_3$ were reported in 2014 by Schelter and co-workers in 2014 [2]. These cerium(IV) amide-halide complexes have great potential to push the field of molecular tetravalent cerium chemistry forward. $CeF[N(SiMe_3)_2]_3$ can serve as a gateway to numerous new complexes via fluorotrimethylsilane elimination reactions, and $CeCl[N(SiMe_3)_2]_3$, $CeBr[N(SiMe_3)_2]_3$, and $CeI[N(SiMe_3)_2]_3$ and can serve as gateways to numerous new complexes via salt metathesis reactions [2]. These cerium(IV) amide-halide complexes have great potential as molecular precursors to advanced

cerium(IV) materials. Furthermore, cerium(IV) is considered to be a suitable plutonium(IV) model because of their similar ionic radii (Ce^{4+}, 0.87 Å; Pu^{4+}, 0.86 Å) and similar chemical behavior [12]. These cerium(IV) amide-halide complexes, and complexes derived from these precursors, can be used to indirectly study plutonium(IV).

Cerium(IV) has a closed-shell configuration, and its compounds are typically colorless [13]. In fact, cerium(IV) oxide is very important in the glass industry due to this property [14]. However, $CeF[N(SiMe_3)_2]_3$ and other molecular tetravalent organometallic/inorganometallic complexes of cerium are highly colored [15,16]. This can be attributed ligand-to-metal charge transfer [1]. Herein the syntheses and NMR spectroscopy of highly colored, red-orange, cerium(IV) tris(amido) phosphinimide complexes, $Ce[NPR_3][N(SiMe_3)_2]_3$, are reported.

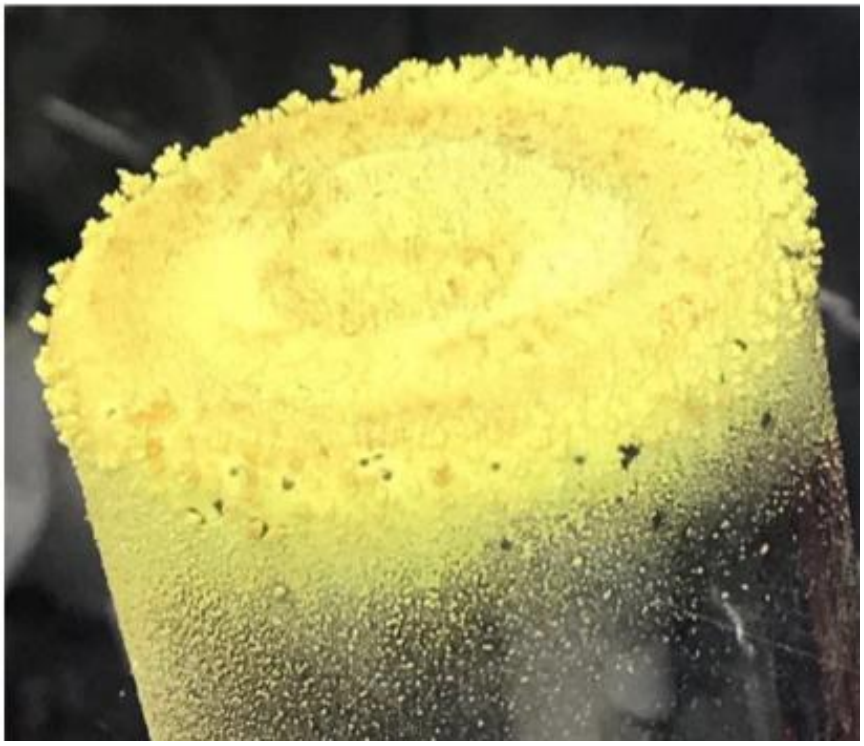

Figure 3.1: Sublimed $Ce[N(SiMe_3)_2]_3$

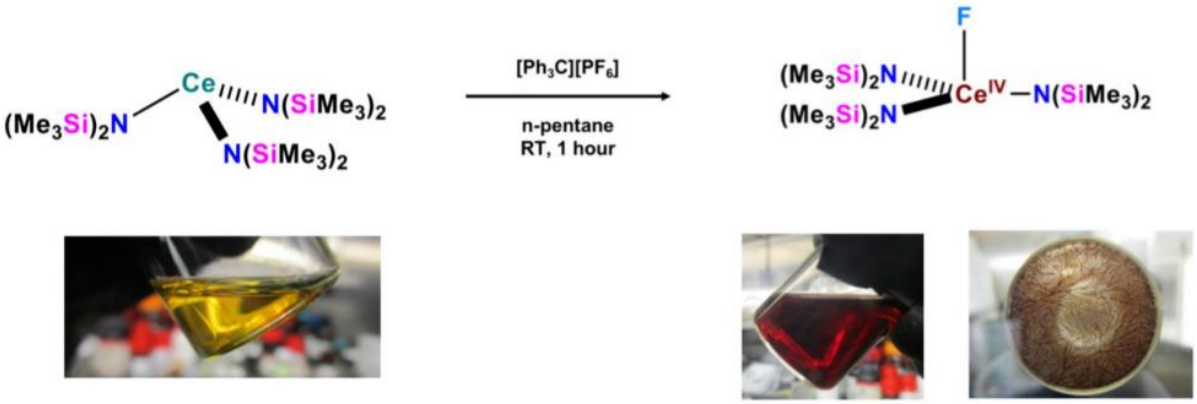

Scheme 3.1: Synthesis of $CeF[N(SiMe_3)_2]_3$

Experimental

All experimental operations were conducted with rigorous exclusion of air and moisture using Schlenk techniques and standard glove-box methods using a Vacuum Atmospheres glovebox with a recirculating dinitrogen atmosphere. Solvents were bought anhydrous or HPLC-grade (pentane, hexane, toluene, acetonitrile) and further purified using a Vacuum Atmospheres Solvent Purifier System. Tetrahydrofuran and diethyl ether were dried over sodium benzophenone ketyl, and degassed using three freeze-pump-thaw cycles prior to use. All solvents were stored under dinitrogen in a glove-box, and stored over 4 Å molecular sieves for at least 24 hours prior to use. Glassware was dried at 150°C before use. ^{1}H and ^{31}P NMR spectra were recorded using a Bruker 400 MHz spectrometer at 298 K. Deuterated benzene (Cambridge Isotopes) was stored over 4 Å molecular sieves for at least 24 hours prior to use.

$CeCl_3$ (anhydrous) , $PrCl_3$ (anhydrous), $KN(SiMe_3)_2$, XeF_2 were used as purchased (Aldrich). *N*-trimethylsilyl phosphinimines were synthesized using literature methods [17] from commercially available tertiary phosphines and azidotrimethylsilane (Aldrich). $Ce[N(SiMe_3)_2]_3$ and $Pr[N(SiMe_3)_2]_3$ were prepared as previously reported [18-22] and sublimed prior to use. $CeF[N(SiMe_3)_2]_3$ was prepared as previously reported [1].

Synthesis of $Ce[NPCy_3][N(SiMe_3)_2]_3$

0.006 grams (0.009 mmol) of $CeF[N(SiMe_3)_2]_3$ was dissolved in 5 mL of THF. 0.004 grams (0.009 mmol) of $Me_3Si\text{-}N{=}PCy_3$ was dissolved in 5 mL of THF and added to the $CeF[N(SiMe_3)_2]_3$ solution dropwise at room temperature. The solution was stirred

overnight at room temperature. The THF was removed *in vacuo* and a red solid was afforded (0.010 grams). The solid was redissolved in C_6D_6 for NMR analysis.

^{1}H *NMR Data* (C_6D_6, 298 K): δ 0.39 ppm ($SiMe_3$), δ 1.1-1.86 ppm (cyclohexyl).
^{31}P *NMR Data* (C_6D_6, 298 K): δ 637.34 ppm.

Synthesis of Ce[NP(*p*-anisyl)$_3$][N($SiMe_3$)$_2$]$_3$

0.021 grams (0.033 mmol) of CeF[N($SiMe_3$)$_2$]$_3$ was dissolved in 5 mL of THF. 0.015 grams (0.033 mmol) of Me_3Si-N=P(*p*-MeOPh)$_3$ was dissolved in 5 mL of THF and added to the CeF[N($SiMe_3$)$_2$]$_3$ solution dropwise at room temperature. The dark-red solution quickly changed color to a transparent cherry-red, and the solution was stirred overnight at room temperature. The THF was removed *in vacuo* and a red solid was afforded in 94% yield (0.030 grams). The solid was redissolved in C_6D_6 for NMR analysis.

^{31}P *NMR Data* (C_6D_6, 298 K): δ 636.79 ppm.

Attempted Synthesis of Ce[NP(*p*-tolyl)$_3$][N($SiMe_3$)$_2$]$_3$

0.017 grams (0.027 mmol) of CeF[N($SiMe_3$)$_2$]$_3$ was dissolved in 10 mL of THF. 0.011 grams (0.027 mmol) of Me_3Si-N=P(*p*-tolyl)$_3$ was dissolved in 5 mL of THF and added to the CeF[N($SiMe_3$)$_2$]$_3$ solution dropwise at room temperature. The solution was stirred overnight at room temperature. The THF was removed *in vacuo* and a red solid was afforded (0.026 grams). The solid was redissolved in C_6D_6 for NMR analysis. NMR data was inconclusive.

Attempted Synthesis of Ce[NP(*t*-butyl)$_3$][N(SiMe$_3$)$_2$]$_3$

0.050 grams (0.078 mmol) of CeF[N(SiMe$_3$)$_2$]$_3$ was dissolved in 10 mL of THF. 0.023 grams (0.079 mmol) of Me$_3$Si-N=P(*t*-butyl)$_3$ was dissolved in 5 mL of THF and added to the CeF[N(SiMe$_3$)$_2$]$_3$ solution dropwise at room temperature. The solution was stirred overnight at room temperature. The THF was removed *in vacuo* and a red solid was afforded. The solid was redissolved in C_6D_6 for NMR analysis.

Attempted Synthesis of PrF[N(SiMe$_3$)$_2$]$_3$

0.031 grams (0.500 mmol) of Pr[N(SiMe$_3$)$_2$]$_3$ was dissolved in 10 mL of pentane. 0.005 grams (0.025 mmol) of XeF_2 was added to the Pr[N(SiMe$_3$)$_2$]$_3$ solution at room temperature. No color change was observed. After 3 hours the pentane was removed *in vacuo*, and the solid was sealed and stored for further characterization.

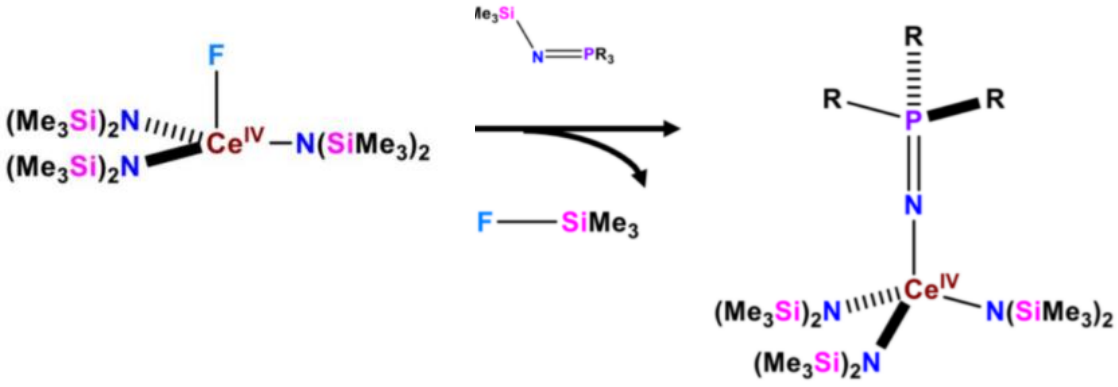

Scheme 3.2: General Synthesis of Ce[NPR$_3$][N(SiMe$_3$)$_2$]$_3$ via Fluorotrimethylsilane Elimination.

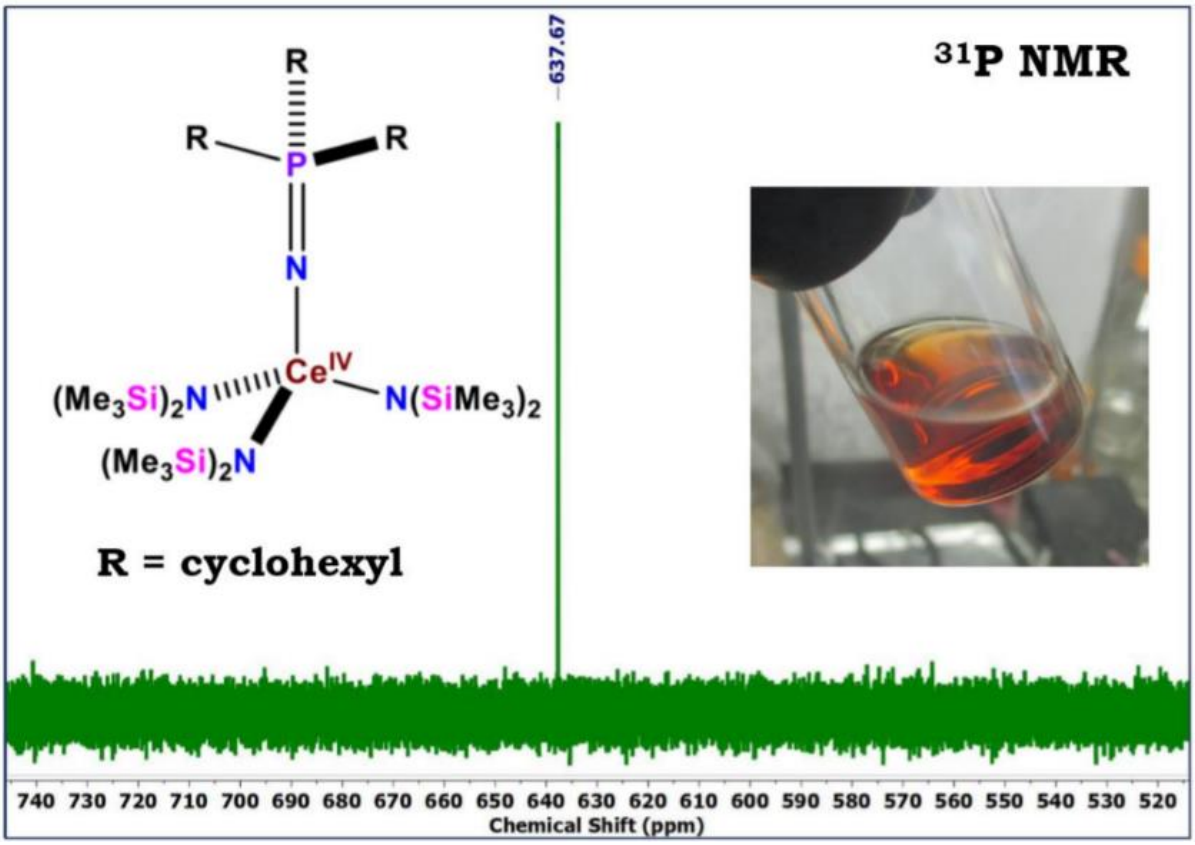

Figure 3.2: ^{31}P NMR spectrum for Ce[NPCy$_3$][N(SiMe$_3$)$_2$]$_3$.

Results and Discussion

Reactions were carried out between *N*-trimethylsilyl phosphinimines and CeF[N(SiMe$_3$)$_2$]$_3$, and solution phase ^{1}H, ^{19}F, and ^{31}P NMR analyses of the resulting residues suggest partial formation of cerium(IV) phosphinimide complexes, Ce[NPR$_3$][N(SiMe$_3$)$_2$]$_3$. The formation of the remarkably strong Si-F bond in F-SiMe$_3$ provides the thermodynamic driving force for these reactions [2,7]. Because fluorotrimethylsilane is volatile, this by-product can be conveniently removed under reduced pressure [7]. These reactions can also be conveniently monitored by ^{1}H, ^{19}F, and ^{31}P NMR.

Anhydrous $CeCl_3$ was stirred with 2.99 equivalents of $KN(SiMe_3)_2$ in THF/toluene (1:1) at room temperature for 24 hours, yielding the well-known trivalent tris(silylamide) complex, $Ce[N(SiMe_3)_2]_3$. After filtering off the KCl by-products, extracting with pentane, and evaporating to dryness, this volatile three-coordinate complex can be purified via sublimation under vacuum at 90-100°C. This high-symmetry precursor was oxidized to $CeF[N(SiMe_3)_2]_3$ using triphenylcarbenium hexafluorophosphate, $[Ph_3C][PF_6]$. $CeF[N(SiMe_3)_2]_3$ has only recently been reported (2014), and this compound is very understudied. Schelter and coworkers reported halide exchange reactions of $CeF[N(SiMe_3)_2]_3$ with X-$SiMe_3$ to form $CeX[N(SiMe_3)_2]_3$ (X = Cl, Br, I) via fluorotrimethylsilane (F-$SiMe_3$) elimination. Inspired by these results, we attempted to extend the fluorotrimethylsilane elimination chemistry of $CeF[N(SiMe_3)_2]_3$ to *N*-trimethylsilyl-substituted phosphinimines (Me_3Si-NPR_3) with the intention of synthesizing tris(silylamido)-phosphinimide complexes of cerium(IV), $Ce[NPR_3][N(SiMe_3)_2]_3$. Fluorotrimethylsilane elimination has been used to synthesize tungsten(VI)-phosphinimide complexes, and chlorotrimethylsilane elimination has been used to synthesize uranium(VI)-phosphinimide complexes. Given these previous reports, we were confident that fluorotrimethylsilane elimination would be a suitable strategy for synthesizing cerium(IV)-phosphinimide complexes.

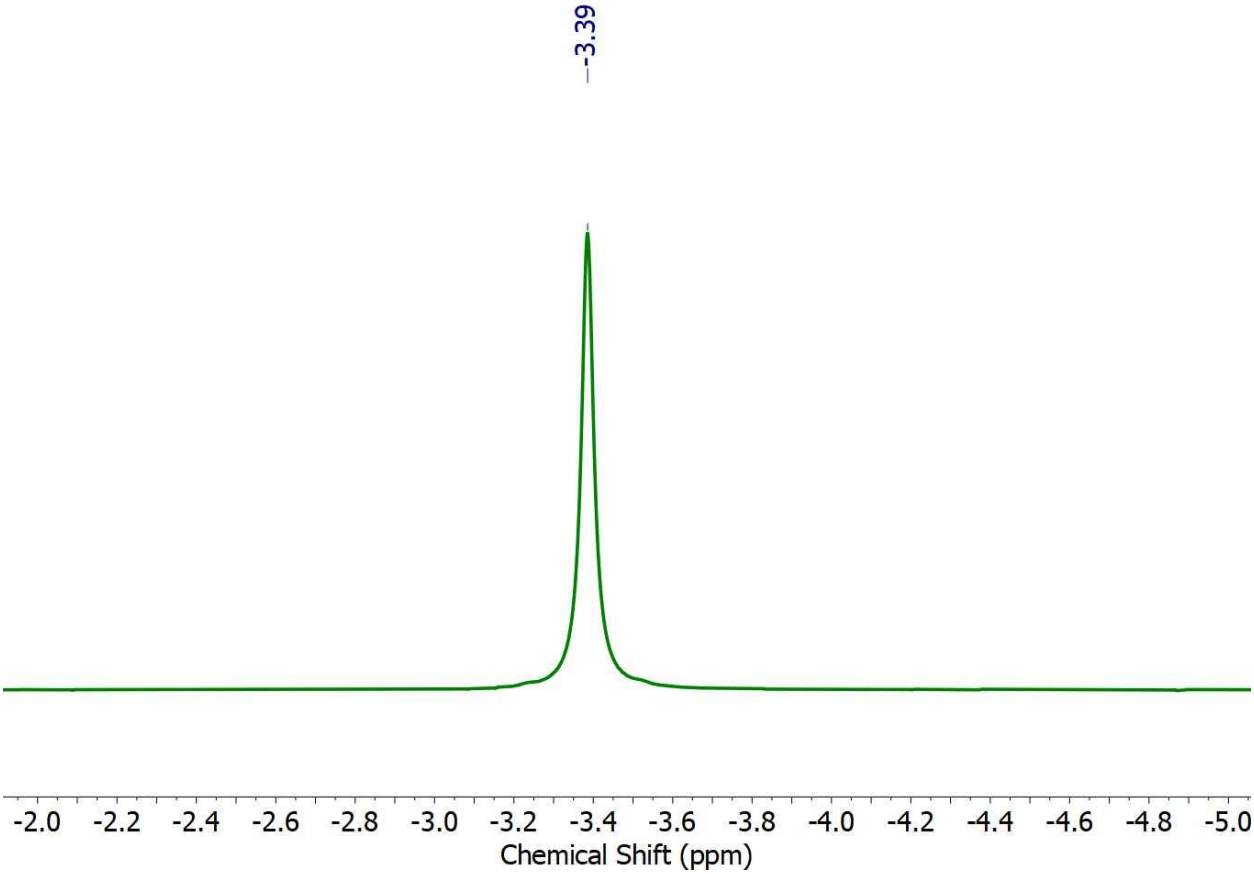

Figure 3.3: ^{1}H NMR signal for $Ce[N(SiMe_3)_2]_3$

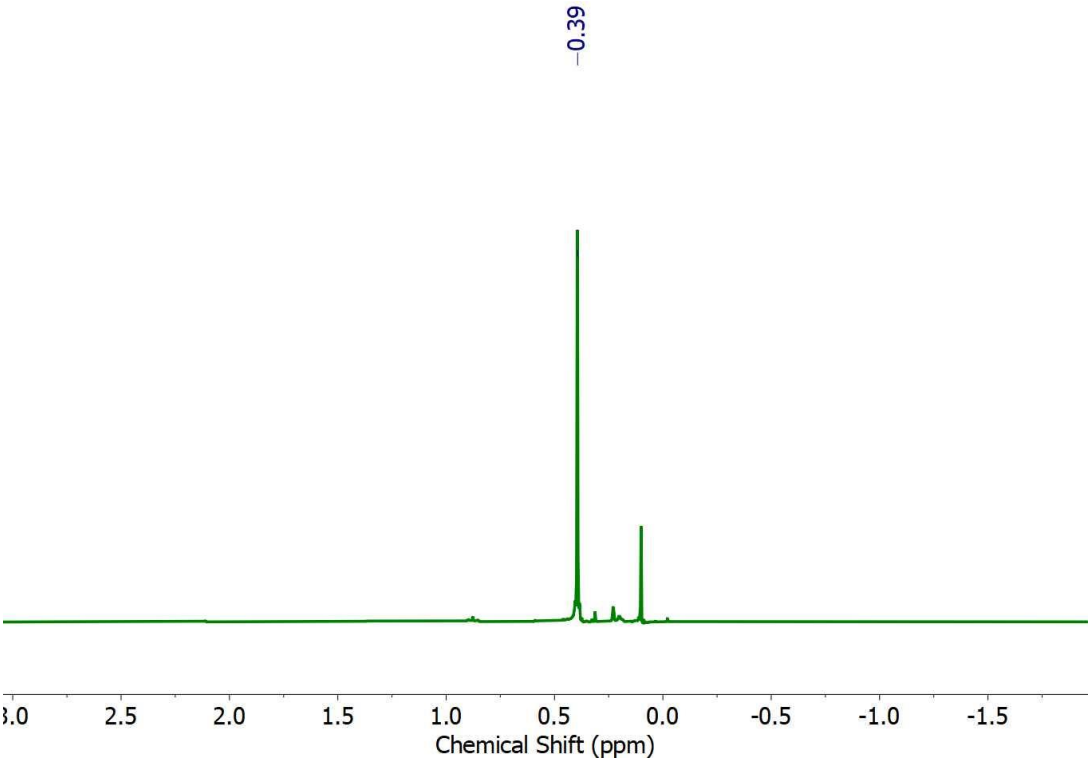

Figure 3.4: ^{1}H NMR signal for $CeF[N(SiMe_3)_2]_3$

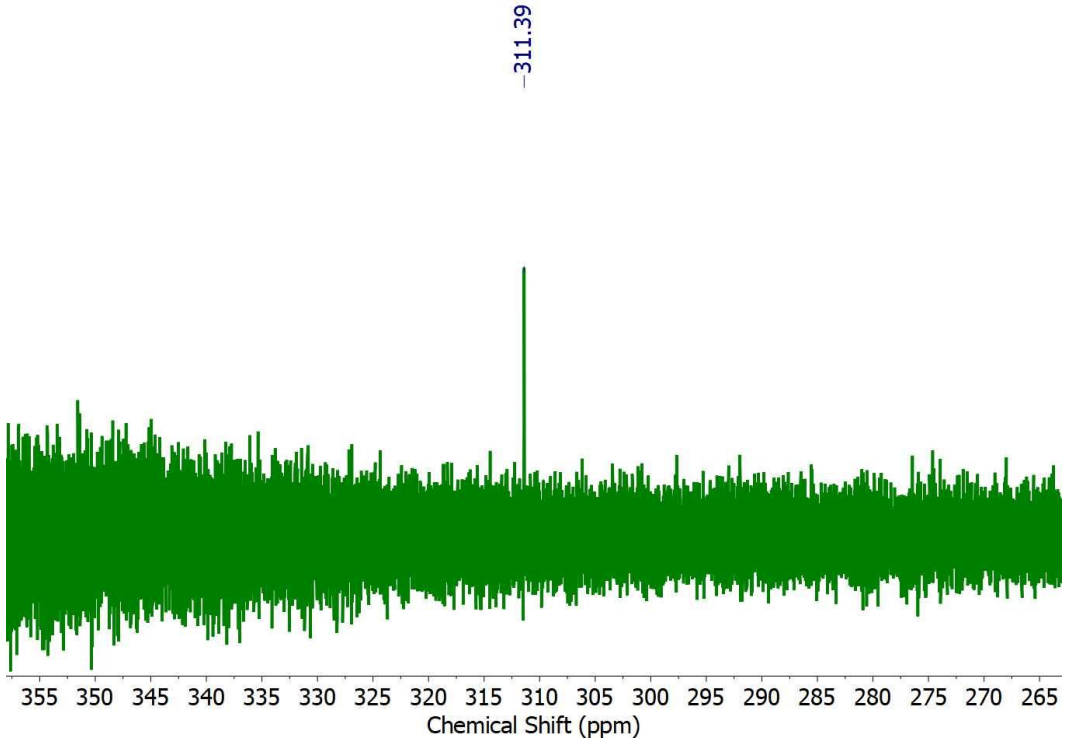

Figure 3.5: ^{19}F NMR signal for $CeF[N(SiMe_3)_2]_3$

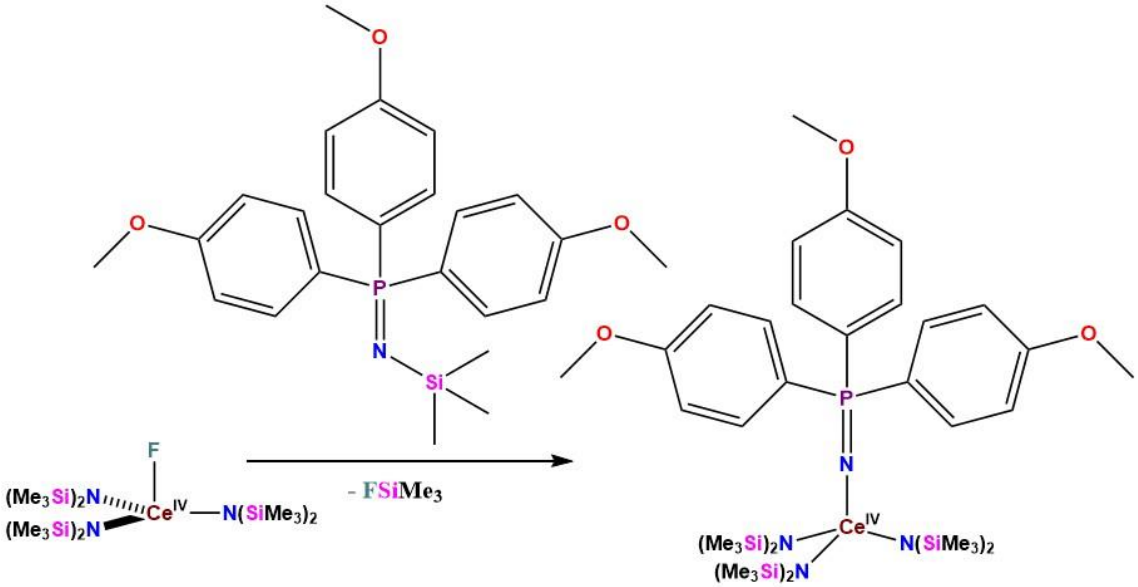

Scheme 3.3: Fluorotrimethylsilane elimination synthesis of tris(*p*-anisyl)phosphinimide complex.

Me_3Si-NP(*p*-anisyl)$_3$ was dissolved in THF, and added to a THF solution of $CeF[N(SiMe_3)_2]_3$. This solution was stirred at room temperature for 24 hours. Upon addition of the phosphinimine solution to the Ce(IV) fluoro-amide complex, the solution became more transparent, and the color shifted from dark cherry-red to a lighter red-orange color. Insoluble by-products were removed by filtration, and the solution was evaporated to dryness. The residue was extracted with pentane, filtered, evaporated to dryness, and dissolved in C_6D_6 for NMR analysis. The ^{19}F NMR signal for $CeF[N(SiMe_3)_2]_3$ was still present in this residue, indicating that the reaction did not go to completion. Additionally, the $SiMe_3$ signals for the starting materials were still present in the ^1H, in addition to free $HNSiMe_3$ at δ 0.1 ppm. However, it appears that new $SiMe_3$ peak formed at around δ 0.3 ppm, which could potential represent desymmetrization of

the silylamide ligands due to phosphinimide coordination. The ^{31}P NMR signal for the *N*-silyl aryl-phosphinimine was still present, further indicating incomplete reaction. However, a ^{31}P NMR resonance was also observed at δ 636.79 ppm. This corresponds to a coordination chemical shift (Δδ) of 637.49 relative to the starting phosphinimine (δ -0.7). This is an extremely deshielded resonance, far downfield from typical phosphinimide ligand resonances. Efforts to further investigate this reaction were cut short, but work should be done to verify that this resonance corresponds to the target complex. If verified, this enormously deshielded ^{31}P resonance would represent an enormous amount of cerium(IV)-phosphinimide covalency and significant *π*-donation into the empty 4f/5d Ce(IV) orbitals. The Ce(IV)-phosphinimide interaction is expected to have significant multiple-bond character, with electron density delocalization along the entire Ce-N-P moiety.

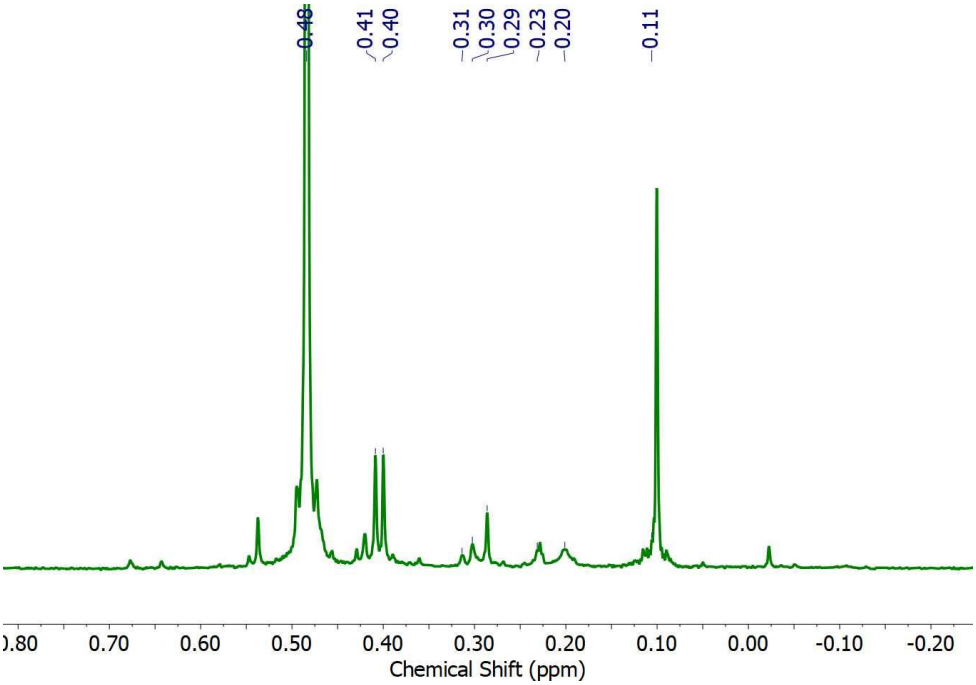

Figure 3.6: ^{1}H NMR signal for Ce[NP(*p*-anisyl)$_3$][N(SiMe$_3$)$_2$]$_3$

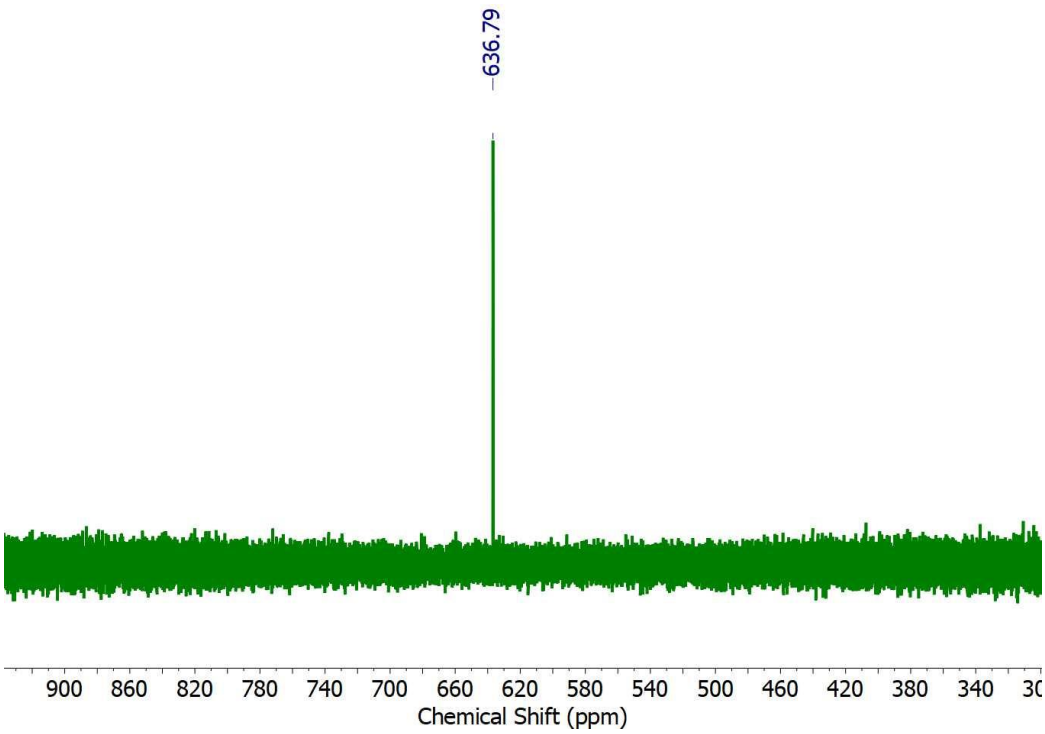

Figure 3.7: ^{131}P NMR signal for Ce[NP(*p*-anisyl)$_3$][N(SiMe$_3$)$_2$]$_3$

Me$_3$Si-NP(*p*-tolyl)$_3$ was also reacted with CeF[N(SiMe$_3$)$_2$]$_3$ under the same conditions as above. Interestingly, no ^{31}P signals were observed, not even for the starting material. This could potentially be due to low sample concentration. The ^{19}F NMR resonance for CeF[N(SiMe$_3$)$_2$]$_3$ was still present, indicating an incomplete reaction. However, similar to the previous example, it appears that new upfield shifted SiMe$_3$ resonances formed, potentially representing desymmetrization of the silylamide ligands with coordination of the phosphinimide ligand.

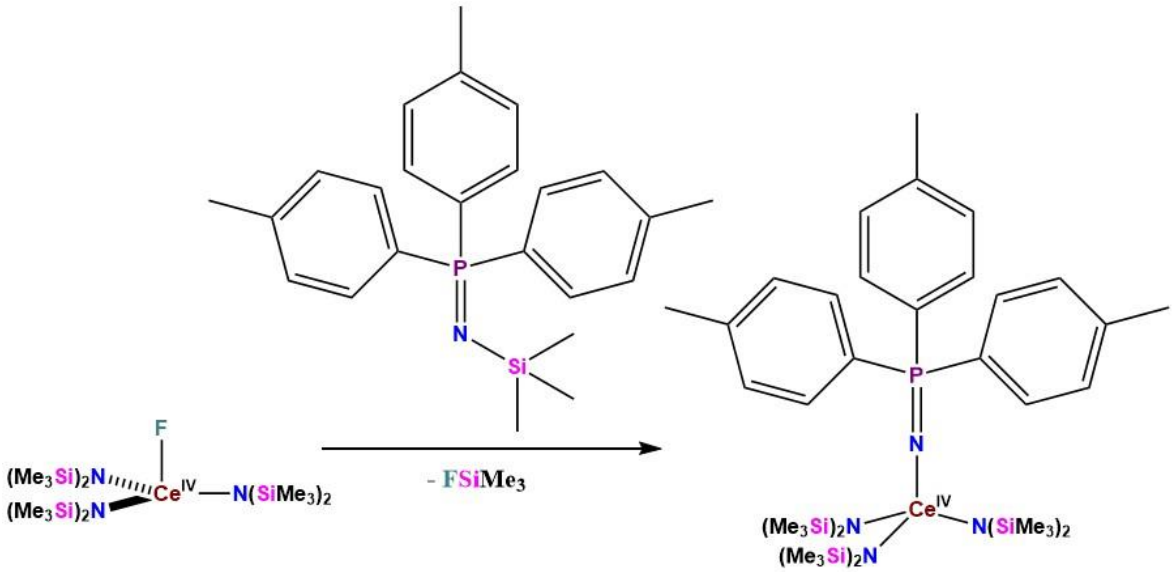

Scheme 3.4: Fluorotrimethylsilane elimination synthesis of tris(*p*-tolyl)phosphinimide complex.

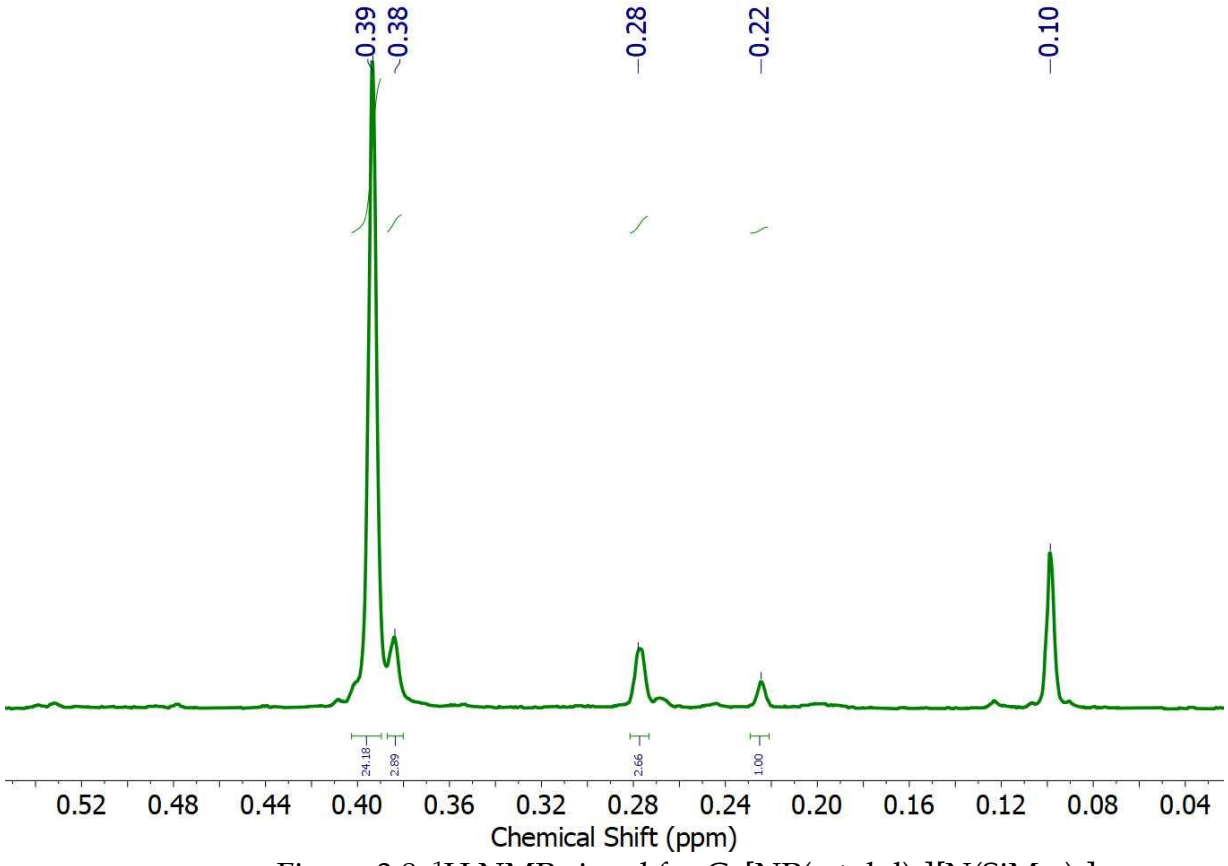

Figure 3.8: ^{1}H NMR signal for Ce[NP(*p*-tolyl)$_3$][N(SiMe$_3$)$_2$]$_3$

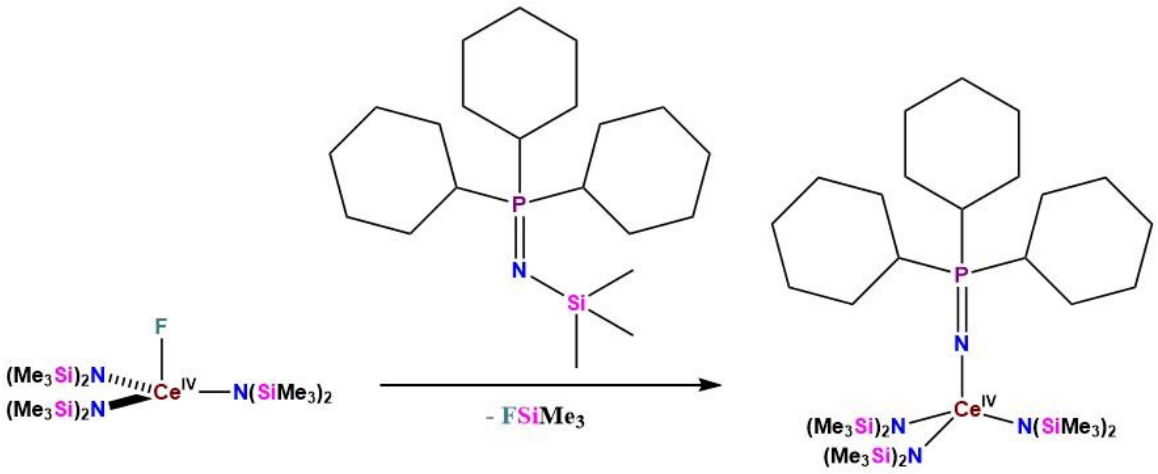

Scheme 3.5: Fluorotrimethylsilane elimination synthesis of tris(cyclohexyl)phosphinimide complex.

Me_3Si-$NPCy_3$ was also reacted with $CeF[N(SiMe_3)_2]_3$ under the same conditions. As above, the ^{19}F NMR of the Ce(IV) precursor was still present, indicating an incomplete reaction. The $SiMe_3$ peaks of the starting materials were still present in the ^1H NMR spectrum, however, as above, new peaks were observed in the $SiMe_3$ region that could potentially represent amide ligand desymmetrization. Furthermore, it appears that a new broad upfield-shifted cyclohexyl resonance emerged. The ^{31}P NMR signal for $Ce[NPCy_3][N(SiMe_3)_2]_3$ is very deshielded (637.34 ppm). The ^{31}P NMR resonance for the alkyl-phosphinimide derivative, $Ce[NPCy_3][N(SiMe_3)_2]_3$, is slightly more deshielded than the ^{31}P NMR resonance of the aryl-phosphinimide derivative, Ce[NP(*p*-anisyl)$_3$][$N(SiMe_3)_2]_3$. This is not a surprise, since ^{31}P NMR resonances for alkylphosphinimines are more deshielded than the resonances for arylphosphinimines. The fundamental difference in the electronic structure of alkyl- and arylphosphinimines

is observed when comparing the moisture sensitivity of alkyl- versus aryl-phosphinimines [23]. Aryl-phosphinimines are highly moisture-sensitive and are easily hydrolyzed to aryl-phosphine oxides unless moisture is rigorously excluded [23]. Alkyl-phosphinimines are much less sensitive to moisture and are not as easily hydrolyzed.

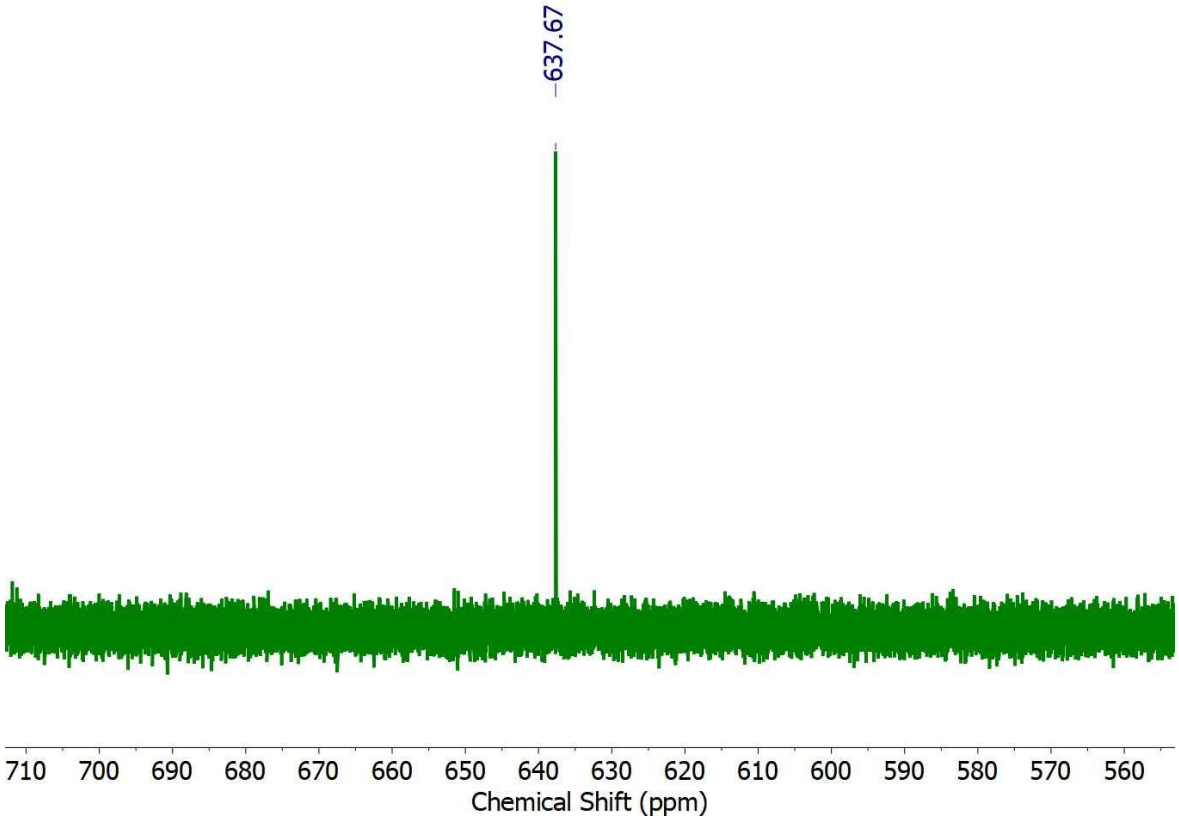

Figure 3.9: ^{31}P NMR signal for $Ce[NPCy_3][N(SiMe_3)_2]_3$

The ^{31}P NMR resonance for $Cy_3PN\text{-}SiMe_3$ is observed at 17 ppm [17]. The signal for $(p\text{-anisyl})_3PN\text{-}SiMe_3$ is more shielded, and is observed at -0.7 ppm [17]. Therefore, it is not surprising that the ^{31}P NMR resonance for $Ce[NPCy_3][N(SiMe_3)_2]_3$ is more deshielded than $Ce[NP(p\text{-anisyl})_3][N(SiMe_3)_2]_3$. This difference in the nuclear magnetic

shielding of the phosphorus nucleus in these two complexes suggests that the electronic structures of the Ce-N-P systems in these two complexes are different, and have different degrees of cerium(IV)-phosphinimide orbital mixing (i.e. different degrees of cerium-ligand covalency). Moreover, the coordination chemical shift for the *p*-anisyl derivative ($\Delta\delta$ = 637.49 ppm) is larger than the coordination chemical shift of the cyclohexyl derivative ($\Delta\delta$ = 620.34 ppm), which further suggests differences in Ce-phosphinimide bonding in these two systems.

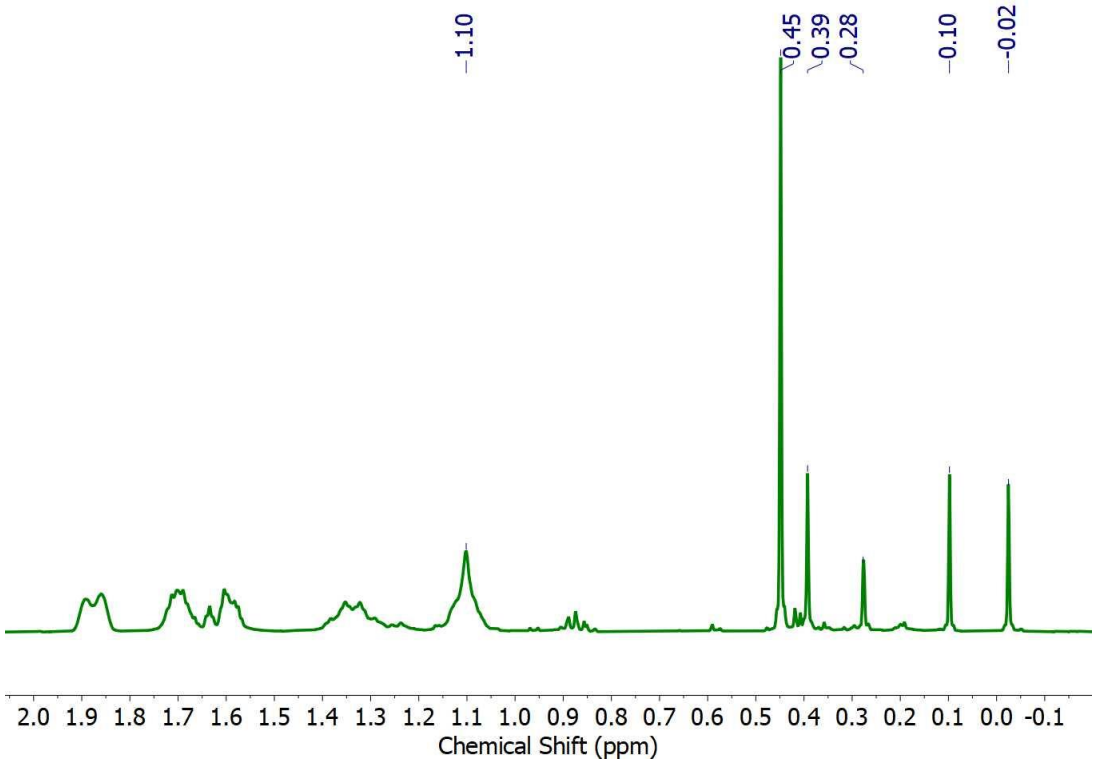

Figure 3.10: ^{1}H NMR signal for $Ce[NPCy_3][N(SiMe_3)_2]_3$

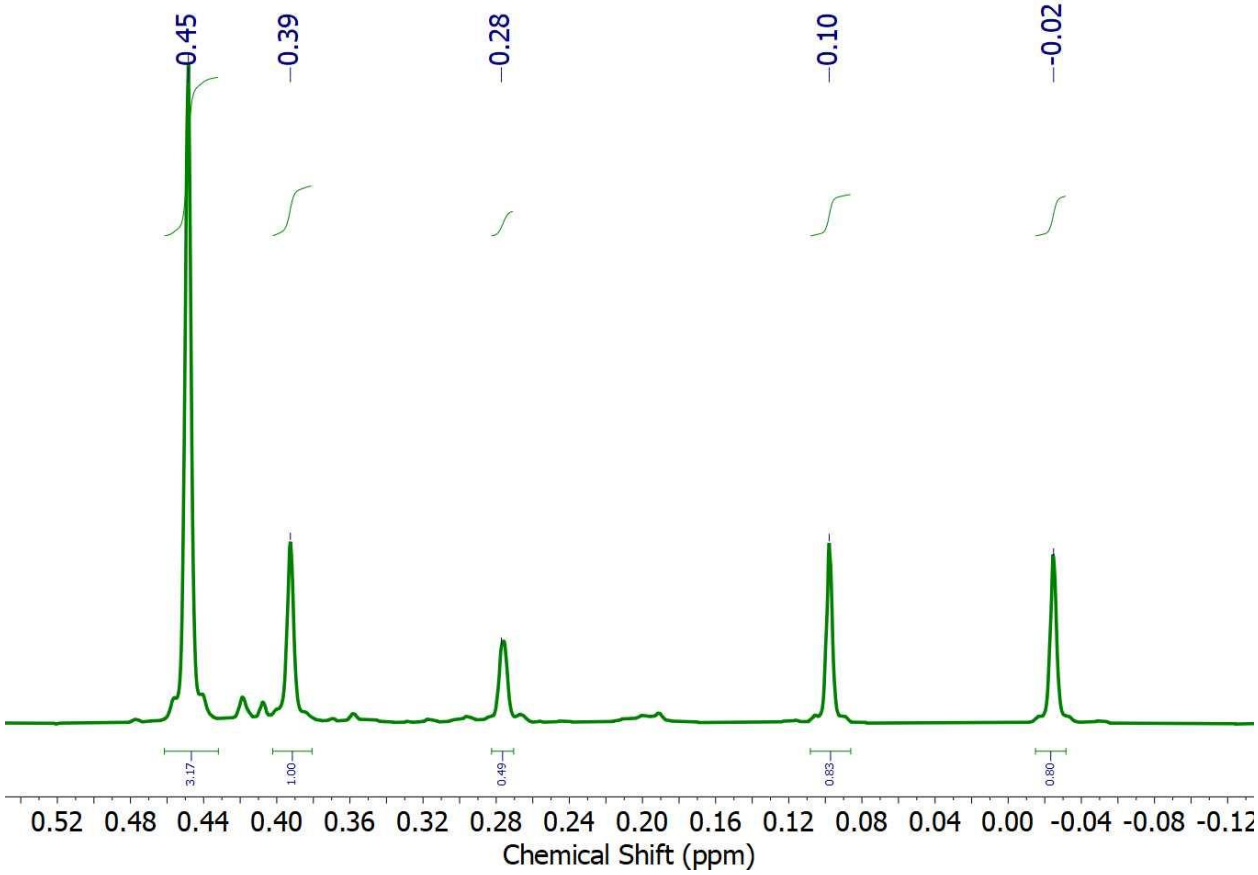

Figure 3.11: ^{1}H NMR signal for $Ce[NPCy_3][N(SiMe_3)_2]_3$ ($SiMe_3$ region)

The phosphorus resonances observed at δ 636.79 ppm and δ 637.34 ppm for $Ce[NPR_3][N(SiMe_3)_2]_3$ (R = *p*-anisyl, cyclohexyl) are comparable to the resonance observed at 689.3 ppm for the analogous uranium complex $U[NP(t\text{-butyl})_3][N(SiMe_3)_2]_3$. The phosphorus resonance for $(t\text{-butyl})_3PNSiMe_3$ is observed at 32.4 ppm [17], which is more deshielded than $Cy_3PNSiMe_3$ (17 ppm) [17]. This difference (Δδ 15.4 ppm) is smaller

than the difference between the cerium(IV) and uranium(IV) complexes (Δδ 53.52 ppm and Δδ 51.96 ppm). Uranium(IV) has a slightly larger Shannon ionic radius than cerium(IV) (0.89 Å vs. 0.87 Å) [24]. Uranium(IV) has an f^2 electronic configuration and is paramagnetic [13]; cerium(IV) has an f^0 electronic configuration and is diamagnetic [13]. It is unclear whether the relatively large difference between the phosphorus resonances of Ce[NPR_3][$N(SiMe_3)_2$]$_3$ and U[NP(*t*-butyl)$_3$][$N(SiMe_3)_2$]$_3$ can be attributed to differences in ionic radii, electronic configuration, and/or orbital mixing. Computational studies, additional spectroscopic investigations, and additional pseudo-isostructural complexes for comparison are necessary in order for such discussions to move beyond speculation. However, the comparable levels of deshielding observed in the ^{31}P NMR spectra for the pseudo-isostructural complexes Ce[NPR_3][$N(SiMe_3)_2$]$_3$ and U[NP(*t*-butyl)$_3$][$N(SiMe_3)_2$]$_3$ seem to suggest comparable levels of metal-ligand covalency. Moreover, the tris(*p*-anisyl)-phosphinimide ligand has a larger coordination shift (Δδ) than the tris(cyclohexyl)phosphinimide by about 17.15 ppm; this stronger deshielding effect could potentially correspond to differences in Ce(IV)-phosphinimide covalency. More characterization is needed to confirm if the phosphorus resonances indeed correspond to the target complexes, and electronic structure studies are necessary to elucidate the nature of the metal-ligand bonding in these complexes.

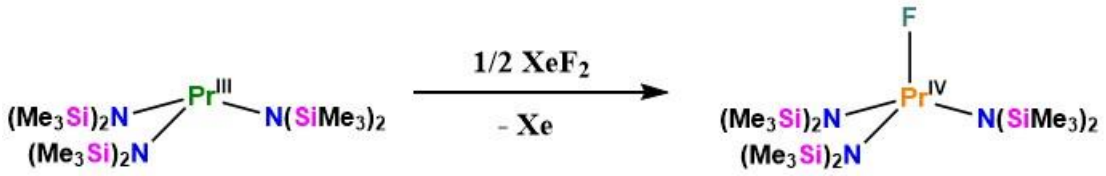

Scheme 3.6: Attempted oxidation of signal for $Pr[N(SiMe_3)_2]_3$

Efforts were initiated to explore the exotic tetravalent oxidation state of praseodymium. The chemistry of praseodymium(IV) is very limited, and the first molecular coordination complexes of Pr(IV) have only recently been reported. To contribute to the expansion of this rare oxidation state, the synthesis of $F\text{-}Pr[N(SiMe_3)_2]_3$ was attempted. The fluoro[tris(bis(trimethylsilyl)amido] motif, $F\text{-}M[N(SiMe_3)_2]_3$ is known for titanium(IV), cerium(IV), and uranium(IV). $F\text{-}Th[N(SiMe_3)_2]_3$ has not been reported and should be the focus of future efforts. Plans were made to synthesize $F\text{-}Th[N(SiMe_3)_2]_3$ using a method recently reported from Los Alamos by Kiplinger and coworkers for the synthesis of $F\text{-}U[N(SiMe_3)_2]_3$. This method involved a halide exchange reaction between $Cl\text{-}U[N(SiMe_3)_2]_3$ and $FSnMe_3$, forming $F\text{-}U[N(SiMe_3)_2]_3$ as the product, and volatile $Cl\text{-}SnMe_3$ as a by-product, which can be converted back to $FSnMe_3$ for reuse using KF. However, work with radioactive materials was discontinued before this plan could be executed.

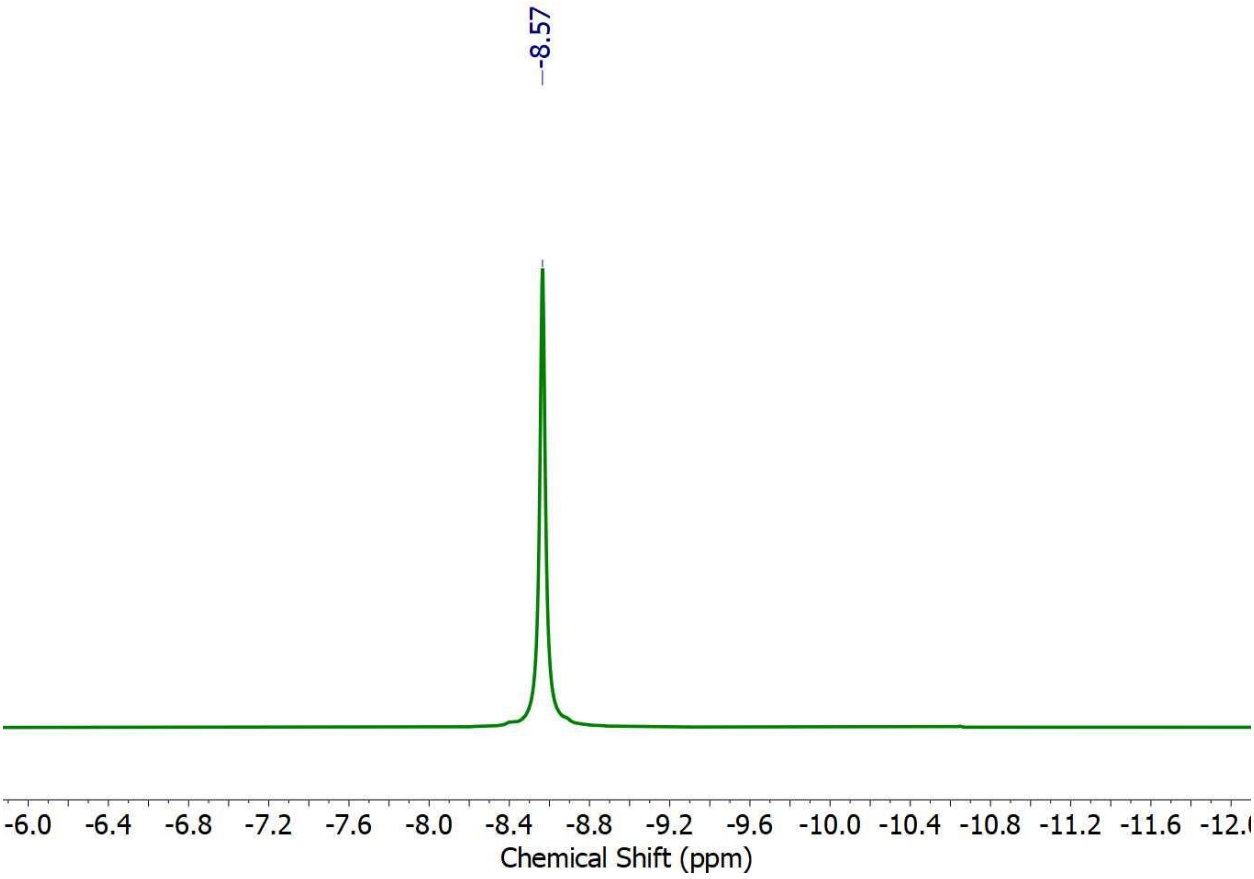

Figure 3.12: ^{1}H NMR signal for $Pr[N(SiMe_3)_2]_3$

$Pr[N(SiMe_3)_2]_3$ was synthesized from anhydrous $PrCl_3$ as previously reported, and sublimed prior to use. Praseodymium(III) is paramagnetic with an f^2 configuration, and the ^{1}H NMR spectrum of $Pr[N(SiMe_3)_2]_3$ features a broad, paramagnetically shielded resonance at δ -8.57 ppm. $Pr[N(SiMe_3)_2]_3$ was dissolved in pentane and half an equivalent of xenon difluoride, XeF_2, was added, and the solution was stirred at room temperature for a few hours. However, work was abruptly discontinued in the glove-box containing the residue of this reaction, and characterization was not completed. Efforts should be made to synthesize F-$Pr[N(SiMe_3)_2]_3$, F-$Th[N(SiMe_3)_2]_3$, F-$Np[N(SiMe_3)_2]_3$, and F-$Pu[N(SiMe_3)_2]_3$ as soon as possible. Successful synthesis of these compounds would

generate a comparative isostructural series, F-M[N(SiMe$_3$)$_2$]$_3$ (M = Ti, Ce, Pr, Th, U, Np, Pu), that could be studied spectroscopically using ^{19}F NMR. ^{19}F NMR could potentially be used to empirically study the differences in the metal-fluoride bonds for these metals, especially for diamagnetic Ti(IV), Ce(IV), and Th(IV) systems. ^{19}F NMR might be difficult to use for paramagnetic Pr(IV), U(IV), Np(IV) and Pu(IV) systems with direct metal-fluoride bonds. To my knowledge, F-U[N(SiMe$_3$)$_2$]$_3$ is ^{19}F NMR-silent, and a ^{19}F resonance has not been reported for this complex. As a result, different analytical methods may need to be employed to study the metal-fluoride bonds in paramagnetic complexes, especially ones that are unaffected by the strong paramagnetism of many of the f-block elements. One method that could be used to study F-M[N(SiMe$_3$)$_2$]$_3$ complexes and other fluoride systems is an esoteric method called time-differential perturbed angular distribution (TD-PAD) analysis. In this method, an accelerator-generated proton beam is used to induce non-resonant nuclear reactions with ^{19}F, thereby inducing fluorine gamma-ray emission. An array of gamma detectors, coupled with a beam chopper for time resolution, can be used to measure the anisotropy of the fluorine gamma-ray distribution generated by fluoride materials, thereby enabling nuclear electric field gradient studies of metal-fluoride covalency. The anisotropy of the gamma-rays is influenced by the relative ionicity/covalency of fluoride bonds, since valence shell electron distributions affect the core energy levels and s-electron densities at fluorine nuclei. Covalency studies using Mössbauer spectroscopy are based on the same phenomena, but this method requires a Mössbauer-active nucleus and therefore has limited applicability. TD-PAD has been used in previous work to study ionicity/covalency differences in transition-metal and main-

group fluorides. This method should be extended to covalency studies of the lanthanide and actinide fluorides [25].

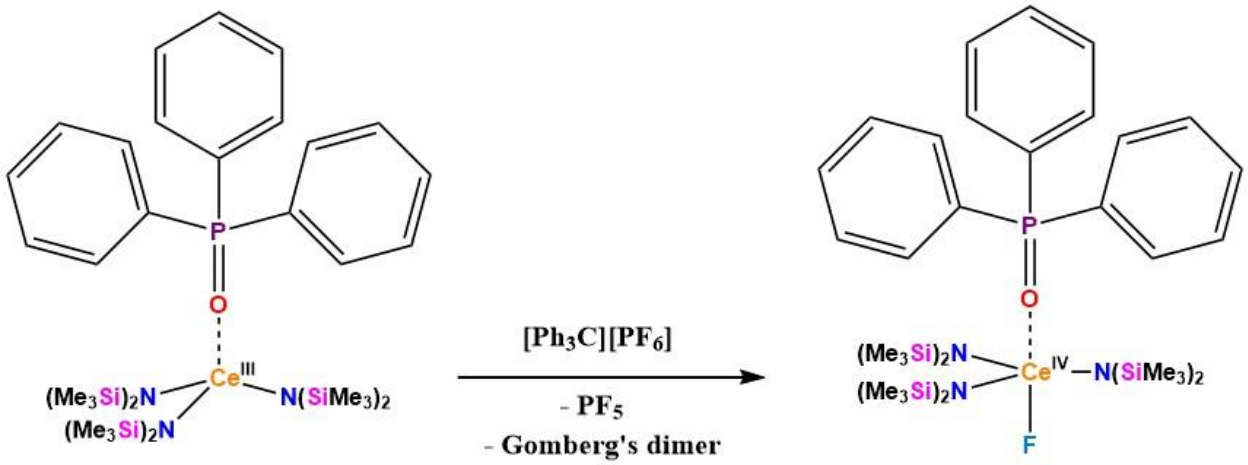

Scheme 3.7: Oxidation of $Ce[OPPh_3][N(SiMe_3)_2]_3$

During the course of this work, oxidation of a previously unreported Lewis-base adduct, $Ce[OPPh_3][N(SiMe_3)_2]_3$, was attempted. The synthesis and characterization of this Lewis-base adduct is detailed in Chapter 4; however, oxidation of this compound is discussed here in the context of tetravalent cerium-fluoride chemistry. Crystals of $Ce[OPPh_3][N(SiMe_3)_2]_3$ were dissolved in toluene, and this solution was added to a vial containing one equivalent of triphenylcarbenium hexafluorophosphate, $[Ph_3C][PF_6]$. An immediate color change was observed from colorless to dark red, indicating that oxidation from Ce(III) to Ce(IV) occurred. However, it is clear from the ^1H NMR results that the reaction did not go to completion, since a large paramagnetic signal

corresponding to $Ce[OPPh_3][N(SiMe_3)_2]_3$ was observed at δ -0.8 ppm. Free $Ce[N(SiMe_3)_2]_3$ was also observed at δ -3.3 ppm. However, a prominent signal was observed at δ 0.39 ppm corresponding to cerium(IV)-coordinated silylamide ligands, as a well as upfield-shifted aromatic resonances corresponding to the aromatic phosphine oxide protons, with the expected ratios with respect to the $SiMe_3$ signal at δ 0.39 ppm. Similar to the four-coordinate F-$Ce[N(SiMe_3)_2]_3$ compound, F-$Ce[OPPh_3][N(SiMe_3)_2]_3$ generates a ^{19}F resonance at δ 311.74 ppm. Two ^{31}P NMR resonances were observed. The most prominent signal at δ 53.43 ppm corresponds to the Ce(III) precursor. A small deshielded peak was observed at δ 79.39 ppm, which likely corresponds to the fluoro-phosphine oxide-amide target complex, albeit, in very small yield. This corresponds to a chemical shift (Δδ) equal to +25.96 ppm with respect to the Ce(III) precursor, indicating that oxidation from Ce(III) to Ce(IV) has an electron-withdrawing effect on the phosphine oxide ligands, which suggests increased levels of Ce(IV)-phosphine oxide covalency compared to the Ce(III)-phosphine oxide interaction.

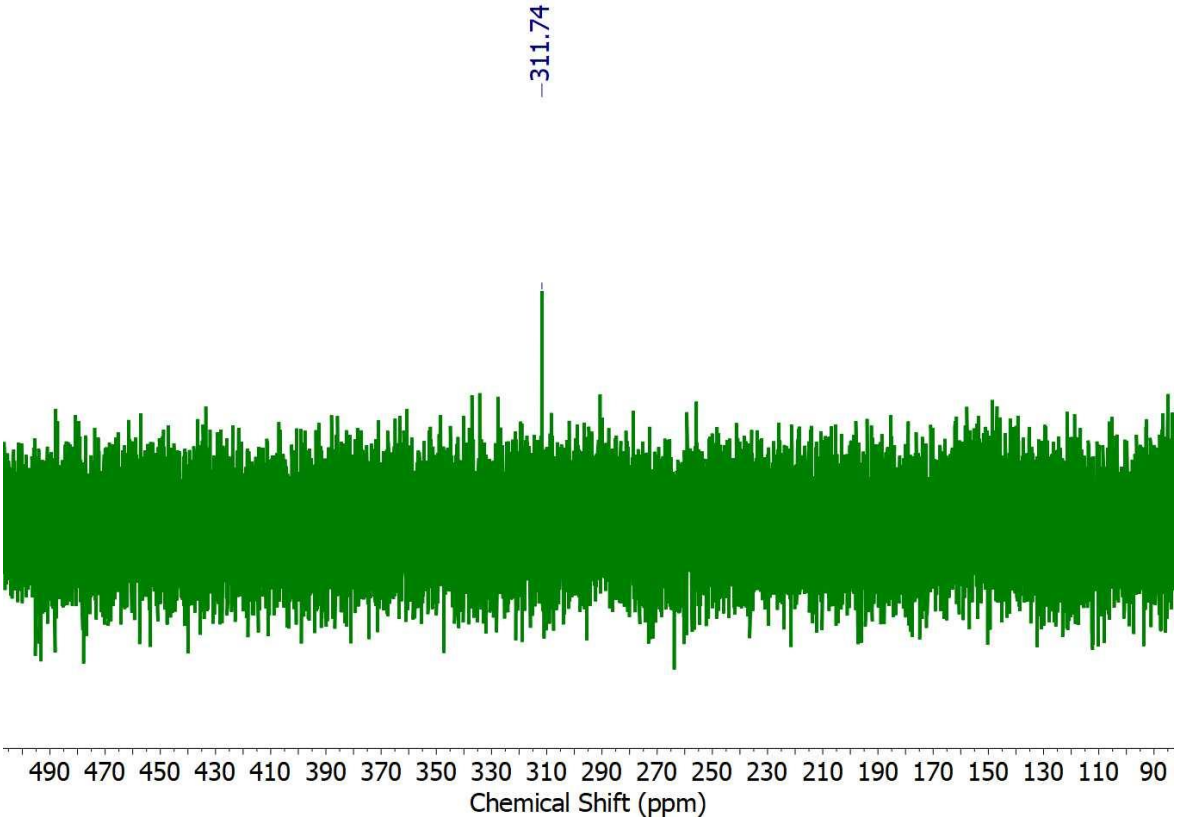

Figure 3.13: ^{19}F NMR signal for F-Ce[$OPPh_3$][$N(SiMe_3)_2$]$_3$

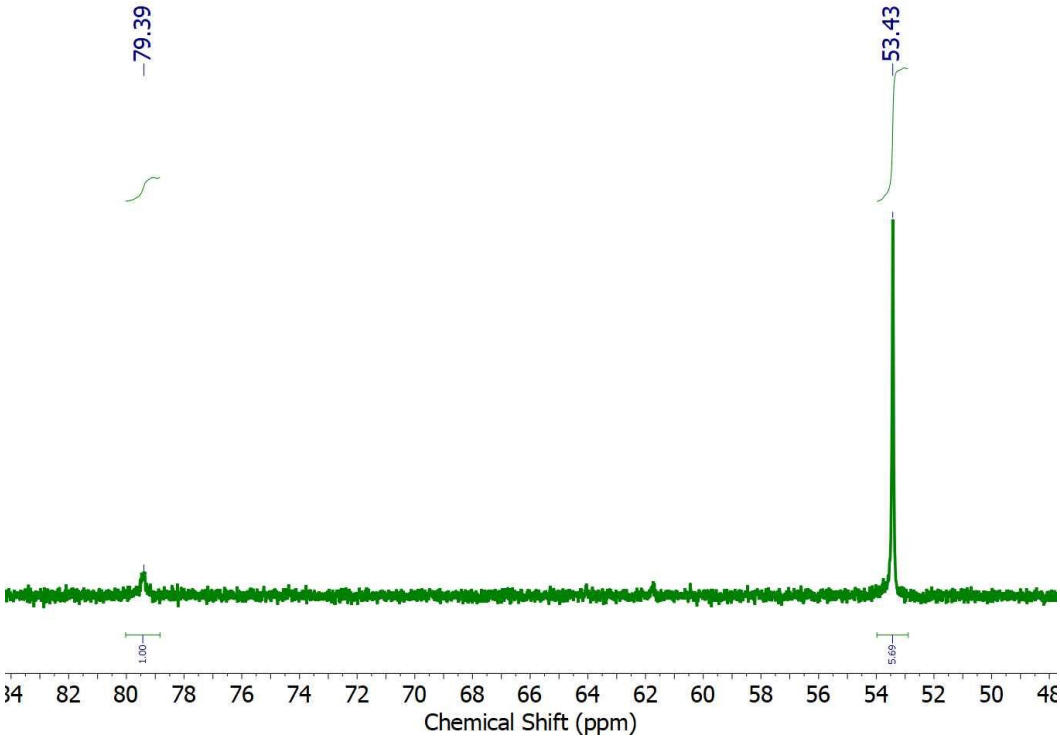

Figure 3.14: ^{31}P NMR spectrum for F-Ce[$OPPh_3$][$N(SiMe_3)_2$]

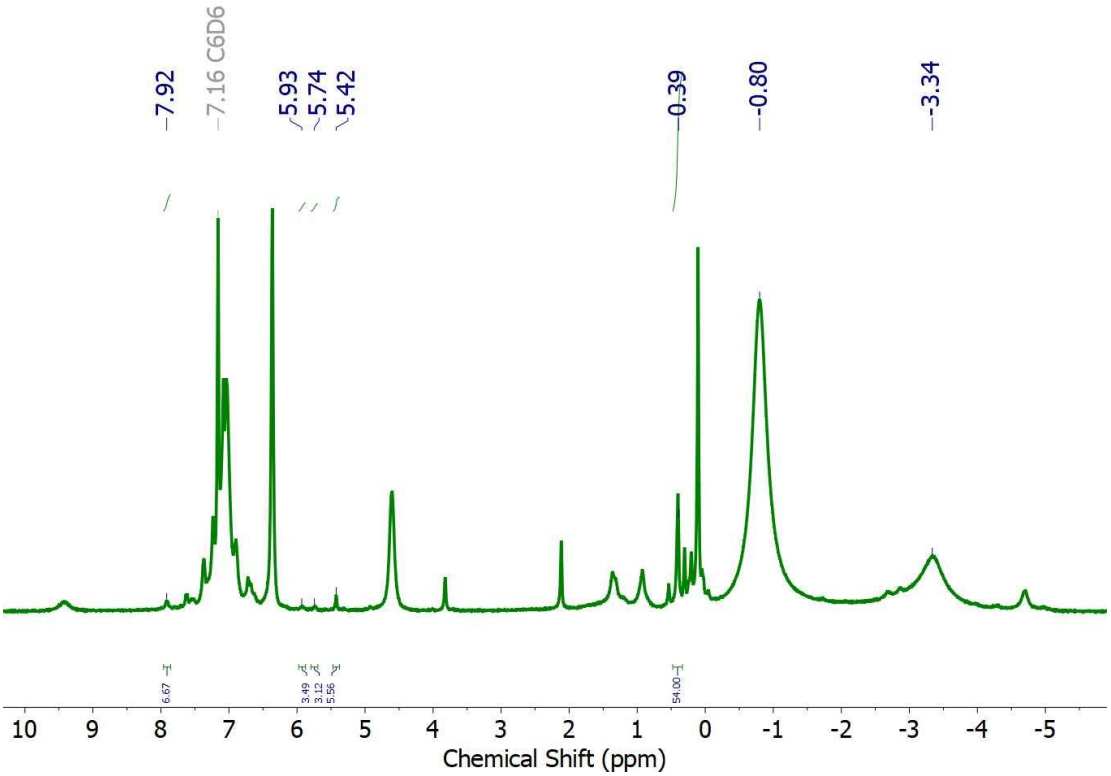

Figure 3.15: ^{1}H NMR spectrum for F-Ce[$OPPh_3$][$N(SiMe_3)_2$]

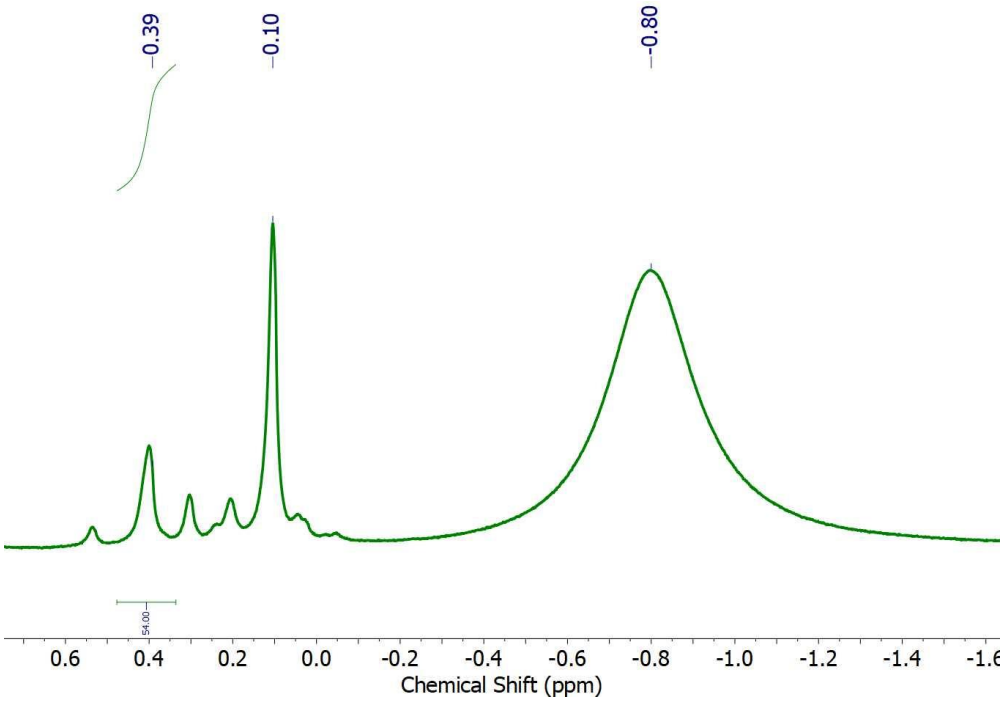

Figure 3.16: ^{1}H NMR spectrum for F-Ce[$OPPh_3$][$N(SiMe_3)_2$] ($SiMe_3$ region)

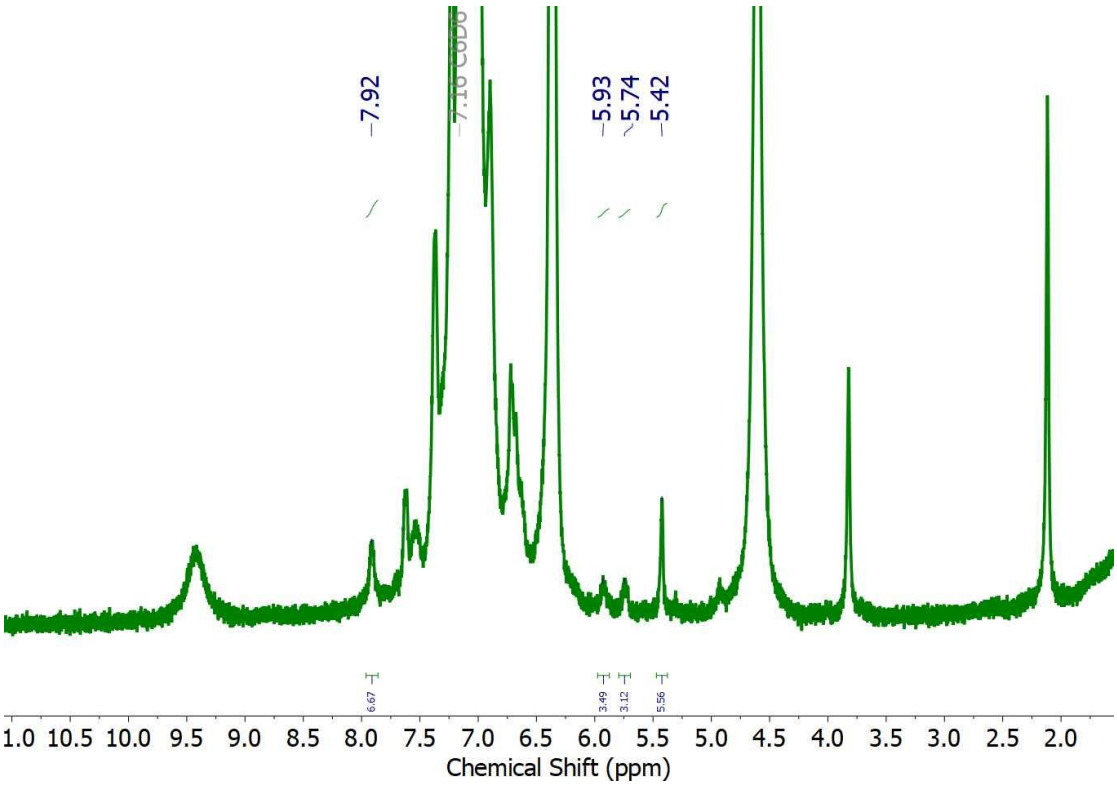

Figure 3.17: ^{1}H NMR spectrum for F-Ce[OPPh$_3$][N(SiMe$_3$)$_2$] (aromatic region)

Concluding Remarks and Future Opportunities

In this chapter, the synthesis and NMR characterization of tetravalent cerium phosphinimide-amide complexes Ce[NPR$_3$][N(SiMe$_3$)$_2$]$_3$ (R = cyclohexyl, *p*-tolyl) was reported. This work is a contribution to molecular cerium(IV) chemistry, and lays the groundwork for further elaboration of the Ce[L][N(SiMe$_3$)$_2$]$_3$ (L = ligand) framework using CeF[N(SiMe$_3$)$_2$]$_3$ as a precursor. More work on the Ce[NPR$_3$][N(SiMe$_3$)$_2$]$_3$ framework should be carried out, and a library of pseudo-isostructural alkyl-, aryl, and amino-phosphinimide complexes should be synthesized in order to enable detailed comparative studies of the bonding interactions in these systems. Such work would

enable one to understand how changing the identity of the substituents on phosphorus influences the relative cerium 4*f* and 5*d* contributions to the σ and π interactions in the Ce-N-P system. A library of isostructural thorium(IV), uranium(IV), and plutonium(IV) complexes with identical ligand frameworks should also be synthesized for comparison. Describing the bonding interactions in M-N-P using ^{31}P spectroscopy is complicated by the fact that the phosphorus atom is not directly bound to the metal center. Nevertheless, the phosphorus nucleus is very sensitive to the electronic structure of the metal-nitrogen bond because the electron density is delocalized between all three atoms in the M-N-P system through multiple π interactions [7]. For highly paramagnetic *f*-metals, situating an intervening atom like nitrogen between phosphorus and the paramagnetic metal center might be necessary to study paramagnetic complexes via ^{31}P NMR spectroscopy, since phosphorus-NMR resonances are often not observed when the phosphorus atom is bound directly to a paramagnetic metal-center. Though monoanionic, phosphinimide ligands can exhibit multiple bond character [7], and in monomeric complexes where the M-N-P system approaches linearity, the metal-nitrogen bond is often described as a triple bond [7]. Cerium phosphinimide complexes offer great potential to investigate the nature of orbital interactions in molecular cerium(IV) complexes, and they could also prove to be useful precursors for the synthesis of advanced Ce(IV) materials. The uranium-like covalency that has been observed by previous researchers challenges traditional understandings of chemical bonding [3,4], and cerium(IV) complexes featuring π-donating phosphinimide ligands provide an avenue to further investigate the anomalous behavior of the cerium(IV) ion.

References

[1] Williams, Ursula J., Jerome R. Robinson, Andrew J. Lewis, Patrick J. Carroll, Patrick J. Walsh, and Eric J. Schelter. 2014. Synthesis, Bonding, and Reactivity of a Cerium(IV) Fluoride Complex. *Inorganic Chemistry* 53: 27-29.

[2] Williams, Ursula J., Patrick J. Carroll, and Eric J. Schelter. 2014. Synthesis and Analysis of a Family of Cerium(IV) Halide and Pseudohalide Compounds. *Inorganic Chemistry* 53: 6338-6345.

[3] Gregson, Matthew, Erli Lu, Floriana Tuna, Eric J.L. McInnes, Christoph Hennig, Andreas C. Scheinost, Jonathan McMaster, William Lewis, Alexander J. Blacke, Andrew Kerridge, and Stephen T. Liddle. 2016. Emergence of comparable covalency in isostructural cerium(IV)- and uranium(IV)-carbon multiple bonds. *Chemical Science* 7(5): 3286-3297.

[4] Löble, Matthias W., Jason M. Keith, Alison B. Altman, S. Chantal E. Stieber, Enrique R. Batista, Kevin S. Boland, Steven D. Conradson, David L. Clark, Juan Lezama Pacheco, Stosh A. Kozimor, Richard L. Martin, Stephan G. Minasian, Angela C. Olson, Brian L. Scott, David K. Shuh, Tolek Tyliszczak, Marianne P. Wilkerson, and Ralph A. Zehnder. 2015. Covalency in Lanthanides. An X-ray Absorption Spectroscopy and Density Function Theory Study of $LnCl_6^{x-}$ (x = 3, 2). *Journal of the American Chemical Society* 137: 2506-2523.

[5] Roesky, Herbert W., Kattesh V. Katti, Ulrich Seseke, Uwe Scholz, Regine Herbst, Ernst Egert, and George M. Scheldrick. 1986. Reacktionen von Wolframhexafluorid mit N-Trimethylsilyliminotriphosphoranen – Kristallstruktur von $(Me_3P=N)_2WF_4$. *Zeitschrift für Naturforschungen* 41b: 1509-1512.

[6] Nugent, William A. and James M. Mayer. 1988. *Metal-Ligand Multiple Bonds*. John Wiley & Sons, New York.

[7] Dehnicke, Kurt and Joachim Strähle. 1989. Phosphorane Iminato Complexes of Transition Metals. *Polyhedron* 8(6): 707-726.

[8] Anfang, S., G. Seybert, K. Harms, G. Geiseler, W. Massa, and K. Dehnicke. 1998. Reacktionen von $LiNPPh_3$ mit den Cyclooctatetraenid-Komplexen $[Ln(C_8H_8)Cl(THF)_2]_2$ von Cer und Samarium. Die Kristallstrukturen von $[LiNPPh_3]_6$, $[Ln(C_8H_8)Li_3Cl_2(NPPh_3)_2(THF)_3]$ (Ln = Ce, Sm) und $[Li(THF)_4][Sm(C_8H_8)_2]$. *Zeitschrift für anorganishe und allgemeine Chemie* 624: 1187-1192.

[9] Dehnicke, Kurt and Frank Weller. 1997. Phosphorane iminato complexes of main group elements. *Coordination Chemistry Reviews* 158: 103-169.

[10] Dehnicke, Kurt, Matthais Krieger, and Werner Massa. 1999. Phosphoraneiminato complexes of transition metals. *Coordination Chemistry Reviews* 182: 19-65.

[11] Dehnicke, Kurt and Andreas Greiner. 2003. Unusual Complex Chemistry of Rare Earth Elements: Large Ionic Radii-Small Coordination Numbers. *Angewandte Chemie International Edition* 42: 1340-1354.

[12] Gaunt, Andrew J., Sean D. Reilly, Alejandro E. Enriquez, Trevor W Hayton, James M. Boncella, Brian L Scott, and Mary P. Neu. 2008. Low-Valent Molecular Plutonium Halide Complexes. *Inorganic Chemistry* 47: 8412-8419.

[13] Aspinall, Helen C. 2001. *Chemistry of the f-Block Elements*. Gordon and Breach Science Publishers, Amsterdam.

[14] Jha, A.R. 2014. *Rare Earth Materials: Properties and Applications*. CRC Press, Boca Raton.

[15] Anwander, Reiner, Michael Dolg, and Frank T. Edelmann. 2017. The difficult search for organocerium(IV) compounds. *Chemical Society Reviews* 46: 6697-6709.

[16] So, Yat Ming and Wa-Hung Leung. 2017. Recent Advances in the coordination chemistry of cerium(IV) complexes. *Coordination Chemistry Reviews* 340: 172-197.

[17] Stephan, Douglas W., Jeffrey C. Stewart, Frédéric Guérin, Silke Courtenay, James Kickham, Emily Hollink, Chad Beddie Aaron Hoskin, Todd Graham, Pingrong Wei, Rupert E. v.H. Spence, Wei Xu, Linda Koch, Xiaoliang Gao, and Daryll G. Harrison. 2003. An Approach to Catalyst Design: Cyclopentadienyl-Titanium Phosphinimide Complexes in Ethylene Polymerization. *Organometallics* 22: 1937-1947.

[18] Edleman, Nikki L., Anchuan Wang, John A. Belot, Andrew W. Metz, Jason R. Babcock, Amber M. Kawaoka, Jun Ni, Matthew V. Metz, Christine J. Flashenriem, Charlotte L. Stern, Louise M. Liable-Sands, Arnold L. Rhinegold, Paul R. Markworth, Robert P. H. Chang, Michael P. Chidzik, Carl R. Kannewurf, and Tobin J. Marks. 2002. Synthesis and Characterization of Volatile, Fluorine-Free β-Ketoiminate Lanthanide MOCVD Precursors and Their Implementation in Low-Temperature Growth of Epitaxial CeO_2 Buffer Layers for Superconducting Electronics. *Inorganic Chemistry* 41: 5005-5023.

[19] Rees, Jr., William S., Oliver Just, and Donald S. Van Derveer. 1999. Molecular design of dopant precursors for atomic layer epitaxy of SrS : Ce. *Journal of Materials Chemistry* 9: 249-252.

[20] Stecher, Hilmar, Ayusman Sen, and Arnold L. Rhinegold. 1988. Synthesis, Structure, and Reactivity of Tricoordinate Cerium(III) Aryloxides. The First Structurally Characterized Monomeric $Ln(OR)_3$ Complexes. *Inorganic Chemistry* 27: 1130-1132.

[21] Fjeldberg, Torgny and Richard A. Andersen. 1985. Gas-Phase Electron Diffraction Studies of Two Sterically Hindered Three-Coordinate Lanthanide Amides: Tris(Bis(Trimethylsilyl)Amido)Cerium(III) and -Praseodymium(III). $M\{N(Si(CH_3)_3)_2\}_3$, M = Ce and Pr. *Journal of Molecular Structure* 129: 93-105.

[22] Bradley, Donald C., Joginder S. Ghotra, and F. Alan Hart. 1973. Low Co-ordination numbers in Lanthanide and Actinide Compounds. Part 1. The Preparation and

Characterization of Tris{bis(trimethylsilyl)amido}lanthanides. *Journal of the Chemical Society, Dalton Transactions* 1973: 1021.

[23] Birkofer, L. and A. Ritter. 1965. New Methods of Preparative Organic Chemistry IV. The Use of Silylation in Organic Synthesis. *Angewandte Chemie International Edition* 4(5): 417-429.

[24] Shannon, R. 1976. *Acta Crystallographica, Section A* 32: 751-767.

[25] Blank, H. -R., M. Frank, M. GeÍger, J. -M. Greneche, M. Ismaier, M. Kaltenhäuser, R. Kapp, W. Kreische, M. Leblanc, U. Lossen, and B. Zapf. 1994. "Systematic Investigation of MF_3 Crystalline Compounds (M = Al, Cr, Fe, Ga, In, Sc, Ti, and V) and $Fe_{1-x}M_xF_3$ Mixed Series (M = Ga, Cr, V)." *Zeitschrift für Naturforschung* 49a: 361-366.

Chapter 4

High-Symmetry Low-Coordinate Complexes of Cerium(III) and Uranium(III): Tris[bis(trimethylsilyl)amido] Phosphine Oxide Compounds for Empirical *f*-Element Electronic Structure Investigations

Introduction

This work reports the synthesis and characterization of trivalent four-coordinate tris(silylamide) phosphine oxide complexes of uranium and cerium with approximate C_3 symmetry. Cerium and uranium, along with the rest of the lanthanide and actinide elements, are considered "hard" Lewis acids and have large ionic radii [1-9]. The coordination chemistry of these elements is dominated by high coordination numbers (typically CN=7 or greater) and they tend to form complexes with "hard" fluoride and oxygen-donor ligands. Coordination numbers less than 6 are extremely rare in *f*-block coordination chemistry, and they were not observed for lanthanides until the three-coordinate tris[bis(trimethylsilyl)amide] complexes were synthesized in the 1970's [10-13]. These volatile, low-coordinate complexes with bulky silyl-amide ligands have led to important advances in the field [14-18]. They have served as gateways to new uncharted areas of *f*-block coordination chemistry via the "silyl-amide protonolysis route" [15, 19-23]; for example, the tris[bis(trimethylsilyl)amides] of the lanthanides have been used to install anionic,

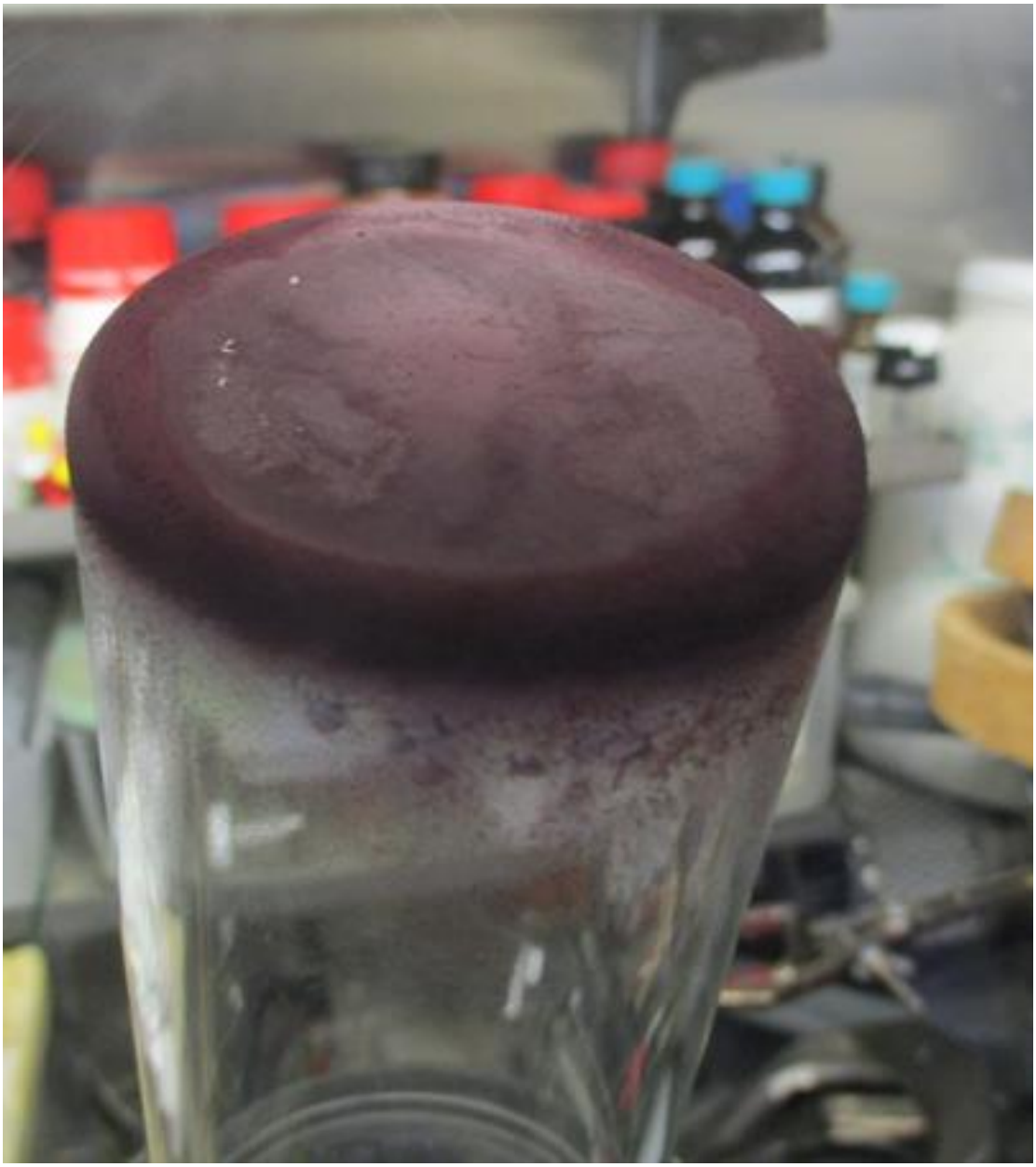

Figure 4.1: Sublimed $U[N(SiMe_3)_2]_3$

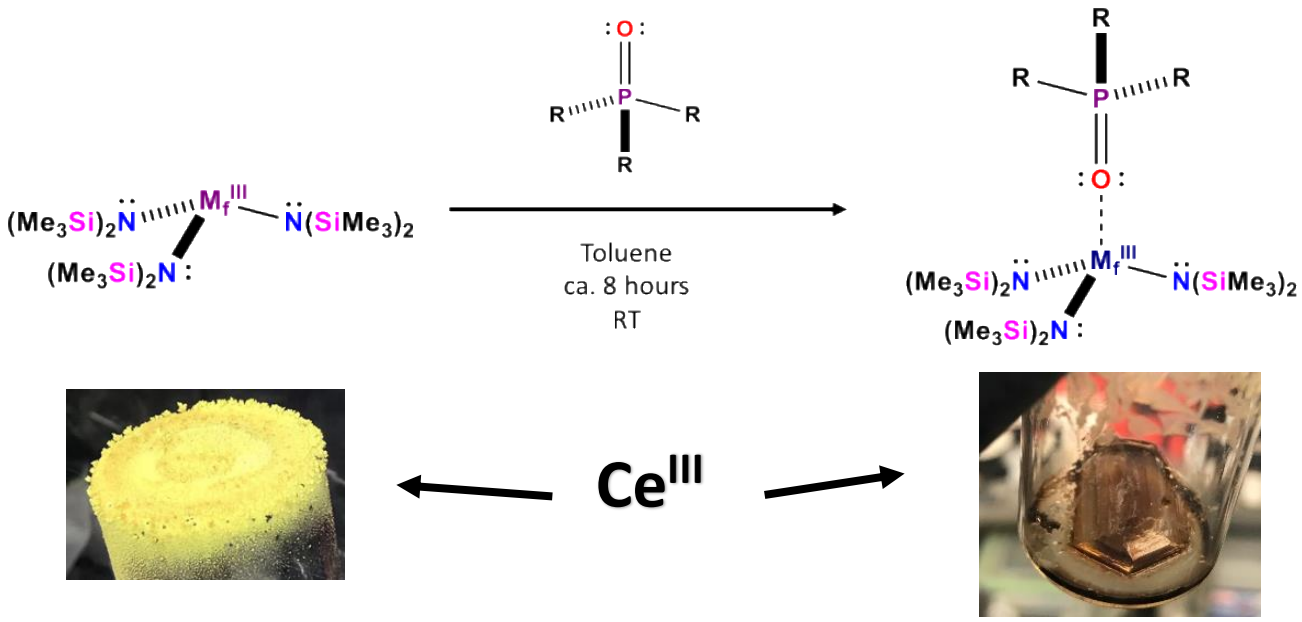

Scheme 4.1: General Synthesis of $M_f^{III}[OPR_3][N(SiMe_3)_2]_3$

"soft-donor" sulfido [20,21], selenido [21], tellurido [22], and phosphido [19] ligands via protonolysis. The volatility of lanthanide and actinide tris(silyl)amides makes them naturally attractive for metal-organic chemical vapor deposition (MOCVD) applications. The sulfido (thiolate) complexes have been used as precursors for the synthesis of high-purity lanthanide sulfide (Ln_2S_3) materials [2]. The tris-silylamides themselves can be used for the synthesis of lanthanide nitride (LnN) materials [15,24, 25], and uranium tris-amides can also be used to make uranium nitride (UN) [26], which has been attracting a lot of attention as a next generation nuclear fuel [26]. Nitride fuels have several advantages, such as high thermal conductivity, thermal stability, and fissile metal density; however, the synthesis of high purity actinide nitrides has been proven very difficult using conventional carbothermic reduction methods from metal oxides [26].

Molecular actinide amide precursors provide a potential alternative for the synthesis of high purity actinide nitride fuels [26].

$Gd[N(SiMe_3)_2]_3$ and $Nd[N(SiMe_3)_2]_3$ have recently been used as single-source precursors for the synthesis of bimetallic MRI contrasts agents (Gd) [27] and efficient photoabsorbers (Nd) [28], respectively. $U[N(SiMe_3)_2]_3$ and $Er[N(SiMe_3)_2]_3$ exhibit slow magnetic relaxation and are single-ion magnets [29,30]. *f*-Element single-ion magnets, and their potential applications in quantum technologies, has been the subject of a few excellent review articles in recent years [30-33]. $Ce[N(SiMe_3)_2]_3$ (Figure 1a) has served as a gateway for the synthesis of four-coordinate Cerium(IV) halide complexes [34-38]. These new tetravalent Cerium halide compounds represent an important advance in Ce^{IV} chemistry [38] and provide a high-symmetry platform for investigating the uranium-like covalency that has recently been observed in Ce^{IV} metal-ligand bonding [8]. Tris(silyl)amides have also provided straightforward and reliable routes to low-coordinate tetravalent uranium [39,40] and plutonium [24,25] halide compounds, as well as tetravalent, pentavalent, and hexavalent uranium complexes with metal-ligand multiple bonds [33-38]. Indeed, it is an exciting time to be involved in *f*-element coordination chemistry.

Over the decades since $Ln[N(SiMe_3)_2]_3$ compounds were first synthesized, they have also been used to synthesize four-coordinate trivalent adducts with Lewis-bases, such as triphenylphosphine oxide [49-51]. The triphenylphosphine oxide adducts have exhibtied interesting reactivity. In a previous study, the four-coordinate

triphenylphosphine oxide adducts showed enhanced protonolysis reactivity with diphenylphosphine ($HPPh_2$) compared to the base-free three-coordinate $Ln[N(SiMe_3)_2]_3$ compounds [19]. These protonolysis reactions resulted in the synthesis of lanthanum, europium, and yttrium phosphido complexes. Very few lanthanide complexes with anionic phosphorus-donor ligands have been reported in the literature [2,19,52,53]. This observed enhancement in reactivity has yet to be further explored since it was first reported decades ago, and it is worth revisiting and investigating further. The pseudo-C_3 symmetric four-coordinate tris[bis(trimethylsilyl)amido] triphenylphosphine oxide framework has only been reported for La [19], Sm [51], Eu [19], Er [50], Lu [19], Y [19], and U [39]. Only the lanthanum and uranium derivatives that have been characterized by X-ray crystallography [19,39], and ^{31}P NMR spectra have only been reported for the diamagnetic derivatives (La and Y) [19]. To our knowledge, tris(silylamido) phosphine oxide complexes with *substituted-aryl* phosphine oxide ligands have not been characterized via XRD or NMR. Substituted aryl-derivatives exhibit different reactivities and spectroscopic properties than the simple triphenylphosphine oxide framework, because the relative electron density on the phosphorus and oxygen atoms is highly influenced by the electronic character of the organic substituents bound to the phosphorus. The nature of the organic substituents on phosphorus therefore highly influences the nature of the metal-oxygen bond in phosphine oxide coordination complexes.

These axially symmetric four-coordinate silyl-amide phosphine oxide complexes are suitable models for studying the relative differences in Ln/An metal-ligand covalency using ^{31}P-NMR spectroscopy and X-ray emission spectroscopy. Expanding this structural framework to other lanthanide and actinide metals, and fully characterizing a series of *pseudo*-isostructural complexes featuring various organic substituents on the phosphine oxide (beyond triphenylphosphine oxide), would provide considerable insight concerning phosphine oxide bonding interactions with *f*-block metals. In addition to being convenient ligands for spectroscopic studies of *f*-element electronic structure, phosphine oxides (and the details of their interactions with *f*-block metals) are directly relevant to the nuclear fuel cycle [54]. Phosphine oxides have been used effectively for advanced trivalent lanthanide/actinide separations [54-56]. The fundamental nature of *f*-block metal-phosphine oxide bonds is not well understood [7,57,58,59], and deeper empirical insight into the nature of these interactions is needed in order to facilitate large-scale computational screening of potential extractants for trivalent Ln/An separations.

Herein we report the synthesis, X-ray crystallography, and paramagnetic NMR spectroscopy of a series of trivalent cerium and uranium tris(silylamido) phosphine oxide complexes, as well as the X-ray and gamma emission spectra for $Ce[N(SiMe_3)_2]_3[OPPh_3]$.

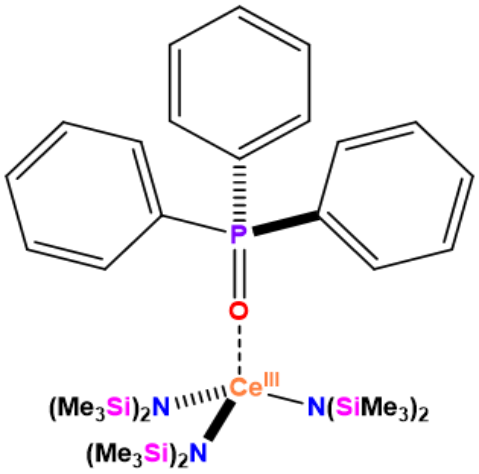

This work

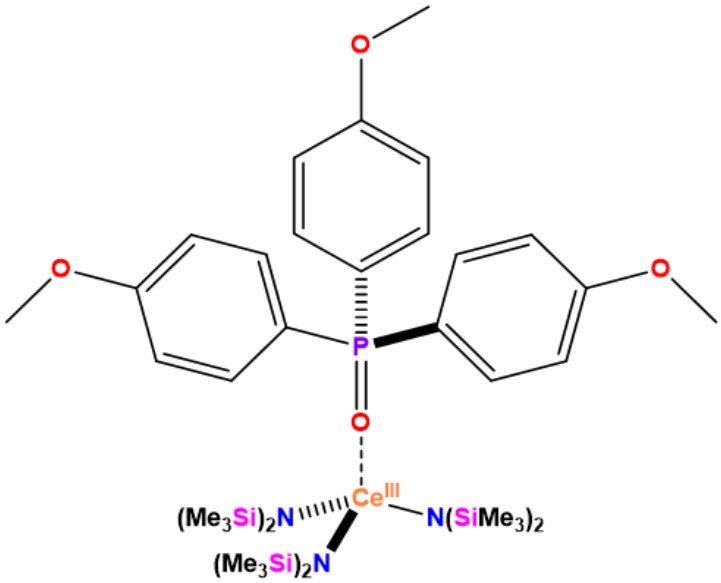

This work

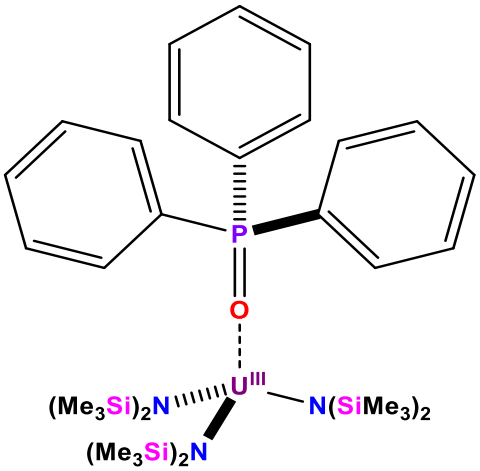

Stewart, J.L. 1988 PhD Thesis, Berkeley

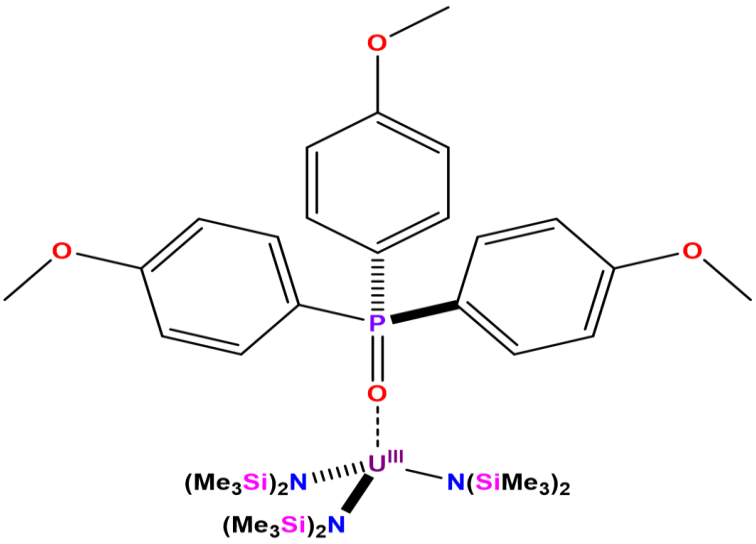

This work

Figure 4.2: Structurally Characterized $M_f^{III}[OPAr_3][N(SiMe_3)_2]_3$ Compounds

Experimental

All experimental operations were conducted with rigorous exclusion of air and moisture using Schlenk techniques, standard glove-box methods using a Vacuum Atmospheres glovebox with a recirculating dinitrogen atmosphere, and standard glove-bag methods using a Captair Pyramid disposable glove-box under Argon. Solvents were bought anhydrous or HPLC grade (pentane, hexane, toluene, acetonitrile, THF, diethyl ether) and further purified using a Vacuum Atmospheres Solvent Purifier System. 1,4-dioxane, THF, and diethyl ether were dried over sodium benzophenone ketyl, and degassed by three freeze-pump-thaw cycles prior to use. All solvents were stored under dinitrogen in a glove-box, and stored over 4 Å molecular sieves for at least 24 hours prior to use. Glassware was dried at 150°C before use. ^{1}H and ^{31}P NMR spectra were recorded using a Bruker 400 MHz spectrometer at 298 K. Deuterated benzene (Cambridge Isotopes) was stored over 4 Å molecular sieves for at least 24 hours prior to use. Elemental analysis was conducted using particle-induced X-ray emission spectrometry (PIXE) and particle-induced gamma-ray emission spectrometry (PIGE) using a 3 MeV proton beam generated by a 3MV Tandem Accelerator (National Electrostatics Corporation). X-rays were detected using two high-energy Bruker SDD detectors, and one low-energy Bruker SDD detector. Gamma-rays were detected using a liquid nitrogen-cooled high-purity germanium (HPGe) detector. The sample for elemental analysis was secured between two pieces of 8 μm Kapton film under nitrogen and brought out into the atmosphere for

external ion beam analysis. Single crystal X-ray diffraction was conducted using a Bruker XRD instrument with a Mo-Kα X-ray source.

Oxide encrustations were removed from the uranium metal using concentrated nitric acid [60]. Once the turnings achieved a brilliant lustre, the nitric acid was decanted, and the turnings were rinsed with acetone and stored in a dinitrogen atmosphere glovebox. Iodine (sublimed) was used as purchased (Aldrich). $KN(SiMe_3)_2$ and $CeCl_3$ (anhydrous) was used as purchased (Aldrich). Phosphine oxides were synthesized from commercially obtained tertiary-arylphosphines (Aldrich) using literature methods [61, 62]. $UI_3(1,4\text{-dioxane})_{1.5}$ was prepared using literature methods [60]. $Ce[N(SiMe_3)_2]_3$ [63] and $U[N(SiMe_3)_2]_3$ [60] were synthesized using literature methods and sublimed prior to use.

Caution! *Depleted uranium (primary isotope ^{238}U) is a weak α-emitter (4.197 MeV) with a half-life of 4.47 x 10^9 years; manipulations and reactions should be carried out in monitored fume hoods or in an inert atmosphere drybox in a radiation laboratory equipped with α-counting equipment*.

Synthesis of $Ce[OPPh_3][N(SiMe_3)_2]_3$

0.739 grams (1.19 mmol) of freshly sublimed $Ce[N(SiMe_3)_2]_3$ was dissolved in 10 mL of toluene, and added to a flask with 0.331 grams (1.19 mmol) of triphenylphosphine oxide, and stirred overnight at room temperature. The vibrant yellow color of the $Ce[N(SiMe_3)_2]_3$ slowly fades to transparent as the triphenylphosphine oxide coordinates to the Cerium ion. The solvent was removed *in-vacuo*, and the residue was extracted with 20 mL of pentane, and filtered through a Celite-padded, medium porosity fritted-filter.

The pentane was removed from the product *in vacuo*, and a beige-tan solid was afforded in 87% yield (0.928 grams). Large crystals we grown from a concentrated pentane solution with a minimal amount of toluene. The crystals initially submitted were twinned, and the product was recrystallized from a pentane/toluene solution to yield a large (ca. 0.5 g) crystal with smaller single crystals surrounding it. The smaller crystals were submitted for single crystal X-ray diffraction, and the crystal structure obtained confirmed that the compound was indeed the four-coordinate complex tris(silyl) amide phosphine oxide complex. The proton NMR for the complex features a large, broad, paramagnetically shifted $SiMe_3$ peak at -0.78 ppm, which is relatively more deshielded than the three-coordinate precursor (-3.3 ppm). Very broad aromatic NMR signals also show up at 6.4 ppm and 4.6 ppm, relatively more shielded compared to the free ligand. The observation of only two aromatic signals is consistent with the isostructural Yttrium complex [49]. Only one ^{31}P NMR resonance was observed at 54 ppm, significantly deshielded compared to the free ligand at 29 ppm. The large crystal was submitted for ion beam analysis, and the X-ray spectrum obtained via PIXE nearly confirms the correct stoichiometry of the complex. The relative Ce and Si concentrations were almost correct; however, the P concentrations were somewhat high, presumably due to the phosphine oxide crust that formed on the crystal over time. *Crystal Data*: $C_{36}H_{69}CeN_3OPSi_6$ (1-Ce), M = 899.57, triclinic, space group $P\bar{1}$, a = 12.3341(10) Å, b = 12.3809(10) Å, c = 19.7051(17) Å, α = 100.0905(13)°, β = 93.0661(14)°, γ = 118.9017(12)°, U = 2560.0(4) Å^3, Z = 2, D_c = 1.167 g cm^{-3}, Mo-Kα radiation [λ = 0.71073 Å, μ(Mo-Kα) = 1.087 mm^{-1}]. *NMR Data* (C_6D_6): ^1H δ -0.78 ppm ($SiMe_3$ 54H), δ 6.4 ppm (aromatic 9H), δ 4.6 ppm (aromatic 6H); ^{31}P δ 53.57 ppm.

Elemental Analysis (PIXE): Calculated Ce 15.58 P 3.44 Si 18.73; Found: Ce 15.58 P 6.48 Si 19.67.

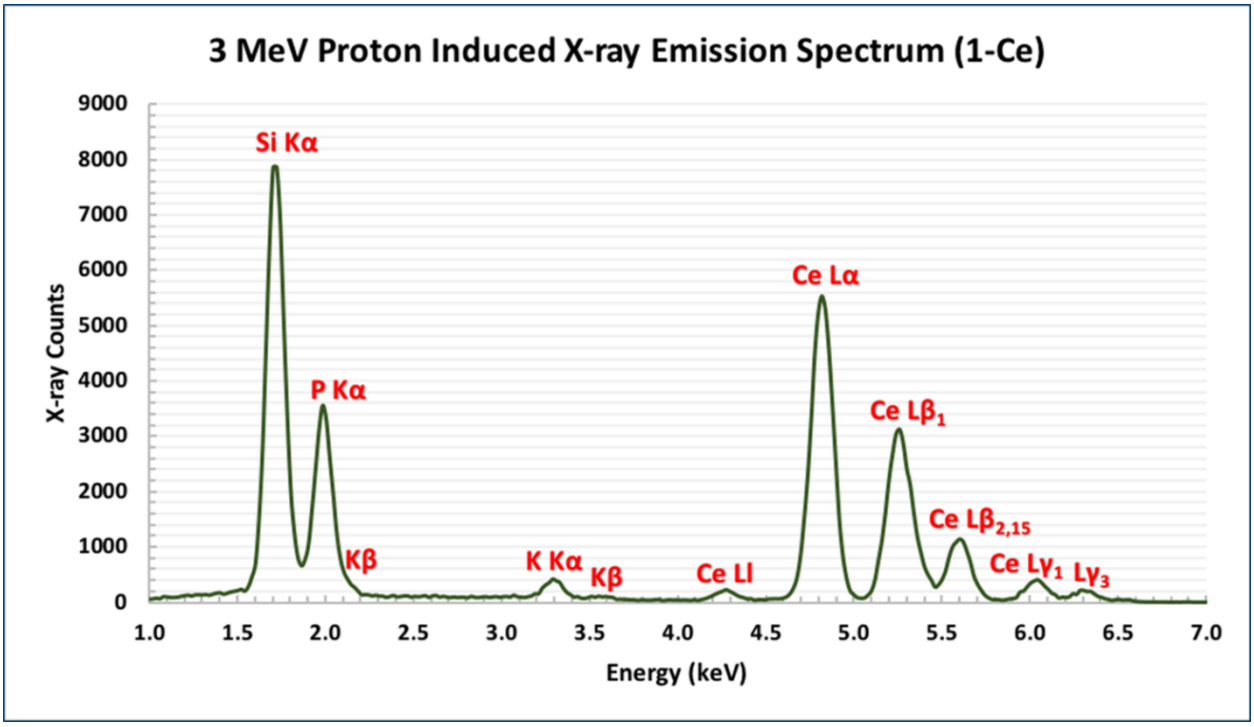

Figure 4.3: Energy-Dispersive X-ray Emission Spectrum for $Ce[OPPh_3][N(SiMe_3)_2]_3$

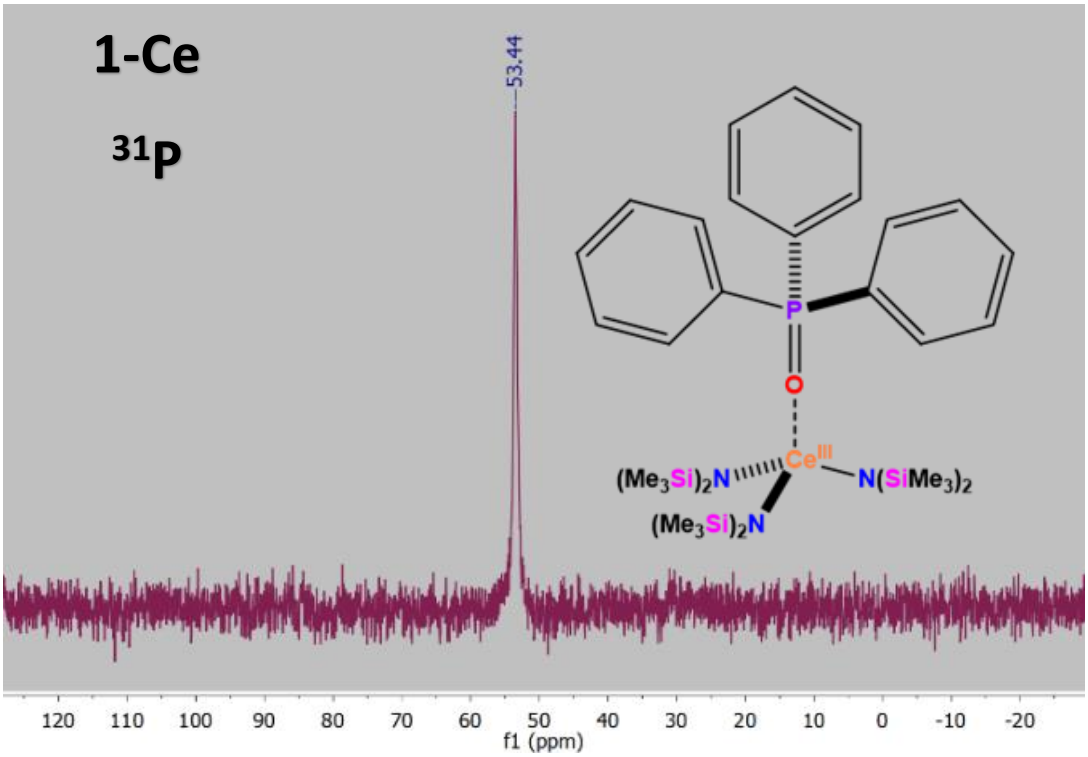

Figure 4.4: ^{31}P NMR Spectrum for $Ce[OPPh_3][N(SiMe_3)_2]_3$

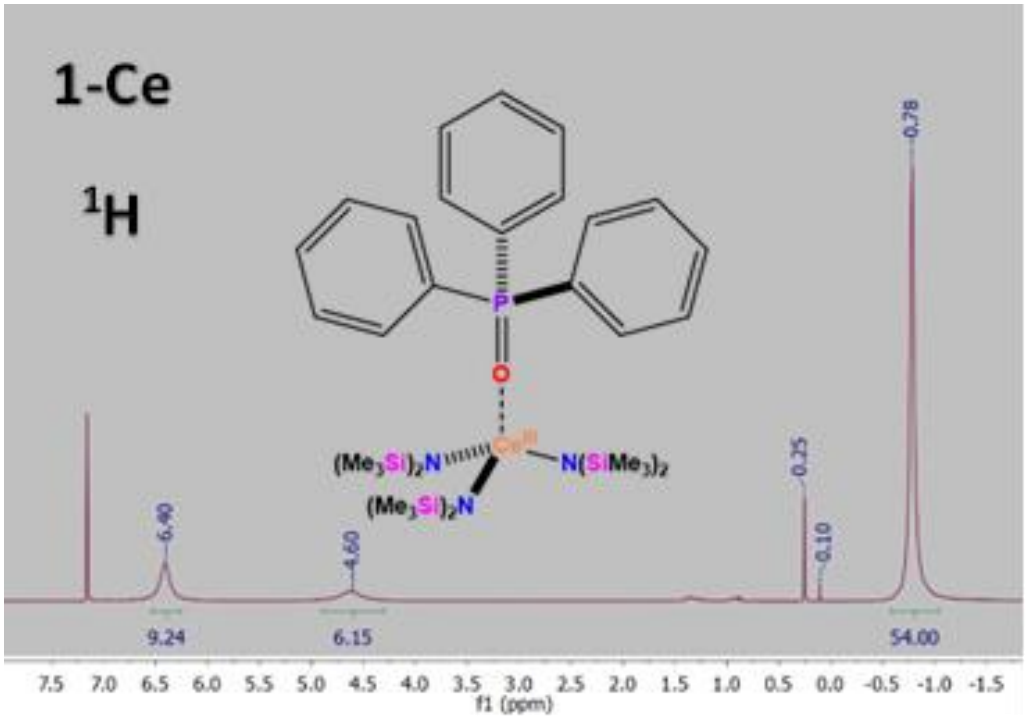

Figure 4.5: ^{1}H NMR Spectrum for $Ce[OPPh_3][N(SiMe_3)_2]_3$

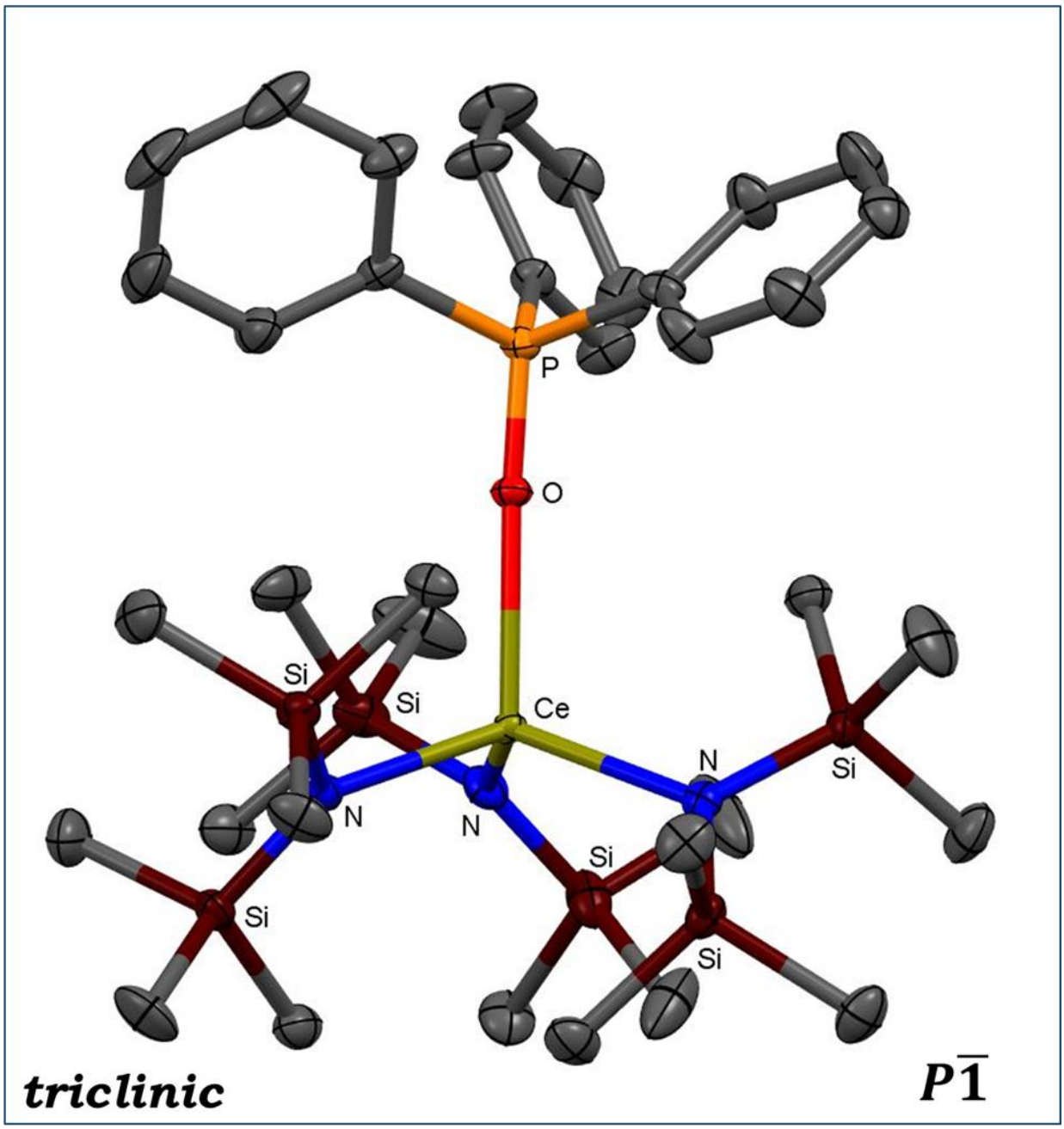

Figure 4.6: Single-Crystal XRD Structure for $Ce[OPPh_3][N(SiMe_3)_2]_3$

Synthesis of Ce[OP(*p*-anisyl)$_3$][N(SiMe$_3$)$_2$]$_3$

0.021 grams (0.034 mmol) of freshly sublimed Ce[N(SiMe$_3$)$_2$]$_3$ was dissolved in 3 mL of toluene, and added to a flask with 0.012 grams (0.034 mmol) of tris(*p*-anisyl)phosphine oxide, and stirred overnight at room temperature. The vibrant yellow color of the Ce[N(SiMe$_3$)$_2$]$_3$ slowly fades to transparent as the tris(*p*-anisyl)phosphine oxide coordinates to the cerium ion. The solvent was removed *in-vacuo*, and the residue was extracted with 10 mL of pentane, and filtered through a Celite-padded, medium porosity fritted-filter. The pentane was removed from the product *in vacuo*, and a colorless solid was afforded in ca. 100% yield (0.033 grams). Single crystals were grown from a concentrated pentane solution via slow evaporation at room temperature after a few days and submitted for X-ray diffraction. *Crystal* Data: $C_{39}H_{75}CeN_3O_4PSi_6$ (2-Ce), M = 989.65, monoclinic, space group $P2_1/c$, a = 16.1035(9) Å, b = 13.8776(8) Å, c = 23.0565(13) Å, α = 90°, β = 91.9766(9)°, γ = 90°, U = 5149.6(5) Å^3, Z = 4, D_c = 1.276 g cm^{-3}, Mo-Kα radiation [λ = 0.71073 Å, μ(Mo-Kα) = 1.092 mm^{-1}]. *NMR Data* (C_6D_6): ^{1}H δ -0.77 ppm (SiMe$_3$ 54H), δ 6.14 ppm (aromatic 6H), δ 4.92 ppm (aromatic 6H), δ 2.98 ppm (OCH$_3$ 9H); ^{31}P δ 54.39 ppm.

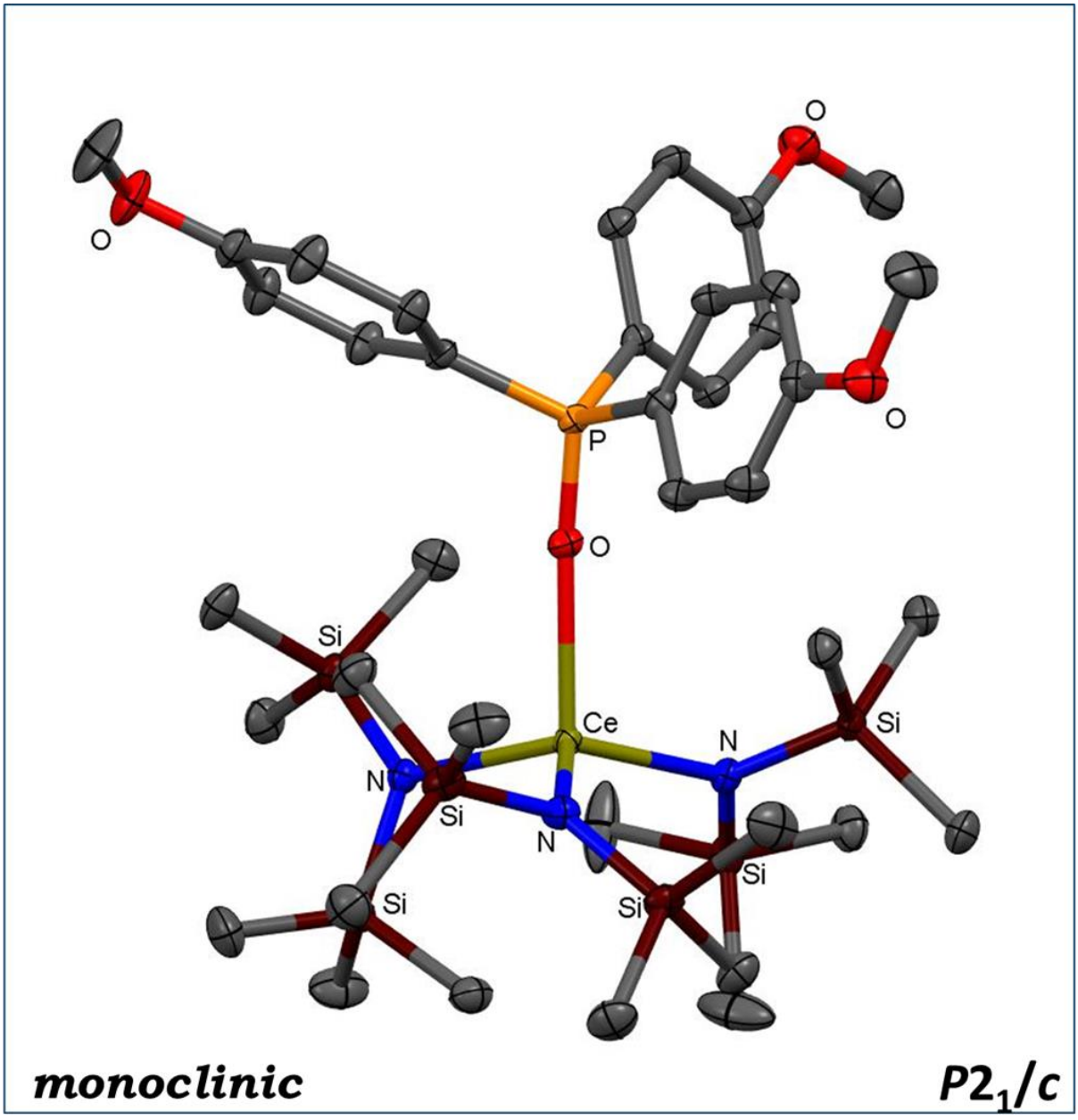

Figure 4.7: Single-Crystal XRD Structure for Ce[OP(*p*-anisyl)$_3$][N(SiMe$_3$)$_2$]$_3$

Synthesis of $U[OP(p\text{-anisyl})_3][N(SiMe_3)_2]_3$

0.719 grams (1.03 mmol) of freshly sublimed $U[N(SiMe_3)_2]_3$ was dissolved in 10 mL of toluene, and added to a flask with 0.379 grams (1.03 mmol) of tris(*p*-anisyl)phosphine oxide, and stirred overnight at room temperature. The reddish-purple color of the $U[N(SiMe_3)_2]_3$ appears to gradually change to a darker shade of purple very subtly as the tris(*p*-anisyl)phosphine oxide coordinates to the uranium ion. The solvent was removed *in-vacuo*, and the residue was extracted with 20 mL of pentane, and filtered through a Celite-padded, medium porosity fritted-filter. The pentane was removed from the product *in vacuo*, and a purple solid was afforded in 46% yield (0.519 grams).

Alternative procedure 0.051 grams (0.068 mmol) of $UI_3(1,4\text{-dioxane})_{1.5}$ was dissolved in 5 mL of THF. Three equivalents of $KN(SiMe_3)_2$ and a threefold excess of t tris(*p*-anisyl)phosphine oxide (with respect to uranium) was dissolved in 5 mL of THF, and added dropwise to the UI_3/THF solution while stirring at room temperature with slight evolution of fumes upon addition. The dark brown (almost black) solution was stirred overnight, and the solvent was removed *in vacuo*. The residue was extracted with toluene, and the potassium iodide salts were removed by filtering the extract through a Celite-padded medium porosity fritted filter. The solvent was removed *in vacuo* yielding a dark-brown/black solid, and the residue was extracted with *n*-pentane. The remaining salts and unidentified insoluble by-products were removed by filtering the purple *n*-pentane extract through a Celite-padded medium-porosity fritted filter. The solvent was removed *in vacuo*, affording a purple solid in ca 50% yield. Purple single-crystals of the complex

were grown from a concentrated pentane solution via slow evaporation at -30°C after a few days and submitted for X-ray diffraction. *Crystal Data*: $C_{39}H_{75}N_3O_4PSi_6U$ (3-U), M = 1087.56, monoclinic, space group $P2_1/c$, a = 16.063(2) Å, b = 13.9300(19) Å, c = 23.043(3) Å, α =90°, β = 91.895(2)°, γ = 90°, U = 5153.2(12) Å^3, Z = 4, D_c = 1.402 g cm^{-3}, Mo-Kα radiation [λ = 0.71073 Å, μ(Mo-Kα) = 3.357 mm^{-1}]. *NMR Data* (C_6D_6): ^{1}H δ -5.68 ppm ($SiMe_3$ 54H), δ 4.47 ppm (aromatic 6H), δ -2.51 ppm (aromatic 6H), δ 2.56 ppm (OCH_3 9H); ^{31}P δ 102.6 ppm.

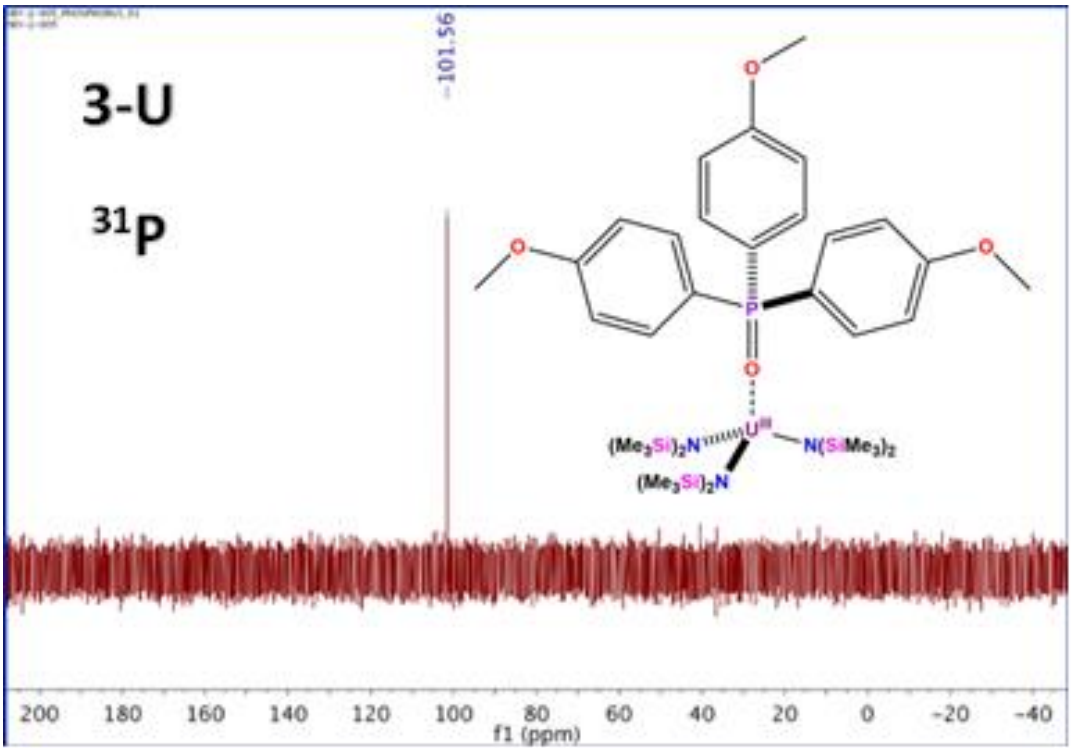

Figure 4.8: ^{31}P NMR Spectrum for U[OP(*p*-anisyl)$_3$][N(SiMe$_3$)$_2$]$_3$

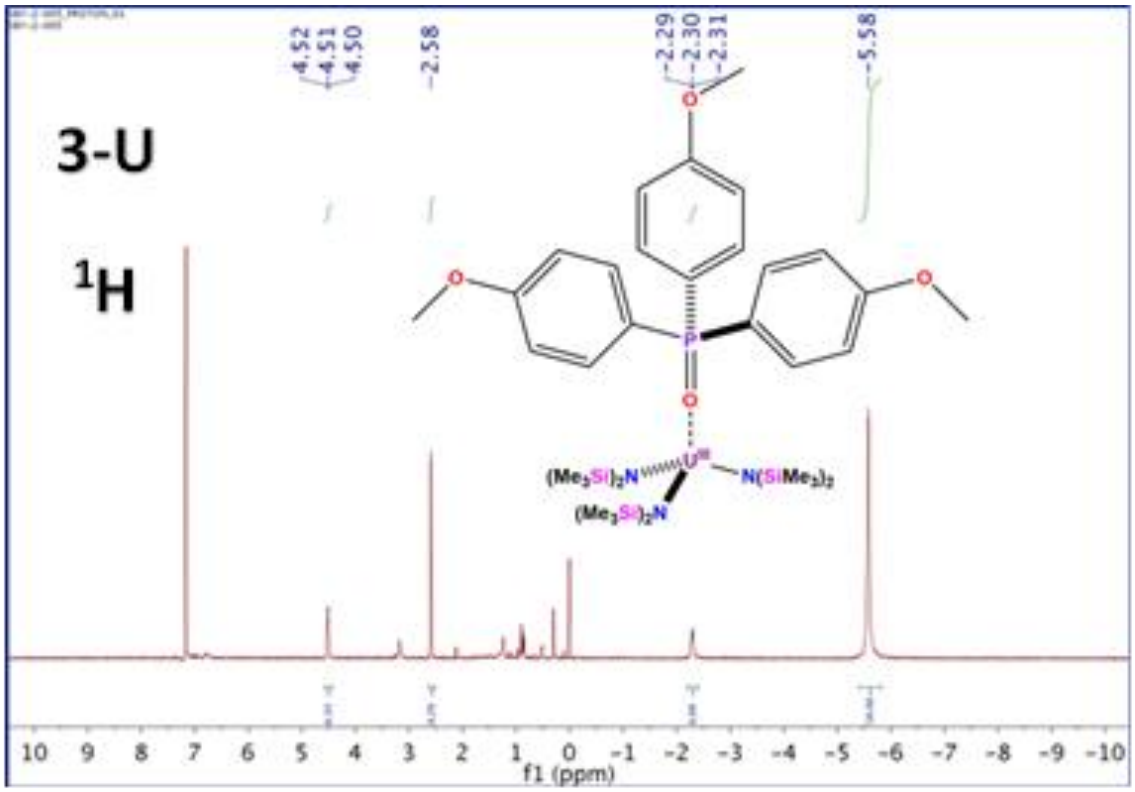

Figure 4.9: ^{1}H NMR Spectrum for U[OP(*p*-anisyl)$_3$][N(SiMe$_3$)$_2$]$_3$

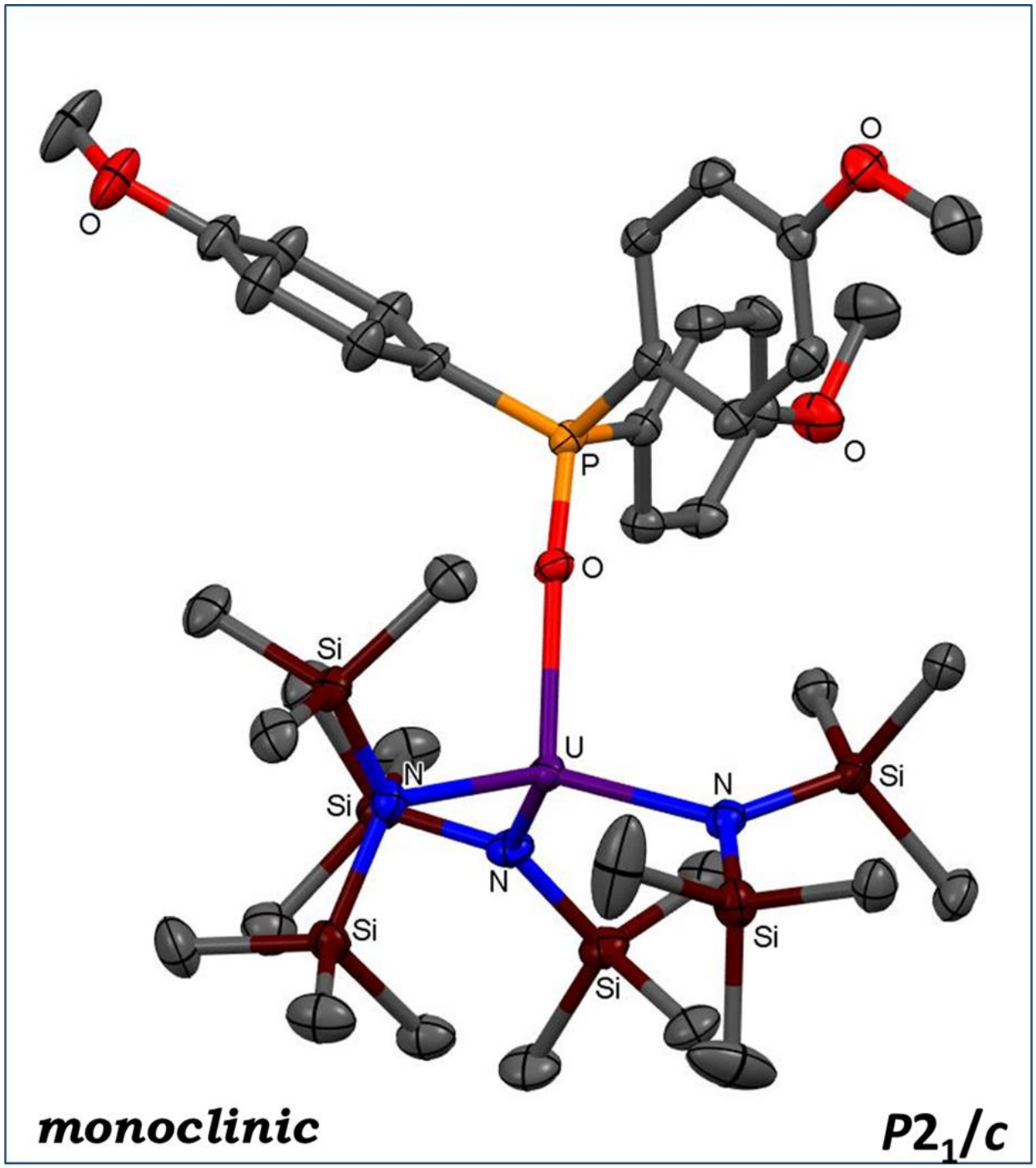

Figure 4.10: Single-Crystal XRD Structure for U[OP(*p*-anisyl)$_3$][N(SiMe$_3$)$_2$]$_3$

Synthesis of Ce[OP(*p*-tolyl$_3$][N(SiMe$_3$)$_2$]$_3$

0.009 grams (0.0148 mmol) of freshly sublimed Ce[N(SiMe$_3$)$_2$]$_3$ was dissolved in 3 mL of toluene, and added to a flask with 0.005 grams (0.0148 mmol) of tris(*p*-tolyl)phosphine oxide, and stirred overnight at room temperature. The vibrant yellow color of the Ce[N(SiMe$_3$)$_2$]$_3$ slowly fades to transparent as the tris(*p*-tolyl)phosphine oxide coordinates to the cerium ion. The solvent was removed *in-vacuo*, and the residue was extracted with 10 mL of pentane, and filtered through a Celite-padded, medium porosity fritted-filter. The pentane was removed from the product *in vacuo*, and a beige solid was afforded in 52 % yield (0.007 grams). *NMR Data* (C_6D_6): ^{1}H δ -0.74 ppm (SiMe$_3$ 54H), δ 5.45 ppm (aromatic 9H), δ 4.67 ppm (aromatic 6H); ^{31}P δ 54.55 ppm.

Table 1. Crystallographic Data for R_3P=O-Met-[N(SiMe$_3$)$_2$]$_3$

		bond length (Å)						bond angle (˚)					
R	**Met**	**Met-O**	**O-P**	**Met-N1**	**Met-N2**	**Met-N3**	**M-N$_{avg}$**	**Met-O=P**	**N1-Met-N2**	**N1-Met-N3**	**N2-Met-N3**	**N-Met-N$_{avg}$**	**ref**
MeOPh	Ce	2.3952(12)	1.5161(12)	2.3612(14)	2.4000(14)	2.4065(14)	2.389	174.44(7)	107.37(5)	114.43(5)	121.53(5)	114.44	
Ph	Ce	2.403(2)	1.512(2)	2.357(2)	2.373(3)	2.388(2)	2.373	176.85(13)	108.83(9)	110.90(9)	116.96(9)	112.23	
MeOPh	U	2.376(3)	1.519(3)	2.344(4)	2.390(4)	2.398(4)	2.377	174.2(2)	108.55(14)	112.84(14)	120.88(14)	114.09	
Ph	U	2.382(2)	1.512(2)	2.343(4)	2.362(4)	2.367(3)	2.357	176.5(2)	109.8(1)	110.7(1)	115.6(1)	112.03	[26]
Ph	La	2.40(2)	1.52(2)	2.38(2)	2.40(3)	2.41(2)	2.397	174.6	109.2(9)	112.7(8)	116.4(6)	112.77	[49]

Table 2. Data for Ph_3P=O-Met-$[N(SiMe_3)_2]_3$				
NMR data (ppm)				
Met	^{31}P	^{1}H $SiMe_3$	^{1}H Aromatic	ref
U	105.19	-5.66	6.46-4.56	
Ce	53.57	-0.78	6.40, 4.63	
La	39	0.07	7.57	[49]
Y	38	0.3	6.8-7.9	[49]
Sm	N/A	N/A	N/A	[51]
Eu	N/A	-1.43	4.9	[49]
Er	N/A	N/A	N/A	[50]
Lu	N/A	0.1	7.5	[49]

Results and Discussion

Reactions of extremely air sensitive $Ce[N(SiMe_3)_2]_3$ (CeN^*_3) and $U[N(SiMe_3)_2]_3$ (UN^*_3) with one equivalent of aryl-phosphine oxide ligands in toluene at room temperature for several hours afforded $M[OPAr_3][N^*]_3$ compounds in moderate to excellent yields (46%-100%). Optimum yields were obtained for the *para*-methoxy substituted aryl-phosphine oxide derivative (quantitative), and in general, cerium derivatives were obtained in better yields than the uranium derivatives. U[OP(*p*-anisyl)$_3$][$N(SiMe_3)_2]_3$ could also be obtained in one step from directly UI_3(1,4-dioxane)$_{1.5}$, thereby circumventing the difficulties involved with obtaining impurity-free $U[N(SiMe_3)_2]_3$. The four-coordinate aryl-phosphine oxide adducts, unsurprisingly, are more air-stable and robust than their three-coordinate tris-amide precursors; however,

the phosphine oxide adducts are still extremely air/moisture-sensitive, just less so than the extremely coordinatively unsaturated three-coordinate precursors. These aryl-phosphine oxide adducts are highly crystalline, and large single-crystals can be obtained via slow evaporation of *n*-pentane and/or toluene at room temperature or -30°C.

Single-crystal X-ray structures were obtained for U[OP(*p*-anisyl)$_3$][N(SiMe$_3$)$_2$]$_3$, Ce[OP(*p*-anisyl)$_3$][N(SiMe$_3$)$_2$]$_3$, and Ce[OPPh$_3$][N(SiMe$_3$)$_2$]$_3$, which facilitated useful comparisons with the two other structurally characterized tris(silyl)amido-triphenylphosphine oxide complexes reported in the literature, La[OPPh$_3$][N(SiMe$_3$)$_2$]$_3$ and U[OPPh$_3$][N(SiMe$_3$)$_2$]$_3$. These compounds also facilitated useful comparisons with the base-free tri-coordinate M[N(SiMe$_3$)$_2$]$_3$ complexes that have been structurally characterized [M = Ce [64], Pr [65], Nd [66], Sm [67], Eu [68], Tb [69], Dy [70], Er [70], Tm [71], Yb [72], Lu [73], Y [74], Sc [68], U [75], and Pu [76]). Additional comparisons can also be made with other *f*-element phosphine oxide complexes that have been structurally characterized [59]; however, to limit the scope of this discussion, attention will be focused on the extremely short list of monomeric four-coordinate tris[bis(trimethylsilyl)amido] Lewis-base adducts of the *f*-elements that have been structurally characterized. The three crystal structures obtained, along with the previously reported La and U derivatives, are *pseudo*-isostructural, and feature nearly linear metal-oxygen-phosphorus bond angles (174-176°). Bond lengths and bond angles for this *pseudo*-isostructural series are given in Table 1. Table 4 gives the average metal-nitrogen bond lengths for the structurally characterized M[N(SiMe$_3$)$_2$]$_3$ derivatives for comparison.

The XRD data obtained in this work, in conjunction with previous XRD results, indicate that coordination of an aryl-phosphine oxide ligand to the tris(silyl)amido framework results in a subtle, but noticeable, lengthening of the metal-nitrogen bonds compared to the three-coordinate base-free analogues. The cerium-nitrogen bond in CeN^*_3 (2.320 Å) increases to 2.403 Å in $Ce[OPPh_3][N(SiMe_3)_2]_3$ and 2.395 Å in 2-Ce. The uranium-nitrogen bond in UN^*_3 (2.320 Å) increases to 2.382 Å in $U[OPPh_3][N(SiMe_3)_2]_3$ and 2.376 Å in 3-U. The metal-oxygen-phosphorus (M-O-P) bond angles are nearly linear in all the complexes. The M-O-P angles for the triphenylphosphine oxide complexes $Ce[OPPh_3][N(SiMe_3)_2]_3$ and $U[OPPh_3][N(SiMe_3)_2]_3$ are ca. 176°, and 174° for $Ce[OP(p\text{-anisyl})_3][N(SiMe_3)_2]_3$, $U[OP(p\text{-anisyl})_3][N(SiMe_3)_2]_3$, and $La[OPPh_3][N(SiMe_3)_2]_3$. The three triphenylphosphine oxide complexes have N-M-N angles of about 112° (average), and the angles for the substituted aryl derivatives are slightly larger, 114° (average). As a whole, the geometrical parameters are extremely similar for the five tris(silyl)amido-phosphine oxide complexes that have been structurally characterized by XRD in this work and previous work.

Table 3. Data for R_3P=O-Met-$[N(SiMe_3)_2]_3$						
NMR data (ppm)						
R	Met	^{31}P	^{1}H $SiMe_3$	^{1}H Aromatic	^{1}H Alkyl	ref
t-Bu	Ce	91.77	-1.17	-	-5.14	
MePh	Ce	54.55	-0.74	5.45, 4.67	1.56	
MeOPh	Ce	54.39	-0.77	6.14, 4.92	2.98	
Ph	Ce	53.57	-0.78	6.40, 4.63	-	
MePh	U	98.34	-5.53	6.25, 4.63	-7.22	
t-Bu	U	368.58	-3.16	-	-8.75	
MeOPh	U	102.6	-5.68	4.47, -2.51	2.56	
Ph_2(tolyl)	U	104.48	-5.52	6.85-4.51	-2.83	
Ph	U	105.19	-5.66	6.46-4.56	-	
Ph	La	39	0.07	7.57	-	[49]

Table 4. $M_f^{III}[N(SiMe_3)_2]_3$				
$Ln^{III}[N(SiMe_3)_2]_3$	^{1}H NMR	ref	Ln-N Bond	ref
La	0.25	[10]		
Ce	-3.39	[63]	2.320(3)	[64]
Pr	-8.64	[10]	2.31(4)	[65]
Nd	-6.25	[63]	2.29(4)	[66]
Sm	-1.58	[10]	2.284(3)	[67]
Eu	6.43	[10]	2.259(9)	[68]
Gd	-11.07	[63]		
Tb			2.233(12)	[69]
Dy			2.212(2)	[70]
Ho				
Er	62.89	[63]	2.21(1)	[70]
Tm			2.198(9)	[71]
Yb			2.158(13)	[72]
Lu	0.1	[10]	2.168(12)	[73]
Y	0.28	[10]	2.224(6)	[74]
Sc			2.047(6)	[68]
$An^{III}[N(SiMe_3)_2]_3$				
U	-11	[14]	2.320(4)	[75]
Np	3.01	[14]		
Pu	0.74	[14]	2.315(10)	[76]

The data in Table 4 shows a gradual decrease in lanthanide-nitrogen bond distances across the 4*f* series from Ce-Yb as the relative ionic radius of the lanthanide ion decreases. The metal-nitrogen bond lengths in $Ce[N(SiMe_3)_2]_3$ and $U[N(SiMe_3)_2]_3$ are identical (2.320 Å), which is consistent with their nearly identical trivalent ionic radii. Since the ionic radii of La^{3+} (117.2 pm), Ce^{3+} (115 pm), and U^{3+} (116 pm) [2] are so similar, one might expect there to be little to no difference in the metal-oxygen bond lengths shown in Table 1. However, the uranium-oxygen bonds are measurably shorter than the cerium and lanthanum bonds. The differences in bond lengths are very subtle (only about 0.02 Å); however, this could be evidence of increased metal-ligand covalency in the uranium complexes compared to the cerium and lanthanum analogues, presumably due to slightly increased ligand 2*p* orbital mixing into 6*d* and 7*p* manifolds. However, very little can be said definitively about the orbital interactions involved based on this slight difference in bond length.

The bonding in these *f*-element amide complexes is largely ionic in character, and most of the structural data can be rationalized in terms of the ionic radius of the central metal cation, and the steric properties of the ligand framework. However, the relative amount of metal-ligand covalency in lanthanide amide complexes appears to have been initially underestimated, with the assumption that the limited radial extent of the core-like 4*f* orbitals prevented nitrogen-metal π-interactions, leading to negligible metal-ligand covalency. Photoelectron studies seemed to confirm this assertion [77]. However, subsequent computational studies suggested that lanthanide amides have a considerable

degree of covalent character. While affirming the conclusions of previous studies with respect to the non-involvement of the 4*f* electrons in chemical bonding, some computational results emphasize the importance of the 5*d* and 6*p* orbitals in lanthanide-nitrogen bonds [93]. Empirical structural and spectroscopic data for lanthanide amide and phosphine oxide complexes are scarce, and more isostructural complexes of the other members of the lanthanide series and actinide series need to be synthesized and characterized. Sophisticated computational and spectroscopic studies must also be conducted on these complexes before any real conclusions about the nature of the metal-ligand bonds in these complexes can be made. This work is a small step in that direction.

Paramagnetic ^{1}H and ^{31}P NMR spectra were obtained for Ce[OP(*p*-anisyl)$_3$][N(SiMe$_3$)$_2$]$_3$, Ce[OPPh$_3$][N(SiMe$_3$)$_2$]$_3$, and U[OP(*p*-anisyl)$_3$][N(SiMe$_3$)$_2$]$_3$, along with other substituted aryl- and alkyl-derivatives. Derivatives other than Ce[OP(*p*-anisyl)$_3$][N(SiMe$_3$)$_2$]$_3$, Ce[OPPh$_3$][N(SiMe$_3$)$_2$]$_3$, and U[OP(*p*-anisyl)$_3$][N(SiMe$_3$)$_2$]$_3$ have not yet been fully characterized or obtained in pure form; however, tentative assignments for additional aryl and alkyl derivatives could still be made for the paramagnetically shifted NMR resonances that were observed, so they are included here for comparison. Table 2 features the NMR data for Ce[OPPh$_3$][N(SiMe$_3$)$_2$]$_3$, as well as all the NMR data available in the literature for M[OPPh$_3$][N(SiMe$_3$)$_2$]$_3$complexes. Table 3 features the NMR data for Ce[OP(*p*-anisyl)$_3$][N(SiMe$_3$)$_2$]$_3$, Ce[OPPh$_3$][N(SiMe$_3$)$_2$]$_3$, and U[OP(*p*-anisyl)$_3$][N(SiMe$_3$)$_2$]$_3$, along with additional data for complexes that have not been fully characterized or obtained in pure form. Tables 2 and 3 also include NMR data for the

previously reported $U[OPPh_3][N(SiMe_3)_2]_3$. No NMR data was previously reported for this complex, though its crystal structure was reported in Stewart's 1988 dissertation. Synthetic difficulties were encountered in this work while trying to reproduce the $U[OPPh_3][N(SiMe_3)_2]_3$ complex, similar to the difficulties Stewart reported in her 1988 dissertation. Presumably the instability of the complex is what prevented the NMR data from being acquired. Stewart reported that the purple solid complex decomposed to a brown microcrystalline solid after prolonged exposure to vacuum. In our hands, the characteristic purple color of the complex persisted for a short time while in an inert-atmosphere glove-box; however, by the time the compound was worked-up, isolated, and analyzed by NMR, the purple color had turned to brown, and complex NMR spectra were obtained that were difficult to assign. However, synthesis of $U[OPPh_3][N(SiMe_3)_2]_3$ directly from $UI_3(1,4\text{-dioxane})_{1.5}$ (described in the experimental section for the alternative synthesis $U[OP(p\text{-anisyl})_3][N(SiMe_3)_2]_3$), yielded NMR spectra that could be assigned with a relatively high degree of confidence. One of the more interesting results of this work is that the *para*-methoxy-substituted aryl-phosphine oxide complex, $U[OP(p\text{-anisyl})_3][N(SiMe_3)_2]_3$, seems to be more stable than $U[N(SiMe_3)_2]_3[OPPh_3]$. $U[OP(p\text{-anisyl})_3][N(SiMe_3)_2]_3$ repeatedly gave clear, easily assignable NMR spectra. The alternative route directly from $UI_3(1,4\text{-dioxane})_{1.5}$ gave cleaner, reproducible results for the synthesis of $U[OP(p\text{-anisyl})_3][N(SiMe_3)_2]_3$ and the other aryl- and alkyl-substituted phosphine oxide complexes shown in Table 3.

The NMR spectra obtained for Ce[OP(*p*-anisyl)$_3$][N(SiMe$_3$)$_2$]$_3$, Ce[OPPh$_3$][N(SiMe$_3$)$_2$]$_3$, and U[OP(*p*-anisyl)$_3$][N(SiMe$_3$)$_2$]$_3$, and other less characterized systems, exhibited large paramagnetic shifts in both the ^{1}H and ^{31}P NMR spectra. The paramagnetic shifts for the uranium complexes were much larger than the cerium complexes, which is consistent with the fact that uranium has more unpaired *f*-electrons with an f^3 configuration compared to cerium with an f^1 configuration. The pseudocontact contribution is the primary influence on the NMR spectra of *f*-elements [2,10,49,78,79], and the large shifts caused by the interactions between unpaired *f*-electrons and ligand nuclei in Ce[OP(*p*-anisyl)$_3$][N(SiMe$_3$)$_2$]$_3$, Ce[OPPh$_3$][N(SiMe$_3$)$_2$]$_3$, and U[OP(*p*-anisyl)$_3$][N(SiMe$_3$)$_2$]$_3$ are mainly dipolar in origin [2,80]. *f*-electrons are very localized and core-like, and do not tend to delocalize onto ligand atoms to a large extent. *f*-electron interactions with ligand nuclei are "through-space" interactions [2,80]. These "through-space" interactions require the *f*-metal ion to have an anisotropic distribution of *f*-electrons [81]. The following equation predicts the relative variation in dipolar shifts for the lanthanide series (assuming axial symmetry):

$$\delta^{pcs} = \frac{-\mu_0}{4\pi}\frac{g_J^2\mu_B^2 J(J+1)(2J-1)(2J+3)}{60(kT)^2}\frac{D_z(3cos^2\theta-1)}{r^3}$$

where

$$g_J = 1 + \frac{J(J+1) - L(L+1) + S(S+1)}{2J(J+1)}$$

Cerium(III) has a $^2F_{5/2}$ ground state [2,81]; therefore, the Landé factor (g_J) is equal to 6/7. Uranium(III) has a $^4I_{9/2}$ ground state [2,82], with a Landé factor (g_J) equal to 8/11. In some rare cases, when suitable delocalization mechanisms are involved, a small covalent contribution to metal-ligand bonding in *f*-element systems can occur. As a result, a "contact" shift can occur due to delocalization of unpaired *f*-electron density onto the ligand atoms [2,80,81]. The mechanism of the spin density delocalization is due to weak covalent bonding involving the 6*s* orbital, which in turn can transfer unpaired spin density onto ligand nuclei via spin polarization from 4*f* orbitals [81].

Table 5. ^{31}P NMR Chemical Shifts for $M[N(SiMe_3)_2]_3[OPR_3]$						
NMR data (ppm)						
f^n	**M**	**R**	**$M[N(SiMe_3)_2]_3[OPR_3]$**	**$[OPR_3]$**	**Δδ**	**ref**
f^1	Ce	*t*-Bu	91.77	41	50.77	
f^1	Ce	MePh	54.55	29.88	24.67	
f^1	Ce	MeOPh	54.39	29.3	25.09	
f^1	Ce	Ph	53.57	29.65	23.92	
f^3	U	*t*-Bu	368.58	41	327.6	
f^3	U	MePh	98.34	29.88	68.46	
f^3	U	MeOPh	102.6	29.3	73.3	
f^3	U	Ph_2(tolyl)	104.48	27.71	76.77	
f^3	U	Ph	105.19	29.65	75.54	
f^0	La	Ph	39	29.65	9.35	[49]

NMR studies of $Ln[N(SiMe_3)_2]_3$ and $Ln[N(SiMe_3)_2]_3[OPPh_3]$ demonstrate the predominance of the pseudo-contact contribution to the paramagnetic shifts in this series [10,49]; however, some of the data suggest that a contact contribution is involved, and there is considerable evidence that lanthanide amides have significant contact contributions to their paramagnetic shifts [10,49]. Separating the pseudocontact and contact contributions for the shifts observed for $Ce[OP(p\text{-anisyl})_3][N(SiMe_3)_2]_3$, $Ce[OPPh_3][N(SiMe_3)_2]_3$, and $U[OP(p\text{-anisyl})_3][N(SiMe_3)_2]_3$ is beyond the scope of this discussion, and is the subject of future work using Density Functional Theory (DFT) and Quantum Theory of Atoms in Molecules (QTAIM). QTAIM has recently been used to analyze the paramagnetic NMR shifts of actinide complexes in order to estimate relative metal-ligand covalency via the QTAIM *delocalization index* [83].

Table 6. ^{1}H NMR Chemical Shifts ($SiMe_3$-54H)

NMR data (ppm)						
f^n	M	R	$M[N(SiMe_3)_2]_3[OPR_3]$	Free $M[N(SiMe_3)_2]_3$	Δδ	ref
f^1	Ce	*t*-Bu	-1.17	-3.39	2.22	
f^1	Ce	MePh	-0.74	-3.39	2.65	
f^1	Ce	MeOPh	-0.77	-3.39	2.62	
f^1	Ce	Ph	-0.78	-3.39	2.61	
f^3	U	*t*-Bu	-3.16	-11	7.84	
f^3	U	MePh	-5.53	-11	5.47	
f^3	U	MeOPh	-5.68	-11	5.32	
f^3	U	Ph_2(tolyl)	-5.52	-11	5.48	
f^3	U	Ph	-5.66	-11	5.34	
f^0	La	Ph	0.7	0.25	-0.45	[10,49]
f^0	Y	Ph	0.3	0.28	-0.02	[10,49]
f^{14}	Lu	Ph	0.1	0.3	0.2	[10,49]
f^6	Eu	Ph	-1.43	6.43	-7.86	[10,49]

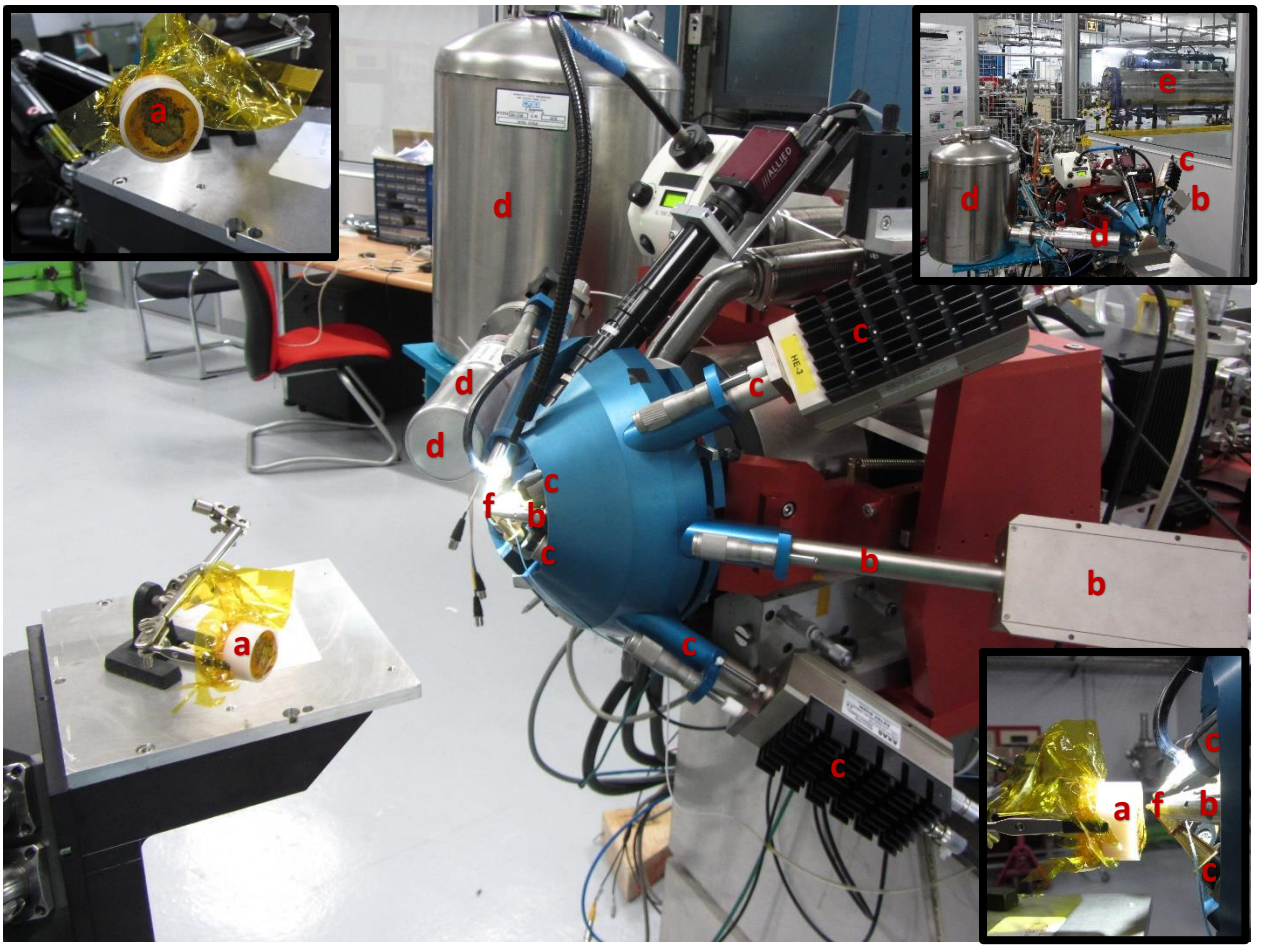

Figure 4.11: External Ion Beam Analysis setup at AGLAE, Louvre Museum, Paris, France. a) $Ce[OPPh_3][N(SiMe_3)_2]_3$ in sample holder, b) low-energy SDD X-ray detector, c) high-energy SDD X-ray detectors, d) HPGe Gamma detector, e) 3 MV Tandem Accelerator, f) 3 MeV proton beam exit window (Si_3N_4).

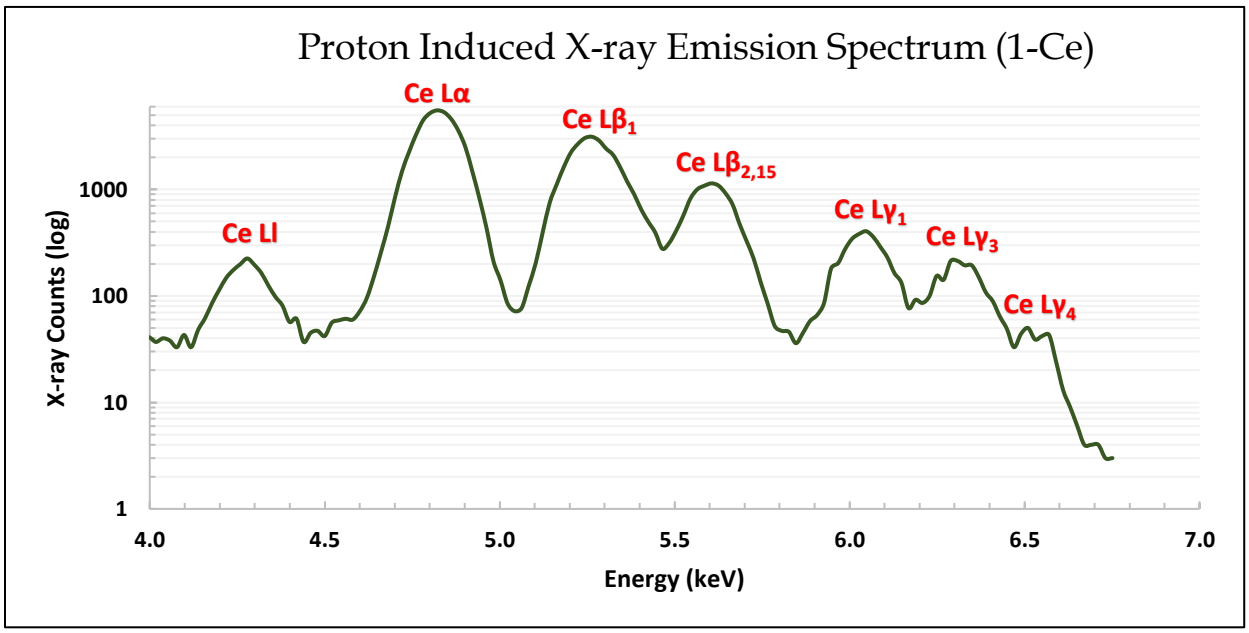

Figure 4.12: Cerium L X-ray Emission Series for $Ce[OPPh_3][N(SiMe_3)_2]_3$.

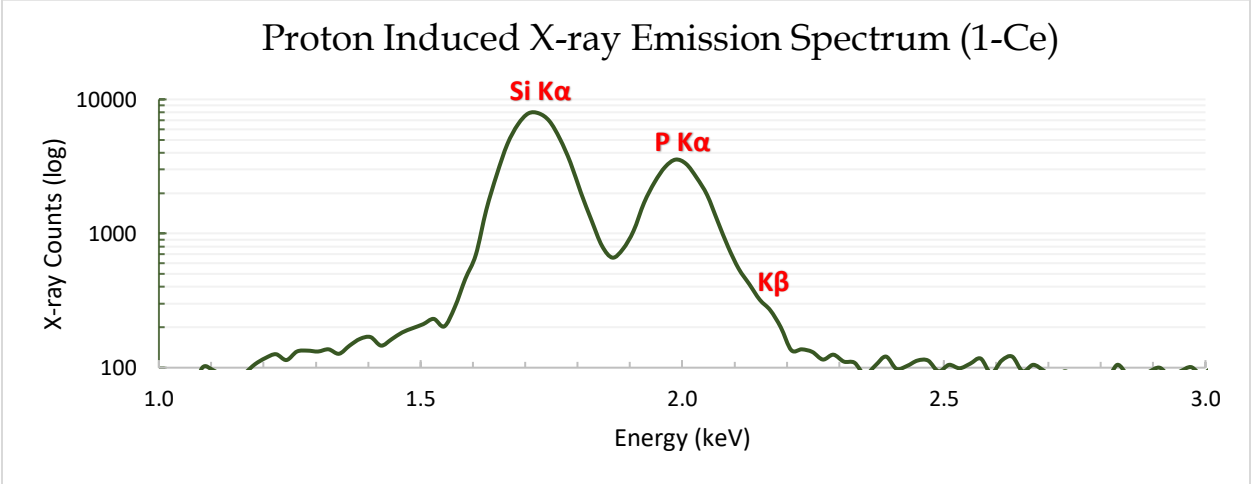

Figure 4.13: Silicon and Phosphorus K X-ray Emissions for $Ce[OPPh_3][N(SiMe_3)_2]_3$.

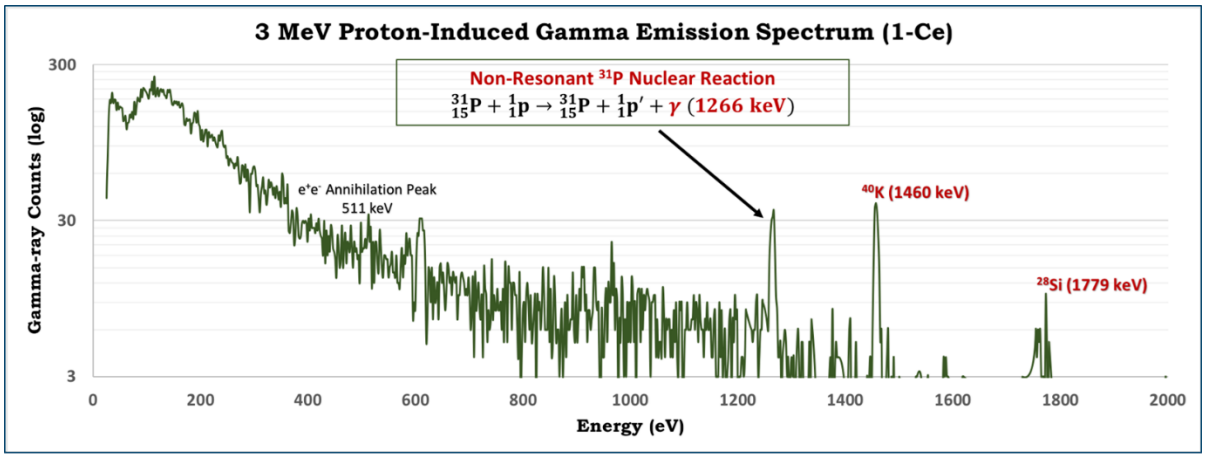

Figure 4.14: Proton-Induced Gamma Emission Spectrum for $Ce[OPPh_3][N(SiMe_3)_2]_3$.

The X-ray emission spectrum for $Ce[OPPh_3][N(SiMe_3)_2]_3$ (obtained using a low-energy SDD detector) is shown in Figure 4.3. The characteristic X-ray lines for cerium, phosphorus, and silicon are present, and concentrations obtained from the Ce Lα (4.84 keV), P Kα (2.015 keV), and Si Kα (1.739 keV) peaks are close to the predict values (Calculated: Ce 15.58 P 3.44 Si 18.73; Found: Ce 15.58 P 6.48 Si 19.67). The relative cerium/silicon ratio is almost correct, but the relative phosphorus concentration is a little high (presumably due to the formation of a phosphine oxide crust on the crystal and sample decomposition over time). Potassium is also present in trace amounts (6578 ppm, 0.65 wt. %) due to the presence of unremoved KCl or unreacted $K(SiMe_3)_2$. This result shows that multiple sublimations are indeed necessary to remove the potassium salts, as has been done by some researchers [77]. The cerium Kα peak was also observed at 34.717 keV in the high-energy X-ray emission spectrum with very low statistics.

In addition to the cerium Lα$_1$ X-ray emission, the Lβ$_1$, Lβ$_{2,15}$, Lγ$_1$, Ll emissions were also observed (Figures 4.3 and 4.12). The 4.84 keV Lα$_1$ X-ray emission is a $M_5 \rightarrow L_3$, ($3d_{5/2} \rightarrow 2p_{3/2}$) electronic transition. The 4.3 keV Ll X-ray emission is a $M_1 \rightarrow L_3$ ($3s_{1/2} \rightarrow 2p_{3/2}$) electronic transition. The 5.262 keV Lβ$_1$ X-ray emission is a $M_4 \rightarrow L_2$ ($3d_{3/2} \rightarrow 2p_{1/2}$) electronic transition. The Lβ$_2$ and Lβ$_{15}$ X-ray emissions at ca. 5.7 keV are $N_5 \rightarrow L_3$ and $N_4 \rightarrow L_3$ ($4d_{5/2} \rightarrow 2p_{3/2}$ and $4d_{3/2} \rightarrow 2p_{3/2}$) electronic transitions, respectively. The 6.1 keV Lγ$_1$ X-ray emission is a $N_4 \rightarrow L_2$ ($4d_{3/2} \rightarrow 2p_{1/2}$) electronic transition. The 6.33 keV Lγ$_3$ X-ray emission is a $N_3 \rightarrow L_1$ ($4p_{3/2} \rightarrow 2s_{1/2}$) electronic transition. The 6.53 keV Lγ$_4$ X-ray emission is a $O_3 \rightarrow L_1$ ($5p_{3/2} \rightarrow 2s_{1/2}$) electronic transition. A fair degree of fine structure can also be seen in the *L*γ emissions. TD-DFT calculations could potentially be used to analyze the fine structure observed. The *L* emission series of cerium is sensitive to the chemical state of the complex, especially the higher energy transitions. It has recently been shown that the *L* emission energies and intensity ratios in energy-dispersive X-ray emission spectra vary depending on the chemical environment of rare-earth cations [84,85]. Comparison of the *L* emissions for a variety of Ce^{III} and Ce^{IV} compounds should be the subject of future work.

In addition to the silicon and phosphorus Kα X-ray emissions peaks ($L_{2,3} \rightarrow K$ or $2p \rightarrow 1s$ transitions), the phosphorus Kβ emission was also observed (Figure 4.13), albeit with very low statistics. The phosphorus Kβ$_1$ X-ray emission is a $M_3 \rightarrow K$, or $3p_{3/2} \rightarrow 1s$, electronic transition. This transition is highly sensitive to the chemical environment of the phosphorus atom because it is a valence-to-core transition. However, high resolution

wavelength-dispersive X-ray emission using a crystal monochromator is required in order to achieve high enough resolution to carry out phosphorus Kβ analysis. Recent studies have shown that small ion accelerators can be used to perform wavelength-dispersive phosphorus Kβ X-ray emission spectroscopy (WD-PIXE) [89]. These studies demonstrated that WD-PIXE yields results comparable to those obtained from advanced synchrotron light sources [89]. Phosphorus X-ray emission studies from other groups over the past several decades [86-89] have motivated us to use WD-PIXE for phosphorus Kβ analysis for a variety of lanthanide and actinide compounds with phosphorus-based ligands. The phosphorus Kβ X-ray emission from phosphine oxides and other phosphorus-based ligands has the potential to provide great insight into the nature *f*-metal-ligand bonding, especially when combined with results from phosphorus-31 NMR spectroscopy. This XES/NMR approach can facilitate the investigation of both *orbital-energy near-degeneracy driven covalency*, and *symmetry-restricted overlap driven covalency* in lanthanide and actinide coordination complexes. This should be the subject of future work. Such studies could potentially reveal periodic trends in metal-ligand orbital mixing for the *f*-block elements.

The proton-induced gamma emission spectrum for $Ce[OPPh_3][N(SiMe_3)_2]_3$ is shown is Figure 4.14. The gamma-emission at 1266 keV corresponds to the non-resonant $^{31}P(p, p\gamma)^{31}P$ nuclear reaction. The e^+e^- annihilation peak was also observed at 511 keV. The observation of the emission resulting from the $^{31}P_{3/2} \rightarrow {}^{31}P_{1/2}$ nuclear transition has inspired us to use this signal for nuclear electric field gradient studies *f*-metal complexes,

similar to NQR (nuclear quadrupole resonance) electric field gradient studies that have been conducted on metal fluorides using time-differential perturbed angular distribution analysis (TD-PAD), which involves using an MeV proton beam to induce fluorine gamma-emission [90-92]. This should be the subject of future work.

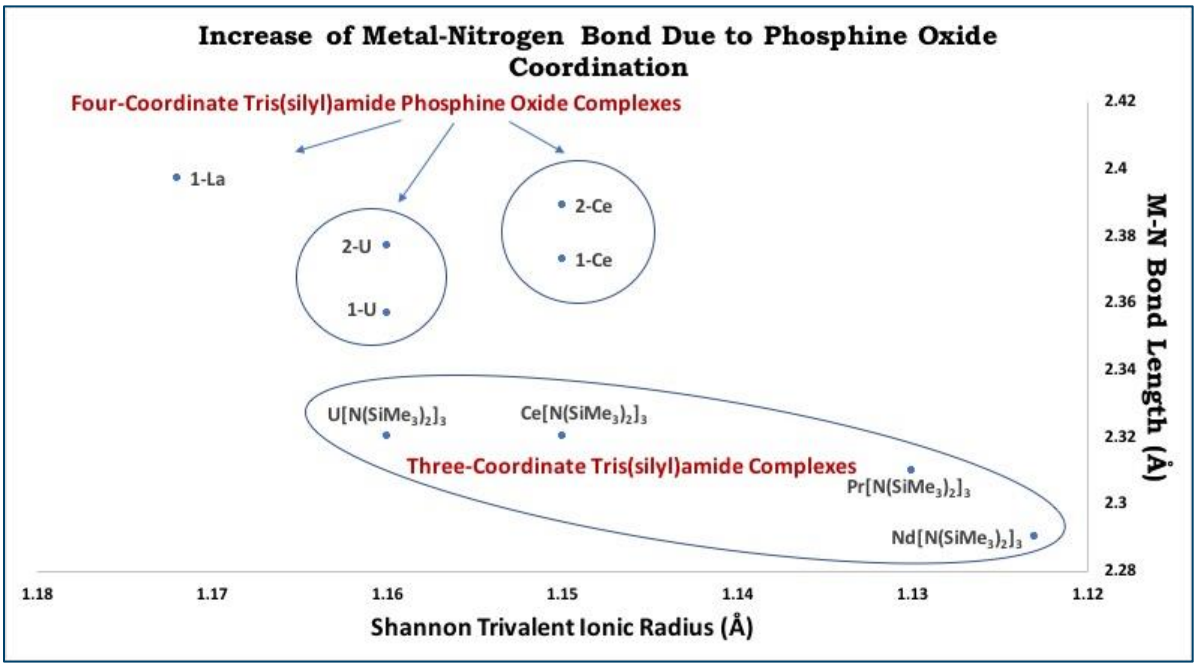

Figure 4.15: Increase in Metal-Nitrogen Bond Length with Phosphine Oxide Coordination

Conclusion

Four-coordinate complexes of the lanthanides and actinides are extremely rare, and Ce[OP(*p*-anisyl)$_3$][N(SiMe$_3$)$_2$]$_3$, Ce[OPPh$_3$][N(SiMe$_3$)$_2$]$_3$, and U[OP(*p*-anisyl)$_3$][N(SiMe$_3$)$_2$]$_3$ are valuable contributions to *f*-element coordination chemistry. The

X-ray crystal structures and paramagnetic NMR spectra for Ce[OP(*p*-anisyl)$_3$][N(SiMe$_3$)$_2$]$_3$, Ce[OPPh$_3$][N(SiMe$_3$)$_2$]$_3$, and U[OP(*p*-anisyl)$_3$][N(SiMe$_3$)$_2$]$_3$ are reported in this work, along with X-ray and gamma emission spectra for Ce[OPPh$_3$][N(SiMe$_3$)$_2$]$_3$. The results were presented in the context of data available from the previous literature, which allowed further insight into the nature of monomeric cerium(III) and uranium(III) complexes with silylamide and phosphine oxide ligands. More insight will be achieved in future theoretical and experimental investigations of these model complexes. Ce[OP(*p*-anisyl)$_3$][N(SiMe$_3$)$_2$]$_3$, Ce[OPPh$_3$][N(SiMe$_3$)$_2$]$_3$, and U[OP(*p*-anisyl)$_3$][N(SiMe$_3$)$_2$]$_3$ can be used to investigate the previously observed enhancement in protonolysis reactivity of phosphine oxide adducts with diphenylphosphine (HPPh$_2$) compared to the base-free three-coordinate Ln[N(SiMe$_3$)$_2$]$_3$ compounds [19]. It was observed in this work that phosphine oxide coordination to the metal center increases the length of the metal-amide bond (see Figure 4.15), which could perhaps explain the enhanced protonolysis reactivity observed for similar rare-earth complexes decades ago [19].

References

[1] Kaltsoyannis, Nikolas and Peter Scott. 1999. *The f elements*. Oxford University Press, Oxford.

[2] Aspinall, Helen C. 2001. *Chemistry of the f-Block Elements*. Gordon and Breach Science Publishers, Amsterdam.

[3] Sastri, V.S., J.-C. Bünzli, V. Ramachandra Rao, G.V.S. Rayudu, and J.R. Perumareddi. 2003. *Modern Aspects of Rare Earths and their Complexes.* Elsevier, Amsterdam.

[4] Cotton, Simon. 2006. *Lanthanide and Actinide Chemistry*. John Wiley & Sons, Ltd, Cichester.

[5] Morss, Lester R., Norman M. Edelstein, Jean Fuger, Joseph J. Katz. *The Chemistry of the Actinide and Transactinide Elements*. Third edition. Springer, Dordrecht.

[6] Atwood, David A. 2012. *The Rare Earth Elements: Fundamentals and Applications*. John Wiley & Sons, Ltd, Chichester.

[7] Kaltsoyannis, Nikolas and Andrew Kerridge. 2014. "Chemical Bonding of Lanthanides and Actinides." In *The Chemical Bond: Chemical Bonding Across the Periodic Table*, pp.337-355, edited by Gernot Frenking and Sason Shaik. Wiley-VCH, Weinheim.

[8] Kerridge, Andrew. 2017. "Quantification of f-element covalency through analysis of the electron density: insights from simulation." *Chemical Communication* 53: 6685-6695.

[9] Dognon, Jean-Pierre. 2017. "Electronic structure theory to decipher the chemical bonding in actinide systems." *Coordination Chemistry Reviews* 344: 150-162.

[10] Bradley, Donald C., Joginder S. Ghotra, and F. Alan Hart. "Low Co-ordination Numbers in Lanthanide and Actinide Compounds. Part I. The Preparation and

Characterization of Tris{bis(trimethylsilyl)-amido}lanthanides." *Journal of the Chemical Society Dalton Transactions* 1973: 1021.

[11] Ghotra, Joginder S., Michael B. Hursthouse, and Alan J. Welch. "Three-co-oridinate Scandium(III) and Europium(III); Crystal aand Molecular Structures of their Trishexamethyldisilylamides." 1973: 669.

[12] Bradley, D.C. and J.S. Ghotra. 1975. "Mass Spectroscopic Studies on Metal Organosilylamides. Part I. Mass Spectra of Tris{bis(trimethylsilyl)amido}lanthanides. *Inorganic Chimica Acta* 13: 11-16.

[13] Andersen, Richard A. 1979. "Tris((hexamethyldisilyl)amido)uranium(III): Preparation and Coordination Chemistry. *Inorganic Chemistry* 18(6): 1507.

[14] Avens, Larry R., Simon G. Bott, David L. Clark, Alfred Sattelberger, John G. Watkin, and Bill D. Zwick. 1994. "A Convenient Entry into Trivalent Actinide Chemistry: Synthesis and Characterization of $AnI_3(THF)_4$ and $An[N(SiMe_3)_2]_3$ (An = U, Np, Pu)." *Inorganic Chemistry* 33: 2248-2256.

[15] Anwander, Reiner. 1996. "Lanthanide Amides." *Topics in Current Chemistry* 179: 33-112.

[16] Drożdżyński, Janusz. 2005. "Tervalent uranium compounds." *Coordination Chemistry Reviews* 249: 2351-2373. University of Wroclaw, Poland.

[17] Baker, Robert J. 2012. "The coordination and organometallic chemistry of UI_3 and $U\{N(SiMe_3)_2\}_3$: Synthetic reagents par excellence." *Coordination Chemistry Reviews* 256: 2843-2871.

[18] Emslie, David J. H. 2018. "Actinides: Amido Complexes." *Encyclopedia of Inorganic and Bioinorganic Chemistry*, John Wiley & Sons, Ltd., pp. 1-18.

[19] Aspinall, Helen C., Donald C. Bradley, and Keith D. Sales. 1988. "Diphenylphosphido Complexes of the Lanthanides: Reactions of Compounds $[Ln\{N(SiMe_3)_2\}_3]$ (Ln = La or Eu) or $[Ln\{N(SiMe_3)_2\}_3(Ph_3PO)]$ (Ln = La, Eu, or Y) with Ph_2PH to give $[Ln\{N(SiMe_3)_2\}_2(PPh_2)]$ or $[Ln\{N(SiMe_3)_2\}_2(PPh_2)(Ph_3PO)]$." *Journal of the Chemical Society Dalton Transactions*: 2211-2213.

[20] Roger, Mathieu, Noémi Barros, Thérèse Arliguie, Pierre Thuéry, Laurent Maron, and Michel Ephritikhine. 2006. "$U(SMes^*)_n$ (n = 3, 4) and $Ln(SMes^*)_3$ (Ln = La, Ce, Pr, Nd): Lanthanide(III)/Actinide(III) Differentiation in Agostic Interactions and an Unprecedented η^3 Ligation Mode of the Arylthiolate Ligand, from X-ray Diffraction and DFT Analysis." *Journal of the American Chemical Society* 128: 8790-8802.

[21] Aspinall, Helen C., Sharron A. Cunningham, Patirck Maestro, and Pierre Macaudierre. 1998. "Lanthanide Tris(*tert*-butylthiolates) and the Crystal Structure of $[Yb(SBu^t)_2(\mu_2\text{-}SBu^t)(Bipy)]_2$." *Inorganic Chemistry* 37: 5396-5398.

[22] Cary, Douglas R. and John Arnold. 1993. "Preparation of Lanthanide Tellurolates and Evidence for the Formation of Cluster Intermediates in Their Thermal Decomposition to Bulk Metal Tellurides." *Journal of the American Chemical Society* 115: 2520-2521.

[23] Gaunt, Andrew J., Sean D. Reilly, Alejanddro E. Enriquez, Brian L. Scott, James A. Ibers, Permal Sekar, Kieran I.M. Ingram, Nikolas Kaltsoyannis, and Mary P. Neu. 2008. "Experimental and Theoretical Comparison of Actinide and Lanthanide Bonding in $M[N(EPR_2)_2]_3$ Complexes (M = U, Pu, La, Ce; E = S, Se, Te; R = Ph, *i*Pr, H)." *Inorganic Chemistry* 47: 29-41.

[24] LaDuca, Robert L. and Peter T. Wolczanski. 1992. "Preparation of Lanthanide Nitrides via Ammonolysis of Molten $\{(Me_3Si)_2N\}_3Ln$: Onset of Crystallization Catalyzed by $LiNH_2$ and LiCl." *Inorganic Chemistry* 31: 1311-1313.

[25] Baxter, David V., Malcom H. Chrisholm, Gennaro J. Gama, and Vincent F. Distasi. 1996. "Molecular Routes to Metal Carbides, Nitrides, and Oxides. 2. Studies of the Ammonolysis of Metal Dialkylamides and Hexamethyldisilylamides." *Chemistry of Materials* 8: 1222-1228.

[26] Czerwinski, K., and T. Hartmann. 2006. *Solution-Based Synthesis of Nitride Fuels*. UNLV, Fuels Campaign: Transmutation Research Program Projects.

[27] Siribbal, Shifaa M., Johannes Schläfer, Shaista Liyas, Zhangjun Hu, Kajsa Uvdal, Martin Valldor, and Sanjay Mathur. 2018. "Air-Stable Gadolinium Precursors for

the Facile Microwave-Assisted Synthesis of Gd_2O_3 Nanocontrast Agents for Magnetic Resonances Imaging." *Crystal Growth and Design* 18: 633-641.

[28] Jamil, Aida, Johannes Schläfer, Yakup Gönüllü, Ashish Lepcha, and Sanjay Mathur. 2016. "Precursor-Derived Rare Earth Metal Pyrochlores: $Nd_2Sn_2O_7$ Nanofibers and Thin Films As Efficient Photoabsorbers." *Crystal Growth and Design* 16: 5260-5267.

[29] Zhang, Peng, Li Zhang, Chao Wang, Shufang Xue, Shuang-Yan Lin, and Jinkui Tang. 2014. "Equatorially Coordinated Lanthanide Single Ion Magnets." *Journal of the American Chemical Society* 136: 4484-4487.

[30] McAdams, Simon G., Ana-Maria Ariciu, Andreas K. Kostopoulos, James P.S. Walsh, and Floriana Tuna. 2017. "Molecular single-ion magnets based on lanthanides and actinides: Design considerations and new advances in the context of quantum technologies." *Coordination Chemistry Reviews* 346: 216-239.

[31] Liddle, Stephen T. and Joris van Slageren. 2015. "Improving f-element single molecule magnets." *Chemical Society Reviews* 44: 6655-6669.

[32] Meihaus, Katie R. and Jeffery R. Long. 2015. "Actinide-based single-molecule magnets." *Daltons Transactions* 44: 2517-2528.

[33] a) Tang, J. and P Zhang. 2015. *Lanthanide Single Molecule Magnets*. Springer-Verlag, Berlin. b) Layfield, Richard A. and Muralee Murugesu. 2015. *Lanthanides and Actinides in Molecular Magnetism*. Wiley-VCH, Verlag.

[34] Eisenstein, Odlie, Peter B. Hitchcock, Alexander G. Hulkes, Michael F. Lappert, and Laurent Maron. 2001. "Cerium masquerading as a Group 4 element: synthesis, structure and computational characterization of [CeCl{N(SiMe$_3$)$_2$}$_3$]." *Chemical Communications*: 1560-1561.

[35] Dröse, Peter, Alan R. Crozier, Samira Lashkari, Jochen Gottriedsen, Steffen Blaurock, Cristian G. Hrib, Cäcilla Maichle-Mössmer, Christoph Schädle, Reiner Anwander, and Frank T. Edelmann. 2010. "Facile Access to tetravalent Cerium Compounds: One-Electron Oxidation Using Iodine(III) Reagents." *Journal of the American Chemical Society Communication* 132: 14046-14047.

[36] Williams, Ursula J., Jerome R. Robinson, Andrew J. Lewis, Patirick J. Caroll, Patrick J. Walsh, and Eric J. Schelter. 2014. "Synthesis, Bonding, and Reactvity of a Cerium(IV) Fluoride Complex." *Inorganic Chemistry* 53: 27-29.

[37] Williams, Ursula J., Patrick J. Carroll, and Eric J. Schelter. 2014. "Synthesis and Analysis of a Family of Cerium(IV) Halide and Pseudohalide Compounds." *Inorganic Chemistry* 53: 6338-6345.

[38] So, Yat-Ming and Wa-Hung Leung. 2017. "Recent advances in the coordination chemistry of cerium(IV) complexes." *Coordination Chemistry Reviews* 340: 172-197.

[39] Stewart, Joanne Lee. 1988. *Tris[bis(trimethylsilyl)amido]uranium: Compounds with Tri-, Tetra-, and Penta-valent Uranium*. PhD Dissertation, University of California, Berkeley. Berkeley, California.

[40] Thomson, R.K., C.R. Graves, B.L. Scott, and J.L. Kiplinger. 2011. "Straightforward and efficient oxidation of tris(aryloxide) and tris(amide) uranium(III) complexes using copper(I) halide reagents." *Inorganic Chemistry Communications* 14: 1742-1744.

[41] Gaunt, Andrew J., Alejandro E. Enriquez, Sean D. Reilly, Brian L. Scott, and Mary P. Neu. 2008. "Structural Characterization of $Pu[N(SiMe_3)_2]_3$, a Synthetically Useful Nonaqueous Plutonium(III) Precursor." *Inorganic Chemistry* 47: 26-28.

[42] Gaunt, Andrew J., Sean D. Reillym Alejandro E. Enriquez, Trevor W. Hayton, James M. Boncella, Brian L. Scott, and Mary P. Neu. 2008. "Low Valent molecular Plutonium Halide Complexes." *Inorganic Chemistry* 47: 8412-8419.

[43] Fortier, Skye, Jessie L. Brown, Nikolas Kaltsoyannis, Guang Wu, and Trevor Hayton. 2012. "Synthesis, Molecular, and Electronic Structure of $U^V(O)[N(SiMe_3)_2]_3$." *Inorganic Chemstry* 51: 1625-1633.

[34] Lewis, Andrew J., Eiko Nakamaru-Ogiso, James M. Kikkawa, Patrick J. Carroll, and Eric J. Schelter. 2012. "Pentavalent uranium *trans*-dihalides and -pseudohalides." *Chemical Communications* 48: 4977-4979.

[35] Brown, Jessie L., Skye Fortier, Richard A. Lewis, Guang Wu, and Trevor W. Hayton. 2012. "A Complete Family of Terminal Uranium Chalcogenides, $[U(N\{SiMe_3\}_2)_3]^-$ (E = O, S, Se, Te)." *Journal of the American Chemical Society* 134: 15468-15475.

[36] Smiles, Danil E., Guang Wu, and Trevor Hayton. 2014. "Synthesis of Uranium-Ligand Multiple Bonds by Cleavage of a Trityl Protecting Group." *Journal of the American Chemical Society* 136: 96-99.

[37] Smiles, Danil E., Guang Wu, and Trevor Hayton. 2014. "Reversible Chalcogen-Atom Transfer to a Terminal Uranium Sulfide." *Inorganic Chemistry* 53: 12683-12685.

[48] Smiles, Danil E., Guang Wu, and Trevor Hayton. 2014. "Synthesis of Terminal Monochalcogenide and Dichalcogenide Complexes of Uranium Using Polychalcogenides, $[E_n]^{2-}$ (E = Te, n = 2; E = Se, n = 4), as Chalcogen Atom Transfer Reagents." *Inorganic Chemistry* 53: 10240-10247.

[49] Bradley, Donald C., Joginder S. Ghotra, F. Alan Hart, Michael B. Hursthouse, and Paul R. Raithby. 1977. "Low Co-ordination Numbers in Lanthanoid and Actinoid Compounds. Part 2. Syntheses, Properties, and Crystal and Molecular Structures of Triphenylphosphine Oxide and Peroxo-derivatives of [Bis(trimethylsilyl)-amido]lanthanoids." *Journal of the Chemical Society Dalton Transactions*: 1166-1172.

[50] Jank, Stefan, Clemens Guteenberger, Hauke Reddmann, Jan Hanss, and Hanns-Dieter Amberger. 2006. "Zur Electronenstruktur hochsymmetrischer Verbindungen der f-Elemente. 41. Syntheses, Kristall-, Molekül- und Elektronenstruktur eines Bis(cyclohexylisonitrol)-Addukts des Grundkörpers Tris(bis(trimethylsilyl)amidoerbium(III) sowie Electronenstrukturen

ausgewählter Monoaddukte." *Zeitschrift für Anorganische und Allgemeine Chemie* 632: 2429-2438.

[51] Jank, Stefan, Hauke reddmann, Lixin Zhang, and Hanns-Dieter Amberger. 2012. "Zur Electronenstruktur hochsymmetrischer Verbindungen der f-Elemente. 45. Ungewöhnliche spektrochemische Eigenschaften des Triphenylphosphanoxido-Liganden im Falle von Mono- und Bisaddukten homoleptischer Samaraium(III)silylamide." *Zeitschrift für Anorganische und Allgemeine Chemie* 638: 1159-1166.

[52] Schumann, H. and G.M. Frisch. 1982. *Zeitschrift für Naturforschung, Teil B* 36: 1244.

[53] Evans, W.J., I. Bloom, W.E. Hunter, and J.L. Atwood. 1983. *Organometallics* 2: 709.

[54] Law, J.D., K.N. Brewer, R.S. Herbst, T.A. Todd, and D.J. Wood. 1999. "Development and demonstration of solvent extraction processes for the separation of radionuclides from acidic radioactive waste." *Waste Management* 19: 27-37.

[55] Krahn, Elizabeth, Cécile Marie, and Kenneth Nash. 2016. Probing organic phase ligand exchange kinetics of 4f/5f solvent extraction systems with NMR spectroscopy. *Coordination Chemistry Reviews* 316: 21-35.

[56] Romanovsky, V.N. 1998. *R&D Activities on Partitioning in Russia*. V.G. Khlopin Radium Institute, pp. 1-9.

[57] Häller, L.J.L, N. Kaltsoyannis, M.J. Sarsfield, L. May, S.M. Cornet, M.P. Redmond, and M. Helliwell. 2007. *Inorganic Chemistry* 46: 4868.

[58] Platt, Andrew W.G. 2017. "Lanthanide phosphine oxide complexes." *Coordination Chemistry Reviews* 340: 62-78.

[59] Lobana, T.S. 1992. "Coordination chemistry of phosphine chalcogenides and their analytical and catalytic applications." In *The Chemistry of Organophosphorus Compounds, Volume 2, Phosphine Oxides, Sulphides, Selenides, and Tellurides*, edited by Frank Hartley, pp. 409-566. John Wiley & Sons, Ltd.

[60] Monreal, Marisa J., Robert K. Thomson, Thibault Cantat, Micholas E. Travia, Brian L. Scott, and Jaqueline L. Kiplinger. 2011. "UI_4(1,4-dioxane)$_2$, [UCl_4(1,4-dioxane)]$_2$, and UI_3(1,4-dioxane)$_{1.5}$: Stable and Versatile Starting Materials for Low- and High-Valent Uranium Chemistry." *Organometallics* 30: 2031-2038

[61] Woollins, J. Derek. 2010. *Inorganic Experiments. Third Edition*. Wiley-VCH, Weinheim.

[62] Denton, Ross M., Jie An, Beatrice Adeniran, Alexander J. Blake, William Lewis, and Andrew Poulton. 2011. "Catalytic Phosphorus(V)-Mediated Nucleophilic Substitution Reactions: Development of a Catalytic Appel Reaction." *Journal of Organic Chemistry* 76: 6749-6767.

[63] Edleman, Nikki L., Anchuan Wang, John A. Belot, Andrew W. Metz, Jason R. Babcock, Amber M. Kawaoka, Jun Ni, Matthew V. Metz, Christine J. Flashenriem,

Charlotte L. Stern, Louise M. Liable-Sands, Arnold L. Rheingold, Paul R. Markworth, Robert P.H. Chang, Michael P. Chudzik, Carl R. Kannewurf, and Tobin J. Marks. 2002. "Synthesis and Characterization of Volatile, Fluorine-Free β-Ketoiminate Lanthanide MOCVD Precursors and Their Implementation in Low-Temperature Growth of Epitaxial CeO_2 Buffer Layers for Superconducting Electronics." *Inorganic Chemistry* 41: 5005-5023.

[64] Rees, Jr., William S., Oliver Just, and Donald S. van Derveer. 1999. "Molecular design of dopant precursors for atomic layer epitaxy of SrS:Ce." *Journal of Material Chemistry* 9: 249-252.

[65] Fjeldberg, T., Andersen, R.A. 1985. *Journal of Molecular Structure* 129: 93.

[66] Andersen, R.A., D.H. Templeton, and A. Zalkin. 1978. *Inorganic Chemistry* 8: 2317.

[67] Brady, Erik D., David L. Clark, John C. Gordon, P. Jeffery Hay, D. Webster Keogh, Rinaldo Poli, Brian L. Scott, and John G. Watkin. 2003. "Tris(bis(trimethylsilyl)amido)samarium: X-ray Structure and DFT Study." *Inorganic Chemistry* 42: 6682-6690.

[68] Ghotra, J.S., M.B. Hursthouse, and A.J. Welch. 1973. *Journal of the Chemical Society Chemical Communications*: 669.

[69] Hitchcock, Peter B., Alexander G. Hulkes, Michael F. Lappert, and Zhengning Li. 2004. "Cerium(III) dialkyl dithiocarbamates from $[Ce\{N(SiMe_3)_2\}_3]$ and

tetraalkylthiuram disulfides, and [Ce(κ^2-S_2CNEt_2)$_4$] from the Ce^{III} precursor; Tb^{III} and Nd^{III} analogues." *Dalton Transactions* 129-136.

[70] Hermann, W.A., R. Anwander, F.C. Munck, W. Scherer, V. Dufaud, N.W. Huber, and G.R.J. Artus. 1994. *Zeitschrift für Naturforschung* B49: 1789.

[71] Bienfait, André M., Benjamin M. Wolf, Karl W. Törnoos, and Reiner Anwander. 2018. "Trivalent Rare-earth-Metal Bis(trimethylsilyl)amide Halide Complexes by Targeted Oxidations." *Inorganic Chemistry* 57: 5204-5212.

[72] Niemeyer, Mark. 2002. "Synthese und strukturelle Charakteriserung verschiedener Ytterdiumbis(trimethylsilyl)amide darunter σ-donorfreies [Yb{$N(SiMe_3)_2$}$_2$(μ-Cl)]$_2$ – Ein koordinativ ungesättiger Komplex mit zusätzlichen agostichen Yb···(H_3C-Si) Wechselwirkungen." *Zeitschrift für Anorganische und Allgemeine Chemie* 628: 647-657.

[73] Anwander, R. 1992. Thesis. Technical University, Munich.

[74] Westerhausen, M., M. Hartmann, A. Pfitzner, and W. Schwarz. 1995. *Zeitschrift für Anorganische und Allgemeine Chemie* 621:837.

[75] Stewart, Joanne L. and Richard A. Andersen. 1998. "Trivalent uranium chemistry: molecular structure of [$(Me_3Si)_2N]_3U$." *Polyhedron* 17(5-6): 953-958.

[76] Gaunt, Andrew J., Alejandro E. Enriquez, Sean D. Reilly, Brian L. Scott, and Mary P. Neu. 2008. "Structural Characterization of Pu[$N(SiMe_3)_2]_3$, a Synthetically Useful Nonaqueous Plutonium(III) Precursor." *Inorganic Chemistry* 47: 26-28.

[77] Lappert, M.F., J.B. Pedley, G.J. Sharp, D.C. Bradely. 1976. *Journal of the Chemical Society Dalton Transactions*: 1737. Green, J.C., M. Payne, E.A. Seddon, R.A. Andersen. 1982. *Journal of the Chemical Society Dalton Transactions*: 887.

[78] Bleaney, B., C.M. Dobson, B.A. Levine, R.B. Martin, R.J.P. Williams, and A.V. Xavier. 1972. *Journal of the Chemical Society Chemical Communications* 791.

[79] Bleaney, B. 1972. *Journal of Magnetic Resonance* 8: 91.

[80] Le Mar, G.N., W. DeW. Horrocks, Jr., R.H. Holm. 1973. *NMR of Paramagnetic Molecules*. Academic Press, Inc.

[81] Bertini, Ivano, Claudio Luchinat, Giacomo Parigi, and Enrico Ravera. 2017. *NMR of Paramagnetic Molecules*. Elsevier.

[82] Boudreaux, E.A. and L.N. Mulay. 1976. *Theory and Applications of Molecular Paramagnetism.* John Wiley & Sons, New York.

[83] Smiles, Danil E., Guang Wu, Peter Hrobárik, and Trevor W. Hayton. 2016. "Use of ^{77}Se and NMR Spectroscopy to Probe Covalency of the Actinide-Chalcogen Bonding in $[Th(E_n)\{N(SiMe_3)_2\}_3]^-$ (E = Se, Te; *n* = 1, 2) and Their Oxo-Uranium(VI) Congeners." *Journal of the American Chemical Society* 138: 814-825.

[84] Durdağı, Sevil. 2017. "Chemical environment change analysis on *L* X-ray emission spectra of some lanthanide compounds." *Microchemical Journal* 130: 27-32.

[85] Durdağı, Sevil. 2013. "Effect of applied external magnetic field on the *L* X-ray emission line structures of the lanthanide elements." *Radiation Physics and Chemistry* 92: 1-7.

[86] Takahashi, Yoshihitio. 1972. "The X-ray Emission Spectra of the Compounds of Third-Period Elements. II. The *K* Spectra of Phosphorus in Compounds." *Bulletin of the Chemical Society of Japan* 45(4): 4-7.

[87] Yumatov, V.D., L.N. Mazalov, and E.A. Il'inchik. 1980. "Electronic Structure of a Series of Organic Compounds of Phosphrous and the Nature of the Chemical Bond Between Phosphorus and Oxygen." *Zhurnal Strukturnoi Khimii* 21(5): 24-28.

[88] Sugiura, Chikara, Hiroharu Yorikawa, and Shinji Muramatsu. 1996. "*K*β X-Ray Emission Spectra and Chemical Environments of Phosphorus in Some Selected Compounds." *Journal of the Physical Society of Japan* 65(9): 2940-2945.

[89] Petric, Marko, Rok Bohinc, Klemen Bučar, Matjaž Žitnik, Jakub Szlachetko, and Matjaž Kavčič. 2015. "Chemical State Analysis of Phosphorus Performed by X-ray Emission Spectroscopy." *Analytical Chemical* 87: 5632-5639.

[90] Blank, H. -R., M. Frank, M. GeÍger, J. -M. Greneche, M. Ismaier, M. Kaltenhäuser, R. Kapp, W. Kreische, M. Leblanc, U. Lossen, and B. Zapf. 1994. "Systematic Investigation of MF_3 Crystalline Compounds (M = Al, Cr, Fe, Ga, In, Sc, Ti, and V) and $Fe_{1-x}M_xF_3$ Mixed Series (M = Ga, Cr, V)." *Zeitschrift für Naturforschung* 49a: 361-366.

[91] Smith, J.A.S. 1986. "Nuclear Quadrupole Resonance: The Present State and Further Development." *Zeitschrift für Naturforschung* 41a: 453-462.

[92] Frank, Michael. 1999. "On Systematics in the ^{19}F Electric Hyperfine Interactions." *Forschritte der Physik* 4: 335-388.

[93] Jingqing, Ren and Xu Guangxian. 1987. "Electronic Structure and Chemical Bonding of Bis(Trimethylsilyl) Amide Derivatives of Lanthanides ($Ln(N(SiMe_3)_2)_3$, Ln = Nd, Eu, Yb)." *Scientia Sinica B* 30(4): 337-346.

Conclusion

At the time of this writing, the geopolitics of the actinide elements is taking center stage. The Doomsday Clock, maintained by the *Bulletin of the Atomic Scientists*, stands 100 seconds to midnight; the closest we have ever been to global catastrophe, in the form of nuclear catastrophe and environmental collapse. At this moment, nuclear weapons and nuclear warfare are on the minds of many people around the world in the wake of Russia's invasion of the sovereign nation of Ukraine. As Russia bombards cities of millions of people like Kiev and Kharkiv (where the Soviet atomic bomb was born), and as diabolical thermobaric weapons ravage Ukraine, millions fear that the conflict could escalate into an all-out nuclear war. In 2017, I was offered the opportunity to perform accelerator-based ion beam analysis on some samples at the Kharkiv Institute of Physics and Technology (I was not able to follow through on the offer); this institute and the city of Kharkiv are currently being destroyed by Russian artillery, and the citizens of Kharkiv are being terrorized by indiscriminate bombing. Many feel that this is the beginning of World War III, and a COVID-weary global populace may soon feel the wrath of fourth-generation nuclear weapons and super-sonic intercontinental ballistic missiles, coupled with chemical, biological, electronic, and information warfare. In violation of international norms, nuclear power plants have been targeted during the invasion. The opening act of the invasion was the occupation of the Chernobyl Nuclear Complex, the site of the 1986 nuclear disaster that accelerated the demise of the Soviet Union. As the Soviet Union broke up in the late 1980's and early 1990's, Ukraine gained its

independence; however, it gave up its vast nuclear weapons arsenal to Russia in order to gain recognition of its sovereignty and boundaries, and security guarantees from the NATO Alliance. These agreements made in the 1990's are being put to the test. American troops are being deployed to eastern NATO allies like Poland, Romania, and the Baltic States, and NATO stands on the brink of nuclear war with the Russia-China-Iran-North Korea tetrad. In the midst of the war in Ukraine, the United States, Europe, Russia, and Iran are negotiating, with the intention of reviving the Iranian Nuclear Agreement (JCPOA). At the center of all this, in the form of nuclear fuel, nuclear reactors, and the fission primaries of thermonuclear weapons, are the actinide elements: uranium and plutonium. Now more than ever, we can see how intertwined the actinide elements and national sovereignty really are.

The vital importance of the actinide elements is clear; the chemical behavior of these elements is not. The fundamental nature of actinide-ligand bonding remains a mystery. Nevertheless, much progress has been made towards the demystification of actinide-ligand covalency. Parallel advances have been made in lanthanide chemistry, and a more nuanced understanding of the electronic structure of cerium(IV)-ligand bonding is emerging from recent observations of uranium-like covalency in molecular Ce(IV) complexes [1, 2]. Long-standing assumptions about the ionicity of *f*-elements, and long-standing bonding paradigms like FEUDAL (f's essentially unaffected, d's accommodate ligands), are being challenged [1, 2]. The paradigmatic inverse-trans influence (ITI) is a dominant theme in modern theoretical actinide and lanthanide

chemistry. Liddle and co-workers have recently published results showing that ionic and covalent effects work against each other, in contradiction to the accepted ITI paradigm, suggesting a "non-FEUDAL, structure directing role for the f-orbitals" [1]. Furthermore, the distinction between orbital energy-near-degeneracy-driven covalency and overlap-driven covalency in actinide systems has become clearer in recent years [2, 3]. As we study and analyze the *f*-elements, our knowledge and understanding of these elements increases, and this enables us to become better managers and stewards of these elements, which are of vital of importance to high-energy industrial societies.

In this work, new *pseudo*-organometallic (inorganometallic) models of uranium, thorium, and cerium were synthesized and studied using nuclear magnetic resonance spectroscopy, X-ray diffraction, and X-ray emission spectrometry. A *pseudo*-isostructural series of tris[bis(trimethylsilyl)]amides of uranium and cerium complexes bearing phosphinimide and phosphine oxide ligands was developed. Other results were obtained that do not conform to the structural motif shown in Scheme 5.1, such as the previously unreported crystal structure of $UCl_4[OP(p\text{-anisyl})_3]_2$ shown in Figure 5.1, and the results described in Chapter 1. However, the most informative results of this work are the structural and spectroscopic results obtained for the previously unreported phosphinimide and phosphine oxide complexes that conform to the general structural motif shown in Scheme 5.1.

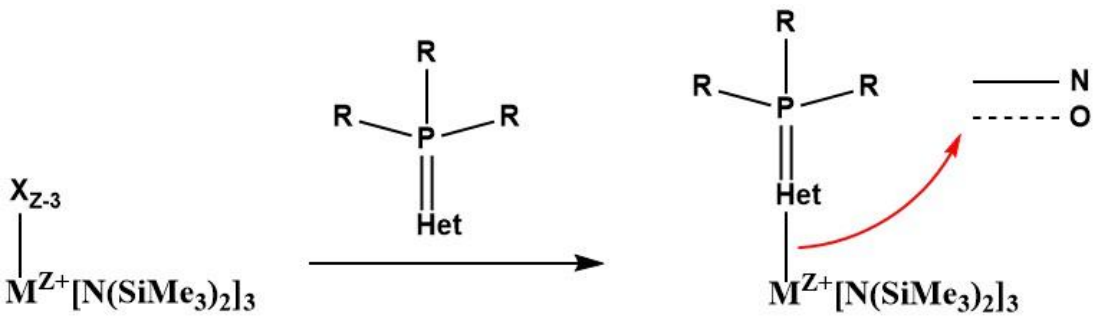

M = Ce, U
Z = 3, 4
Het = O, N
X = halogen
R = Ph, *p*-tolyl, *p*-anisyl, cyclohexyl, *t*-butyl

Scheme 5.1: General Formula for Isostructural Series

Structural results were obtained using single-crystal X-ray diffraction for the previously unreported compounds $Ce[OPR_3][N(SiMe_3)_2]_3$ (R = Ph, anisyl) and U[OP(*p*-anisyl)$_3$][$N(SiMe_3)_2]_3$. Similar compounds have been reported, including $U[OPPh_3][N(SiMe_3)_2]_3$ and $La[OPPh_3][N(SiMe_3)_2]$ [4, 5], and a comparative series of new and previously reported compounds was developed. These results were discussed in Chapter 4. The near linearity of the metal-oxygen-phosphorus systems in these complexes suggests these systems have multiple-bond character. The M-O-P angle in these systems ranges from about 174-176°. Note that the M-O-P angle in $UCl_4[OP(anisyl)_3]$ shown in Figure 5.1 is much less linear (about 163°), despite having a slightly shorter metal-oxygen bond. The silylamide complexes are much more bulky and sterically congested, and it is not surprising that the silylamide complexes have slightly longer metal-oxygen bonds. Caution must be used when using XRD bonds lengths to make

statements and comparisons about metal-ligand covalency, especially for non-isostructural complexes with different oxidation states. Analysis of the structural results in this comparative series showed that coordination of the phosphine oxide ligand to the metal center elongated the silylamide metal-nitrogen bonds in all three cases, when compared to the phosphine oxide-free three-coordinate complexes, $Ce[N(SiMe_3)_2]_3$ and $U[N(SiMe_3)_2]_3$. In light of these new results, the enhanced reactivity of $Ln[OPPh_3][N(SiMe_3)_2]_3$ versus $Ln[N(SiMe_3)_2]_3$ in protonolysis reactions with $HPPh_2$ to form lanthanide-phosphido complexes makes more sense. The elongated amide bonds in the phosphine oxide complexes are more labile and more reactive. Perhaps the phosphine oxide complexes could serve as more robust and more reactive precursors than the phosphine oxide-free three-coordinate metal-amide precursors in lanthanide and actinide coordination chemistry and materials science.

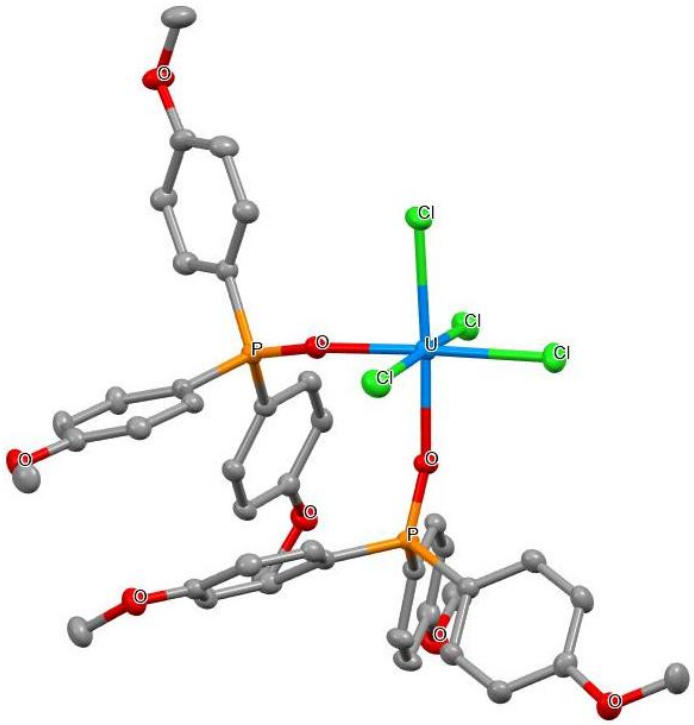

Figure 5.1: Single-Crystal XRD Structure of $UCl_4[OP(p\text{-anisyl})_3]_2$

Nuclear magnetic resonance spectroscopy (^{1}H and ^{31}P) data was obtained for $U[NP(t\text{-butyl})_3][N(SiMe_3)_2]_3$, $Ce[NPR_3][N(SiMe_3)_2]_3$ (R = cyclohexyl, *p*-anisyl), $U[OPR_3][N(SiMe_3)_2]_3$ (R = Ph, *p*-tolyl, Ph_2(*p*-tolyl), *p*-anisyl, *t*-butyl) , and $Ce[OPR_3][N(SiMe_3)_2]_3$ (R = Ph, *p*-tolyl, *p*-anisyl, *t*-butyl). The three aryl-phosphine oxide derivatives of cerium had similar phosphorus-31 chemical shifts ranging from 53.57-54.55 ppm, with the substituted-aryl derivatives being slightly more deshielded than the triphenylphosphine oxide derivative. Similarly, the four aryl-phosphine oxide derivatives of uranium have similar phosphorus-31 chemical shifts, ranging from 98.34-105.19 ppm, with the substituted-aryl derivatives being slightly less deshielded than the triphenylphosphine oxide derivative. Note that this is a reversal of the trend observed for the aryl-phosphine oxide complexes for cerium. This reversal warrants future investigation, and more isostructural substituted-aryl phosphine oxide complexes for all the *f*-elements need to be synthesized, so that these NMR trends can be better understood, and so the influence of aryl-substituents on the electronic structure of the metal-phosphine oxide system (M-O-P) can be better understood. The alkyl-phosphine oxide complex, $Ce[OP(t\text{-butyl})_3][N(SiMe_3)_2]_3$, is much more deshielded than its aryl-phosphine oxide analogues, with a phosphorus-31 chemical shift of 91.77 ppm. Similarly, the uranium derivative $U[OP(t\text{-butyl})_3][N(SiMe_3)_2]_3$, is also much more deshielded than its aryl-phosphine oxide analogues, with a chemical shift of 368.58 ppm. Both cases suggest an increased degree of metal-phosphine oxide covalency in the alkyl derivatives versus

the aryl derivatives. It is well-known that alkyl- and aryl-phosphine oxides have very different electronic distributuions. The electron donation of the alkyl groups results in a greater δ^- on the oxygen, and there is greater electron density available to donate to the metal center as a result. The electron distribution is delocalized throughout the metal-oxygen-phosphorus system, which makes the phosphorus nuclear magnetic shielding tensor very sensitive to the orbital interactions in the metal-oxygen bond. When the phosphine oxide ligand coordinates to the metal center, the phosphorus nucleus becomes more deshielded as electron density is drawn toward the metal center. Qualitative comparisons can be made regarding the degree of metal-ligand covalency in isostructural complexes using NMR chemical shifts, with increased deshielding of the NMR nucleus being indicative of increased covalency (orbital mixing). These comparisons can be made quantitative through the use of DFT and Quantum Theory of Atoms in Molecules (QTAIM); however, such calculations are beyond the scope of this work.

The ^{31}P NMR shifts for U[NP(*t*-butyl)$_3$][N(SiMe$_3$)$_2$]$_3$ and Ce[NPR$_3$][N(SiMe$_3$)$_2$]$_3$ (R = cyclohexyl, *p*-anisyl) are much more deshielded than the phosphine oxide complexes, with chemical shifts of 689.3 ppm, 637.34 ppm, and 636.79 ppm, respectively. Similar to the results observed for the phosphine oxide complexes, the alkyl-phosphinimide complex, Ce[NPCy$_3$][N(SiMe$_3$)$_2$]$_3$, is more deshielded than the aryl-phosphinimide complex, Ce[NP(*p*-anisyl)$_3$][N(SiMe$_3$)$_2$]$_3$. The orbital mixing in the metal-nitrogen bonds in the tetravalent complexes with formally anionic phosphinimide ligands is expected to be much greater than the orbital mixing in the metal-oxygen bonds in the trivalent

complexes with formally neutral phosphine oxide ligands. Both systems are expected to have multiple bond character in the metal-phosphine oxide and metal-phosphinimide bonds; however, based on significantly greater level of ^{31}P NMR deshielding observed for the phosphinimide complexes, it seems apparent that there is much more covalency (orbital mixing) in the metal-phosphinimide bonds. These preliminary results suggest that ^{31}P NMR can be a very useful tool for studying metal-ligand covalency in both paramagnetic and diamagnetic *f*-element complexes bearing phosphinimide and phosphine oxide ligands. Actinide-oxygen-phosphorus interactions are ubiquitous in the nuclear fuel cycle, and this work shows that phosphorus NMR can be a very useful tool for studying the orbital interactions in model systems, and can help decipher the underlying principles governing the interactions of *f*-elements with phosphorus-based extractants. Such an understanding is necessary in order for trivalent *f*-element separations to evolve from an empirical science to a more theory-driven endeavor based on first-principles.

Ion beam analysis (IBA) using an external 3 MeV proton beam was performed, and X-ray and gamma-ray emission (PIXE and PIGE) data for $Ce[OPPh_3][N(SiMe_3)_2]_3$ was obtained. This work was performed at the AGLAE accelerator facility (C2RMF) located in the Louvre Palace in Paris, France. These results demonstrate the feasibility of using external ion beam analysis for the study of air- and moisture-sensitive *f*-element coordination complexes. This work has inspired me to pursue further ion beam analysis studies of *f*-element complexes, in conjunction with NMR spectroscopy and X-ray

diffraction, with the intention of using these methods to study metal-ligand covalency. The analysis of the metal-chloride bonds in $M^{IV}Cl[N(SiMe_3)_2]_3$ (M = Ce, Th, U, Np, Pu) and $U^{V}Cl_2[N(SiMe_3)_2]_3$ should be a priority for future work [6-11]. Wavelength-dispersive particle-induced X-ray emission spectrometry (WD-PIXE) can be used to conduct chlorine Kβ X-ray emission analysis of these compounds, and coupled with time-dependent density functional theory (TD-DFT), this analytical approach can provide detailed information about the orbital interactions in metal-chlorine bonds in low-coordinate silyl-amide complexes. The chlorine Kβ X-ray emission is a valence-to-core electronic transition and is very sensitive to the orbital interactions in metal-chlorine bonds. In addition, it would be beneficial to develop an isostructural series with the formula $M^{III}[PR_2]_3$ (M = U, Np, Pu, Am, Cm, La, Ce, Pr, Nd, Pm, Sm, Eu, Gd, Tb, Dy, Ho, Er, Tm, Yb, Lu). Such as series could be studied using phosphorus Kβ X-ray emission spectrometry, coupled with ^{31}P NMR spectroscopy, TD-DFT, and QTAIM computational studies. Such an approach would allow one to study both energy-near-degeneracy-driven covalency *and* overlap-driven covalency in trivalent actinide and lanthanide phosphido complexes. There remains much to learn and explore in *f*-block chemistry.

Figure 5.2: Purification of $U^{V}Cl_2[N(SiMe_3)_2]_3$

References

[1] Lu, Erli, Saira Sajjad, Victoria E.J. Berryman, Ashley J. Wooles, Nikolas Kaltsoyannis, and Stephen Liddle. 2019. Emergence of the structure-directing role of f-orbital overlap-driven covalency. *Nature Communications* 10: 634.

[2] Löble, Matthias W., Jason M. Keith, Alison B. Altman, S. Chantal E. Stieber, Enrique R. Batista, Kevin S. Boland, Steven D. Conradson, David L. Clark, Juan Lezama Pacheco, Stosh A. Kozimor, Richard L. Martin, Stephan G. Minasian, Angela C. Olson, Brian L. Scott, David K. Shuh, Tolek Tyliszczak, Marianne P. Wilkerson, and Ralph A. Zehnder. 2015. Covalency in Lanthanides. An X-ray

Absorption Spectroscopy and Density Function Theory Study of $LnCl_6^{x-}$ (x = 3, 2). *Journal of the American Chemical Society* 137: 2506-2523.

[3] Neidig, Michael L., David L. Clark, and Richard L. Martin. 2013. Covalency in f-element complexes. *Coordination Chemistry Reviews* 257: 394-406.

[4] Stewart, Joanne Lee. 1988. *Tris[bis(trimethylsilyl)amido]uranium: Compounds with Tri-, Tetra-, and Penta-valent Uranium*. PhD Dissertation, University of California, Berkeley. Berkeley, California.

[5] Aspinall, Helen C., Donald C. Bradley, and Keith D. Sales. 1988. "Diphenylphosphido Complexes of the Lanthanides: Reactions of Compounds $[Ln\{N(SiMe_3)_2\}_3]$ (Ln = La or Eu) or $[Ln\{N(SiMe_3)_2\}_3(Ph_3PO)]$ (Ln = La, Eu, or Y) with Ph_2PH to give $[Ln\{N(SiMe_3)_2\}_2(PPh_2)]$ or $[Ln\{N(SiMe_3)_2\}_2(PPh_2)(Ph_3PO)]$." *Journal of the Chemical Society Dalton Transactions*: 2211-2213.

[6] Williams, Ursula J., Patrick J. Carroll, and Eric J. Schelter. 2014. "Synthesis and Analysis of a Family of Cerium(IV) Halide and Pseudohalide Compounds." *Inorganic Chemistry* 53: 6338-6345.

[7] Smiles, Danil E.; Guang Wu, Nikolas Kaltsoyannis, and Tevor W. Hayton. 2015. Thorium-ligand multiple bonds via reductive deprotection of a trityl group. *Chemical Science* 6(7): 3891-3899.

[8] Turner, Howard W., Richard A. Andersen, Allan Zalkin, and David H. Templeton. 1979. Chloro-, Methyl-, and

(Tetrahydroborato)tris((hexamethyldisilyl)amido)thorium(IV) and -uranium(IV). Crystal Structure of (Tetrahydroborato)tris((hexamethyldisilyl)amido)thorium(IV). *Inorganic Chemistry* 18(5): 1221.

[9] Staun, Selena L., Lauren M. Stevens, Danil E. Smiles, Conrad A. P. Goodwin, Brennan S. Billow, Brian L. Scott, Guang Wu, Aaron M. Tondreau, Andrew J. Gaunt, and Trevor W. Hayton. 2021. Expanding the Nonaqueous Chemistry of Neptunium: Synthesis and Structural Characterization of $[Np(NR_2)_3Cl]$, $[Np(NR_2)_3Cl]^-$, and $[Np\{N®(SiMe_2CH_2)\}_2(NR_2)]^-$ (R = $SiMe_3$). *Inorganic Chemistry* 60: 2740-2748.

[10] Gaunt, Andrew J., Sean D. Reilly, Alejandro E. Enriquez, Trevor W Hayton, James M. Boncella, Brian L Scott, and Mary P. Neu. 2008. Low-Valent Molecular Plutonium Halide Complexes. *Inorganic Chemistry* 47: 8412-8419.

[11] Lewis, Andrew J., Eiko Nakamaru-Ogiso, James M. Kikkawa, Patrick J. Carroll, and Eric J. Schelter. 2012. "Pentavalent uranium *trans*-dihalides and -pseudohalides." *Chemical Communications* 48: 4977-4979.

Appendix I: X-ray Crystallography Data

Table 1. Crystal data and structure refinement for SBY-4-061.

Empirical formula	C_{36} H_{69} Ce N_3 O P Si_6	
Formula weight	899.57	
Crystal system	triclinic	
Space group	$P\bar{1}$	
Unit cell dimensions	a = 12.3341(10) Å	a= 100.0905(13)°
	b = 12.3809(10) Å	b= 93.0661(14)°
	c = 19.7051(17) Å	c= 118.9017(12)°
Volume	2560.0(4) $Å^3$	
Z, Z'	2, 1	
Density (calculated)	1.167 Mg/m^3	
Wavelength	0.71073 Å	
Temperature	100(2) K	
F(000)	942	
Absorption coefficient	1.087 mm^{-1}	
Absorption correction	semi-empirical from equivalents	
Max. and min. transmission	0.832 and 0.777	
Theta range for data collection	1.063 to 29.630°	
Reflections collected	56447	
Independent reflections	14033 [R(int) = 0.0291]	
Data / restraints / parameters	14033 / 0 / 434	
$wR(F^2$ all data)	$wR2$ = 0.1182	
R(F obsd data)	$R1$ = 0.0432	
Goodness-of-fit on F^2	0.855	
Observed data [I > 2s(I)]	11600	
Largest and mean shift / s.u.	0.003 and 0.000	
Largest diff. peak and hole	2.004 and -1.063 $e/Å^3$	

$wR2 = \{ S [w(F_o^2 - F_c^2)^2] / S [w(F_o^2)^2] \}^{1/2}$

$R1 = S ||F_o| - |F_c|| / S |F_o|$

Table 2. Atomic coordinates and equivalent isotropic displacement parameters for SBY-4-061. U(eq) is defined as one third of the trace of the orthogonalized U_{ij} tensor.

	x	y	z	U(eq)
Ce(1)	0.74096(2)	0.59797(2)	0.76164(2)	0.01212(5)
P(1)	0.45911(7)	0.26748(7)	0.76802(4)	0.01445(15)
Si(1)	0.52779(9)	0.65818(10)	0.67414(5)	0.0262(2)
Si(2)	0.69852(11)	0.86921(10)	0.79546(5)	0.0280(2)
Si(3)	0.81781(9)	0.65596(9)	0.94211(4)	0.02001(18)
Si(4)	1.04343(8)	0.72967(9)	0.87271(4)	0.01870(17)
Si(5)	0.86373(8)	0.44040(9)	0.65719(5)	0.01979(18)
Si(6)	0.88129(8)	0.66160(9)	0.60707(4)	0.02095(18)
O(1)	0.56615(19)	0.3945(2)	0.76304(11)	0.0161(4)
N(1)	0.6481(3)	0.7214(3)	0.74274(14)	0.0211(5)
N(2)	0.8845(2)	0.6709(2)	0.86752(13)	0.0164(5)
N(3)	0.8397(2)	0.5676(2)	0.66681(13)	0.0168(5)
C(1)	0.4342(3)	0.1441(3)	0.69523(16)	0.0183(6)
C(2)	0.4517(3)	0.1719(4)	0.62993(18)	0.0287(8)
C(3)	0.4287(4)	0.0769(4)	0.5721(2)	0.0395(10)
C(4)	0.3881(4)	-0.0452(4)	0.5797(2)	0.0396(10)
C(5)	0.3706(4)	-0.0735(4)	0.6438(2)	0.0372(9)
C(6)	0.3934(3)	0.0212(3)	0.7022(2)	0.0275(7)
C(7)	0.3148(3)	0.2699(3)	0.77002(16)	0.0185(6)
C(8)	0.3198(3)	0.3803(3)	0.80597(19)	0.0275(7)
C(9)	0.2097(4)	0.3834(4)	0.81205(19)	0.0302(8)
C(10)	0.0950(3)	0.2769(4)	0.7832(2)	0.0321(8)
C(11)	0.0901(4)	0.1680(4)	0.7470(3)	0.0406(10)
C(12)	0.1997(3)	0.1640(3)	0.7401(2)	0.0291(8)
C(13)	0.4886(3)	0.2227(3)	0.84584(16)	0.0182(6)
C(14)	0.6012(4)	0.2261(4)	0.8614(2)	0.0300(8)
C(15)	0.6285(4)	0.1953(4)	0.9219(2)	0.0334(8)
C(16)	0.5435(4)	0.1621(4)	0.96785(19)	0.0306(8)
C(17)	0.4308(4)	0.1573(4)	0.9528(2)	0.0379(9)
C(18)	0.4025(3)	0.1876(4)	0.89199(19)	0.0297(8)
C(19)	0.4885(4)	0.4918(4)	0.6346(2)	0.0376(10)
C(20)	0.5623(4)	0.7444(4)	0.60107(19)	0.0317(8)
C(21)	0.3803(4)	0.6476(5)	0.7008(3)	0.0555(14)
C(22)	0.7072(4)	0.9924(4)	0.7485(2)	0.0310(8)
C(23)	0.5954(6)	0.8627(5)	0.8631(3)	0.0624(17)
C(24)	0.8611(5)	0.9362(4)	0.8419(2)	0.0473(12)

C(25)	0.6425(3)	0.5792(3)	0.91914(18)	0.0256(7)
C(26)	0.8627(4)	0.8083(4)	1.00584(19)	0.0350(9)
C(27)	0.8491(5)	0.5557(5)	0.9915(2)	0.0434(11)
C(28)	1.1400(3)	0.8497(4)	0.95579(19)	0.0309(8)
C(29)	1.0881(4)	0.6033(4)	0.8670(2)	0.0304(8)
C(30)	1.1069(3)	0.8129(4)	0.80121(19)	0.0300(8)
C(31)	0.8021(3)	0.3546(3)	0.72872(18)	0.0242(7)
C(32)	1.0325(3)	0.4811(4)	0.6622(2)	0.0321(8)
C(33)	0.7755(4)	0.3195(4)	0.57332(19)	0.0330(8)
C(34)	0.7595(4)	0.5921(4)	0.52688(18)	0.0352(9)
C(35)	0.9084(3)	0.8227(3)	0.64753(18)	0.0269(7)
C(36)	1.0303(4)	0.6883(4)	0.5742(2)	0.0406(10)

Table 3. Bond lengths [Å] and angles [°] for SBY-4-061.

Ce(1)-N(3)	2.357(2)	Si(4)-C(29)	1.882(4)
Ce(1)-N(1)	2.373(3)	Si(5)-N(3)	1.719(3)
Ce(1)-N(2)	2.388(2)	Si(5)-C(33)	1.877(4)
Ce(1)-O(1)	2.403(2)	Si(5)-C(32)	1.882(4)
Ce(1)-Si(5)	3.4809(9)	Si(5)-C(31)	1.885(3)
Ce(1)-Si(3)	3.4853(9)	Si(6)-N(3)	1.724(3)
P(1)-O(1)	1.512(2)	Si(6)-C(35)	1.870(4)
P(1)-C(1)	1.794(3)	Si(6)-C(34)	1.875(4)
P(1)-C(13)	1.796(3)	Si(6)-C(36)	1.876(4)
P(1)-C(7)	1.797(3)	C(1)-C(6)	1.388(5)
Si(1)-N(1)	1.713(3)	C(1)-C(2)	1.391(5)
Si(1)-C(21)	1.870(5)	C(2)-C(3)	1.391(5)
Si(1)-C(19)	1.876(4)	C(2)-H(2)	0.9500
Si(1)-C(20)	1.886(4)	C(3)-C(4)	1.384(6)
Si(2)-N(1)	1.726(3)	C(3)-H(3)	0.9500
Si(2)-C(24)	1.864(5)	C(4)-C(5)	1.370(6)
Si(2)-C(23)	1.876(5)	C(4)-H(4)	0.9500
Si(2)-C(22)	1.881(4)	C(5)-C(6)	1.397(5)
Si(3)-N(2)	1.718(3)	C(5)-H(5)	0.9500
Si(3)-C(27)	1.867(4)	C(6)-H(6)	0.9500
Si(3)-C(26)	1.878(4)	C(7)-C(12)	1.386(4)
Si(3)-C(25)	1.882(4)	C(7)-C(8)	1.395(5)
Si(4)-N(2)	1.719(3)	C(8)-C(9)	1.389(5)
Si(4)-C(30)	1.872(4)	C(8)-H(8)	0.9500
Si(4)-C(28)	1.880(4)	C(9)-C(10)	1.383(6)

C(9)-H(9)	0.9500	C(25)-H(25B)	0.9798
C(10)-C(11)	1.382(6)	C(25)-H(25C)	0.9799
C(10)-H(10)	0.9500	C(26)-H(26A)	0.9799
C(11)-C(12)	1.389(5)	C(26)-H(26B)	0.9798
C(11)-H(11)	0.9500	C(26)-H(26C)	0.9800
C(12)-H(12)	0.9500	C(27)-H(27A)	0.9799
C(13)-C(14)	1.385(5)	C(27)-H(27B)	0.9799
C(13)-C(18)	1.392(4)	C(27)-H(27C)	0.9800
C(14)-C(15)	1.387(5)	C(28)-H(28A)	0.9800
C(14)-H(14)	0.9500	C(28)-H(28B)	0.9799
C(15)-C(16)	1.379(5)	C(28)-H(28C)	0.9798
C(15)-H(15)	0.9500	C(29)-H(29A)	0.9798
C(16)-C(17)	1.376(6)	C(29)-H(29B)	0.9799
C(16)-H(16)	0.9500	C(29)-H(29C)	0.9799
C(17)-C(18)	1.392(5)	C(30)-H(30A)	0.9799
C(17)-H(17)	0.9500	C(30)-H(30B)	0.9799
C(18)-H(18)	0.9500	C(30)-H(30C)	0.9800
C(19)-H(19A)	0.9799	C(31)-H(31A)	0.9799
C(19)-H(19B)	0.9800	C(31)-H(31B)	0.9800
C(19)-H(19C)	0.9798	C(31)-H(31C)	0.9799
C(20)-H(20A)	0.9800	C(32)-H(32A)	0.9798
C(20)-H(20B)	0.9800	C(32)-H(32B)	0.9800
C(20)-H(20C)	0.9799	C(32)-H(32C)	0.9799
C(21)-H(21A)	0.9799	C(33)-H(33A)	0.9800
C(21)-H(21B)	0.9800	C(33)-H(33B)	0.9800
C(21)-H(21C)	0.9799	C(33)-H(33C)	0.9798
C(22)-H(22A)	0.9798	C(34)-H(34A)	0.9800
C(22)-H(22B)	0.9799	C(34)-H(34B)	0.9799
C(22)-H(22C)	0.9800	C(34)-H(34C)	0.9799
C(23)-H(23A)	0.9800	C(35)-H(35A)	0.9799
C(23)-H(23B)	0.9799	C(35)-H(35B)	0.9799
C(23)-H(23C)	0.9799	C(35)-H(35C)	0.9799
C(24)-H(24A)	0.9799	C(36)-H(36A)	0.9800
C(24)-H(24B)	0.9799	C(36)-H(36B)	0.9799
C(24)-H(24C)	0.9798	C(36)-H(36C)	0.9799
C(25)-H(25A)	0.9800		

N(3)-Ce(1)-N(1)	110.90(9)	N(2)-Ce(1)-O(1)	108.11(8)
N(3)-Ce(1)-N(2)	108.83(9)	N(3)-Ce(1)-Si(5)	26.25(7)
N(1)-Ce(1)-N(2)	116.96(9)	N(1)-Ce(1)-Si(5)	134.79(7)
N(3)-Ce(1)-O(1)	107.24(8)	N(2)-Ce(1)-Si(5)	99.01(6)
N(1)-Ce(1)-O(1)	104.27(9)	O(1)-Ce(1)-Si(5)	88.18(5)

N(3)-Ce(1)-Si(3)	133.73(6)	N(3)-Si(5)-C(31)	109.43(14)
N(1)-Ce(1)-Si(3)	106.03(7)	C(33)-Si(5)-C(31)	105.47(17)
N(2)-Ce(1)-Si(3)	26.48(6)	C(32)-Si(5)-C(31)	106.08(16)
O(1)-Ce(1)-Si(3)	89.16(5)	N(3)-Si(5)-Ce(1)	37.34(8)
Si(5)-Ce(1)-Si(3)	117.63(2)	C(33)-Si(5)-Ce(1)	123.99(13)
O(1)-P(1)-C(1)	111.42(13)	C(32)-Si(5)-Ce(1)	127.57(14)
O(1)-P(1)-C(13)	111.68(13)	C(31)-Si(5)-Ce(1)	72.10(11)
C(1)-P(1)-C(13)	107.21(15)	N(3)-Si(6)-C(35)	110.34(14)
O(1)-P(1)-C(7)	111.50(14)	N(3)-Si(6)-C(34)	112.55(16)
C(1)-P(1)-C(7)	107.77(14)	C(35)-Si(6)-C(34)	108.75(18)
C(13)-P(1)-C(7)	107.01(15)	N(3)-Si(6)-C(36)	113.85(17)
N(1)-Si(1)-C(21)	113.2(2)	C(35)-Si(6)-C(36)	105.77(19)
N(1)-Si(1)-C(19)	108.75(15)	C(34)-Si(6)-C(36)	105.2(2)
C(21)-Si(1)-C(19)	106.4(2)	P(1)-O(1)-Ce(1)	176.85(13)
N(1)-Si(1)-C(20)	115.24(15)	Si(1)-N(1)-Si(2)	120.69(16)
C(21)-Si(1)-C(20)	106.28(19)	Si(1)-N(1)-Ce(1)	117.35(14)
C(19)-Si(1)-C(20)	106.48(19)	Si(2)-N(1)-Ce(1)	121.96(14)
N(1)-Si(2)-C(24)	110.13(17)	Si(3)-N(2)-Si(4)	119.77(15)
N(1)-Si(2)-C(23)	111.9(2)	Si(3)-N(2)-Ce(1)	115.22(13)
C(24)-Si(2)-C(23)	107.8(3)	Si(4)-N(2)-Ce(1)	124.96(13)
N(1)-Si(2)-C(22)	115.29(16)	Si(5)-N(3)-Si(6)	120.32(15)
C(24)-Si(2)-C(22)	104.9(2)	Si(5)-N(3)-Ce(1)	116.41(13)
C(23)-Si(2)-C(22)	106.3(2)	Si(6)-N(3)-Ce(1)	123.22(14)
N(2)-Si(3)-C(27)	112.92(17)	C(6)-C(1)-C(2)	119.7(3)
N(2)-Si(3)-C(26)	115.87(17)	C(6)-C(1)-P(1)	121.5(3)
C(27)-Si(3)-C(26)	107.0(2)	C(2)-C(1)-P(1)	118.8(3)
N(2)-Si(3)-C(25)	109.87(14)	C(1)-C(2)-C(3)	120.0(4)
C(27)-Si(3)-C(25)	107.0(2)	C(1)-C(2)-H(2)	120.0
C(26)-Si(3)-C(25)	103.34(17)	C(3)-C(2)-H(2)	120.0
N(2)-Si(3)-Ce(1)	38.31(9)	C(4)-C(3)-C(2)	119.9(4)
C(27)-Si(3)-Ce(1)	126.84(15)	C(4)-C(3)-H(3)	120.1
C(26)-Si(3)-Ce(1)	125.35(14)	C(2)-C(3)-H(3)	120.1
C(25)-Si(3)-Ce(1)	71.58(11)	C(5)-C(4)-C(3)	120.6(3)
N(2)-Si(4)-C(30)	111.76(14)	C(5)-C(4)-H(4)	119.7
N(2)-Si(4)-C(28)	114.54(15)	C(3)-C(4)-H(4)	119.7
C(30)-Si(4)-C(28)	104.92(18)	C(4)-C(5)-C(6)	120.0(4)
N(2)-Si(4)-C(29)	113.12(16)	C(4)-C(5)-H(5)	120.0
C(30)-Si(4)-C(29)	106.90(18)	C(6)-C(5)-H(5)	120.0
C(28)-Si(4)-C(29)	104.90(17)	C(1)-C(6)-C(5)	119.9(4)
N(3)-Si(5)-C(33)	112.66(17)	C(1)-C(6)-H(6)	120.0
N(3)-Si(5)-C(32)	115.25(16)	C(5)-C(6)-H(6)	120.0
C(33)-Si(5)-C(32)	107.31(18)	C(12)-C(7)-C(8)	119.8(3)

C(12)-C(7)-P(1)	121.9(3)	Si(1)-C(20)-H(20B)	109.4
C(8)-C(7)-P(1)	118.2(2)	H(20A)-C(20)-H(20B)	109.5
C(9)-C(8)-C(7)	119.9(3)	Si(1)-C(20)-H(20C)	109.5
C(9)-C(8)-H(8)	120.0	H(20A)-C(20)-H(20C)	109.5
C(7)-C(8)-H(8)	120.0	H(20B)-C(20)-H(20C)	109.5
C(10)-C(9)-C(8)	120.1(3)	Si(1)-C(21)-H(21A)	110.2
C(10)-C(9)-H(9)	119.9	Si(1)-C(21)-H(21B)	108.8
C(8)-C(9)-H(9)	119.9	H(21A)-C(21)-H(21B)	109.5
C(11)-C(10)-C(9)	119.9(3)	Si(1)-C(21)-H(21C)	109.4
C(11)-C(10)-H(10)	120.0	H(21A)-C(21)-H(21C)	109.5
C(9)-C(10)-H(10)	120.0	H(21B)-C(21)-H(21C)	109.5
C(10)-C(11)-C(12)	120.5(4)	Si(2)-C(22)-H(22A)	109.6
C(10)-C(11)-H(11)	119.8	Si(2)-C(22)-H(22B)	109.4
C(12)-C(11)-H(11)	119.8	H(22A)-C(22)-H(22B)	109.5
C(7)-C(12)-C(11)	119.8(3)	Si(2)-C(22)-H(22C)	109.4
C(7)-C(12)-H(12)	120.1	H(22A)-C(22)-H(22C)	109.5
C(11)-C(12)-H(12)	120.1	H(22B)-C(22)-H(22C)	109.5
C(14)-C(13)-C(18)	119.0(3)	Si(2)-C(23)-H(23A)	110.1
C(14)-C(13)-P(1)	119.3(2)	Si(2)-C(23)-H(23B)	109.3
C(18)-C(13)-P(1)	121.8(3)	H(23A)-C(23)-H(23B)	109.5
C(13)-C(14)-C(15)	120.8(3)	Si(2)-C(23)-H(23C)	109.0
C(13)-C(14)-H(14)	119.6	H(23A)-C(23)-H(23C)	109.5
C(15)-C(14)-H(14)	119.6	H(23B)-C(23)-H(23C)	109.5
C(16)-C(15)-C(14)	119.9(3)	Si(2)-C(24)-H(24A)	109.6
C(16)-C(15)-H(15)	120.0	Si(2)-C(24)-H(24B)	109.7
C(14)-C(15)-H(15)	120.0	H(24A)-C(24)-H(24B)	109.5
C(17)-C(16)-C(15)	119.9(3)	Si(2)-C(24)-H(24C)	109.1
C(17)-C(16)-H(16)	120.0	H(24A)-C(24)-H(24C)	109.5
C(15)-C(16)-H(16)	120.0	H(24B)-C(24)-H(24C)	109.5
C(16)-C(17)-C(18)	120.4(3)	Si(3)-C(25)-H(25A)	109.4
C(16)-C(17)-H(17)	119.8	Si(3)-C(25)-H(25B)	109.7
C(18)-C(17)-H(17)	119.8	H(25A)-C(25)-H(25B)	109.5
C(13)-C(18)-C(17)	119.9(3)	Si(3)-C(25)-H(25C)	109.4
C(13)-C(18)-H(18)	120.1	H(25A)-C(25)-H(25C)	109.5
C(17)-C(18)-H(18)	120.1	H(25B)-C(25)-H(25C)	109.5
Si(1)-C(19)-H(19A)	109.4	Si(3)-C(26)-H(26A)	109.4
Si(1)-C(19)-H(19B)	109.5	Si(3)-C(26)-H(26B)	109.7
H(19A)-C(19)-H(19B)	109.5	H(26A)-C(26)-H(26B)	109.5
Si(1)-C(19)-H(19C)	109.6	Si(3)-C(26)-H(26C)	109.2
H(19A)-C(19)-H(19C)	109.5	H(26A)-C(26)-H(26C)	109.5
H(19B)-C(19)-H(19C)	109.5	H(26B)-C(26)-H(26C)	109.5
Si(1)-C(20)-H(20A)	109.6	Si(3)-C(27)-H(27A)	109.5

Si(3)-C(27)-H(27B)	109.6	Si(5)-C(32)-H(32B)	109.5
H(27A)-C(27)-H(27B)	109.5	H(32A)-C(32)-H(32B)	109.5
Si(3)-C(27)-H(27C)	109.3	Si(5)-C(32)-H(32C)	109.4
H(27A)-C(27)-H(27C)	109.5	H(32A)-C(32)-H(32C)	109.5
H(27B)-C(27)-H(27C)	109.5	H(32B)-C(32)-H(32C)	109.5
Si(4)-C(28)-H(28A)	109.2	Si(5)-C(33)-H(33A)	109.3
Si(4)-C(28)-H(28B)	109.6	Si(5)-C(33)-H(33B)	109.8
H(28A)-C(28)-H(28B)	109.5	H(33A)-C(33)-H(33B)	109.5
Si(4)-C(28)-H(28C)	109.6	Si(5)-C(33)-H(33C)	109.3
H(28A)-C(28)-H(28C)	109.5	H(33A)-C(33)-H(33C)	109.5
H(28B)-C(28)-H(28C)	109.5	H(33B)-C(33)-H(33C)	109.5
Si(4)-C(29)-H(29A)	109.1	Si(6)-C(34)-H(34A)	109.2
Si(4)-C(29)-H(29B)	109.8	Si(6)-C(34)-H(34B)	109.5
H(29A)-C(29)-H(29B)	109.5	H(34A)-C(34)-H(34B)	109.5
Si(4)-C(29)-H(29C)	109.5	Si(6)-C(34)-H(34C)	109.8
H(29A)-C(29)-H(29C)	109.5	H(34A)-C(34)-H(34C)	109.5
H(29B)-C(29)-H(29C)	109.5	H(34B)-C(34)-H(34C)	109.5
Si(4)-C(30)-H(30A)	109.6	Si(6)-C(35)-H(35A)	109.4
Si(4)-C(30)-H(30B)	109.5	Si(6)-C(35)-H(35B)	109.6
H(30A)-C(30)-H(30B)	109.5	H(35A)-C(35)-H(35B)	109.5
Si(4)-C(30)-H(30C)	109.4	Si(6)-C(35)-H(35C)	109.4
H(30A)-C(30)-H(30C)	109.5	H(35A)-C(35)-H(35C)	109.5
H(30B)-C(30)-H(30C)	109.5	H(35B)-C(35)-H(35C)	109.5
Si(5)-C(31)-H(31A)	109.3	Si(6)-C(36)-H(36A)	109.7
Si(5)-C(31)-H(31B)	109.6	Si(6)-C(36)-H(36B)	109.5
H(31A)-C(31)-H(31B)	109.5	H(36A)-C(36)-H(36B)	109.5
Si(5)-C(31)-H(31C)	109.5	Si(6)-C(36)-H(36C)	109.2
H(31A)-C(31)-H(31C)	109.5	H(36A)-C(36)-H(36C)	109.5
H(31B)-C(31)-H(31C)	109.5	H(36B)-C(36)-H(36C)	109.5
Si(5)-C(32)-H(32A)	109.5		

Table 4. Anisotropic displacement parameters ($Å^2 x\ 10^3$) for SBY-4-061. The anisotropic displacement factor exponent takes the form:
$-2\ p^2[\ h^2\ a^{*2}\ U_{11} + ... + 2\ h\ k\ a^*\ b^*\ U_{12}]$

	U_{11}	U_{22}	U_{33}	U_{23}	U_{13}	U_{12}
Ce(1)	10(1)	12(1)	13(1)	2(1)	1(1)	5(1)
P(1)	13(1)	13(1)	18(1)	3(1)	4(1)	7(1)
Si(1)	15(1)	30(1)	35(1)	18(1)	1(1)	10(1)
Si(2)	47(1)	28(1)	22(1)	9(1)	10(1)	28(1)
Si(3)	25(1)	21(1)	15(1)	2(1)	2(1)	12(1)
Si(4)	17(1)	20(1)	19(1)	1(1)	-3(1)	11(1)
Si(5)	15(1)	20(1)	23(1)	2(1)	7(1)	8(1)
Si(6)	18(1)	25(1)	17(1)	7(1)	6(1)	8(1)
O(1)	13(1)	13(1)	19(1)	4(1)	4(1)	4(1)
N(1)	24(1)	22(1)	23(1)	10(1)	7(1)	14(1)
N(2)	18(1)	16(1)	18(1)	3(1)	2(1)	10(1)
N(3)	14(1)	19(1)	14(1)	2(1)	4(1)	6(1)
C(1)	11(1)	16(1)	25(1)	-1(1)	3(1)	7(1)
C(2)	27(2)	24(2)	27(2)	-1(1)	8(1)	8(1)
C(3)	31(2)	41(2)	28(2)	-11(2)	6(2)	10(2)
C(4)	29(2)	32(2)	44(2)	-20(2)	-6(2)	15(2)
C(5)	33(2)	21(2)	50(2)	-10(2)	-13(2)	16(2)
C(6)	26(2)	19(2)	35(2)	2(1)	-2(1)	11(1)
C(7)	13(1)	22(2)	22(1)	4(1)	5(1)	10(1)
C(8)	21(2)	23(2)	37(2)	-1(1)	2(1)	13(1)
C(9)	32(2)	35(2)	35(2)	3(2)	7(2)	27(2)
C(10)	22(2)	42(2)	46(2)	15(2)	10(2)	25(2)
C(11)	15(2)	34(2)	66(3)	1(2)	2(2)	10(2)
C(12)	15(2)	19(2)	49(2)	2(2)	3(1)	7(1)
C(13)	19(2)	14(1)	23(1)	6(1)	5(1)	9(1)
C(14)	29(2)	44(2)	34(2)	24(2)	16(2)	26(2)
C(15)	29(2)	43(2)	41(2)	22(2)	8(2)	24(2)
C(16)	38(2)	32(2)	28(2)	14(2)	6(2)	19(2)
C(17)	35(2)	59(3)	30(2)	23(2)	17(2)	26(2)
C(18)	24(2)	42(2)	29(2)	14(2)	11(1)	19(2)
C(19)	30(2)	28(2)	37(2)	12(2)	-16(2)	2(2)
C(20)	27(2)	32(2)	33(2)	15(2)	-5(1)	11(2)
C(21)	29(2)	71(3)	92(4)	54(3)	24(2)	31(2)

C(22)	42(2)	27(2)	33(2)	12(2)	5(2)	23(2)
C(23)	121(5)	56(3)	51(3)	30(2)	56(3)	65(3)
C(24)	75(3)	29(2)	35(2)	-4(2)	-22(2)	31(2)
C(25)	22(2)	22(2)	25(2)	1(1)	6(1)	6(1)
C(26)	30(2)	37(2)	28(2)	-10(2)	2(2)	15(2)
C(27)	63(3)	53(3)	34(2)	27(2)	14(2)	39(2)
C(28)	22(2)	35(2)	31(2)	-3(2)	-6(1)	15(2)
C(29)	28(2)	32(2)	38(2)	5(2)	1(2)	23(2)
C(30)	18(2)	37(2)	32(2)	14(2)	3(1)	10(2)
C(31)	23(2)	22(2)	32(2)	9(1)	10(1)	13(1)
C(32)	21(2)	39(2)	46(2)	19(2)	15(2)	18(2)
C(33)	31(2)	31(2)	30(2)	-4(2)	11(2)	13(2)
C(34)	40(2)	37(2)	22(2)	7(2)	-2(2)	14(2)
C(35)	24(2)	24(2)	26(2)	9(1)	0(1)	8(1)
C(36)	36(2)	50(3)	45(2)	27(2)	28(2)	22(2)

Table 5. Hydrogen coordinates and isotropic displacement parameters for SBY-4-061.

	x	y	z	U(eq)
H(2)	0.479195	0.255735	0.624807	0.034
H(3)	0.440923	0.095864	0.527507	0.047
H(4)	0.372276	-0.109995	0.540147	0.047
H(5)	0.342990	-0.157553	0.648609	0.045
H(6)	0.381052	0.001560	0.746664	0.033
H(8)	0.398557	0.453206	0.826261	0.033
H(9)	0.213145	0.458801	0.836070	0.036
H(10)	0.019584	0.278513	0.788263	0.038
H(11)	0.011217	0.095315	0.726704	0.049
H(12)	0.195801	0.089051	0.714999	0.035
H(14)	0.660445	0.249798	0.830194	0.036
H(15)	0.705623	0.197003	0.931775	0.040
H(16)	0.562729	0.142593	1.009802	0.037
H(17)	0.371833	0.133172	0.984198	0.045
H(18)	0.324665	0.184379	0.881988	0.036
H(19A)	0.565786	0.490725	0.626749	0.056

H(19B)	0.432236	0.460626	0.590003	0.056
H(19C)	0.447060	0.437110	0.666407	0.056
H(20A)	0.569305	0.827344	0.617146	0.048
H(20B)	0.494030	0.694346	0.561353	0.048
H(20C)	0.641312	0.755955	0.586653	0.048
H(21A)	0.350423	0.592720	0.733851	0.083
H(21B)	0.316306	0.612240	0.659122	0.083
H(21C)	0.396755	0.732557	0.722787	0.083
H(22A)	0.754887	0.994857	0.710045	0.046
H(22B)	0.749101	1.075562	0.781247	0.046
H(22C)	0.622220	0.970982	0.729951	0.046
H(23A)	0.517622	0.855278	0.841924	0.094
H(23B)	0.639936	0.940174	0.900270	0.094
H(23C)	0.575240	0.788964	0.882759	0.094
H(24A)	0.861258	0.883305	0.873437	0.071
H(24B)	0.891583	1.022707	0.868872	0.071
H(24C)	0.915959	0.937711	0.807466	0.071
H(25A)	0.622568	0.621590	0.887030	0.038
H(25B)	0.606306	0.586488	0.961616	0.038
H(25C)	0.607246	0.489451	0.896600	0.038
H(26A)	0.953369	0.865758	1.011058	0.052
H(26B)	0.840113	0.791032	1.051247	0.052
H(26C)	0.818071	0.847724	0.988260	0.052
H(27A)	0.829525	0.476206	0.959584	0.065
H(27B)	0.796706	0.537022	1.028303	0.065
H(27C)	0.937771	0.601385	1.012656	0.065
H(28A)	1.126694	0.922334	0.959995	0.046
H(28B)	1.228964	0.878187	0.954815	0.046
H(28C)	1.114406	0.811303	0.995810	0.046
H(29A)	1.053833	0.555835	0.902879	0.046
H(29B)	1.179716	0.642447	0.874703	0.046
H(29C)	1.053615	0.545481	0.820777	0.046
H(30A)	1.062155	0.754793	0.755810	0.045
H(30B)	1.196515	0.840844	0.804273	0.045
H(30C)	1.095367	0.886650	0.806196	0.045
H(31A)	0.833757	0.416012	0.773833	0.036
H(31B)	0.830330	0.293001	0.729135	0.036
H(31C)	0.710201	0.310213	0.720452	0.036
H(32A)	1.060737	0.498637	0.617815	0.048
H(32B)	1.040245	0.409692	0.671441	0.048
H(32C)	1.084317	0.556252	0.700000	0.048
H(33A)	0.689874	0.305094	0.565976	0.049

H(33B)	0.772509	0.239696	0.575582	0.049
H(33C)	0.817864	0.350988	0.534514	0.049
H(34A)	0.754927	0.514360	0.501135	0.053
H(34B)	0.782468	0.653188	0.497200	0.053
H(34C)	0.677609	0.572159	0.540251	0.053
H(35A)	0.831129	0.815020	0.662778	0.040
H(35B)	0.932558	0.875426	0.613221	0.040
H(35C)	0.975599	0.862051	0.687884	0.040
H(36A)	1.098246	0.722924	0.613811	0.061
H(36B)	1.052149	0.748240	0.543869	0.061
H(36C)	1.018027	0.607480	0.547725	0.061

Table 6. Torsion angles [°] for SBY-4-061.

C(21)-Si(1)-N(1)-Si(2)	-56.5(3)	C(33)-Si(5)-N(3)-Si(6)	-60.7(2)
C(19)-Si(1)-N(1)-Si(2)	-174.4(2)	C(32)-Si(5)-N(3)-Si(6)	62.9(2)
C(20)-Si(1)-N(1)-Si(2)	66.1(2)	C(31)-Si(5)-N(3)-Si(6)	-177.66(17)
C(21)-Si(1)-N(1)-Ce(1)	123.5(2)	Ce(1)-Si(5)-N(3)-Si(6)	-177.5(3)
C(19)-Si(1)-N(1)-Ce(1)	5.6(2)	C(33)-Si(5)-N(3)-Ce(1)	116.84(16)
C(20)-Si(1)-N(1)-Ce(1)	-113.86(19)	C(32)-Si(5)-N(3)-Ce(1)	-119.56(17)
C(24)-Si(2)-N(1)-Si(1)	-159.0(2)	C(31)-Si(5)-N(3)-Ce(1)	-0.15(19)
C(23)-Si(2)-N(1)-Si(1)	81.0(3)	C(35)-Si(6)-N(3)-Si(5)	-156.35(17)
C(22)-Si(2)-N(1)-Si(1)	-40.6(3)	C(34)-Si(6)-N(3)-Si(5)	82.0(2)
C(24)-Si(2)-N(1)-Ce(1)	21.0(2)	C(36)-Si(6)-N(3)-Si(5)	-37.6(2)
C(23)-Si(2)-N(1)-Ce(1)	-99.0(2)	C(35)-Si(6)-N(3)-Ce(1)	26.3(2)
C(22)-Si(2)-N(1)-Ce(1)	139.39(18)	C(34)-Si(6)-N(3)-Ce(1)	-95.4(2)
C(27)-Si(3)-N(2)-Si(4)	-56.7(2)	C(36)-Si(6)-N(3)-Ce(1)	145.06(19)
C(26)-Si(3)-N(2)-Si(4)	67.2(2)	O(1)-P(1)-C(1)-C(6)	146.7(3)
C(25)-Si(3)-N(2)-Si(4)	-176.15(17)	C(13)-P(1)-C(1)-C(6)	24.2(3)
Ce(1)-Si(3)-N(2)-Si(4)	-177.7(3)	C(7)-P(1)-C(1)-C(6)	-90.7(3)
C(27)-Si(3)-N(2)-Ce(1)	121.0(2)	O(1)-P(1)-C(1)-C(2)	-35.9(3)
C(26)-Si(3)-N(2)-Ce(1)	-115.05(18)	C(13)-P(1)-C(1)-C(2)	-158.4(3)
C(25)-Si(3)-N(2)-Ce(1)	1.57(19)	C(7)-P(1)-C(1)-C(2)	86.7(3)
C(30)-Si(4)-N(2)-Si(3)	-151.07(19)	C(6)-C(1)-C(2)-C(3)	-0.3(5)
C(28)-Si(4)-N(2)-Si(3)	-31.9(2)	P(1)-C(1)-C(2)-C(3)	-177.7(3)
C(29)-Si(4)-N(2)-Si(3)	88.2(2)	C(1)-C(2)-C(3)-C(4)	0.3(6)
C(30)-Si(4)-N(2)-Ce(1)	31.5(2)	C(2)-C(3)-C(4)-C(5)	-0.2(6)
C(28)-Si(4)-N(2)-Ce(1)	150.59(17)	C(3)-C(4)-C(5)-C(6)	0.2(6)
C(29)-Si(4)-N(2)-Ce(1)	-89.3(2)	C(2)-C(1)-C(6)-C(5)	0.3(5)

P(1)-C(1)-C(6)-C(5)	177.6(3)
C(4)-C(5)-C(6)-C(1)	-0.2(6)
O(1)-P(1)-C(7)-C(12)	146.6(3)
C(1)-P(1)-C(7)-C(12)	24.0(3)
C(13)-P(1)-C(7)-C(12)	-91.0(3)
O(1)-P(1)-C(7)-C(8)	-36.7(3)
C(1)-P(1)-C(7)-C(8)	-159.3(3)
C(13)-P(1)-C(7)-C(8)	85.7(3)
C(12)-C(7)-C(8)-C(9)	0.4(5)
P(1)-C(7)-C(8)-C(9)	-176.4(3)
C(7)-C(8)-C(9)-C(10)	0.7(6)
C(8)-C(9)-C(10)-C(11)	-1.4(6)
C(9)-C(10)-C(11)-C(12)	0.9(7)
C(8)-C(7)-C(12)-C(11)	-0.9(6)
P(1)-C(7)-C(12)-C(11)	175.7(3)
C(10)-C(11)-C(12)-C(7)	0.3(7)
O(1)-P(1)-C(13)-C(14)	-51.1(3)
C(1)-P(1)-C(13)-C(14)	71.2(3)
C(7)-P(1)-C(13)-C(14)	-173.4(3)
O(1)-P(1)-C(13)-C(18)	127.3(3)
C(1)-P(1)-C(13)-C(18)	-110.4(3)
C(7)-P(1)-C(13)-C(18)	5.0(3)
C(18)-C(13)-C(14)-C(15)	-0.1(6)
P(1)-C(13)-C(14)-C(15)	178.3(3)
C(13)-C(14)-C(15)-C(16)	-0.7(6)
C(14)-C(15)-C(16)-C(17)	1.2(6)
C(15)-C(16)-C(17)-C(18)	-1.0(7)
C(14)-C(13)-C(18)-C(17)	0.3(6)
P(1)-C(13)-C(18)-C(17)	-178.0(3)
C(16)-C(17)-C(18)-C(13)	0.2(6)

Table 1. Crystal data and structure refinement for SBY-3-077.

Empirical formula	$C_{39}\ H_{75}\ Ce\ N_3\ O_4\ P\ Si_6$	
Formula weight	989.65	
Crystal system	monoclinic	
Space group	$P2_1/c$	
Unit cell dimensions	a = 16.1035(9) Å	a= 90°
	b = 13.8776(8) Å	b= 91.9766(9)°
	c = 23.0565(13) Å	c= 90°
Volume	5149.6(5) $Å^3$	
Z, Z'	4, 2	
Density (calculated)	1.276 Mg/m^3	
Wavelength	0.71073 Å	
Temperature	100(2) K	
$F(000)$	2076	
Absorption coefficient	1.092 mm^{-1}	
Absorption correction	semi-empirical from equivalents	
Max. and min. transmission	0.958 and 0.721	
Theta range for data collection	1.265 to 27.511°	
Reflections collected	52967	
Independent reflections	11818 [R(int) = 0.0272]	
Data / restraints / parameters	11818 / 0 / 487	
$wR(F^2$ all data)	$wR2$ = 0.0577	
$R(F$ obsd data)	$R1$ = 0.0219	
Goodness-of-fit on F^2	0.892	
Observed data [I > 2s(I)]	10247	
Largest and mean shift / s.u.	0.003 and 0.000	
Largest diff. peak and hole	0.541 and -0.267 $e/Å^3$	

$wR2 = \{ S [w(F_o^2 - F_c^2)^2] / S [w(F_o^2)^2] \}^{1/2}$

$R1 = S ||F_o| - |F_c|| / S |F_o|$

Table 2. Atomic coordinates and equivalent isotropic displacement parameters for SBY-3-077. U(eq) is defined as one third of the trace of the orthogonalized U_{ij} tensor.

	x	y	z	U(eq)
Ce(1)	0.80737(2)	0.14849(2)	0.37234(2)	0.01283(3)
P(1)	0.62380(3)	0.26823(3)	0.28366(2)	0.01418(9)
Si(1)	0.89332(3)	0.10210(4)	0.23346(2)	0.01802(10)
Si(2)	0.95225(3)	-0.01916(4)	0.33627(2)	0.01878(10)
Si(3)	0.82719(3)	0.36101(3)	0.45200(2)	0.01744(10)
Si(4)	0.99228(3)	0.29147(4)	0.41816(2)	0.02000(10)
Si(5)	0.67426(3)	-0.05039(4)	0.39490(2)	0.02098(11)
Si(6)	0.73256(3)	0.04585(4)	0.50470(2)	0.01970(10)
O(1)	0.69724(7)	0.22009(9)	0.31468(5)	0.0168(2)
O(2)	0.69902(9)	0.66563(9)	0.20467(6)	0.0259(3)
O(3)	0.35428(8)	0.30974(10)	0.45171(6)	0.0268(3)
O(4)	0.51040(9)	0.06459(11)	0.06898(6)	0.0317(3)
N(1)	0.89353(9)	0.07180(10)	0.30556(6)	0.0164(3)
N(2)	0.88575(9)	0.27914(10)	0.41566(6)	0.0163(3)
N(3)	0.72823(9)	0.04022(11)	0.42991(6)	0.0178(3)
C(1)	0.65109(11)	0.38572(12)	0.25792(7)	0.0155(3)
C(2)	0.71427(11)	0.43758(13)	0.28626(7)	0.0182(3)
C(3)	0.73314(11)	0.53136(13)	0.26968(8)	0.0195(4)
C(4)	0.68811(11)	0.57367(12)	0.22371(7)	0.0182(3)
C(5)	0.62599(12)	0.52171(13)	0.19393(7)	0.0208(4)
C(6)	0.60767(11)	0.42885(13)	0.21096(7)	0.0193(4)
C(7)	0.53983(11)	0.28137(12)	0.33223(7)	0.0166(3)
C(8)	0.53779(11)	0.22470(13)	0.38242(8)	0.0193(4)
C(9)	0.47506(11)	0.23603(14)	0.42094(8)	0.0221(4)
C(10)	0.41231(11)	0.30359(13)	0.41032(8)	0.0199(4)
C(11)	0.41253(12)	0.35999(13)	0.36031(8)	0.0220(4)
C(12)	0.47648(12)	0.34890(13)	0.32199(8)	0.0206(4)
C(13)	0.58625(11)	0.20353(12)	0.22091(7)	0.0167(3)
C(14)	0.63781(12)	0.19553(14)	0.17318(8)	0.0227(4)
C(15)	0.61062(13)	0.14853(14)	0.12344(8)	0.0250(4)
C(16)	0.53083(12)	0.10866(13)	0.12016(8)	0.0224(4)
C(17)	0.47954(13)	0.11518(15)	0.16704(8)	0.0266(4)
C(18)	0.50764(12)	0.16328(13)	0.21713(8)	0.0226(4)
C(19)	0.75947(13)	0.72328(14)	0.23554(9)	0.0300(4)
C(20)	0.28417(14)	0.37088(18)	0.44042(10)	0.0388(5)

C(21)	0.42891(15)	0.02378(19)	0.06276(9)	0.0431(6)
C(22)	0.86424(12)	0.23233(14)	0.22410(9)	0.0259(4)
C(23)	0.81828(13)	0.02624(15)	0.18921(8)	0.0265(4)
C(24)	0.99700(12)	0.08996(15)	0.19895(8)	0.0263(4)
C(25)	0.93710(12)	-0.01496(15)	0.41675(8)	0.0248(4)
C(26)	0.91819(16)	-0.14209(14)	0.31140(10)	0.0358(5)
C(27)	1.06720(13)	-0.01096(18)	0.32634(10)	0.0355(5)
C(28)	0.71460(12)	0.32426(14)	0.44529(8)	0.0233(4)
C(29)	0.83156(13)	0.48829(13)	0.42302(8)	0.0254(4)
C(30)	0.85049(13)	0.36961(14)	0.53243(8)	0.0265(4)
C(31)	1.03027(12)	0.41633(14)	0.43357(9)	0.0260(4)
C(32)	1.04366(15)	0.21787(18)	0.47731(13)	0.0510(7)
C(33)	1.03800(16)	0.2600(2)	0.34765(12)	0.0568(9)
C(34)	0.67413(14)	-0.02954(15)	0.31405(8)	0.0289(4)
C(35)	0.56290(13)	-0.05790(17)	0.41606(10)	0.0349(5)
C(36)	0.71724(14)	-0.17536(15)	0.40716(9)	0.0311(5)
C(37)	0.64244(14)	0.11315(18)	0.53480(9)	0.0359(5)
C(38)	0.73402(14)	-0.07390(15)	0.54283(9)	0.0302(4)
C(39)	0.83089(13)	0.10677(15)	0.53033(8)	0.0264(4)

Table 3. Bond lengths [Å] and angles [°] for SBY-3-077.

Ce(1)-N(1)	2.3612(14)	Si(2)-C(25)	1.8808(19)
Ce(1)-O(1)	2.3952(12)	Si(3)-N(2)	1.7138(15)
Ce(1)-N(3)	2.4000(14)	Si(3)-C(28)	1.885(2)
Ce(1)-N(2)	2.4065(14)	Si(3)-C(30)	1.8830(19)
Ce(1)-Si(2)	3.4179(5)	Si(3)-C(29)	1.891(2)
Ce(1)-Si(3)	3.4834(5)	Si(4)-N(2)	1.7230(16)
P(1)-O(1)	1.5161(12)	Si(4)-C(33)	1.860(2)
P(1)-C(13)	1.7901(17)	Si(4)-C(31)	1.8676(19)
P(1)-C(7)	1.7944(18)	Si(4)-C(32)	1.873(2)
P(1)-C(1)	1.7948(18)	Si(5)-N(3)	1.7146(16)
Si(1)-N(1)	1.7147(14)	Si(5)-C(35)	1.878(2)
Si(1)-C(23)	1.8773(19)	Si(5)-C(34)	1.886(2)
Si(1)-C(22)	1.878(2)	Si(5)-C(36)	1.885(2)
Si(1)-C(24)	1.882(2)	Si(6)-N(3)	1.7253(15)
Si(2)-N(1)	1.7155(15)	Si(6)-C(39)	1.873(2)
Si(2)-C(26)	1.876(2)	Si(6)-C(37)	1.879(2)
Si(2)-C(27)	1.877(2)	Si(6)-C(38)	1.880(2)

O(2)-C(4)	1.363(2)	C(21)-H(21A)	0.9800
O(2)-C(19)	1.431(2)	C(21)-H(21B)	0.9800
O(3)-C(10)	1.361(2)	C(21)-H(21C)	0.9800
O(3)-C(20)	1.429(3)	C(22)-H(22A)	0.9800
O(4)-C(16)	1.359(2)	C(22)-H(22B)	0.9800
O(4)-C(21)	1.432(3)	C(22)-H(22C)	0.9800
C(1)-C(2)	1.391(2)	C(23)-H(23A)	0.9800
C(1)-C(6)	1.403(2)	C(23)-H(23B)	0.9800
C(2)-C(3)	1.393(2)	C(23)-H(23C)	0.9800
C(2)-H(2)	0.9500	C(24)-H(24A)	0.9800
C(3)-C(4)	1.393(2)	C(24)-H(24B)	0.9800
C(3)-H(3)	0.9500	C(24)-H(24C)	0.9800
C(4)-C(5)	1.394(3)	C(25)-H(25A)	0.9800
C(5)-C(6)	1.382(2)	C(25)-H(25B)	0.9800
C(5)-H(5)	0.9500	C(25)-H(25C)	0.9800
C(6)-H(6)	0.9500	C(26)-H(26A)	0.9800
C(7)-C(12)	1.399(2)	C(26)-H(26B)	0.9800
C(7)-C(8)	1.401(2)	C(26)-H(26C)	0.9800
C(8)-C(9)	1.377(3)	C(27)-H(27A)	0.9800
C(8)-H(8)	0.9500	C(27)-H(27B)	0.9800
C(9)-C(10)	1.394(3)	C(27)-H(27C)	0.9800
C(9)-H(9)	0.9500	C(28)-H(28A)	0.9800
C(10)-C(11)	1.394(3)	C(28)-H(28B)	0.9800
C(11)-C(12)	1.388(3)	C(28)-H(28C)	0.9800
C(11)-H(11)	0.9500	C(29)-H(29A)	0.9800
C(12)-H(12)	0.9500	C(29)-H(29B)	0.9800
C(13)-C(18)	1.384(3)	C(29)-H(29C)	0.9800
C(13)-C(14)	1.406(2)	C(30)-H(30A)	0.9800
C(14)-C(15)	1.378(2)	C(30)-H(30B)	0.9800
C(14)-H(14)	0.9500	C(30)-H(30C)	0.9800
C(15)-C(16)	1.399(3)	C(31)-H(31A)	0.9800
C(15)-H(15)	0.9500	C(31)-H(31B)	0.9800
C(16)-C(17)	1.386(3)	C(31)-H(31C)	0.9800
C(17)-C(18)	1.396(3)	C(32)-H(32A)	0.9800
C(17)-H(17)	0.9500	C(32)-H(32B)	0.9800
C(18)-H(18)	0.9500	C(32)-H(32C)	0.9800
C(19)-H(19A)	0.9800	C(33)-H(33A)	0.9800
C(19)-H(19B)	0.9800	C(33)-H(33B)	0.9800
C(19)-H(19C)	0.9800	C(33)-H(33C)	0.9800
C(20)-H(20A)	0.9800	C(34)-H(34A)	0.9800
C(20)-H(20B)	0.9800	C(34)-H(34B)	0.9800
C(20)-H(20C)	0.9800	C(34)-H(34C)	0.9800

C(35)-H(35A)	0.9800	C(37)-H(37C)	0.9800
C(35)-H(35B)	0.9800	C(38)-H(38A)	0.9800
C(35)-H(35C)	0.9800	C(38)-H(38B)	0.9800
C(36)-H(36A)	0.9800	C(38)-H(38C)	0.9800
C(36)-H(36B)	0.9800	C(39)-H(39A)	0.9800
C(36)-H(36C)	0.9800	C(39)-H(39B)	0.9800
C(37)-H(37A)	0.9800	C(39)-H(39C)	0.9800
C(37)-H(37B)	0.9800		

N(1)-Ce(1)-O(1)	105.40(4)	N(1)-Si(2)-Ce(1)	39.49(5)
N(1)-Ce(1)-N(3)	114.43(5)	C(26)-Si(2)-Ce(1)	119.91(8)
O(1)-Ce(1)-N(3)	99.76(4)	C(27)-Si(2)-Ce(1)	132.29(8)
N(1)-Ce(1)-N(2)	107.37(5)	C(25)-Si(2)-Ce(1)	68.04(6)
O(1)-Ce(1)-N(2)	106.59(4)	N(2)-Si(3)-C(28)	108.93(8)
N(3)-Ce(1)-N(2)	121.53(5)	N(2)-Si(3)-C(30)	115.42(8)
N(1)-Ce(1)-Si(2)	27.52(4)	C(28)-Si(3)-C(30)	104.86(9)
O(1)-Ce(1)-Si(2)	130.23(3)	N(2)-Si(3)-C(29)	114.76(8)
N(3)-Ce(1)-Si(2)	95.07(4)	C(28)-Si(3)-C(29)	105.74(9)
N(2)-Ce(1)-Si(2)	105.14(4)	C(30)-Si(3)-C(29)	106.28(9)
N(1)-Ce(1)-Si(3)	132.86(4)	N(2)-Si(3)-Ce(1)	38.99(5)
O(1)-Ce(1)-Si(3)	89.66(3)	C(28)-Si(3)-Ce(1)	69.95(6)
N(3)-Ce(1)-Si(3)	106.21(4)	C(30)-Si(3)-Ce(1)	125.76(6)
N(2)-Ce(1)-Si(3)	26.62(4)	C(29)-Si(3)-Ce(1)	127.48(6)
Si(2)-Ce(1)-Si(3)	130.824(12)	N(2)-Si(4)-C(33)	111.79(10)
O(1)-P(1)-C(13)	113.36(8)	N(2)-Si(4)-C(31)	114.69(8)
O(1)-P(1)-C(7)	110.04(7)	C(33)-Si(4)-C(31)	104.32(11)
C(13)-P(1)-C(7)	108.33(8)	N(2)-Si(4)-C(32)	112.60(9)
O(1)-P(1)-C(1)	111.12(7)	C(33)-Si(4)-C(32)	109.27(15)
C(13)-P(1)-C(1)	105.56(8)	C(31)-Si(4)-C(32)	103.52(11)
C(7)-P(1)-C(1)	108.21(8)	N(3)-Si(5)-C(35)	113.05(9)
N(1)-Si(1)-C(23)	111.66(8)	N(3)-Si(5)-C(34)	109.63(8)
N(1)-Si(1)-C(22)	109.85(8)	C(35)-Si(5)-C(34)	107.27(10)
C(23)-Si(1)-C(22)	108.90(9)	N(3)-Si(5)-C(36)	115.25(9)
N(1)-Si(1)-C(24)	114.57(8)	C(35)-Si(5)-C(36)	105.01(10)
C(23)-Si(1)-C(24)	106.50(9)	C(34)-Si(5)-C(36)	106.10(10)
C(22)-Si(1)-C(24)	105.02(9)	N(3)-Si(6)-C(39)	109.91(8)
N(1)-Si(2)-C(26)	113.07(9)	N(3)-Si(6)-C(37)	112.74(9)
N(1)-Si(2)-C(27)	115.92(9)	C(39)-Si(6)-C(37)	108.33(11)
C(26)-Si(2)-C(27)	107.29(11)	N(3)-Si(6)-C(38)	115.26(9)
N(1)-Si(2)-C(25)	107.22(8)	C(39)-Si(6)-C(38)	104.76(9)
C(26)-Si(2)-C(25)	106.46(10)	C(37)-Si(6)-C(38)	105.31(10)
C(27)-Si(2)-C(25)	106.30(9)	P(1)-O(1)-Ce(1)	174.44(7)

C(4)-O(2)-C(19)	117.17(15)	C(12)-C(11)-C(10)	119.17(17)
C(10)-O(3)-C(20)	117.82(15)	C(12)-C(11)-H(11)	120.4
C(16)-O(4)-C(21)	117.29(16)	C(10)-C(11)-H(11)	120.4
Si(1)-N(1)-Si(2)	124.28(9)	C(11)-C(12)-C(7)	121.29(16)
Si(1)-N(1)-Ce(1)	122.69(7)	C(11)-C(12)-H(12)	119.4
Si(2)-N(1)-Ce(1)	112.98(7)	C(7)-C(12)-H(12)	119.4
Si(3)-N(2)-Si(4)	118.80(8)	C(18)-C(13)-C(14)	118.86(16)
Si(3)-N(2)-Ce(1)	114.39(7)	C(18)-C(13)-P(1)	122.42(14)
Si(4)-N(2)-Ce(1)	126.59(7)	C(14)-C(13)-P(1)	118.70(13)
Si(5)-N(3)-Si(6)	120.41(9)	C(15)-C(14)-C(13)	120.66(17)
Si(5)-N(3)-Ce(1)	117.97(7)	C(15)-C(14)-H(14)	119.7
Si(6)-N(3)-Ce(1)	121.37(8)	C(13)-C(14)-H(14)	119.7
C(2)-C(1)-C(6)	118.62(16)	C(14)-C(15)-C(16)	119.82(18)
C(2)-C(1)-P(1)	119.89(13)	C(14)-C(15)-H(15)	120.1
C(6)-C(1)-P(1)	121.44(13)	C(16)-C(15)-H(15)	120.1
C(1)-C(2)-C(3)	121.17(16)	O(4)-C(16)-C(17)	124.99(17)
C(1)-C(2)-H(2)	119.4	O(4)-C(16)-C(15)	114.79(17)
C(3)-C(2)-H(2)	119.4	C(17)-C(16)-C(15)	120.21(17)
C(4)-C(3)-C(2)	119.33(16)	C(16)-C(17)-C(18)	119.45(18)
C(4)-C(3)-H(3)	120.3	C(16)-C(17)-H(17)	120.3
C(2)-C(3)-H(3)	120.3	C(18)-C(17)-H(17)	120.3
O(2)-C(4)-C(3)	124.77(16)	C(13)-C(18)-C(17)	120.99(17)
O(2)-C(4)-C(5)	115.08(15)	C(13)-C(18)-H(18)	119.5
C(3)-C(4)-C(5)	120.15(16)	C(17)-C(18)-H(18)	119.5
C(6)-C(5)-C(4)	119.93(16)	O(2)-C(19)-H(19A)	109.4
C(6)-C(5)-H(5)	120.0	O(2)-C(19)-H(19B)	109.5
C(4)-C(5)-H(5)	120.0	H(19A)-C(19)-H(19B)	109.5
C(5)-C(6)-C(1)	120.77(16)	O(2)-C(19)-H(19C)	109.5
C(5)-C(6)-H(6)	119.6	H(19A)-C(19)-H(19C)	109.5
C(1)-C(6)-H(6)	119.6	H(19B)-C(19)-H(19C)	109.5
C(12)-C(7)-C(8)	118.54(16)	O(3)-C(20)-H(20A)	109.4
C(12)-C(7)-P(1)	121.56(13)	O(3)-C(20)-H(20B)	109.5
C(8)-C(7)-P(1)	119.89(14)	H(20A)-C(20)-H(20B)	109.5
C(9)-C(8)-C(7)	120.50(17)	O(3)-C(20)-H(20C)	109.5
C(9)-C(8)-H(8)	119.8	H(20A)-C(20)-H(20C)	109.5
C(7)-C(8)-H(8)	119.8	H(20B)-C(20)-H(20C)	109.5
C(8)-C(9)-C(10)	120.47(17)	O(4)-C(21)-H(21A)	109.4
C(8)-C(9)-H(9)	119.8	O(4)-C(21)-H(21B)	109.5
C(10)-C(9)-H(9)	119.8	H(21A)-C(21)-H(21B)	109.5
O(3)-C(10)-C(11)	124.49(17)	O(4)-C(21)-H(21C)	109.5
O(3)-C(10)-C(9)	115.47(16)	H(21A)-C(21)-H(21C)	109.5
C(11)-C(10)-C(9)	120.03(17)	H(21B)-C(21)-H(21C)	109.5

Si(1)-C(22)-H(22A)	109.5	Si(3)-C(29)-H(29A)	109.5
Si(1)-C(22)-H(22B)	109.5	Si(3)-C(29)-H(29B)	109.5
H(22A)-C(22)-H(22B)	109.5	H(29A)-C(29)-H(29B)	109.5
Si(1)-C(22)-H(22C)	109.5	Si(3)-C(29)-H(29C)	109.4
H(22A)-C(22)-H(22C)	109.5	H(29A)-C(29)-H(29C)	109.5
H(22B)-C(22)-H(22C)	109.5	H(29B)-C(29)-H(29C)	109.5
Si(1)-C(23)-H(23A)	109.4	Si(3)-C(30)-H(30A)	109.5
Si(1)-C(23)-H(23B)	109.5	Si(3)-C(30)-H(30B)	109.5
H(23A)-C(23)-H(23B)	109.5	H(30A)-C(30)-H(30B)	109.5
Si(1)-C(23)-H(23C)	109.5	Si(3)-C(30)-H(30C)	109.5
H(23A)-C(23)-H(23C)	109.5	H(30A)-C(30)-H(30C)	109.5
H(23B)-C(23)-H(23C)	109.5	H(30B)-C(30)-H(30C)	109.5
Si(1)-C(24)-H(24A)	109.5	Si(4)-C(31)-H(31A)	109.5
Si(1)-C(24)-H(24B)	109.5	Si(4)-C(31)-H(31B)	109.5
H(24A)-C(24)-H(24B)	109.5	H(31A)-C(31)-H(31B)	109.5
Si(1)-C(24)-H(24C)	109.5	Si(4)-C(31)-H(31C)	109.4
H(24A)-C(24)-H(24C)	109.5	H(31A)-C(31)-H(31C)	109.5
H(24B)-C(24)-H(24C)	109.5	H(31B)-C(31)-H(31C)	109.5
Si(2)-C(25)-H(25A)	109.5	Si(4)-C(32)-H(32A)	109.4
Si(2)-C(25)-H(25B)	109.5	Si(4)-C(32)-H(32B)	109.5
H(25A)-C(25)-H(25B)	109.5	H(32A)-C(32)-H(32B)	109.5
Si(2)-C(25)-H(25C)	109.5	Si(4)-C(32)-H(32C)	109.5
H(25A)-C(25)-H(25C)	109.5	H(32A)-C(32)-H(32C)	109.5
H(25B)-C(25)-H(25C)	109.5	H(32B)-C(32)-H(32C)	109.5
Si(2)-C(26)-H(26A)	109.5	Si(4)-C(33)-H(33A)	109.5
Si(2)-C(26)-H(26B)	109.5	Si(4)-C(33)-H(33B)	109.4
H(26A)-C(26)-H(26B)	109.5	H(33A)-C(33)-H(33B)	109.5
Si(2)-C(26)-H(26C)	109.5	Si(4)-C(33)-H(33C)	109.5
H(26A)-C(26)-H(26C)	109.5	H(33A)-C(33)-H(33C)	109.5
H(26B)-C(26)-H(26C)	109.5	H(33B)-C(33)-H(33C)	109.5
Si(2)-C(27)-H(27A)	109.4	Si(5)-C(34)-H(34A)	109.5
Si(2)-C(27)-H(27B)	109.5	Si(5)-C(34)-H(34B)	109.5
H(27A)-C(27)-H(27B)	109.5	H(34A)-C(34)-H(34B)	109.5
Si(2)-C(27)-H(27C)	109.5	Si(5)-C(34)-H(34C)	109.4
H(27A)-C(27)-H(27C)	109.5	H(34A)-C(34)-H(34C)	109.5
H(27B)-C(27)-H(27C)	109.5	H(34B)-C(34)-H(34C)	109.5
Si(3)-C(28)-H(28A)	109.4	Si(5)-C(35)-H(35A)	109.5
Si(3)-C(28)-H(28B)	109.4	Si(5)-C(35)-H(35B)	109.5
H(28A)-C(28)-H(28B)	109.5	H(35A)-C(35)-H(35B)	109.5
Si(3)-C(28)-H(28C)	109.6	Si(5)-C(35)-H(35C)	109.4
H(28A)-C(28)-H(28C)	109.5	H(35A)-C(35)-H(35C)	109.5
H(28B)-C(28)-H(28C)	109.5	H(35B)-C(35)-H(35C)	109.5

Si(5)-C(36)-H(36A)	109.5	Si(6)-C(38)-H(38A)	109.5
Si(5)-C(36)-H(36B)	109.4	Si(6)-C(38)-H(38B)	109.5
H(36A)-C(36)-H(36B)	109.5	H(38A)-C(38)-H(38B)	109.5
Si(5)-C(36)-H(36C)	109.5	Si(6)-C(38)-H(38C)	109.5
H(36A)-C(36)-H(36C)	109.5	H(38A)-C(38)-H(38C)	109.5
H(36B)-C(36)-H(36C)	109.5	H(38B)-C(38)-H(38C)	109.5
Si(6)-C(37)-H(37A)	109.5	Si(6)-C(39)-H(39A)	109.5
Si(6)-C(37)-H(37B)	109.5	Si(6)-C(39)-H(39B)	109.4
H(37A)-C(37)-H(37B)	109.5	H(39A)-C(39)-H(39B)	109.5
Si(6)-C(37)-H(37C)	109.4	Si(6)-C(39)-H(39C)	109.5
H(37A)-C(37)-H(37C)	109.5	H(39A)-C(39)-H(39C)	109.5
H(37B)-C(37)-H(37C)	109.5	H(39B)-C(39)-H(39C)	109.5

Table 4. Anisotropic displacement parameters ($Å^2 x\ 10^3$ for SBY-3-077. The anisotropic displacement factor exponent takes the form:
$-2\ p^2[\ h^2\ a^{*2}\ U_{11} + ... + 2\ h\ k\ a^*\ b^*\ U_{12}\ ]$

	U_{11}	U_{22}	U_{33}	U_{23}	U_{13}	U_{12}
Ce(1)	13(1)	14(1)	11(1)	0(1)	1(1)	0(1)
P(1)	14(1)	16(1)	13(1)	0(1)	-1(1)	-1(1)
Si(1)	20(1)	20(1)	15(1)	-1(1)	4(1)	-2(1)
Si(2)	18(1)	20(1)	19(1)	-2(1)	2(1)	3(1)
Si(3)	20(1)	19(1)	14(1)	-4(1)	0(1)	1(1)
Si(4)	17(1)	19(1)	24(1)	-3(1)	3(1)	-3(1)
Si(5)	19(1)	23(1)	20(1)	5(1)	0(1)	-5(1)
Si(6)	19(1)	25(1)	15(1)	5(1)	4(1)	1(1)
O(1)	15(1)	20(1)	15(1)	1(1)	-1(1)	0(1)
O(2)	32(1)	18(1)	27(1)	4(1)	-1(1)	-4(1)
O(3)	20(1)	35(1)	27(1)	1(1)	9(1)	4(1)
O(4)	37(1)	40(1)	18(1)	-9(1)	-1(1)	-17(1)
N(1)	17(1)	18(1)	15(1)	-2(1)	2(1)	0(1)
N(2)	18(1)	17(1)	14(1)	-2(1)	1(1)	-1(1)
N(3)	16(1)	21(1)	17(1)	3(1)	2(1)	0(1)
C(1)	15(1)	16(1)	15(1)	1(1)	2(1)	0(1)
C(2)	18(1)	20(1)	16(1)	1(1)	-2(1)	-1(1)
C(3)	18(1)	20(1)	21(1)	-1(1)	0(1)	-3(1)

C(4)	22(1)	16(1)	17(1)	1(1)	6(1)	0(1)
C(5)	24(1)	23(1)	15(1)	3(1)	-2(1)	1(1)
C(6)	19(1)	22(1)	18(1)	0(1)	-2(1)	-2(1)
C(7)	15(1)	19(1)	16(1)	-1(1)	0(1)	-3(1)
C(8)	16(1)	20(1)	22(1)	3(1)	0(1)	0(1)
C(9)	20(1)	25(1)	22(1)	6(1)	3(1)	-1(1)
C(10)	17(1)	21(1)	22(1)	-3(1)	3(1)	-3(1)
C(11)	18(1)	22(1)	26(1)	1(1)	1(1)	4(1)
C(12)	22(1)	21(1)	19(1)	4(1)	-1(1)	0(1)
C(13)	19(1)	17(1)	14(1)	1(1)	-3(1)	-2(1)
C(14)	19(1)	28(1)	21(1)	-3(1)	1(1)	-7(1)
C(15)	26(1)	30(1)	19(1)	-5(1)	4(1)	-7(1)
C(16)	29(1)	21(1)	17(1)	-2(1)	-3(1)	-6(1)
C(17)	24(1)	33(1)	23(1)	-3(1)	0(1)	-14(1)
C(18)	24(1)	27(1)	17(1)	-2(1)	2(1)	-7(1)
C(19)	34(1)	21(1)	35(1)	1(1)	2(1)	-9(1)
C(20)	26(1)	54(2)	38(1)	1(1)	10(1)	15(1)
C(21)	44(1)	59(2)	26(1)	-11(1)	-6(1)	-30(1)
C(22)	23(1)	26(1)	29(1)	5(1)	5(1)	-1(1)
C(23)	33(1)	32(1)	15(1)	-1(1)	1(1)	-8(1)
C(24)	30(1)	28(1)	21(1)	1(1)	9(1)	0(1)
C(25)	23(1)	31(1)	21(1)	4(1)	1(1)	5(1)
C(26)	45(1)	22(1)	41(1)	-9(1)	0(1)	7(1)
C(27)	21(1)	51(1)	35(1)	11(1)	6(1)	8(1)
C(28)	23(1)	25(1)	22(1)	-5(1)	3(1)	3(1)
C(29)	30(1)	21(1)	26(1)	-4(1)	-4(1)	2(1)
C(30)	34(1)	29(1)	17(1)	-6(1)	-1(1)	2(1)
C(31)	25(1)	23(1)	30(1)	-5(1)	0(1)	-5(1)
C(32)	25(1)	40(1)	87(2)	25(1)	-18(1)	-4(1)
C(33)	37(1)	73(2)	63(2)	-48(2)	30(1)	-30(1)
C(34)	35(1)	27(1)	24(1)	2(1)	-4(1)	-10(1)
C(35)	21(1)	45(1)	38(1)	11(1)	-1(1)	-8(1)
C(36)	36(1)	25(1)	32(1)	3(1)	0(1)	-5(1)
C(37)	36(1)	47(1)	26(1)	7(1)	15(1)	12(1)
C(38)	35(1)	32(1)	23(1)	9(1)	2(1)	-2(1)
C(39)	29(1)	33(1)	18(1)	1(1)	0(1)	-3(1)

Table 5. Hydrogen coordinates and isotropic displacement parameters for SBY-3-077.

	x	y	z	U(eq)
H(2)	0.7451	0.4085	0.3175	0.022
H(3)	0.7763	0.5661	0.2895	0.023
H(5)	0.5963	0.5501	0.1620	0.025
H(6)	0.5652	0.3938	0.1906	0.023
H(8)	0.5800	0.1781	0.3900	0.023
H(9)	0.4745	0.1975	0.4550	0.027
H(11)	0.3695	0.4055	0.3525	0.026
H(12)	0.4772	0.3879	0.2882	0.025
H(14)	0.6919	0.2228	0.1752	0.027
H(15)	0.6460	0.1432	0.0915	0.030
H(17)	0.4257	0.0871	0.1651	0.032
H(18)	0.4723	0.1685	0.2491	0.027
H(19A)	0.7451	0.7276	0.2764	0.045
H(19B)	0.7603	0.7880	0.2186	0.045
H(19C)	0.8145	0.6937	0.2327	0.045
H(20A)	0.3031	0.4376	0.4363	0.058
H(20B)	0.2464	0.3667	0.4727	0.058
H(20C)	0.2550	0.3504	0.4045	0.058
H(21A)	0.4217	-0.0250	0.0929	0.065
H(21B)	0.4220	-0.0062	0.0244	0.065
H(21C)	0.3873	0.0746	0.0667	0.065
H(22A)	0.8107	0.2442	0.2417	0.039
H(22B)	0.8599	0.2479	0.1827	0.039
H(22C)	0.9070	0.2729	0.2431	0.039
H(23A)	0.8334	-0.0418	0.1935	0.040
H(23B)	0.8204	0.0447	0.1483	0.040
H(23C)	0.7619	0.0362	0.2027	0.040
H(24A)	1.0386	0.1279	0.2210	0.039
H(24B)	0.9927	0.1136	0.1589	0.039
H(24C)	1.0137	0.0221	0.1990	0.039
H(25A)	0.9488	0.0502	0.4312	0.037
H(25B)	0.9750	-0.0608	0.4363	0.037
H(25C)	0.8796	-0.0322	0.4247	0.037
H(26A)	0.8593	-0.1510	0.3192	0.054
H(26B)	0.9512	-0.1911	0.3323	0.054

H(26C)	0.9263	-0.1483	0.2696	0.054
H(27A)	1.0786	-0.0162	0.2850	0.053
H(27B)	1.0952	-0.0635	0.3476	0.053
H(27C)	1.0878	0.0511	0.3412	0.053
H(28A)	0.6930	0.3382	0.4059	0.035
H(28B)	0.6827	0.3605	0.4734	0.035
H(28C)	0.7096	0.2551	0.4531	0.035
H(29A)	0.8730	0.5253	0.4458	0.038
H(29B)	0.7769	0.5187	0.4259	0.038
H(29C)	0.8471	0.4868	0.3823	0.038
H(30A)	0.8319	0.3106	0.5514	0.040
H(30B)	0.8212	0.4252	0.5482	0.040
H(30C)	0.9104	0.3775	0.5395	0.040
H(31A)	1.0053	0.4609	0.4050	0.039
H(31B)	1.0909	0.4181	0.4313	0.039
H(31C)	1.0145	0.4355	0.4726	0.039
H(32A)	1.0157	0.2292	0.5138	0.076
H(32B)	1.1022	0.2366	0.4819	0.076
H(32C)	1.0399	0.1494	0.4672	0.076
H(33A)	1.0187	0.1959	0.3354	0.085
H(33B)	1.0987	0.2598	0.3521	0.085
H(33C)	1.0207	0.3076	0.3183	0.085
H(34A)	0.6427	0.0291	0.3044	0.043
H(34B)	0.6482	-0.0847	0.2939	0.043
H(34C)	0.7314	-0.0222	0.3018	0.043
H(35A)	0.5606	-0.0672	0.4581	0.052
H(35B)	0.5358	-0.1123	0.3960	0.052
H(35C)	0.5342	0.0020	0.4051	0.052
H(36A)	0.7775	-0.1746	0.4025	0.047
H(36B)	0.6914	-0.2197	0.3788	0.047
H(36C)	0.7052	-0.1967	0.4465	0.047
H(37A)	0.6419	0.1793	0.5199	0.054
H(37B)	0.6480	0.1144	0.5773	0.054
H(37C)	0.5905	0.0808	0.5230	0.054
H(38A)	0.6815	-0.1076	0.5344	0.045
H(38B)	0.7411	-0.0637	0.5848	0.045
H(38C)	0.7802	-0.1128	0.5292	0.045
H(39A)	0.8768	0.0604	0.5303	0.040
H(39B)	0.8243	0.1313	0.5698	0.040
H(39C)	0.8430	0.1605	0.5043	0.040

Table 6. Torsion angles [°] for SBY-3-077.

C(23)-Si(1)-N(1)-Si(2)	85.45(12)	C(13)-P(1)-C(1)-C(2)	-150.48(14)
C(22)-Si(1)-N(1)-Si(2)	-153.62(10)	C(7)-P(1)-C(1)-C(2)	93.71(15)
C(24)-Si(1)-N(1)-Si(2)	-35.71(13)	O(1)-P(1)-C(1)-C(6)	155.52(14)
C(23)-Si(1)-N(1)-Ce(1)	-91.91(10)	C(13)-P(1)-C(1)-C(6)	32.24(17)
C(22)-Si(1)-N(1)-Ce(1)	29.02(11)	C(7)-P(1)-C(1)-C(6)	-83.57(16)
C(24)-Si(1)-N(1)-Ce(1)	146.93(9)	C(6)-C(1)-C(2)-C(3)	1.6(3)
C(26)-Si(2)-N(1)-Si(1)	-67.99(13)	P(1)-C(1)-C(2)-C(3)	-175.72(14)
C(27)-Si(2)-N(1)-Si(1)	56.49(14)	C(1)-C(2)-C(3)-C(4)	-0.3(3)
C(25)-Si(2)-N(1)-Si(1)	174.99(10)	C(19)-O(2)-C(4)-C(3)	-2.0(3)
Ce(1)-Si(2)-N(1)-Si(1)	-177.58(15)	C(19)-O(2)-C(4)-C(5)	177.25(16)
C(26)-Si(2)-N(1)-Ce(1)	109.59(10)	C(2)-C(3)-C(4)-O(2)	177.90(16)
C(27)-Si(2)-N(1)-Ce(1)	-125.93(10)	C(2)-C(3)-C(4)-C(5)	-1.3(3)
C(25)-Si(2)-N(1)-Ce(1)	-7.43(10)	O(2)-C(4)-C(5)-C(6)	-177.72(16)
C(28)-Si(3)-N(2)-Si(4)	-176.37(9)	C(3)-C(4)-C(5)-C(6)	1.6(3)
C(30)-Si(3)-N(2)-Si(4)	-58.78(12)	C(4)-C(5)-C(6)-C(1)	-0.2(3)
C(29)-Si(3)-N(2)-Si(4)	65.34(12)	C(2)-C(1)-C(6)-C(5)	-1.4(3)
Ce(1)-Si(3)-N(2)-Si(4)	-174.97(14)	P(1)-C(1)-C(6)-C(5)	175.93(14)
C(28)-Si(3)-N(2)-Ce(1)	-1.39(10)	O(1)-P(1)-C(7)-C(12)	159.08(14)
C(30)-Si(3)-N(2)-Ce(1)	116.19(9)	C(13)-P(1)-C(7)-C(12)	-76.48(16)
C(29)-Si(3)-N(2)-Ce(1)	-119.69(9)	C(1)-P(1)-C(7)-C(12)	37.50(16)
C(33)-Si(4)-N(2)-Si(3)	-142.49(13)	O(1)-P(1)-C(7)-C(8)	-19.47(16)
C(31)-Si(4)-N(2)-Si(3)	-24.00(13)	C(13)-P(1)-C(7)-C(8)	104.96(15)
C(32)-Si(4)-N(2)-Si(3)	94.04(14)	C(1)-P(1)-C(7)-C(8)	-141.06(14)
C(33)-Si(4)-N(2)-Ce(1)	43.22(15)	C(12)-C(7)-C(8)-C(9)	-0.5(3)
C(31)-Si(4)-N(2)-Ce(1)	161.71(9)	P(1)-C(7)-C(8)-C(9)	178.07(14)
C(32)-Si(4)-N(2)-Ce(1)	-80.25(13)	C(7)-C(8)-C(9)-C(10)	0.5(3)
C(35)-Si(5)-N(3)-Si(6)	55.51(13)	C(20)-O(3)-C(10)-C(11)	6.8(3)
C(34)-Si(5)-N(3)-Si(6)	175.13(10)	C(20)-O(3)-C(10)-C(9)	-173.99(18)
C(36)-Si(5)-N(3)-Si(6)	-65.28(13)	C(8)-C(9)-C(10)-O(3)	-179.00(17)
C(35)-Si(5)-N(3)-Ce(1)	-130.24(9)	C(8)-C(9)-C(10)-C(11)	0.3(3)
C(34)-Si(5)-N(3)-Ce(1)	-10.62(11)	O(3)-C(10)-C(11)-C(12)	178.23(17)
C(36)-Si(5)-N(3)-Ce(1)	108.97(10)	C(9)-C(10)-C(11)-C(12)	-1.0(3)
C(39)-Si(6)-N(3)-Si(5)	152.11(10)	C(10)-C(11)-C(12)-C(7)	0.9(3)
C(37)-Si(6)-N(3)-Si(5)	-86.92(13)	C(8)-C(7)-C(12)-C(11)	-0.2(3)
C(38)-Si(6)-N(3)-Si(5)	34.04(13)	P(1)-C(7)-C(12)-C(11)	-178.76(14)
C(39)-Si(6)-N(3)-Ce(1)	-21.94(12)	O(1)-P(1)-C(13)-C(18)	115.73(15)
C(37)-Si(6)-N(3)-Ce(1)	99.03(11)	C(7)-P(1)-C(13)-C(18)	-6.70(18)
C(38)-Si(6)-N(3)-Ce(1)	-140.01(10)	C(1)-P(1)-C(13)-C(18)	-122.42(16)
O(1)-P(1)-C(1)-C(2)	-27.20(16)	O(1)-P(1)-C(13)-C(14)	-65.96(16)

C(7)-P(1)-C(13)-C(14)	171.60(14)
C(1)-P(1)-C(13)-C(14)	55.89(16)
C(18)-C(13)-C(14)-C(15)	0.1(3)
P(1)-C(13)-C(14)-C(15)	-178.32(15)
C(13)-C(14)-C(15)-C(16)	0.3(3)
C(21)-O(4)-C(16)-C(17)	1.5(3)
C(21)-O(4)-C(16)-C(15)	-179.01(19)
C(14)-C(15)-C(16)-O(4)	179.59(18)
C(14)-C(15)-C(16)-C(17)	-0.9(3)
O(4)-C(16)-C(17)-C(18)	-179.41(19)
C(15)-C(16)-C(17)-C(18)	1.1(3)
C(14)-C(13)-C(18)-C(17)	0.2(3)
P(1)-C(13)-C(18)-C(17)	178.49(15)
C(16)-C(17)-C(18)-C(13)	-0.8(3)

Table 1. Crystal data and structure refinement for SBY-2-005.

Empirical formula	C_{39} H_{75} N_3 O_4 P Si_6 U	
Formula weight	1087.56	
Crystal system	monoclinic	
Space group	$P2_1/c$	
Unit cell dimensions	a = 16.063(2) Å	a= 90°
	b = 13.9300(19) Å	b= 91.895(2)°
	c = 23.043(3) Å	c= 90°
Volume	5153.2(12) $Å^3$	
Z, Z'	4, 1	
Density (calculated)	1.402 Mg/m^3	
Wavelength	0.71073 Å	
Temperature	100(2) K	
F(000)	2212	
Absorption coefficient	3.357 mm^{-1}	
Absorption correction	semi-empirical from equivalents	
Max. and min. transmission	0.4305 and 0.2231	
Theta range for data collection	1.268 to 27.545°	
Reflections collected	98212	
Independent reflections	11873 [R(int) = 0.0588]	
Data / restraints / parameters	11873 / 0 / 487	
$wR(F^2$ all data)	$wR2$ = 0.1136	
R(F obsd data)	$R1$ = 0.0403	
Goodness-of-fit on F^2	1.002	
Observed data [I > 2s(I)]	9681	
Largest and mean shift / s.u.	0.003 and 0.000	
Largest diff. peak and hole	7.285 and -0.810 $e/Å^3$	

$wR2 = \{ S [w(F_o^2 - F_c^2)^2] / S [w(F_o^2)^2] \}^{1/2}$

$R1 = S ||F_o| - |F_c|| / S |F_o|$

Table 2. Atomic coordinates and equivalent isotropic displacement parameters for SBY-2-005. U(eq) is defined as one third of the trace of the orthogonalized U_{ij} tensor.

	x	y	z	U(eq)
U(1)	0.19346(2)	0.84859(2)	0.62826(2)	0.01900(6)
P(1)	0.37628(7)	0.72926(8)	0.71655(5)	0.0188(2)
Si(1)	0.17506(9)	0.63662(10)	0.54778(6)	0.0241(3)
Si(2)	0.01007(9)	0.70732(10)	0.58170(6)	0.0276(3)
Si(3)	0.10719(9)	0.89703(10)	0.76589(6)	0.0237(3)
Si(4)	0.04852(9)	1.01953(10)	0.66386(6)	0.0251(3)
Si(5)	0.32594(9)	1.04760(11)	0.60517(6)	0.0275(3)
Si(6)	0.26608(9)	0.95249(11)	0.49584(6)	0.0267(3)
O(1)	0.3016(3)	0.3333(3)	0.79612(17)	0.0326(8)
O(2)	0.4885(3)	0.9329(3)	0.93100(16)	0.0399(10)
O(3)	0.6469(2)	0.6907(3)	0.54834(17)	0.0343(9)
O(4)	0.3025(2)	0.7773(2)	0.68559(14)	0.0209(7)
N(2)	0.1168(3)	0.7185(3)	0.58419(17)	0.0224(8)
N(3)	0.1076(2)	0.9267(3)	0.69365(17)	0.0211(8)
N(4)	0.2704(2)	0.9577(3)	0.57062(17)	0.0239(8)
C(1)	0.3490(3)	0.6123(3)	0.7422(2)	0.0206(9)
C(2)	0.2856(3)	0.5603(4)	0.7143(2)	0.0243(10)
C(3)	0.2669(3)	0.4669(4)	0.7311(2)	0.0259(10)
C(4)	0.3120(3)	0.4249(3)	0.7769(2)	0.0253(10)
C(5)	0.3743(3)	0.4769(4)	0.8062(2)	0.0265(10)
C(6)	0.3927(3)	0.5695(4)	0.7891(2)	0.0248(10)
C(7)	0.2416(4)	0.2754(4)	0.7653(3)	0.0393(13)
C(8)	0.4135(3)	0.7939(3)	0.77912(19)	0.0210(9)
C(9)	0.3618(3)	0.8021(4)	0.8269(2)	0.0300(11)
C(10)	0.3886(4)	0.8494(4)	0.8767(2)	0.0330(12)
C(11)	0.4683(4)	0.8890(4)	0.8800(2)	0.0302(11)
C(12)	0.5200(4)	0.8824(4)	0.8333(2)	0.0340(12)
C(13)	0.4926(3)	0.8341(4)	0.7830(2)	0.0277(11)
C(14)	0.5702(5)	0.9726(6)	0.9376(3)	0.056(2)
C(15)	0.4603(3)	0.7164(3)	0.6675(2)	0.0207(9)
C(16)	0.4629(3)	0.7745(4)	0.6183(2)	0.0247(10)
C(17)	0.5257(3)	0.7642(4)	0.5796(2)	0.0275(11)

C(18)	0.5886(3)	0.6962(4)	0.5899(2)	0.0260(10)
C(19)	0.5878(3)	0.6389(4)	0.6390(2)	0.0279(11)
C(20)	0.5235(3)	0.6489(4)	0.6775(2)	0.0264(10)
C(21)	0.7168(4)	0.6293(5)	0.5593(3)	0.0485(17)
C(22)	0.2880(3)	0.6714(4)	0.5541(2)	0.0310(11)
C(23)	0.1694(4)	0.5096(4)	0.5773(2)	0.0317(12)
C(24)	0.1510(4)	0.6287(4)	0.4673(2)	0.0349(12)
C(25)	-0.0288(4)	0.5839(4)	0.5666(3)	0.0348(12)
C(26)	-0.0405(4)	0.7802(6)	0.5227(4)	0.065(2)
C(27)	-0.0361(5)	0.7392(7)	0.6519(4)	0.073(3)
C(28)	0.1355(4)	0.7671(4)	0.7758(2)	0.0315(11)
C(29)	0.0035(4)	0.9100(4)	0.8003(2)	0.0333(12)
C(30)	0.1825(4)	0.9722(4)	0.8105(2)	0.0349(12)
C(31)	-0.0664(4)	1.0112(5)	0.6737(3)	0.0435(15)
C(32)	0.0825(5)	1.1407(4)	0.6911(3)	0.0457(16)
C(33)	0.0622(3)	1.0191(4)	0.5831(2)	0.0351(12)
C(34)	0.3298(4)	1.0268(4)	0.6859(2)	0.0378(13)
C(35)	0.4371(3)	1.0550(5)	0.5821(3)	0.0406(14)
C(36)	0.2831(4)	1.1722(4)	0.5944(3)	0.0396(13)
C(37)	0.2641(4)	1.0719(4)	0.4582(2)	0.0391(13)
C(38)	0.3565(4)	0.8861(5)	0.4652(3)	0.0430(15)
C(39)	0.1681(4)	0.8911(5)	0.4698(2)	0.0363(13)

Table 3. Bond lengths [Å] and angles [°] for SBY-2-005.

U(1)-N(3)	2.344(4)	Si(2)-C(25)	1.858(6)
U(1)-O(4)	2.376(3)	Si(2)-C(26)	1.862(7)
U(1)-N(4)	2.390(4)	Si(3)-N(3)	1.715(4)
U(1)-N(2)	2.398(4)	Si(3)-C(29)	1.877(5)
U(1)-Si(4)	3.4481(14)	Si(3)-C(28)	1.878(5)
P(1)-O(4)	1.519(3)	Si(3)-C(30)	1.880(6)
P(1)-C(8)	1.786(5)	Si(4)-N(3)	1.732(4)
P(1)-C(1)	1.793(5)	Si(4)-C(31)	1.871(6)
P(1)-C(15)	1.797(5)	Si(4)-C(32)	1.876(6)
Si(1)-N(2)	1.712(4)	Si(4)-C(33)	1.882(6)
Si(1)-C(22)	1.879(6)	Si(5)-N(4)	1.717(4)
Si(1)-C(24)	1.885(5)	Si(5)-C(36)	1.881(6)
Si(1)-C(23)	1.899(6)	Si(5)-C(34)	1.883(6)
Si(2)-N(2)	1.721(4)	Si(5)-C(35)	1.883(6)
Si(2)-C(27)	1.855(7)	Si(6)-N(4)	1.724(4)

Si(6)-C(39)	1.873(6)	C(19)-C(20)	1.392(7)
Si(6)-C(37)	1.876(6)	C(19)-H(19)	0.9500
Si(6)-C(38)	1.878(6)	C(20)-H(20)	0.9500
O(1)-C(4)	1.364(6)	C(21)-H(21A)	0.9799
O(1)-C(7)	1.427(7)	C(21)-H(21B)	0.9800
O(2)-C(11)	1.354(6)	C(21)-H(21C)	0.9801
O(2)-C(14)	1.428(7)	C(22)-H(22A)	0.9800
O(3)-C(18)	1.364(6)	C(22)-H(22B)	0.9800
O(3)-C(21)	1.426(7)	C(22)-H(22C)	0.9801
C(1)-C(2)	1.391(7)	C(23)-H(23A)	0.9799
C(1)-C(6)	1.401(7)	C(23)-H(23B)	0.9800
C(2)-C(3)	1.393(7)	C(23)-H(23C)	0.9800
C(2)-H(2)	0.9500	C(24)-H(24A)	0.9799
C(3)-C(4)	1.390(7)	C(24)-H(24B)	0.9800
C(3)-H(3)	0.9500	C(24)-H(24C)	0.9800
C(4)-C(5)	1.391(7)	C(25)-H(25A)	0.9800
C(5)-C(6)	1.384(7)	C(25)-H(25B)	0.9800
C(5)-H(5)	0.9500	C(25)-H(25C)	0.9801
C(6)-H(6)	0.9500	C(26)-H(26A)	0.9801
C(7)-H(7A)	0.9800	C(26)-H(26B)	0.9799
C(7)-H(7B)	0.9802	C(26)-H(26C)	0.9799
C(7)-H(7C)	0.9800	C(27)-H(27A)	0.9800
C(8)-C(13)	1.389(7)	C(27)-H(27B)	0.9801
C(8)-C(9)	1.405(7)	C(27)-H(27C)	0.9800
C(9)-C(10)	1.381(7)	C(28)-H(28A)	0.9800
C(9)-H(9)	0.9500	C(28)-H(28B)	0.9800
C(10)-C(11)	1.394(8)	C(28)-H(28C)	0.9800
C(10)-H(10)	0.9500	C(29)-H(29A)	0.9800
C(11)-C(12)	1.383(8)	C(29)-H(29B)	0.9799
C(12)-C(13)	1.399(7)	C(29)-H(29C)	0.9800
C(12)-H(12)	0.9500	C(30)-H(30A)	0.9801
C(13)-H(13)	0.9500	C(30)-H(30B)	0.9798
C(14)-H(14A)	0.9801	C(30)-H(30C)	0.9800
C(14)-H(14B)	0.9799	C(31)-H(31A)	0.9799
C(14)-H(14C)	0.9800	C(31)-H(31B)	0.9799
C(15)-C(16)	1.395(7)	C(31)-H(31C)	0.9802
C(15)-C(20)	1.397(7)	C(32)-H(32A)	0.9802
C(16)-C(17)	1.377(7)	C(32)-H(32B)	0.9800
C(16)-H(16)	0.9500	C(32)-H(32C)	0.9799
C(17)-C(18)	1.400(7)	C(33)-H(33A)	0.9800
C(17)-H(17)	0.9500	C(33)-H(33B)	0.9800
C(18)-C(19)	1.385(7)	C(33)-H(33C)	0.9800

C(34)-H(34A)	0.9800	C(37)-H(37A)	0.9799
C(34)-H(34B)	0.9802	C(37)-H(37B)	0.9801
C(34)-H(34C)	0.9799	C(37)-H(37C)	0.9800
C(35)-H(35A)	0.9800	C(38)-H(38A)	0.9799
C(35)-H(35B)	0.9801	C(38)-H(38B)	0.9801
C(35)-H(35C)	0.9799	C(38)-H(38C)	0.9801
C(36)-H(36A)	0.9800	C(39)-H(39A)	0.9799
C(36)-H(36B)	0.9801	C(39)-H(39B)	0.9801
C(36)-H(36C)	0.9800	C(39)-H(39C)	0.9800

N(3)-U(1)-O(4)	105.97(12)	C(29)-Si(3)-C(30)	106.3(3)
N(3)-U(1)-N(4)	112.84(14)	C(28)-Si(3)-C(30)	108.8(3)
O(4)-U(1)-N(4)	100.94(13)	N(3)-Si(4)-C(31)	115.8(3)
N(3)-U(1)-N(2)	108.55(14)	N(3)-Si(4)-C(32)	112.9(3)
O(4)-U(1)-N(2)	106.16(12)	C(31)-Si(4)-C(32)	107.0(3)
N(4)-U(1)-N(2)	120.88(14)	N(3)-Si(4)-C(33)	108.0(2)
N(3)-U(1)-Si(4)	27.15(10)	C(31)-Si(4)-C(33)	105.5(3)
O(4)-U(1)-Si(4)	130.34(8)	C(32)-Si(4)-C(33)	107.0(3)
N(4)-U(1)-Si(4)	93.35(10)	N(3)-Si(4)-U(1)	38.14(13)
N(2)-U(1)-Si(4)	106.35(10)	C(31)-Si(4)-U(1)	131.5(2)
O(4)-P(1)-C(8)	113.1(2)	C(32)-Si(4)-U(1)	120.7(2)
O(4)-P(1)-C(1)	111.1(2)	C(33)-Si(4)-U(1)	70.17(18)
C(8)-P(1)-C(1)	105.7(2)	N(4)-Si(5)-C(36)	115.4(3)
O(4)-P(1)-C(15)	109.8(2)	N(4)-Si(5)-C(34)	110.2(2)
C(8)-P(1)-C(15)	108.6(2)	C(36)-Si(5)-C(34)	105.9(3)
C(1)-P(1)-C(15)	108.3(2)	N(4)-Si(5)-C(35)	113.1(3)
N(2)-Si(1)-C(22)	109.4(2)	C(36)-Si(5)-C(35)	104.9(3)
N(2)-Si(1)-C(24)	115.0(2)	C(34)-Si(5)-C(35)	106.7(3)
C(22)-Si(1)-C(24)	104.9(3)	N(4)-Si(6)-C(39)	110.2(2)
N(2)-Si(1)-C(23)	114.3(2)	N(4)-Si(6)-C(37)	115.1(2)
C(22)-Si(1)-C(23)	105.6(3)	C(39)-Si(6)-C(37)	104.8(3)
C(24)-Si(1)-C(23)	106.7(2)	N(4)-Si(6)-C(38)	113.0(2)
N(2)-Si(2)-C(27)	112.1(3)	C(39)-Si(6)-C(38)	107.9(3)
N(2)-Si(2)-C(25)	114.7(2)	C(37)-Si(6)-C(38)	105.3(3)
C(27)-Si(2)-C(25)	104.1(3)	C(4)-O(1)-C(7)	117.1(4)
N(2)-Si(2)-C(26)	112.7(3)	C(11)-O(2)-C(14)	117.4(5)
C(27)-Si(2)-C(26)	109.2(5)	C(18)-O(3)-C(21)	117.6(4)
C(25)-Si(2)-C(26)	103.4(3)	P(1)-O(4)-U(1)	174.2(2)
N(3)-Si(3)-C(29)	114.7(2)	Si(1)-N(2)-Si(2)	118.9(2)
N(3)-Si(3)-C(28)	109.9(2)	Si(1)-N(2)-U(1)	115.4(2)
C(29)-Si(3)-C(28)	104.9(3)	Si(2)-N(2)-U(1)	125.4(2)
N(3)-Si(3)-C(30)	111.9(2)	Si(3)-N(3)-Si(4)	123.0(2)

Si(3)-N(3)-U(1)	122.2(2)	C(11)-C(12)-H(12)	120.1
Si(4)-N(3)-U(1)	114.71(19)	C(13)-C(12)-H(12)	120.1
Si(5)-N(4)-Si(6)	119.8(2)	C(8)-C(13)-C(12)	120.6(5)
Si(5)-N(4)-U(1)	118.4(2)	C(8)-C(13)-H(13)	119.7
Si(6)-N(4)-U(1)	121.6(2)	C(12)-C(13)-H(13)	119.7
C(2)-C(1)-C(6)	118.4(4)	O(2)-C(14)-H(14A)	109.6
C(2)-C(1)-P(1)	120.2(4)	O(2)-C(14)-H(14B)	109.4
C(6)-C(1)-P(1)	121.3(4)	H(14A)-C(14)-H(14B)	109.5
C(1)-C(2)-C(3)	121.3(5)	O(2)-C(14)-H(14C)	109.5
C(1)-C(2)-H(2)	119.3	H(14A)-C(14)-H(14C)	109.5
C(3)-C(2)-H(2)	119.3	H(14B)-C(14)-H(14C)	109.5
C(4)-C(3)-C(2)	119.5(5)	C(16)-C(15)-C(20)	118.9(4)
C(4)-C(3)-H(3)	120.3	C(16)-C(15)-P(1)	119.8(4)
C(2)-C(3)-H(3)	120.3	C(20)-C(15)-P(1)	121.3(4)
O(1)-C(4)-C(3)	125.0(5)	C(17)-C(16)-C(15)	120.6(5)
O(1)-C(4)-C(5)	115.1(4)	C(17)-C(16)-H(16)	119.7
C(3)-C(4)-C(5)	119.9(5)	C(15)-C(16)-H(16)	119.7
C(6)-C(5)-C(4)	120.3(5)	C(16)-C(17)-C(18)	120.0(5)
C(6)-C(5)-H(5)	119.9	C(16)-C(17)-H(17)	120.0
C(4)-C(5)-H(5)	119.9	C(18)-C(17)-H(17)	120.0
C(5)-C(6)-C(1)	120.7(5)	O(3)-C(18)-C(19)	124.5(5)
C(5)-C(6)-H(6)	119.7	O(3)-C(18)-C(17)	115.3(4)
C(1)-C(6)-H(6)	119.7	C(19)-C(18)-C(17)	120.2(5)
O(1)-C(7)-H(7A)	109.4	C(18)-C(19)-C(20)	119.4(5)
O(1)-C(7)-H(7B)	109.6	C(18)-C(19)-H(19)	120.3
H(7A)-C(7)-H(7B)	109.5	C(20)-C(19)-H(19)	120.3
O(1)-C(7)-H(7C)	109.4	C(19)-C(20)-C(15)	120.9(5)
H(7A)-C(7)-H(7C)	109.5	C(19)-C(20)-H(20)	119.6
H(7B)-C(7)-H(7C)	109.5	C(15)-C(20)-H(20)	119.6
C(13)-C(8)-C(9)	118.7(4)	O(3)-C(21)-H(21A)	109.5
C(13)-C(8)-P(1)	122.4(4)	O(3)-C(21)-H(21B)	109.6
C(9)-C(8)-P(1)	118.9(4)	H(21A)-C(21)-H(21B)	109.5
C(10)-C(9)-C(8)	121.0(5)	O(3)-C(21)-H(21C)	109.3
C(10)-C(9)-H(9)	119.5	H(21A)-C(21)-H(21C)	109.5
C(8)-C(9)-H(9)	119.5	H(21B)-C(21)-H(21C)	109.5
C(9)-C(10)-C(11)	119.6(5)	Si(1)-C(22)-H(22A)	109.6
C(9)-C(10)-H(10)	120.2	Si(1)-C(22)-H(22B)	109.4
C(11)-C(10)-H(10)	120.2	H(22A)-C(22)-H(22B)	109.5
O(2)-C(11)-C(12)	124.9(5)	Si(1)-C(22)-H(22C)	109.4
O(2)-C(11)-C(10)	114.7(5)	H(22A)-C(22)-H(22C)	109.5
C(12)-C(11)-C(10)	120.4(5)	H(22B)-C(22)-H(22C)	109.5
C(11)-C(12)-C(13)	119.7(5)	Si(1)-C(23)-H(23A)	109.5

Si(1)-C(23)-H(23B)	109.5	Si(3)-C(30)-H(30B)	109.4
H(23A)-C(23)-H(23B)	109.5	H(30A)-C(30)-H(30B)	109.5
Si(1)-C(23)-H(23C)	109.4	Si(3)-C(30)-H(30C)	109.5
H(23A)-C(23)-H(23C)	109.5	H(30A)-C(30)-H(30C)	109.5
H(23B)-C(23)-H(23C)	109.5	H(30B)-C(30)-H(30C)	109.5
Si(1)-C(24)-H(24A)	109.5	Si(4)-C(31)-H(31A)	109.4
Si(1)-C(24)-H(24B)	109.5	Si(4)-C(31)-H(31B)	109.5
H(24A)-C(24)-H(24B)	109.5	H(31A)-C(31)-H(31B)	109.5
Si(1)-C(24)-H(24C)	109.5	Si(4)-C(31)-H(31C)	109.5
H(24A)-C(24)-H(24C)	109.5	H(31A)-C(31)-H(31C)	109.5
H(24B)-C(24)-H(24C)	109.5	H(31B)-C(31)-H(31C)	109.5
Si(2)-C(25)-H(25A)	109.4	Si(4)-C(32)-H(32A)	109.5
Si(2)-C(25)-H(25B)	109.5	Si(4)-C(32)-H(32B)	109.5
H(25A)-C(25)-H(25B)	109.5	H(32A)-C(32)-H(32B)	109.5
Si(2)-C(25)-H(25C)	109.5	Si(4)-C(32)-H(32C)	109.5
H(25A)-C(25)-H(25C)	109.5	H(32A)-C(32)-H(32C)	109.5
H(25B)-C(25)-H(25C)	109.5	H(32B)-C(32)-H(32C)	109.5
Si(2)-C(26)-H(26A)	109.4	Si(4)-C(33)-H(33A)	109.5
Si(2)-C(26)-H(26B)	109.5	Si(4)-C(33)-H(33B)	109.5
H(26A)-C(26)-H(26B)	109.5	H(33A)-C(33)-H(33B)	109.5
Si(2)-C(26)-H(26C)	109.5	Si(4)-C(33)-H(33C)	109.5
H(26A)-C(26)-H(26C)	109.5	H(33A)-C(33)-H(33C)	109.5
H(26B)-C(26)-H(26C)	109.5	H(33B)-C(33)-H(33C)	109.5
Si(2)-C(27)-H(27A)	109.7	Si(5)-C(34)-H(34A)	109.4
Si(2)-C(27)-H(27B)	109.4	Si(5)-C(34)-H(34B)	109.5
H(27A)-C(27)-H(27B)	109.5	H(34A)-C(34)-H(34B)	109.5
Si(2)-C(27)-H(27C)	109.3	Si(5)-C(34)-H(34C)	109.5
H(27A)-C(27)-H(27C)	109.5	H(34A)-C(34)-H(34C)	109.5
H(27B)-C(27)-H(27C)	109.5	H(34B)-C(34)-H(34C)	109.5
Si(3)-C(28)-H(28A)	109.4	Si(5)-C(35)-H(35A)	109.6
Si(3)-C(28)-H(28B)	109.5	Si(5)-C(35)-H(35B)	109.4
H(28A)-C(28)-H(28B)	109.5	H(35A)-C(35)-H(35B)	109.5
Si(3)-C(28)-H(28C)	109.5	Si(5)-C(35)-H(35C)	109.5
H(28A)-C(28)-H(28C)	109.5	H(35A)-C(35)-H(35C)	109.5
H(28B)-C(28)-H(28C)	109.5	H(35B)-C(35)-H(35C)	109.5
Si(3)-C(29)-H(29A)	109.5	Si(5)-C(36)-H(36A)	109.5
Si(3)-C(29)-H(29B)	109.5	Si(5)-C(36)-H(36B)	109.5
H(29A)-C(29)-H(29B)	109.5	H(36A)-C(36)-H(36B)	109.5
Si(3)-C(29)-H(29C)	109.4	Si(5)-C(36)-H(36C)	109.4
H(29A)-C(29)-H(29C)	109.5	H(36A)-C(36)-H(36C)	109.5
H(29B)-C(29)-H(29C)	109.5	H(36B)-C(36)-H(36C)	109.5
Si(3)-C(30)-H(30A)	109.5	Si(6)-C(37)-H(37A)	109.4

Si(6)-C(37)-H(37B)	109.5
H(37A)-C(37)-H(37B)	109.5
Si(6)-C(37)-H(37C)	109.5
H(37A)-C(37)-H(37C)	109.5
H(37B)-C(37)-H(37C)	109.5
Si(6)-C(38)-H(38A)	109.4
Si(6)-C(38)-H(38B)	109.5
H(38A)-C(38)-H(38B)	109.5
Si(6)-C(38)-H(38C)	109.5
H(38A)-C(38)-H(38C)	109.5
H(38B)-C(38)-H(38C)	109.5
Si(6)-C(39)-H(39A)	109.5
Si(6)-C(39)-H(39B)	109.4
H(39A)-C(39)-H(39B)	109.5
Si(6)-C(39)-H(39C)	109.5
H(39A)-C(39)-H(39C)	109.5
H(39B)-C(39)-H(39C)	109.5

Table 4. Anisotropic displacement parameters ($Å^2 x\ 10^3$) for SBY-2-005. The anisotropic displacement factor exponent takes the form:
$-2\ p^2[\ h^2\ a^{*2}\ U_{11} + ... + 2\ h\ k\ a^*\ b^*\ U_{12}]$

	U_{11}	U_{22}	U_{33}	U_{23}	U_{13}	U_{12}
U(1)	21(1)	21(1)	15(1)	0(1)	2(1)	1(1)
P(1)	20(1)	21(1)	16(1)	0(1)	-2(1)	-2(1)
Si(1)	27(1)	27(1)	18(1)	-4(1)	-1(1)	2(1)
Si(2)	25(1)	27(1)	31(1)	-2(1)	4(1)	-2(1)
Si(3)	28(1)	27(1)	17(1)	0(1)	5(1)	-3(1)
Si(4)	24(1)	26(1)	26(1)	-1(1)	4(1)	4(1)
Si(5)	27(1)	31(1)	24(1)	6(1)	0(1)	-5(1)
Si(6)	28(1)	35(1)	18(1)	5(1)	4(1)	0(1)
O(1)	40(2)	24(2)	34(2)	4(2)	0(2)	-5(2)
O(2)	48(2)	50(2)	22(2)	-9(2)	-2(2)	-21(2)
O(3)	27(2)	42(2)	35(2)	1(2)	9(2)	8(2)
O(4)	19(2)	24(2)	19(2)	-1(1)	-2(1)	1(1)
N(2)	26(2)	24(2)	17(2)	1(2)	1(2)	-1(2)
N(3)	24(2)	21(2)	18(2)	-2(2)	3(2)	-1(2)
N(4)	23(2)	31(2)	18(2)	5(2)	3(2)	1(2)
C(1)	21(2)	23(2)	18(2)	-2(2)	1(2)	-2(2)
C(2)	26(2)	28(2)	19(2)	2(2)	0(2)	-2(2)
C(3)	25(2)	27(2)	26(2)	-1(2)	0(2)	-6(2)
C(4)	30(3)	23(2)	23(2)	0(2)	6(2)	1(2)
C(5)	31(3)	28(3)	20(2)	4(2)	-2(2)	0(2)
C(6)	27(2)	26(2)	21(2)	-1(2)	-4(2)	-1(2)
C(7)	42(3)	28(3)	47(4)	3(3)	6(3)	-9(2)
C(8)	25(2)	23(2)	15(2)	1(2)	-3(2)	-5(2)
C(9)	26(3)	38(3)	25(3)	-7(2)	0(2)	-8(2)
C(10)	33(3)	42(3)	24(3)	-10(2)	3(2)	-13(2)
C(11)	42(3)	28(3)	21(2)	-1(2)	-7(2)	-10(2)
C(12)	34(3)	44(3)	24(3)	-4(2)	-1(2)	-18(2)
C(13)	31(3)	32(3)	20(2)	-1(2)	-1(2)	-11(2)
C(14)	63(4)	72(5)	31(3)	-11(3)	-7(3)	-40(4)
C(15)	23(2)	21(2)	19(2)	-1(2)	0(2)	-2(2)
C(16)	24(2)	26(2)	23(2)	3(2)	1(2)	3(2)

C(17)	27(3)	32(3)	24(2)	7(2)	3(2)	1(2)
C(18)	24(2)	28(3)	25(2)	-3(2)	4(2)	-2(2)
C(19)	25(2)	30(3)	29(3)	2(2)	4(2)	8(2)
C(20)	26(2)	30(3)	23(2)	6(2)	-2(2)	1(2)
C(21)	34(3)	69(5)	43(4)	2(3)	13(3)	19(3)
C(22)	31(3)	34(3)	28(3)	-4(2)	2(2)	3(2)
C(23)	37(3)	29(3)	29(3)	-6(2)	-5(2)	2(2)
C(24)	44(3)	38(3)	23(3)	-7(2)	2(2)	0(3)
C(25)	33(3)	34(3)	37(3)	-8(2)	0(2)	-3(2)
C(26)	29(3)	58(4)	106(7)	36(4)	-17(4)	-2(3)
C(27)	42(4)	98(6)	81(6)	-56(5)	34(4)	-34(4)
C(28)	35(3)	31(3)	29(3)	6(2)	7(2)	-1(2)
C(29)	39(3)	36(3)	25(3)	1(2)	13(2)	0(2)
C(30)	46(3)	40(3)	19(2)	0(2)	0(2)	-9(3)
C(31)	31(3)	58(4)	43(3)	13(3)	9(3)	10(3)
C(32)	53(4)	27(3)	56(4)	-9(3)	4(3)	6(3)
C(33)	29(3)	46(3)	31(3)	7(2)	3(2)	6(2)
C(34)	50(4)	35(3)	28(3)	3(2)	-5(2)	-12(3)
C(35)	28(3)	52(4)	42(3)	13(3)	-2(2)	-10(3)
C(36)	42(3)	35(3)	42(3)	4(3)	2(3)	-2(3)
C(37)	45(3)	46(3)	25(3)	13(2)	3(2)	1(3)
C(38)	41(3)	57(4)	31(3)	9(3)	11(3)	10(3)
C(39)	40(3)	47(3)	21(3)	5(2)	-2(2)	-2(3)

Table 5. Hydrogen coordinates and isotropic displacement parameters for SBY-2-005.

	x	y	z	U(eq)
H(2)	0.254386	0.589032	0.683164	0.029
H(3)	0.223594	0.432184	0.711386	0.031
H(5)	0.404437	0.448650	0.837987	0.032
H(6)	0.435245	0.604519	0.809399	0.030
H(7A)	0.186827	0.306097	0.766431	0.059
H(7B)	0.239097	0.211847	0.783471	0.059
H(7C)	0.257787	0.268517	0.724901	0.059
H(9)	0.307637	0.774653	0.824858	0.036
H(10)	0.352975	0.854853	0.908655	0.040

H(12)	0.573898	0.910502	0.835448	0.041
H(13)	0.528378	0.828836	0.751154	0.033
H(14A)	0.611675	0.922319	0.931764	0.083
H(14B)	0.577755	0.999309	0.976793	0.083
H(14C)	0.577055	1.023689	0.908912	0.083
H(16)	0.420850	0.821511	0.611426	0.030
H(17)	0.526348	0.803286	0.545785	0.033
H(19)	0.630820	0.593244	0.646350	0.033
H(20)	0.522428	0.609236	0.711037	0.032
H(21A)	0.746245	0.649344	0.595212	0.073
H(21B)	0.754585	0.633294	0.526882	0.073
H(21C)	0.697375	0.563034	0.563392	0.073
H(22A)	0.293651	0.740474	0.547324	0.047
H(22B)	0.319271	0.635974	0.525234	0.047
H(22C)	0.310061	0.655684	0.593144	0.047
H(23A)	0.153196	0.511575	0.617888	0.048
H(23B)	0.224096	0.478855	0.574898	0.048
H(23C)	0.128116	0.472855	0.554298	0.048
H(24A)	0.091637	0.615085	0.460603	0.052
H(24B)	0.184107	0.577175	0.450613	0.052
H(24C)	0.164837	0.689865	0.448913	0.052
H(25A)	-0.010372	0.563058	0.528424	0.052
H(25B)	-0.089762	0.583488	0.566734	0.052
H(25C)	-0.006622	0.539948	0.596494	0.052
H(26A)	-0.032931	0.848585	0.531373	0.097
H(26B)	-0.100111	0.765303	0.519923	0.097
H(26C)	-0.015061	0.765173	0.485673	0.097
H(27A)	-0.011198	0.699499	0.682980	0.110
H(27B)	-0.096348	0.728139	0.649330	0.110
H(27C)	-0.025208	0.807099	0.660370	0.110
H(28A)	0.091486	0.726850	0.758133	0.047
H(28B)	0.141586	0.752520	0.817282	0.047
H(28C)	0.188206	0.754110	0.756982	0.047
H(29A)	-0.012694	0.977837	0.800514	0.050
H(29B)	0.007346	0.885917	0.840224	0.050
H(29C)	-0.038414	0.872947	0.777974	0.050
H(30A)	0.238844	0.963768	0.796178	0.052
H(30B)	0.181424	0.952038	0.851178	0.052
H(30C)	0.166493	1.039908	0.807318	0.052
H(31A)	-0.086821	0.949224	0.658908	0.065
H(31B)	-0.094581	1.063264	0.652278	0.065
H(31C)	-0.078081	1.016554	0.715058	0.065

H(32A)	0.075639	1.144078	0.733170	0.068
H(32B)	0.048389	1.190448	0.671900	0.068
H(32C)	0.141169	1.150858	0.682510	0.068
H(33A)	0.119226	1.038341	0.574714	0.053
H(33B)	0.022786	1.064281	0.564574	0.053
H(33C)	0.051616	0.954391	0.567824	0.053
H(34A)	0.273689	1.012348	0.698891	0.057
H(34B)	0.350879	1.084558	0.705771	0.057
H(34C)	0.366839	0.972598	0.695211	0.057
H(35A)	0.466944	0.996503	0.593963	0.061
H(35B)	0.464144	1.110824	0.600513	0.061
H(35C)	0.438154	1.061773	0.539783	0.061
H(36A)	0.285353	1.189870	0.553269	0.059
H(36B)	0.316473	1.217730	0.617779	0.059
H(36C)	0.225223	1.174060	0.606449	0.059
H(37A)	0.217621	1.110182	0.472096	0.059
H(37B)	0.257021	1.062192	0.416186	0.059
H(37C)	0.316601	1.105712	0.466636	0.059
H(38A)	0.408646	0.916066	0.479030	0.065
H(38B)	0.352656	0.888606	0.422730	0.065
H(38C)	0.355266	0.819046	0.478040	0.065
H(39A)	0.156456	0.836959	0.495424	0.054
H(39B)	0.174916	0.867529	0.430154	0.054
H(39C)	0.121596	0.936659	0.470114	0.054

Table 6. Torsion angles [°] for SBY-2-005

C(22)-Si(1)-N(2)-Si(2)	176.3(3)
C(24)-Si(1)-N(2)-Si(2)	58.5(3)
C(23)-Si(1)-N(2)-Si(2)	-65.5(3)
C(22)-Si(1)-N(2)-U(1)	1.3(3)
C(24)-Si(1)-N(2)-U(1)	-116.5(3)
C(23)-Si(1)-N(2)-U(1)	119.5(2)
C(27)-Si(2)-N(2)-Si(1)	142.7(4)
C(25)-Si(2)-N(2)-Si(1)	24.3(4)
C(26)-Si(2)-N(2)-Si(1)	-93.6(4)
C(27)-Si(2)-N(2)-U(1)	-42.9(4)
C(25)-Si(2)-N(2)-U(1)	-161.3(3)
C(26)-Si(2)-N(2)-U(1)	80.8(4)
C(29)-Si(3)-N(3)-Si(4)	36.2(4)

C(28)-Si(3)-N(3)-Si(4)	154.1(3)
C(30)-Si(3)-N(3)-Si(4)	-84.9(3)
C(29)-Si(3)-N(3)-U(1)	-146.7(3)
C(28)-Si(3)-N(3)-U(1)	-28.9(3)
C(30)-Si(3)-N(3)-U(1)	92.1(3)
C(31)-Si(4)-N(3)-Si(3)	-57.6(4)
C(32)-Si(4)-N(3)-Si(3)	66.3(4)
C(33)-Si(4)-N(3)-Si(3)	-175.6(3)
U(1)-Si(4)-N(3)-Si(3)	177.2(4)
C(31)-Si(4)-N(3)-U(1)	125.2(3)
C(32)-Si(4)-N(3)-U(1)	-110.9(3)
C(33)-Si(4)-N(3)-U(1)	7.2(3)
C(36)-Si(5)-N(4)-Si(6)	66.8(4)
C(34)-Si(5)-N(4)-Si(6)	-173.4(3)
C(35)-Si(5)-N(4)-Si(6)	-54.1(4)
C(36)-Si(5)-N(4)-U(1)	-109.3(3)
C(34)-Si(5)-N(4)-U(1)	10.5(3)
C(35)-Si(5)-N(4)-U(1)	129.8(3)
C(39)-Si(6)-N(4)-Si(5)	-153.4(3)
C(37)-Si(6)-N(4)-Si(5)	-35.2(4)
C(38)-Si(6)-N(4)-Si(5)	85.9(4)
C(39)-Si(6)-N(4)-U(1)	22.6(3)
C(37)-Si(6)-N(4)-U(1)	140.8(3)
C(38)-Si(6)-N(4)-U(1)	-98.2(3)
O(4)-P(1)-C(1)-C(2)	27.0(5)
C(8)-P(1)-C(1)-C(2)	150.0(4)
C(15)-P(1)-C(1)-C(2)	-93.7(4)
O(4)-P(1)-C(1)-C(6)	-155.5(4)
C(8)-P(1)-C(1)-C(6)	-32.4(5)
C(15)-P(1)-C(1)-C(6)	83.8(4)
C(6)-C(1)-C(2)-C(3)	-1.8(7)
P(1)-C(1)-C(2)-C(3)	175.8(4)
C(1)-C(2)-C(3)-C(4)	0.5(7)
C(7)-O(1)-C(4)-C(3)	2.2(7)
C(7)-O(1)-C(4)-C(5)	-176.5(5)
C(2)-C(3)-C(4)-O(1)	-177.6(5)
C(2)-C(3)-C(4)-C(5)	1.1(7)
O(1)-C(4)-C(5)-C(6)	177.6(5)
C(3)-C(4)-C(5)-C(6)	-1.2(8)
C(4)-C(5)-C(6)-C(1)	-0.1(8)
C(2)-C(1)-C(6)-C(5)	1.6(7)
P(1)-C(1)-C(6)-C(5)	-176.0(4)

O(4)-P(1)-C(8)-C(13)	-116.0(4)
C(1)-P(1)-C(8)-C(13)	122.2(4)
C(15)-P(1)-C(8)-C(13)	6.2(5)
O(4)-P(1)-C(8)-C(9)	65.9(5)
C(1)-P(1)-C(8)-C(9)	-55.9(5)
C(15)-P(1)-C(8)-C(9)	-171.9(4)
C(13)-C(8)-C(9)-C(10)	0.2(8)
P(1)-C(8)-C(9)-C(10)	178.4(4)
C(8)-C(9)-C(10)-C(11)	-0.5(9)
C(14)-O(2)-C(11)-C(12)	-2.1(9)
C(14)-O(2)-C(11)-C(10)	178.3(6)
C(9)-C(10)-C(11)-O(2)	-179.4(5)
C(9)-C(10)-C(11)-C(12)	1.0(9)
O(2)-C(11)-C(12)-C(13)	179.3(5)
C(10)-C(11)-C(12)-C(13)	-1.1(9)
C(9)-C(8)-C(13)-C(12)	-0.4(8)
P(1)-C(8)-C(13)-C(12)	-178.6(4)
C(11)-C(12)-C(13)-C(8)	0.9(9)
O(4)-P(1)-C(15)-C(16)	20.9(5)
C(8)-P(1)-C(15)-C(16)	-103.2(4)
C(1)-P(1)-C(15)-C(16)	142.5(4)
O(4)-P(1)-C(15)-C(20)	-158.8(4)
C(8)-P(1)-C(15)-C(20)	77.1(4)
C(1)-P(1)-C(15)-C(20)	-37.2(5)
C(20)-C(15)-C(16)-C(17)	1.2(7)
P(1)-C(15)-C(16)-C(17)	-178.5(4)
C(15)-C(16)-C(17)-C(18)	-1.1(8)
C(21)-O(3)-C(18)-C(19)	-7.2(8)
C(21)-O(3)-C(18)-C(17)	174.1(5)
C(16)-C(17)-C(18)-O(3)	178.9(5)
C(16)-C(17)-C(18)-C(19)	0.1(8)
O(3)-C(18)-C(19)-C(20)	-177.9(5)
C(17)-C(18)-C(19)-C(20)	0.7(8)
C(18)-C(19)-C(20)-C(15)	-0.6(8)
C(16)-C(15)-C(20)-C(19)	-0.3(7)
P(1)-C(15)-C(20)-C(19)	179.4(4)

Table 1. Crystal data and structure refinement for SBY-3-043.

Empirical formula	$(C_{42}\ H_{42}\ Cl_4\ O_4\ P_2\ U) \cdot 4(C_6\ D_6)$	
	$C_{66}\ H_{42}\ Cl_4\ D_{24}\ O_8\ P_2\ U$	
Formula weight	1453.10	
Crystal system	monoclinic	
Space group	*P*2/*c*	
Unit cell dimensions	*a* = 12.7103(16) Å	a= 90°
	b = 10.3892(13) Å	b= 104.719(2)°
	c = 24.619(3) Å	c= 90°
Volume	3144.3(7) Å3	
Z, Z'	2, 0.5	
Density (calculated)	1.535 Mg/m3	
Wavelength	0.71073 Å	
Temperature	100(2) K	
F(000)	1432	
Absorption coefficient	2.856 mm-1	
Absorption correction	semi-empirical from equivalents	
Max. and min. transmission	0.4305 and 0.3455	
Theta range for data collection	1.657 to 27.549°	
Reflections collected	29583	
Independent reflections	7241 [R(int) = 0.0422]	
Data / restraints / parameters	7241 / 106 / 370	
wR(*F*2 all data)	*wR*2 = 0.0755	
R(*F* obsd data)	*R*1 = 0.0307	
Goodness-of-fit on *F*2	1.004	

Observed data [I > 2s(I)] 6353

Largest and mean shift / s.u. 0.002 and 0.000

Largest diff. peak and hole 1.302 and -0.611 e/Å3

$wR2 = \{ S [w(Fo2 - Fc2)2] / S [w(Fo 2)2] \}1/2$

$R1 = S ||Fo| - |Fc|| / S |Fo|$

Table 2. Atomic coordinates and equivalent isotropic displacement parameters for SBY-3-043. U(eq) is defined as one third of the trace of the orthogonalized Uij tensor.

	x	y	z	U(eq)
U(1)	1.000000	0.95835(2)	0.250000	0.01802(6)
Cl(1)	0.91764(7)	1.13278(8)	0.30368(4)	0.03225(19)
Cl(2)	0.82367(7)	0.94388(8)	0.16723(4)	0.02924(18)
P(1)	0.86538(6)	0.68280(7)	0.30374(3)	0.01786(16)
O(1)	0.92839(16)	0.80059(19)	0.29264(9)	0.0202(4)
O(2)	0.70325(19)	0.3646(2)	0.10027(10)	0.0277(5)
O(3)	1.13581(19)	0.3852(2)	0.49416(10)	0.0291(5)
C(1)	0.8207(2)	0.5819(3)	0.24354(14)	0.0192(6)
C(2)	0.7404(2)	0.6292(3)	0.19780(13)	0.0215(6)
C(3)	0.7036(3)	0.5549(3)	0.15075(14)	0.0230(7)
C(4)	0.7458(2)	0.4300(3)	0.14859(14)	0.0210(6)
O(4)	0.47242(18)	0.8378(2)	0.37609(11)	0.0304(5)
C(5)	0.8254(2)	0.3823(3)	0.19355(14)	0.0230(7)

C(6)	0.8624(2)	0.4585(3)	0.24063(14)	0.0216(6)
C(7)	0.9491(2)	0.5925(3)	0.36009(13)	0.0190(6)
C(8)	1.0515(2)	0.6374(3)	0.38715(13)	0.0198(6)
C(9)	1.1165(3)	0.5707(3)	0.43244(14)	0.0226(7)
C(10)	1.0781(3)	0.4579(3)	0.45062(14)	0.0240(6)
C(11)	0.9748(3)	0.4124(3)	0.42405(14)	0.0261(7)
C(12)	0.9105(3)	0.4785(3)	0.37921(14)	0.0242(7)
C(13)	0.7456(2)	0.7337(3)	0.32326(13)	0.0198(6)
C(14)	0.7423(3)	0.8550(3)	0.34692(14)	0.0245(7)
C(15)	0.6526(3)	0.8924(3)	0.36509(15)	0.0274(7)
C(16)	0.5646(2)	0.8098(3)	0.35939(14)	0.0230(7)
C(17)	0.5671(3)	0.6881(3)	0.33571(14)	0.0253(7)
C(18)	0.6572(3)	0.6511(3)	0.31788(14)	0.0238(7)
C(19)	0.7369(3)	0.2335(3)	0.09838(17)	0.0352(8)
C(20)	1.2409(3)	0.4296(3)	0.52396(15)	0.0308(8)
C(21)	0.4665(3)	0.9642(4)	0.39951(18)	0.0359(8)
C(1A)	0.3830(2)	0.2425(3)	-0.00100(15)	0.0456(10)
D(1A)	0.408474	0.245791	-0.034073	0.055
C(2A)	0.4402(3)	0.3035(3)	0.04697(17)	0.0598(14)
D(2A)	0.505106	0.348834	0.047048	0.072
C(3A)	0.4034(3)	0.2989(3)	0.09484(16)	0.0610(14)
D(3A)	0.442876	0.340980	0.128050	0.073
C(4A)	0.3094(3)	0.2335(3)	0.09450(14)	0.0530(12)
D(4A)	0.283761	0.230454	0.127503	0.064
C(5A)	0.2525(3)	0.1724(3)	0.04660(13)	0.0390(9)
D(5A)	0.187500	0.127070	0.046521	0.047

C(6A)	0.2892(2)	0.1767(3)	-0.00117(13)	0.0379(9)
D(6A)	0.249857	0.134352	-0.034312	0.045
C(1B)	0.500000	1.3476(6)	0.250000	0.064(2)
D(1B)	0.500000	1.439070	0.250000	0.077
C(2B)	0.5910(3)	1.2812(4)	0.24734(13)	0.0618(14)
D(2B)	0.654711	1.326883	0.245480	0.074
C(3B)	0.5917(3)	1.1493(4)	0.24730(13)	0.081(2)
D(3B)	0.655624	1.104187	0.245409	0.097
C(4B)	0.500000	1.0824(6)	0.250000	0.079(2)
D(4B)	0.500000	0.990923	0.250000	0.095
C(1C)	1.0407(2)	0.1147(3)	0.52522(15)	0.0334(8)
D(1C)	1.068738	0.193660	0.542396	0.040
C(2C)	0.9884(2)	0.0306(3)	0.55267(14)	0.0332(8)
D(2C)	0.980359	0.051546	0.588958	0.040
C(3C)	0.9479(2)	-0.0833(3)	0.52784(15)	0.0337(8)
D(3C)	0.911833	-0.141091	0.547007	0.040

Table 3. Bond lengths [Å] and angles [°] for SBY-3-043.

U(1)-O(1)	2.259(2)	P(1)-C(1)	1.786(3)
U(1)-Cl(1)	2.6133(8)	P(1)-C(13)	1.789(3)
U(1)-Cl(2)	2.6225(8)	O(2)-C(4)	1.357(4)
P(1)-O(1)	1.525(2)	O(2)-C(19)	1.431(4)
P(1)-C(7)	1.785(3)	O(3)-C(10)	1.363(4)

O(3)-C(20)	1.427(4)	C(14)-H(14)	0.9500
C(1)-C(6)	1.396(4)	C(15)-C(16)	1.388(4)
C(1)-C(2)	1.403(4)	C(15)-H(15)	0.9500
C(2)-C(3)	1.371(4)	C(16)-C(17)	1.396(5)
C(2)-H(2)	0.9500	C(17)-C(18)	1.381(4)
C(3)-C(4)	1.410(4)	C(17)-H(17)	0.9500
C(3)-H(3)	0.9500	C(18)-H(18)	0.9500
C(4)-C(5)	1.387(4)	C(19)-H(19A)	0.9800
O(4)-C(16)	1.368(4)	C(19)-H(19B)	0.9800
O(4)-C(21)	1.444(4)	C(19)-H(19C)	0.9800
C(5)-C(6)	1.384(4)	C(20)-H(20A)	0.9800
C(5)-H(5)	0.9500	C(20)-H(20B)	0.9800
C(6)-H(6)	0.9500	C(20)-H(20C)	0.9800
C(7)-C(8)	1.384(4)	C(21)-H(21A)	0.9800
C(7)-C(12)	1.408(4)	C(21)-H(21B)	0.9800
C(8)-C(9)	1.392(4)	C(21)-H(21C)	0.9800
C(8)-H(8)	0.9500	C(1A)-C(6A)	1.373(3)
C(9)-C(10)	1.387(4)	C(1A)-C(2A)	1.374(3)
C(9)-H(9)	0.9500	C(1A)-D(1A)	0.9500
C(10)-C(11)	1.392(5)	C(2A)-C(3A)	1.375(3)
C(11)-C(12)	1.378(5)	C(2A)-D(2A)	0.9500
C(11)-H(11)	0.9500	C(3A)-C(4A)	1.372(3)
C(12)-H(12)	0.9500	C(3A)-D(3A)	0.9500
C(13)-C(14)	1.393(4)	C(4A)-C(5A)	1.372(3)
C(13)-C(18)	1.393(4)	C(4A)-D(4A)	0.9500
C(14)-C(15)	1.382(4)	C(5A)-C(6A)	1.372(3)

C(5A)-D(5A) 0.9500

C(6A)-D(6A) 0.9500

C(1B)-C(2B)#2 1.362(3)

C(1B)-C(2B) 1.362(3)

C(1B)-D(1B) 0.9500

C(2B)-C(3B) 1.370(3)

C(2B)-D(2B) 0.9500

C(3B)-C(4B) 1.373(3)

C(3B)-D(3B) 0.9500

C(4B)-D(4B) 0.9500

C(1C)-C(2C) 1.374(3)

C(1C)-C(3C)#3 1.389(5)

C(1C)-D(1C) 0.9500

C(2C)-C(3C) 1.372(3)

C(2C)-D(2C) 0.9500

C(3C)-D(3C) 0.9500

O(1)-U(1)-O(1)#1 86.96(11)

O(1)-U(1)-Cl(1)#1 177.04(6)

O(1)#1-U(1)-Cl(1)#1 90.44(6)

O(1)-U(1)-Cl(1) 90.44(6)

O(1)#1-U(1)-Cl(1) 177.04(6)

Cl(1)#1-U(1)-Cl(1) 92.19(4)

O(1)-U(1)-Cl(2) 87.35(6)

O(1)#1-U(1)-Cl(2) 87.88(6)

Cl(1)#1-U(1)-Cl(2) 91.14(3)

Cl(1)-U(1)-Cl(2) 93.42(3)

O(1)-U(1)-Cl(2)#1 87.88(6)

O(1)#1-U(1)-Cl(2)#1 87.35(6)

Cl(1)#1-U(1)-Cl(2)#1 93.42(3)

Cl(1)-U(1)-Cl(2)#1 91.14(3)

Cl(2)-U(1)-Cl(2)#1 173.43(4)

O(1)-P(1)-C(7) 108.94(13)

O(1)-P(1)-C(1) 113.13(14)

C(7)-P(1)-C(1) 109.72(14)

O(1)-P(1)-C(13) 109.41(13)

C(7)-P(1)-C(13) 109.08(15)

C(1)-P(1)-C(13) 106.49(14)

P(1)-O(1)-U(1) 163.28(14)

C(4)-O(2)-C(19) 116.7(3)

C(10)-O(3)-C(20) 118.1(3)

C(6)-C(1)-C(2) 119.2(3)

C(6)-C(1)-P(1) 122.5(2)

C(2)-C(1)-P(1) 118.3(2)

C(3)-C(2)-C(1) 120.2(3)

C(3)-C(2)-H(2) 119.9

C(1)-C(2)-H(2) 119.9

C(2)-C(3)-C(4) 119.9(3)

C(2)-C(3)-H(3) 120.0

C(4)-C(3)-H(3) 120.0

O(2)-C(4)-C(5) 124.6(3)

O(2)-C(4)-C(3)	115.0(3)	C(7)-C(12)-H(12)	120.0
C(5)-C(4)-C(3)	120.4(3)	C(14)-C(13)-C(18)	119.2(3)
C(16)-O(4)-C(21)	116.7(3)	C(14)-C(13)-P(1)	119.9(2)
C(6)-C(5)-C(4)	119.2(3)	C(18)-C(13)-P(1)	120.9(2)
C(6)-C(5)-H(5)	120.4	C(15)-C(14)-C(13)	120.3(3)
C(4)-C(5)-H(5)	120.4	C(15)-C(14)-H(14)	119.9
C(5)-C(6)-C(1)	121.1(3)	C(13)-C(14)-H(14)	119.9
C(5)-C(6)-H(6)	119.5	C(14)-C(15)-C(16)	120.2(3)
C(1)-C(6)-H(6)	119.5	C(14)-C(15)-H(15)	119.9
C(8)-C(7)-C(12)	119.2(3)	C(16)-C(15)-H(15)	119.9
C(8)-C(7)-P(1)	119.9(2)	O(4)-C(16)-C(15)	124.5(3)
C(12)-C(7)-P(1)	120.8(2)	O(4)-C(16)-C(17)	115.5(3)
C(7)-C(8)-C(9)	120.8(3)	C(15)-C(16)-C(17)	119.9(3)
C(7)-C(8)-H(8)	119.6	C(18)-C(17)-C(16)	119.6(3)
C(9)-C(8)-H(8)	119.6	C(18)-C(17)-H(17)	120.2
C(10)-C(9)-C(8)	119.6(3)	C(16)-C(17)-H(17)	120.2
C(10)-C(9)-H(9)	120.2	C(17)-C(18)-C(13)	120.8(3)
C(8)-C(9)-H(9)	120.2	C(17)-C(18)-H(18)	119.6
O(3)-C(10)-C(9)	124.0(3)	C(13)-C(18)-H(18)	119.6
O(3)-C(10)-C(11)	115.9(3)	O(2)-C(19)-H(19A)	109.5
C(9)-C(10)-C(11)	120.1(3)	O(2)-C(19)-H(19B)	109.5
C(12)-C(11)-C(10)	120.3(3)	H(19A)-C(19)-H(19B)	109.5
C(12)-C(11)-H(11)	119.9	O(2)-C(19)-H(19C)	109.5
C(10)-C(11)-H(11)	119.9	H(19A)-C(19)-H(19C)	109.5
C(11)-C(12)-C(7)	120.0(3)	H(19B)-C(19)-H(19C)	109.5
C(11)-C(12)-H(12)	120.0	O(3)-C(20)-H(20A)	109.5

O(3)-C(20)-H(20B) 109.5
H(20A)-C(20)-H(20B) 109.5
O(3)-C(20)-H(20C) 109.5
H(20A)-C(20)-H(20C) 109.5
H(20B)-C(20)-H(20C) 109.5
O(4)-C(21)-H(21A) 109.5
O(4)-C(21)-H(21B) 109.5
H(21A)-C(21)-H(21B) 109.5
O(4)-C(21)-H(21C) 109.5
H(21A)-C(21)-H(21C) 109.5
H(21B)-C(21)-H(21C) 109.5
C(6A)-C(1A)-C(2A) 120.1(2)
C(6A)-C(1A)-D(1A) 120.0
C(2A)-C(1A)-D(1A) 120.0
C(1A)-C(2A)-C(3A) 120.0(3)
C(1A)-C(2A)-D(2A) 120.0
C(3A)-C(2A)-D(2A) 120.0
C(4A)-C(3A)-C(2A) 119.8(3)
C(4A)-C(3A)-D(3A) 120.1
C(2A)-C(3A)-D(3A) 120.1
C(3A)-C(4A)-C(5A) 120.2(3)
C(3A)-C(4A)-D(4A) 119.9
C(5A)-C(4A)-D(4A) 119.9
C(6A)-C(5A)-C(4A) 120.1(2)
C(6A)-C(5A)-D(5A) 120.0
C(4A)-C(5A)-D(5A) 120.0
C(5A)-C(6A)-C(1A) 119.9(2)
C(5A)-C(6A)-D(6A) 120.1
C(1A)-C(6A)-D(6A) 120.1
C(2B)#2-C(1B)-C(2B) 119.1(5)
C(2B)#2-C(1B)-D(1B) 120.4
C(2B)-C(1B)-D(1B) 120.4
C(1B)-C(2B)-C(3B) 120.8(3)
C(1B)-C(2B)-D(2B) 119.6
C(3B)-C(2B)-D(2B) 119.6
C(2B)-C(3B)-C(4B) 120.1(3)
C(2B)-C(3B)-D(3B) 120.0
C(4B)-C(3B)-D(3B) 120.0
C(3B)-C(4B)-C(3B)#2 119.1(5)
C(3B)-C(4B)-D(4B) 120.4
C(3B)#2-C(4B)-D(4B) 120.4
C(2C)-C(1C)-C(3C)#3 119.5(3)
C(2C)-C(1C)-D(1C) 120.2
C(3C)#3-C(1C)-D(1C) 120.2
C(3C)-C(2C)-C(1C) 120.2(3)
C(3C)-C(2C)-D(2C) 119.9
C(1C)-C(2C)-D(2C) 119.9
C(2C)-C(3C)-C(1C)#3 120.3(3)
C(2C)-C(3C)-D(3C) 119.9
C(1C)#3-C(3C)-D(3C) 119.9

Symmetry transformations used to generate equivalent atoms:

#1 -x+2, y, -z+1/2 #2 -x+1, y, -z+1/2 #3 -x+2, -y, -z+1

Table 4. Anisotropic displacement parameters (Å2x 103) for SBY-3-043. The anisotropic displacement factor exponent takes the form:

-2 p2[h2 *a**2 U11 + ... + 2 h k *a** *b** U12]

	U11	U22	U33	U23	U13	U12
U(1)	19(1)	14(1)	22(1)	0	5(1)	0
Cl(1)	43(1)	23(1)	33(1)	0(1)	15(1)	7(1)
Cl(2)	25(1)	28(1)	31(1)	3(1)	0(1)	2(1)
P(1)	15(1)	17(1)	22(1)	2(1)	5(1)	1(1)
O(1)	16(1)	19(1)	26(1)	2(1)	6(1)	0(1)
O(2)	31(1)	23(1)	27(1)	-3(1)	4(1)	0(1)
O(3)	31(1)	25(1)	26(1)	5(1)	-4(1)	0(1)
C(1)	15(1)	18(1)	25(2)	-2(1)	7(1)	-2(1)
C(2)	19(1)	18(1)	28(2)	1(1)	6(1)	1(1)
C(3)	20(1)	25(2)	23(2)	5(1)	4(1)	2(1)
C(4)	19(1)	20(2)	24(2)	0(1)	6(1)	-2(1)
O(4)	21(1)	32(1)	40(2)	-8(1)	13(1)	1(1)
C(5)	23(2)	17(1)	31(2)	2(1)	9(1)	2(1)
C(6)	18(1)	21(1)	25(2)	3(1)	4(1)	3(1)
C(7)	18(1)	18(1)	21(2)	2(1)	5(1)	2(1)

C(8)	20(1)	15(1)	25(2)	-1(1)	7(1)	0(1)
C(9)	21(2)	21(2)	24(2)	-3(1)	4(1)	-1(1)
C(10)	26(2)	24(2)	20(2)	1(1)	3(1)	4(1)
C(11)	28(2)	21(2)	28(2)	5(1)	4(1)	-5(1)
C(12)	22(2)	22(2)	27(2)	3(1)	3(1)	-5(1)
C(13)	16(1)	21(2)	21(2)	0(1)	4(1)	-1(1)
C(14)	20(2)	21(2)	32(2)	-2(1)	7(1)	-2(1)
C(15)	24(2)	22(2)	36(2)	-8(1)	7(2)	0(1)
C(16)	15(1)	30(2)	23(2)	0(1)	4(1)	4(1)
C(17)	20(2)	26(2)	31(2)	-4(1)	8(1)	-5(1)
C(18)	21(2)	21(2)	29(2)	-4(1)	7(1)	-3(1)
C(19)	44(2)	24(2)	38(2)	-6(2)	10(2)	0(2)
C(20)	26(2)	35(2)	25(2)	2(1)	-4(1)	1(1)
C(21)	29(2)	35(2)	47(2)	-12(2)	16(2)	2(2)
C(1A)	43(2)	38(2)	60(3)	10(2)	19(2)	13(2)
C(2A)	26(2)	36(2)	109(5)	-1(3)	1(3)	3(2)
C(3A)	59(3)	40(2)	63(3)	-14(2)	-23(3)	18(2)
C(4A)	76(3)	37(2)	42(3)	7(2)	7(2)	26(2)
C(5A)	37(2)	29(2)	48(2)	9(2)	5(2)	6(2)
C(6A)	38(2)	32(2)	37(2)	2(2)	-1(2)	8(2)
C(1B)	74(5)	61(4)	47(4)	0	-6(4)	0
C(2B)	36(2)	111(5)	40(3)	15(3)	12(2)	-8(3)
C(3B)	68(3)	130(6)	33(3)	-19(3)	-7(2)	62(4)
C(4B)	95(4)	61(3)	65(4)	0	-6(3)	0
C(1C)	36(2)	27(2)	37(2)	-1(2)	8(2)	2(2)
C(2C)	38(2)	32(2)	31(2)	4(2)	12(2)	8(2)

C(3C)	35(2)	32(2)	38(2)	10(2)	16(2)	4(2)

Table 5. Hydrogen coordinates and isotropic displacement parameters for SBY-3-043.

	x	y	z	U(eq)
H(2)	0.711380	0.712959	0.199422	0.026
H(3)	0.649862	0.587577	0.119657	0.028
H(5)	0.854079	0.298295	0.192027	0.028
H(6)	0.916982	0.426272	0.271468	0.026
H(8)	1.077790	0.714712	0.374665	0.024
H(9)	1.186646	0.602311	0.450795	0.027
H(11)	0.948590	0.335512	0.436877	0.031
H(12)	0.840042	0.447084	0.361201	0.029
H(14)	0.801906	0.912324	0.350574	0.029
H(15)	0.651097	0.974832	0.381540	0.033
H(17)	0.507225	0.631114	0.331882	0.030
H(18)	0.658904	0.568331	0.301750	0.029
H(19A)	0.814810	0.230767	0.100208	0.053
H(19B)	0.695875	0.193739	0.063292	0.053
H(19C)	0.723119	0.186394	0.130354	0.053
H(20A)	1.288800	0.432471	0.498458	0.046
H(20B)	1.271395	0.370736	0.555092	0.046
H(20C)	1.234611	0.515977	0.538800	0.046

H(21A)	0.524383	0.973436	0.434208	0.054
H(21B)	0.395614	0.975246	0.407801	0.054
H(21C)	0.475555	1.029777	0.372434	0.054

Table 6. Torsion angles [°] for SBY-3-043.

C(7)-P(1)-O(1)-U(1)	137.5(4)	C(4)-C(5)-C(6)-C(1)	0.2(5)
C(1)-P(1)-O(1)-U(1)	15.2(5)	C(2)-C(1)-C(6)-C(5)	-0.3(5)
C(13)-P(1)-O(1)-U(1)	-103.4(4)	P(1)-C(1)-C(6)-C(5)	179.4(2)
O(1)-P(1)-C(1)-C(6)	112.3(3)	O(1)-P(1)-C(7)-C(8)	2.6(3)
C(7)-P(1)-C(1)-C(6)	-9.6(3)	C(1)-P(1)-C(7)-C(8)	127.0(3)
C(13)-P(1)-C(1)-C(6)	-127.5(3)	C(13)-P(1)-C(7)-C(8)	-116.7(3)
O(1)-P(1)-C(1)-C(2)	-68.1(3)	O(1)-P(1)-C(7)-C(12)	179.8(3)
C(7)-P(1)-C(1)-C(2)	170.1(2)	C(1)-P(1)-C(7)-C(12)	-55.9(3)
C(13)-P(1)-C(1)-C(2)	52.2(3)	C(13)-P(1)-C(7)-C(12)	60.4(3)
C(6)-C(1)-C(2)-C(3)	-0.2(5)	C(12)-C(7)-C(8)-C(9)	0.6(5)
P(1)-C(1)-C(2)-C(3)	-179.9(2)	P(1)-C(7)-C(8)-C(9)	177.7(2)
C(1)-C(2)-C(3)-C(4)	0.8(5)	C(7)-C(8)-C(9)-C(10)	0.1(5)
C(19)-O(2)-C(4)-C(5)	5.7(4)	C(20)-O(3)-C(10)-C(9)	1.8(5)
C(19)-O(2)-C(4)-C(3)	-174.7(3)	C(20)-O(3)-C(10)-C(11)	-178.1(3)
C(2)-C(3)-C(4)-O(2)	179.6(3)	C(8)-C(9)-C(10)-O(3)	179.4(3)
C(2)-C(3)-C(4)-C(5)	-0.8(5)	C(8)-C(9)-C(10)-C(11)	-0.7(5)
O(2)-C(4)-C(5)-C(6)	179.9(3)	O(3)-C(10)-C(11)-C(12)	-179.4(3)
C(3)-C(4)-C(5)-C(6)	0.4(5)	C(9)-C(10)-C(11)-C(12)	0.6(5)

C(10)-C(11)-C(12)-C(7)	0.0(5)
C(8)-C(7)-C(12)-C(11)	-0.6(5)
P(1)-C(7)-C(12)-C(11)	-177.7(3)
O(1)-P(1)-C(13)-C(14)	-24.7(3)
C(7)-P(1)-C(13)-C(14)	94.4(3)
C(1)-P(1)-C(13)-C(14)	-147.2(3)
O(1)-P(1)-C(13)-C(18)	158.8(3)
C(7)-P(1)-C(13)-C(18)	-82.2(3)
C(1)-P(1)-C(13)-C(18)	36.2(3)
C(18)-C(13)-C(14)-C(15)	0.4(5)
P(1)-C(13)-C(14)-C(15)	-176.3(3)
C(13)-C(14)-C(15)-C(16)	-0.7(5)
C(21)-O(4)-C(16)-C(15)	2.1(5)
C(21)-O(4)-C(16)-C(17)	-178.6(3)
C(14)-C(15)-C(16)-O(4)	179.9(3)
C(14)-C(15)-C(16)-C(17)	0.6(5)
O(4)-C(16)-C(17)-C(18)	-179.7(3)
C(15)-C(16)-C(17)-C(18)	-0.3(5)
C(16)-C(17)-C(18)-C(13)	0.0(5)
C(14)-C(13)-C(18)-C(17)	-0.1(5)
P(1)-C(13)-C(18)-C(17)	176.5(3)
C(6A)-C(1A)-C(2A)-C(3A)	-0.09(17)
C(1A)-C(2A)-C(3A)-C(4A)	-0.10(17)
C(2A)-C(3A)-C(4A)-C(5A)	0.2(3)
C(3A)-C(4A)-C(5A)-C(6A)	-0.1(4)
C(4A)-C(5A)-C(6A)-C(1A)	-0.1(4)
C(2A)-C(1A)-C(6A)-C(5A)	0.2(3)
C(2B)#2-C(1B)-C(2B)-C(3B)	0.02(6)
C(1B)-C(2B)-C(3B)-C(4B)	-0.03(11)
C(2B)-C(3B)-C(4B)-C(3B)#2	0.02(6)
C(3C)#3-C(1C)-C(2C)-C(3C)	-0.01(12)
C(1C)-C(2C)-C(3C)-C(1C)#3	0.01(12)

Symmetry transformations used to generate equivalent atoms:

#2 -x+1, y, -z+1/2 #3 -x+2, -y, -z+1

Table 7. Hydrogen bonds for SBY-3-043[Å and °].

D-H...A	d(D-H)	d(H...A)	d(D...A)	<(DHA)
C(19)-H(19C)...Cl(2)#4	0.98	2.87	3.492(4)	122.5
C(20)-H(20A)...O(2)#1	0.98	2.56	3.379(5)	141.4
C(21)-H(21B)...Cl(2)#2	0.98	2.94	3.643(4)	129.1

Symmetry transformations used to generate equivalent atoms:

#1 -x+2, y, -z+1/2 #2 -x+1, y, -z+1/2 #4 x, y-1, z

Table 1. Crystal data and structure refinement for SBY-4-023.

Empirical formula	$(C_{64}\ H_{80}\ Li_8\ O_4\ P_8) \cdot 2(C_6\ H_6)$	
	$C_{76}\ H_{92}\ Li_8\ O_4\ P_8$	
Formula weight	1372.77	
Crystal system	triclinic	
Space group	$P\ \bar{1}$	
Unit cell dimensions	a = 13.070(4) Å	a= 90.784(5)°
	b = 14.954(5) Å	b= 101.315(5)°
	c = 20.208(6) Å	c= 91.832(5)°
Volume	3870(2) Å3	
Z, Z'	2, 1	
Density (calculated)	1.178 Mg/m3	
Wavelength	0.71073 Å	
Temperature	100(2) K	
F(000)	1448	
Absorption coefficient	0.225 mm-1	
Absorption correction	semi-empirical from equivalents	
Max. and min. transmission	0.7453 and 0.6370	
Theta range for data collection	1.028 to 21.490°	
Reflections collected	26293	
Independent reflections	8887 [R(int) = 0.0982]	
Data / restraints / parameters	8887 / 660 / 917	
wR(F2 all data)	wR2 = 0.1448	
R(F obsd data)	R1 = 0.0579	
Goodness-of-fit on F2	0.999	

Observed data [I > 2s(I)] 5394

Largest and mean shift / s.u. 0.007 and 0.000

Largest diff. peak and hole 0.355 and -0.308 e/Å3

$wR2 = \{ S [w(Fo2 - Fc2)2] / S [w(Fo 2)2] \}1/2$

$R1 = S ||Fo| - |Fc|| / S |Fo|$

Table 2. Atomic coordinates and equivalent isotropic displacement parameters for SBY-4-023. U(eq) is defined as one third of the trace of the orthogonalized Uij tensor.

	x	y	z	U(eq)
P(1A)	0.57677(12)	-0.16725(10)	0.37304(7)	0.0308(4)
C(1A)	0.6695(4)	-0.2089(3)	0.4444(2)	0.0240(12)
C(2A)	0.6419(4)	-0.2758(3)	0.4864(3)	0.0283(13)
C(3A)	0.7131(5)	-0.3054(4)	0.5396(3)	0.0373(15)
C(4A)	0.8149(5)	-0.2706(4)	0.5537(3)	0.0447(16)
C(5A)	0.8430(5)	-0.2055(4)	0.5125(3)	0.0424(16)
C(6A)	0.7721(4)	-0.1761(4)	0.4591(3)	0.0312(14)
P(1B)	0.58840(12)	0.10727(10)	0.47309(7)	0.0305(4)
C(1B)	0.7230(4)	0.1279(3)	0.5107(2)	0.0265(13)
C(2B)	0.7963(5)	0.0631(4)	0.5071(3)	0.0446(16)
C(3B)	0.9006(6)	0.0761(6)	0.5382(4)	0.071(2)
C(4B)	0.9331(6)	0.1557(7)	0.5745(4)	0.088(3)

C(5B)	0.8629(6)	0.2176(6)	0.5778(4)	0.079(3)
C(6B)	0.7607(5)	0.2049(4)	0.5482(3)	0.0430(16)
P(1C)	0.46410(11)	0.27724(9)	0.30867(7)	0.0284(4)
C(1C)	0.3377(4)	0.2636(3)	0.2546(3)	0.0280(13)
C(2C)	0.2468(4)	0.3026(4)	0.2655(3)	0.0355(14)
C(3C)	0.1508(5)	0.2874(4)	0.2224(3)	0.0459(16)
C(4C)	0.1436(5)	0.2333(4)	0.1662(3)	0.0472(16)
C(5C)	0.2310(5)	0.1929(4)	0.1536(3)	0.0449(16)
C(6C)	0.3259(4)	0.2075(4)	0.1965(3)	0.0336(14)
P(1D)	0.57360(12)	0.33692(10)	0.14691(7)	0.0322(4)
C(1D)	0.6690(4)	0.2957(3)	0.1006(3)	0.0293(13)
C(2D)	0.6485(5)	0.2232(3)	0.0548(3)	0.0327(14)
C(3D)	0.7246(5)	0.1935(4)	0.0222(3)	0.0393(15)
C(4D)	0.8227(5)	0.2330(4)	0.0326(3)	0.0408(16)
C(5D)	0.8455(4)	0.3049(4)	0.0773(3)	0.0355(15)
C(6D)	0.7692(4)	0.3350(3)	0.1106(3)	0.0296(14)
P(1E)	0.41004(11)	0.39279(9)	-0.05160(7)	0.0270(4)
C(1E)	0.2762(4)	0.3661(3)	-0.0463(2)	0.0242(13)
C(2E)	0.2430(4)	0.2850(3)	-0.0190(3)	0.0299(14)
C(3E)	0.1392(4)	0.2680(4)	-0.0170(3)	0.0352(14)
C(4E)	0.0642(5)	0.3288(4)	-0.0398(3)	0.0365(15)
C(5E)	0.0945(4)	0.4086(4)	-0.0653(3)	0.0364(15)
C(6E)	0.1986(4)	0.4256(4)	-0.0683(2)	0.0283(13)
P(1F)	0.59649(12)	0.55941(9)	0.27923(8)	0.0291(4)
C(1F)	0.7360(4)	0.5840(3)	0.2985(3)	0.0264(13)
C(2F)	0.7931(4)	0.5755(3)	0.2469(3)	0.0322(14)

C(3F)	0.8997(5)	0.5889(3)	0.2580(3)	0.0372(15)
C(4F)	0.9535(5)	0.6126(4)	0.3214(3)	0.0402(15)
C(5F)	0.9013(5)	0.6250(4)	0.3739(3)	0.0382(15)
C(6F)	0.7941(4)	0.6121(3)	0.3626(3)	0.0314(14)
P(1G)	0.46494(11)	0.78097(9)	0.18338(7)	0.0263(4)
C(1G)	0.3318(4)	0.7709(3)	0.1966(3)	0.0224(12)
C(2G)	0.3104(4)	0.7200(3)	0.2505(3)	0.0298(14)
C(3G)	0.2101(5)	0.7078(4)	0.2607(3)	0.0424(16)
C(4G)	0.1272(5)	0.7445(4)	0.2189(3)	0.0441(16)
C(5G)	0.1466(4)	0.7955(4)	0.1663(3)	0.0369(15)
C(6G)	0.2473(4)	0.8089(3)	0.1563(3)	0.0294(13)
P(1H)	0.60779(11)	1.05953(9)	0.25431(8)	0.0281(4)
C(1H)	0.7457(4)	1.0862(3)	0.2583(3)	0.0248(13)
C(2H)	0.8154(4)	1.0821(3)	0.3200(3)	0.0310(14)
C(3H)	0.9215(4)	1.1007(3)	0.3249(3)	0.0364(14)
C(4H)	0.9601(5)	1.1254(3)	0.2686(3)	0.0394(15)
C(5H)	0.8931(5)	1.1292(4)	0.2083(3)	0.0392(15)
C(6H)	0.7876(4)	1.1111(3)	0.2024(3)	0.0295(13)
O(1I)	0.3982(2)	0.0294(2)	0.35516(16)	0.0258(9)
C(1I)	0.3392(4)	-0.0213(4)	0.2967(3)	0.0340(14)
C(2I)	0.2284(4)	-0.0240(4)	0.3057(3)	0.0419(16)
C(3I)	0.2192(4)	0.0659(4)	0.3386(3)	0.0389(15)
C(4I)	0.3220(4)	0.0799(3)	0.3855(3)	0.0303(14)
O(1J)	0.7176(3)	0.3141(2)	0.31193(17)	0.0285(9)
C(1J)	0.8171(4)	0.3395(4)	0.2933(3)	0.0351(14)
C(2J)	0.8878(4)	0.3676(4)	0.3581(3)	0.0414(15)

C(3J)	0.8543(4)	0.3053(4)	0.4091(3)	0.0415(15)
C(4J)	0.7377(5)	0.2915(4)	0.3837(3)	0.0445(16)
O(1K)	0.3903(2)	0.5327(2)	0.11614(16)	0.0253(9)
C(1K)	0.3318(4)	0.4823(4)	0.1591(3)	0.0307(14)
C(2K)	0.2215(4)	0.4754(4)	0.1194(3)	0.0337(14)
C(3K)	0.2106(4)	0.5661(3)	0.0851(3)	0.0287(14)
C(4K)	0.3154(4)	0.5823(3)	0.0669(3)	0.0275(13)
O(1L)	0.7152(3)	0.8180(2)	0.24198(16)	0.0262(9)
C(1L)	0.8144(4)	0.8430(4)	0.2864(3)	0.0327(14)
C(2L)	0.8900(17)	0.872(3)	0.2414(6)	0.037(4)
C(3L)	0.8482(8)	0.8177(12)	0.1767(5)	0.035(3)
C(4L)	0.7306(11)	0.8210(15)	0.1718(11)	0.036(5)
C(2L')	0.885(2)	0.876(4)	0.2399(7)	0.040(6)
C(3L')	0.8189(15)	0.8692(14)	0.1698(6)	0.037(4)
C(4L')	0.7387(15)	0.7955(17)	0.1753(14)	0.021(5)
C(1M)	0.3576(6)	0.5486(4)	0.4887(4)	0.068(2)
C(2M)	0.3898(6)	0.5462(4)	0.4281(4)	0.066(2)
C(3M)	0.3199(7)	0.5269(5)	0.3704(4)	0.072(2)
C(4M)	0.2157(7)	0.5108(5)	0.3716(4)	0.077(2)
C(5M)	0.1827(6)	0.5127(5)	0.4318(5)	0.077(2)
C(6M)	0.2522(7)	0.5298(4)	0.4909(4)	0.072(2)
C(1N)	-0.0785(6)	0.0100(4)	0.0363(4)	0.060(2)
C(2N)	0.0241(7)	0.0059(4)	0.0687(4)	0.062(2)
C(3N)	0.1018(6)	-0.0061(4)	0.0328(4)	0.065(2)
C(1O)	0.4511(7)	0.0140(5)	0.0536(4)	0.070(2)
C(2O)	0.5444(7)	-0.0283(5)	0.0616(4)	0.076(2)

C(3O)	0.5948(6)	-0.0419(5)	0.0090(4)	0.070(2)
Li(1)	0.4898(7)	-0.0411(6)	0.4277(5)	0.034(2)
Li(2)	0.5150(7)	0.1198(6)	0.3462(4)	0.029(2)
Li(3)	0.6195(7)	0.2298(6)	0.2513(5)	0.034(2)
Li(4)	0.5901(8)	0.3936(6)	0.2715(5)	0.040(3)
Li(5)	0.4855(7)	0.4596(6)	0.0682(5)	0.035(2)
Li(6)	0.5076(7)	0.6177(6)	0.1600(4)	0.028(2)
Li(7)	0.6207(7)	0.7303(6)	0.2766(4)	0.033(2)
Li(8)	0.5912(7)	0.8940(6)	0.2568(5)	0.035(2)

Table 3. Bond lengths [Å] and angles [°] for SBY-4-023.

P(1A)-C(1A)	1.823(5)	C(4A)-C(5A)	1.376(8)
P(1A)-Li(8)#1	2.573(9)	C(4A)-H(4A)	0.9500
P(1A)-Li(1)	2.578(9)	C(5A)-C(6A)	1.364(7)
P(1A)-Li(7)#1	2.624(9)	C(5A)-H(5A)	0.9500
P(1A)-H(1P)	1.37(4)	C(6A)-H(6A)	0.9500
C(1A)-C(6A)	1.388(7)	P(1B)-C(1B)	1.789(5)
C(1A)-C(2A)	1.403(7)	P(1B)-Li(2)	2.568(9)
C(2A)-C(3A)	1.367(7)	P(1B)-Li(1)	2.593(9)
C(2A)-H(2A)	0.9500	P(1B)-Li(1)#2	2.615(9)
C(3A)-C(4A)	1.388(7)	P(1B)-H(2P)	1.38(4)
C(3A)-H(3A)	0.9500	C(1B)-C(6B)	1.392(7)

C(1B)-C(2B) 1.395(7)
C(2B)-C(3B) 1.391(9)
C(2B)-H(2B) 0.9500
C(3B)-C(4B) 1.400(11)
C(3B)-H(3B) 0.9500
C(4B)-C(5B) 1.333(11)
C(4B)-H(4B) 0.9500
C(5B)-C(6B) 1.358(9)
C(5B)-H(5B) 0.9500
C(6B)-H(6B) 0.9500
P(1C)-C(1C) 1.797(6)
P(1C)-Li(2) 2.551(9)
P(1C)-Li(4) 2.577(10)
P(1C)-Li(3) 2.639(9)
P(1C)-H(3P) 1.38(4)
C(1C)-C(2C) 1.394(7)
C(1C)-C(6C) 1.415(7)
C(2C)-C(3C) 1.390(8)
C(2C)-H(2C) 0.9500
C(3C)-C(4C) 1.372(8)
C(3C)-H(3C) 0.9500
C(4C)-C(5C) 1.374(8)
C(4C)-H(4C) 0.9500
C(5C)-C(6C) 1.376(7)
C(5C)-H(5C) 0.9500
C(6C)-H(6C) 0.9500
P(1D)-C(1D) 1.817(5)
P(1D)-Li(5) 2.593(10)
P(1D)-Li(4) 2.612(9)
P(1D)-Li(3) 2.652(9)
P(1D)-H(4P) 1.48(4)
C(1D)-C(6D) 1.395(7)
C(1D)-C(2D) 1.400(7)
C(2D)-C(3D) 1.378(7)
C(2D)-H(2D) 0.9500
C(3D)-C(4D) 1.371(7)
C(3D)-H(3D) 0.9500
C(4D)-C(5D) 1.382(7)
C(4D)-H(4D) 0.9500
C(5D)-C(6D) 1.390(7)
C(5D)-H(5D) 0.9500
C(6D)-H(6D) 0.9500
P(1E)-C(1E) 1.805(5)
P(1E)-Li(5) 2.601(9)
P(1E)-Li(5)#3 2.618(9)
P(1E)-Li(6)#3 2.628(8)
P(1E)-H(5P) 1.34(4)
C(1E)-C(6E) 1.382(7)
C(1E)-C(2E) 1.429(7)
C(2E)-C(3E) 1.381(7)
C(2E)-H(2E) 0.9500
C(3E)-C(4E) 1.374(7)

C(3E)-H(3E) 0.9500
C(4E)-C(5E) 1.383(7)
C(4E)-H(4E) 0.9500
C(5E)-C(6E) 1.390(7)
C(5E)-H(5E) 0.9500
C(6E)-H(6E) 0.9500
P(1F)-C(1F) 1.813(6)
P(1F)-Li(4) 2.479(10)
P(1F)-Li(7) 2.567(9)
P(1F)-Li(6) 2.634(9)
P(1F)-H(6P) 1.40(4)
C(1F)-C(2F) 1.403(7)
C(1F)-C(6F) 1.419(7)
C(1F)-Li(7) 2.688(10)
C(2F)-C(3F) 1.374(7)
C(2F)-H(2F) 0.9500
C(3F)-C(4F) 1.370(8)
C(3F)-H(3F) 0.9500
C(4F)-C(5F) 1.383(7)
C(4F)-H(4F) 0.9500
C(5F)-C(6F) 1.381(7)
C(5F)-H(5F) 0.9500
C(6F)-H(6F) 0.9500
P(1G)-C(1G) 1.814(5)
P(1G)-Li(8) 2.564(9)
P(1G)-Li(6) 2.579(9)
P(1G)-Li(7) 2.628(9)
P(1G)-H(7P) 1.29(5)
C(1G)-C(6G) 1.380(7)
C(1G)-C(2G) 1.406(7)
C(2G)-C(3G) 1.373(7)
C(2G)-H(2G) 0.9500
C(3G)-C(4G) 1.371(8)
C(3G)-H(3G) 0.9500
C(4G)-C(5G) 1.376(8)
C(4G)-H(4G) 0.9500
C(5G)-C(6G) 1.379(7)
C(5G)-H(5G) 0.9500
C(6G)-H(6G) 0.9500
P(1H)-C(1H) 1.819(5)
P(1H)-Li(8) 2.480(9)
P(1H)-Li(3)#4 2.549(9)
P(1H)-Li(2)#4 2.576(9)
P(1H)-H(8P) 1.39(5)
C(1H)-C(2H) 1.395(7)
C(1H)-C(6H) 1.400(7)
C(1H)-Li(3)#4 2.738(10)
C(2H)-C(3H) 1.389(7)
C(2H)-H(2H) 0.9500
C(3H)-C(4H) 1.384(7)
C(3H)-H(3H) 0.9500
C(4H)-C(5H) 1.357(7)

C(4H)-H(4H) 0.9500
C(5H)-C(6H) 1.378(7)
C(5H)-H(5H) 0.9500
C(6H)-H(6H) 0.9500
O(1I)-C(1I) 1.466(6)
O(1I)-C(4I) 1.487(5)
O(1I)-Li(1) 2.032(10)
O(1I)-Li(2) 2.043(9)
C(1I)-C(2I) 1.494(7)
C(1I)-H(1I1) 0.9900
C(1I)-H(1I2) 0.9900
C(2I)-C(3I) 1.512(7)
C(2I)-H(2I1) 0.9900
C(2I)-H(2I2) 0.9900
C(3I)-C(4I) 1.491(7)
C(3I)-H(3I1) 0.9900
C(3I)-H(3I2) 0.9900
C(4I)-H(4I1) 0.9900
C(4I)-H(4I2) 0.9900
O(1J)-C(1J) 1.465(6)
O(1J)-C(4J) 1.469(6)
O(1J)-Li(3) 1.992(10)
O(1J)-Li(4) 2.116(10)
C(1J)-C(2J) 1.493(7)
C(1J)-H(1J1) 0.9900
C(1J)-H(1J2) 0.9900
C(2J)-C(3J) 1.516(7)
C(2J)-H(2J1) 0.9900
C(2J)-H(2J2) 0.9900
C(3J)-C(4J) 1.515(7)
C(3J)-H(3J1) 0.9900
C(3J)-H(3J2) 0.9900
C(4J)-H(4J1) 0.9900
C(4J)-H(4J2) 0.9900
O(1K)-C(1K) 1.465(5)
O(1K)-C(4K) 1.477(6)
O(1K)-Li(6) 2.016(9)
O(1K)-Li(5) 2.052(9)
C(1K)-C(2K) 1.505(7)
C(1K)-H(1K1) 0.9900
C(1K)-H(1K2) 0.9900
C(2K)-C(3K) 1.529(7)
C(2K)-H(2K1) 0.9900
C(2K)-H(2K2) 0.9900
C(3K)-C(4K) 1.500(6)
C(3K)-H(3K1) 0.9900
C(3K)-H(3K2) 0.9900
C(4K)-H(4K1) 0.9900
C(4K)-H(4K2) 0.9900
O(1L)-C(1L) 1.460(6)
O(1L)-C(4L) 1.47(2)
O(1L)-C(4L') 1.48(3)

O(1L)-Li(7)	1.999(9)	C(2M)-H(2M)	0.9500
O(1L)-Li(8)	2.075(9)	C(3M)-C(4M)	1.380(10)
C(1L)-C(2L)	1.524(11)	C(3M)-H(3M)	0.9500
C(1L)-C(2L')	1.522(13)	C(4M)-C(5M)	1.370(10)
C(1L)-H(1L1)	0.9900	C(4M)-H(4M)	0.9500
C(1L)-H(1L2)	0.9900	C(5M)-C(6M)	1.366(10)
C(2L)-C(3L)	1.525(15)	C(5M)-H(5M)	0.9500
C(2L)-H(2L1)	0.9900	C(6M)-H(6M)	0.9500
C(2L)-H(2L2)	0.9900	C(1N)-C(3N)#5	1.369(9)
C(3L)-C(4L)	1.524(14)	C(1N)-C(2N)	1.375(9)
C(3L)-H(3L1)	0.9900	C(1N)-H(1N)	0.9500
C(3L)-H(3L2)	0.9900	C(2N)-C(3N)	1.374(9)
C(4L)-H(4L1)	0.9900	C(2N)-H(2N)	0.9500
C(4L)-H(4L2)	0.9900	C(3N)-H(3N)	0.9500
C(2L')-C(3L')	1.510(15)	C(1O)-C(3O)#6	1.367(9)
C(2L')-H(2L3)	0.9900	C(1O)-C(2O)	1.374(10)
C(2L')-H(2L4)	0.9900	C(1O)-H(1O)	0.9500
C(3L')-C(4L')	1.517(15)	C(2O)-C(3O)	1.372(9)
C(3L')-H(3L3)	0.9900	C(2O)-H(2O)	0.9500
C(3L')-H(3L4)	0.9900	C(3O)-H(3O)	0.9500
C(4L')-H(4L3)	0.9900	Li(1)-Li(2)	2.981(12)
C(4L')-H(4L4)	0.9900	Li(1)-Li(1)#2	3.114(18)
C(1M)-C(2M)	1.372(9)	Li(2)-Li(3)	3.036(12)
C(1M)-C(6M)	1.406(10)	Li(3)-Li(4)	2.532(13)
C(1M)-H(1M)	0.9500	Li(5)-Li(6)	2.956(12)
C(2M)-C(3M)	1.355(10)	Li(5)-Li(5)#3	3.109(19)

Li(6)-Li(7) 2.990(12)

Li(7)-Li(8) 2.516(13)

C(1A)-P(1A)-Li(8)#1 134.6(3)
C(1A)-P(1A)-Li(1) 102.6(3)
Li(8)#1-P(1A)-Li(1) 103.8(3)
C(1A)-P(1A)-Li(7)#1 99.3(3)
Li(8)#1-P(1A)-Li(7)#1 57.9(3)
Li(1)-P(1A)-Li(7)#1 158.0(3)
C(1A)-P(1A)-H(1P) 106.7(19)
Li(8)#1-P(1A)-H(1P) 111.3(18)
Li(1)-P(1A)-H(1P) 86.1(18)
Li(7)#1-P(1A)-H(1P) 89.7(18)
C(6A)-C(1A)-C(2A) 116.7(5)
C(6A)-C(1A)-P(1A) 120.9(4)
C(2A)-C(1A)-P(1A) 122.3(4)
C(3A)-C(2A)-C(1A) 121.0(5)
C(3A)-C(2A)-H(2A) 119.5
C(1A)-C(2A)-H(2A) 119.5
C(2A)-C(3A)-C(4A) 121.0(6)
C(2A)-C(3A)-H(3A) 119.5
C(4A)-C(3A)-H(3A) 119.5
C(5A)-C(4A)-C(3A) 118.4(6)
C(5A)-C(4A)-H(4A) 120.8
C(3A)-C(4A)-H(4A) 120.8
C(6A)-C(5A)-C(4A) 120.6(6)
C(6A)-C(5A)-H(5A) 119.7
C(4A)-C(5A)-H(5A) 119.7
C(5A)-C(6A)-C(1A) 122.2(5)
C(5A)-C(6A)-H(6A) 118.9
C(1A)-C(6A)-H(6A) 118.9
C(1B)-P(1B)-Li(2) 123.6(3)
C(1B)-P(1B)-Li(1) 129.9(3)
Li(2)-P(1B)-Li(1) 70.6(3)
C(1B)-P(1B)-Li(1)#2 103.0(3)
Li(2)-P(1B)-Li(1)#2 132.7(3)
Li(1)-P(1B)-Li(1)#2 73.4(3)
C(1B)-P(1B)-H(2P) 99.5(18)
Li(2)-P(1B)-H(2P) 96.9(18)
Li(1)-P(1B)-H(2P) 128.2(18)
Li(1)#2-P(1B)-H(2P) 82.0(18)
C(6B)-C(1B)-C(2B) 115.7(5)
C(6B)-C(1B)-P(1B) 123.6(4)
C(2B)-C(1B)-P(1B) 120.6(4)
C(3B)-C(2B)-C(1B) 121.7(6)
C(3B)-C(2B)-H(2B) 119.2
C(1B)-C(2B)-H(2B) 119.2
C(2B)-C(3B)-C(4B) 119.4(7)
C(2B)-C(3B)-H(3B) 120.3
C(4B)-C(3B)-H(3B) 120.3
C(5B)-C(4B)-C(3B) 118.8(8)

C(5B)-C(4B)-H(4B)	120.6	C(2C)-C(3C)-H(3C)	120.1
C(3B)-C(4B)-H(4B)	120.6	C(3C)-C(4C)-C(5C)	119.8(6)
C(4B)-C(5B)-C(6B)	122.0(8)	C(3C)-C(4C)-H(4C)	120.1
C(4B)-C(5B)-H(5B)	119.0	C(5C)-C(4C)-H(4C)	120.1
C(6B)-C(5B)-H(5B)	119.0	C(4C)-C(5C)-C(6C)	120.4(6)
C(5B)-C(6B)-C(1B)	122.4(7)	C(4C)-C(5C)-H(5C)	119.8
C(5B)-C(6B)-H(6B)	118.8	C(6C)-C(5C)-H(5C)	119.8
C(1B)-C(6B)-H(6B)	118.8	C(5C)-C(6C)-C(1C)	122.0(5)
C(1C)-P(1C)-Li(2)	105.3(3)	C(5C)-C(6C)-H(6C)	119.0
C(1C)-P(1C)-Li(4)	115.9(3)	C(1C)-C(6C)-H(6C)	119.0
Li(2)-P(1C)-Li(4)	124.0(3)	C(1D)-P(1D)-Li(5)	102.1(3)
C(1C)-P(1C)-Li(3)	113.9(3)	C(1D)-P(1D)-Li(4)	132.1(3)
Li(2)-P(1C)-Li(3)	71.6(3)	Li(5)-P(1D)-Li(4)	108.0(3)
Li(4)-P(1C)-Li(3)	58.0(3)	C(1D)-P(1D)-Li(3)	96.8(2)
C(1C)-P(1C)-H(3P)	102.5(18)	Li(5)-P(1D)-Li(3)	161.1(3)
Li(2)-P(1C)-H(3P)	111.0(18)	Li(4)-P(1D)-Li(3)	57.5(3)
Li(4)-P(1C)-H(3P)	95.8(18)	C(1D)-P(1D)-H(4P)	99.1(16)
Li(3)-P(1C)-H(3P)	141.5(18)	Li(5)-P(1D)-H(4P)	91.4(17)
C(2C)-C(1C)-C(6C)	115.5(5)	Li(4)-P(1D)-H(4P)	116.1(17)
C(2C)-C(1C)-P(1C)	125.5(4)	Li(3)-P(1D)-H(4P)	85.8(17)
C(6C)-C(1C)-P(1C)	119.0(4)	C(6D)-C(1D)-C(2D)	116.4(5)
C(3C)-C(2C)-C(1C)	122.5(6)	C(6D)-C(1D)-P(1D)	120.4(4)
C(3C)-C(2C)-H(2C)	118.7	C(2D)-C(1D)-P(1D)	123.2(4)
C(1C)-C(2C)-H(2C)	118.7	C(3D)-C(2D)-C(1D)	120.7(5)
C(4C)-C(3C)-C(2C)	119.8(6)	C(3D)-C(2D)-H(2D)	119.7
C(4C)-C(3C)-H(3C)	120.1	C(1D)-C(2D)-H(2D)	119.7

C(4D)-C(3D)-C(2D) 122.2(6)
C(4D)-C(3D)-H(3D) 118.9
C(2D)-C(3D)-H(3D) 118.9
C(3D)-C(4D)-C(5D) 118.6(5)
C(3D)-C(4D)-H(4D) 120.7
C(5D)-C(4D)-H(4D) 120.7
C(4D)-C(5D)-C(6D) 119.6(5)
C(4D)-C(5D)-H(5D) 120.2
C(6D)-C(5D)-H(5D) 120.2
C(5D)-C(6D)-C(1D) 122.6(5)
C(5D)-C(6D)-H(6D) 118.7
C(1D)-C(6D)-H(6D) 118.7
C(1E)-P(1E)-Li(5) 102.0(2)
C(1E)-P(1E)-Li(5)#3 134.5(3)
Li(5)-P(1E)-Li(5)#3 73.1(3)
C(1E)-P(1E)-Li(6)#3 126.7(2)
Li(5)-P(1E)-Li(6)#3 130.9(3)
Li(5)#3-P(1E)-Li(6)#3 68.6(3)
C(1E)-P(1E)-H(5P) 100.0(18)
Li(5)-P(1E)-H(5P) 81.8(18)
Li(5)#3-P(1E)-H(5P) 123.0(18)
Li(6)#3-P(1E)-H(5P) 94.2(18)
C(6E)-C(1E)-C(2E) 115.6(5)
C(6E)-C(1E)-P(1E) 120.7(4)
C(2E)-C(1E)-P(1E) 123.8(4)
C(3E)-C(2E)-C(1E) 121.0(5)
C(3E)-C(2E)-H(2E) 119.5
C(1E)-C(2E)-H(2E) 119.5
C(4E)-C(3E)-C(2E) 121.6(5)
C(4E)-C(3E)-H(3E) 119.2
C(2E)-C(3E)-H(3E) 119.2
C(3E)-C(4E)-C(5E) 118.6(5)
C(3E)-C(4E)-H(4E) 120.7
C(5E)-C(4E)-H(4E) 120.7
C(4E)-C(5E)-C(6E) 120.1(5)
C(4E)-C(5E)-H(5E) 120.0
C(6E)-C(5E)-H(5E) 120.0
C(1E)-C(6E)-C(5E) 123.1(5)
C(1E)-C(6E)-H(6E) 118.4
C(5E)-C(6E)-H(6E) 118.5
C(1F)-P(1F)-Li(4) 101.6(3)
C(1F)-P(1F)-Li(7) 73.5(3)
Li(4)-P(1F)-Li(7) 172.3(3)
C(1F)-P(1F)-Li(6) 112.3(3)
Li(4)-P(1F)-Li(6) 107.2(3)
Li(7)-P(1F)-Li(6) 70.2(3)
C(1F)-P(1F)-H(6P) 97.7(17)
Li(4)-P(1F)-H(6P) 112.0(18)
Li(7)-P(1F)-H(6P) 74.9(18)
Li(6)-P(1F)-H(6P) 123.7(18)
C(2F)-C(1F)-C(6F) 115.9(5)
C(2F)-C(1F)-P(1F) 118.9(4)

C(6F)-C(1F)-P(1F) 125.1(4)
C(2F)-C(1F)-Li(7) 108.8(4)
C(6F)-C(1F)-Li(7) 96.3(4)
P(1F)-C(1F)-Li(7) 66.3(2)
C(3F)-C(2F)-C(1F) 122.5(6)
C(3F)-C(2F)-H(2F) 118.8
C(1F)-C(2F)-H(2F) 118.8
C(4F)-C(3F)-C(2F) 119.7(5)
C(4F)-C(3F)-H(3F) 120.1
C(2F)-C(3F)-H(3F) 120.1
C(3F)-C(4F)-C(5F) 120.6(6)
C(3F)-C(4F)-H(4F) 119.7
C(5F)-C(4F)-H(4F) 119.7
C(6F)-C(5F)-C(4F) 119.7(6)
C(6F)-C(5F)-H(5F) 120.1
C(4F)-C(5F)-H(5F) 120.1
C(5F)-C(6F)-C(1F) 121.4(5)
C(5F)-C(6F)-H(6F) 119.3
C(1F)-C(6F)-H(6F) 119.3
C(1G)-P(1G)-Li(8) 118.4(2)
C(1G)-P(1G)-Li(6) 102.9(2)
Li(8)-P(1G)-Li(6) 124.6(3)
C(1G)-P(1G)-Li(7) 120.5(3)
Li(8)-P(1G)-Li(7) 58.0(3)
Li(6)-P(1G)-Li(7) 70.1(3)
C(1G)-P(1G)-H(7P) 94.8(18)
Li(8)-P(1G)-H(7P) 108.5(19)
Li(6)-P(1G)-H(7P) 102.6(18)
Li(7)-P(1G)-H(7P) 144.7(18)
C(6G)-C(1G)-C(2G) 116.2(5)
C(6G)-C(1G)-P(1G) 124.6(4)
C(2G)-C(1G)-P(1G) 119.1(4)
C(3G)-C(2G)-C(1G) 121.0(5)
C(3G)-C(2G)-H(2G) 119.5
C(1G)-C(2G)-H(2G) 119.5
C(4G)-C(3G)-C(2G) 121.6(6)
C(4G)-C(3G)-H(3G) 119.2
C(2G)-C(3G)-H(3G) 119.2
C(3G)-C(4G)-C(5G) 118.4(6)
C(3G)-C(4G)-H(4G) 120.8
C(5G)-C(4G)-H(4G) 120.8
C(4G)-C(5G)-C(6G) 120.3(6)
C(4G)-C(5G)-H(5G) 119.9
C(6G)-C(5G)-H(5G) 119.9
C(5G)-C(6G)-C(1G) 122.5(5)
C(5G)-C(6G)-H(6G) 118.7
C(1G)-C(6G)-H(6G) 118.7
C(1H)-P(1H)-Li(8) 105.9(3)
C(1H)-P(1H)-Li(3)#4 75.6(3)
Li(8)-P(1H)-Li(3)#4 178.5(3)
C(1H)-P(1H)-Li(2)#4 120.2(3)
Li(8)-P(1H)-Li(2)#4 106.5(3)

Li(3)#4-P(1H)-Li(2)#4	72.6(3)	C(1I)-O(1I)-C(4I)	107.5(4)
C(1H)-P(1H)-H(8P)	97.1(17)	C(1I)-O(1I)-Li(1)	117.0(4)
Li(8)-P(1H)-H(8P)	106.0(18)	C(4I)-O(1I)-Li(1)	109.6(4)
Li(3)#4-P(1H)-H(8P)	73.6(18)	C(1I)-O(1I)-Li(2)	121.6(4)
Li(2)#4-P(1H)-H(8P)	119.7(17)	C(4I)-O(1I)-Li(2)	106.0(4)
C(2H)-C(1H)-C(6H)	116.9(5)	Li(1)-O(1I)-Li(2)	94.0(4)
C(2H)-C(1H)-P(1H)	119.5(4)	O(1I)-C(1I)-C(2I)	105.6(4)
C(6H)-C(1H)-P(1H)	123.7(4)	O(1I)-C(1I)-H(1I1)	110.6
C(2H)-C(1H)-Li(3)#4	112.9(4)	C(2I)-C(1I)-H(1I1)	110.6
C(6H)-C(1H)-Li(3)#4	94.1(4)	O(1I)-C(1I)-H(1I2)	110.6
P(1H)-C(1H)-Li(3)#4	64.4(2)	C(2I)-C(1I)-H(1I2)	110.6
C(3H)-C(2H)-C(1H)	121.1(5)	H(1I1)-C(1I)-H(1I2)	108.8
C(3H)-C(2H)-H(2H)	119.4	C(1I)-C(2I)-C(3I)	102.6(4)
C(1H)-C(2H)-H(2H)	119.4	C(1I)-C(2I)-H(2I1)	111.2
C(4H)-C(3H)-C(2H)	120.4(6)	C(3I)-C(2I)-H(2I1)	111.2
C(4H)-C(3H)-H(3H)	119.8	C(1I)-C(2I)-H(2I2)	111.2
C(2H)-C(3H)-H(3H)	119.8	C(3I)-C(2I)-H(2I2)	111.2
C(5H)-C(4H)-C(3H)	118.9(6)	H(2I1)-C(2I)-H(2I2)	109.2
C(5H)-C(4H)-H(4H)	120.6	C(4I)-C(3I)-C(2I)	103.3(4)
C(3H)-C(4H)-H(4H)	120.6	C(4I)-C(3I)-H(3I1)	111.1
C(4H)-C(5H)-C(6H)	121.5(6)	C(2I)-C(3I)-H(3I1)	111.1
C(4H)-C(5H)-H(5H)	119.2	C(4I)-C(3I)-H(3I2)	111.1
C(6H)-C(5H)-H(5H)	119.2	C(2I)-C(3I)-H(3I2)	111.1
C(5H)-C(6H)-C(1H)	121.1(5)	H(3I1)-C(3I)-H(3I2)	109.1
C(5H)-C(6H)-H(6H)	119.4	O(1I)-C(4I)-C(3I)	106.1(4)
C(1H)-C(6H)-H(6H)	119.4	O(1I)-C(4I)-H(4I1)	110.5

C(3I)-C(4I)-H(4I1)	110.5	C(2J)-C(3J)-H(3J2)	111.0
O(1I)-C(4I)-H(4I2)	110.5	H(3J1)-C(3J)-H(3J2)	109.0
C(3I)-C(4I)-H(4I2)	110.5	O(1J)-C(4J)-C(3J)	106.4(4)
H(4I1)-C(4I)-H(4I2)	108.7	O(1J)-C(4J)-H(4J1)	110.5
C(1J)-O(1J)-C(4J)	108.5(4)	C(3J)-C(4J)-H(4J1)	110.5
C(1J)-O(1J)-Li(3)	118.6(4)	O(1J)-C(4J)-H(4J2)	110.5
C(4J)-O(1J)-Li(3)	115.2(4)	C(3J)-C(4J)-H(4J2)	110.5
C(1J)-O(1J)-Li(4)	115.7(4)	H(4J1)-C(4J)-H(4J2)	108.6
C(4J)-O(1J)-Li(4)	120.2(4)	C(1K)-O(1K)-C(4K)	108.4(3)
Li(3)-O(1J)-Li(4)	76.0(4)	C(1K)-O(1K)-Li(6)	118.9(4)
O(1J)-C(1J)-C(2J)	105.0(4)	C(4K)-O(1K)-Li(6)	108.8(4)
O(1J)-C(1J)-H(1J1)	110.7	C(1K)-O(1K)-Li(5)	116.0(4)
C(2J)-C(1J)-H(1J1)	110.7	C(4K)-O(1K)-Li(5)	110.8(4)
O(1J)-C(1J)-H(1J2)	110.7	Li(6)-O(1K)-Li(5)	93.2(4)
C(2J)-C(1J)-H(1J2)	110.7	O(1K)-C(1K)-C(2K)	104.8(4)
H(1J1)-C(1J)-H(1J2)	108.8	O(1K)-C(1K)-H(1K1)	110.8
C(1J)-C(2J)-C(3J)	103.4(5)	C(2K)-C(1K)-H(1K1)	110.8
C(1J)-C(2J)-H(2J1)	111.1	O(1K)-C(1K)-H(1K2)	110.8
C(3J)-C(2J)-H(2J1)	111.1	C(2K)-C(1K)-H(1K2)	110.8
C(1J)-C(2J)-H(2J2)	111.1	H(1K1)-C(1K)-H(1K2)	108.9
C(3J)-C(2J)-H(2J2)	111.1	C(1K)-C(2K)-C(3K)	102.0(4)
H(2J1)-C(2J)-H(2J2)	109.1	C(1K)-C(2K)-H(2K1)	111.4
C(4J)-C(3J)-C(2J)	103.7(5)	C(3K)-C(2K)-H(2K1)	111.4
C(4J)-C(3J)-H(3J1)	111.0	C(1K)-C(2K)-H(2K2)	111.4
C(2J)-C(3J)-H(3J1)	111.0	C(3K)-C(2K)-H(2K2)	111.4
C(4J)-C(3J)-H(3J2)	111.0	H(2K1)-C(2K)-H(2K2)	109.2

C(4K)-C(3K)-C(2K) 103.0(4)
C(4K)-C(3K)-H(3K1) 111.2
C(2K)-C(3K)-H(3K1) 111.2
C(4K)-C(3K)-H(3K2) 111.2
C(2K)-C(3K)-H(3K2) 111.2
H(3K1)-C(3K)-H(3K2) 109.1
O(1K)-C(4K)-C(3K) 106.1(4)
O(1K)-C(4K)-H(4K1) 110.5
C(3K)-C(4K)-H(4K1) 110.5
O(1K)-C(4K)-H(4K2) 110.5
C(3K)-C(4K)-H(4K2) 110.5
H(4K1)-C(4K)-H(4K2) 108.7
C(1L)-O(1L)-C(4L) 108.1(6)
C(1L)-O(1L)-C(4L') 106.9(7)
C(1L)-O(1L)-Li(7) 117.4(4)
C(4L)-O(1L)-Li(7) 125.0(7)
C(4L')-O(1L)-Li(7) 115.5(8)
C(1L)-O(1L)-Li(8) 114.2(4)
C(4L)-O(1L)-Li(8) 112.0(9)
C(4L')-O(1L)-Li(8) 124.5(11)
Li(7)-O(1L)-Li(8) 76.3(4)
O(1L)-C(1L)-C(2L) 107.1(7)
O(1L)-C(1L)-C(2L') 105.4(8)
O(1L)-C(1L)-H(1L1) 110.3
C(2L)-C(1L)-H(1L1) 110.3
O(1L)-C(1L)-H(1L2) 110.3
C(2L)-C(1L)-H(1L2) 110.3
H(1L1)-C(1L)-H(1L2) 108.6
C(3L)-C(2L)-C(1L) 102.2(9)
C(3L)-C(2L)-H(2L1) 111.3
C(1L)-C(2L)-H(2L1) 111.3
C(3L)-C(2L)-H(2L2) 111.3
C(1L)-C(2L)-H(2L2) 111.3
H(2L1)-C(2L)-H(2L2) 109.2
C(2L)-C(3L)-C(4L) 102.1(12)
C(2L)-C(3L)-H(3L1) 111.4
C(4L)-C(3L)-H(3L1) 111.4
C(2L)-C(3L)-H(3L2) 111.4
C(4L)-C(3L)-H(3L2) 111.4
H(3L1)-C(3L)-H(3L2) 109.2
O(1L)-C(4L)-C(3L) 105.2(12)
O(1L)-C(4L)-H(4L1) 110.7
C(3L)-C(4L)-H(4L1) 110.7
O(1L)-C(4L)-H(4L2) 110.7
C(3L)-C(4L)-H(4L2) 110.7
H(4L1)-C(4L)-H(4L2) 108.8
C(3L')-C(2L')-C(1L) 105.0(11)
C(3L')-C(2L')-H(2L3) 110.8
C(1L)-C(2L')-H(2L3) 110.7
C(3L')-C(2L')-H(2L4) 110.8
C(1L)-C(2L')-H(2L4) 110.8
H(2L3)-C(2L')-H(2L4) 108.8

C(2L')-C(3L')-C(4L')	103.7(13)	C(4M)-C(5M)-H(5M)	119.7
C(2L')-C(3L')-H(3L3)	111.0	C(5M)-C(6M)-C(1M)	119.1(7)
C(4L')-C(3L')-H(3L3)	111.0	C(5M)-C(6M)-H(6M)	120.5
C(2L')-C(3L')-H(3L4)	111.0	C(1M)-C(6M)-H(6M)	120.5
C(4L')-C(3L')-H(3L4)	111.0	C(3N)#5-C(1N)-C(2N)	118.9(7)
H(3L3)-C(3L')-H(3L4)	109.0	C(3N)#5-C(1N)-H(1N)	120.5
O(1L)-C(4L')-C(3L')	100.4(16)	C(2N)-C(1N)-H(1N)	120.5
O(1L)-C(4L')-H(4L3)	111.7	C(3N)-C(2N)-C(1N)	120.8(7)
C(3L')-C(4L')-H(4L3)	111.7	C(3N)-C(2N)-H(2N)	119.6
O(1L)-C(4L')-H(4L4)	111.7	C(1N)-C(2N)-H(2N)	119.6
C(3L')-C(4L')-H(4L4)	111.7	C(1N)#5-C(3N)-C(2N)	120.2(7)
H(4L3)-C(4L')-H(4L4)	109.5	C(1N)#5-C(3N)-H(3N)	119.9
C(2M)-C(1M)-C(6M)	119.9(8)	C(2N)-C(3N)-H(3N)	119.9
C(2M)-C(1M)-H(1M)	120.0	C(3O)#6-C(1O)-C(2O)	119.3(7)
C(6M)-C(1M)-H(1M)	120.0	C(3O)#6-C(1O)-H(1O)	120.4
C(3M)-C(2M)-C(1M)	120.0(8)	C(2O)-C(1O)-H(1O)	120.4
C(3M)-C(2M)-H(2M)	120.0	C(3O)-C(2O)-C(1O)	122.2(8)
C(1M)-C(2M)-H(2M)	120.0	C(3O)-C(2O)-H(2O)	118.9
C(2M)-C(3M)-C(4M)	120.7(8)	C(1O)-C(2O)-H(2O)	118.9
C(2M)-C(3M)-H(3M)	119.7	C(1O)#6-C(3O)-C(2O)	118.5(8)
C(4M)-C(3M)-H(3M)	119.7	C(1O)#6-C(3O)-H(3O)	120.7
C(5M)-C(4M)-C(3M)	119.8(8)	C(2O)-C(3O)-H(3O)	120.7
C(5M)-C(4M)-H(4M)	120.1	O(1I)-Li(1)-P(1A)	110.1(4)
C(3M)-C(4M)-H(4M)	120.1	O(1I)-Li(1)-P(1B)	88.8(3)
C(6M)-C(5M)-C(4M)	120.5(8)	P(1A)-Li(1)-P(1B)	122.6(3)
C(6M)-C(5M)-H(5M)	119.7	O(1I)-Li(1)-P(1B)#2	119.7(4)

P(1A)-Li(1)-P(1B)#2 108.7(3)
P(1B)-Li(1)-P(1B)#2 106.6(3)
O(1I)-Li(1)-Li(2) 43.1(3)
P(1A)-Li(1)-Li(2) 104.9(3)
P(1B)-Li(1)-Li(2) 54.3(2)
P(1B)#2-Li(1)-Li(2) 146.3(4)
O(1I)-Li(1)-Li(1)#2 113.5(5)
P(1A)-Li(1)-Li(1)#2 136.0(5)
P(1B)-Li(1)-Li(1)#2 53.6(3)
P(1B)#2-Li(1)-Li(1)#2 53.0(3)
Li(2)-Li(1)-Li(1)#2 102.3(4)
O(1I)-Li(2)-P(1C) 117.9(4)
O(1I)-Li(2)-P(1B) 89.2(3)
P(1C)-Li(2)-P(1B) 114.4(3)
O(1I)-Li(2)-P(1H)#1 107.6(4)
P(1C)-Li(2)-P(1H)#1 104.5(3)
P(1B)-Li(2)-P(1H)#1 123.2(3)
O(1I)-Li(2)-Li(1) 42.8(3)
P(1C)-Li(2)-Li(1) 150.7(4)
P(1B)-Li(2)-Li(1) 55.1(2)
P(1H)#1-Li(2)-Li(1) 103.2(3)
O(1I)-Li(2)-Li(3) 146.7(4)
P(1C)-Li(2)-Li(3) 55.6(2)
P(1B)-Li(2)-Li(3) 123.9(4)
P(1H)#1-Li(2)-Li(3) 53.3(2)
Li(1)-Li(2)-Li(3) 153.7(4)
O(1J)-Li(3)-Li(4) 54.2(3)
O(1J)-Li(3)-P(1H)#1 128.5(4)
Li(4)-Li(3)-P(1H)#1 162.2(4)
O(1J)-Li(3)-P(1C) 90.8(3)
Li(4)-Li(3)-P(1C) 59.8(3)
P(1H)#1-Li(3)-P(1C) 102.8(3)
O(1J)-Li(3)-P(1D) 97.5(4)
Li(4)-Li(3)-P(1D) 60.5(3)
P(1H)#1-Li(3)-P(1D) 129.4(4)
P(1C)-Li(3)-P(1D) 95.6(3)
O(1J)-Li(3)-C(1H)#1 98.4(4)
Li(4)-Li(3)-C(1H)#1 151.8(5)
P(1H)#1-Li(3)-C(1H)#1 40.06(17)
P(1C)-Li(3)-C(1H)#1 135.7(4)
P(1D)-Li(3)-C(1H)#1 125.5(3)
O(1J)-Li(3)-Li(2) 104.5(4)
Li(4)-Li(3)-Li(2) 108.5(4)
P(1H)#1-Li(3)-Li(2) 54.1(2)
P(1C)-Li(3)-Li(2) 52.9(2)
P(1D)-Li(3)-Li(2) 140.9(4)
C(1H)#1-Li(3)-Li(2) 82.9(3)
O(1J)-Li(4)-P(1F) 123.6(5)
O(1J)-Li(4)-Li(3) 49.8(3)
P(1F)-Li(4)-Li(3) 166.9(5)
O(1J)-Li(4)-P(1C) 89.8(4)
P(1F)-Li(4)-P(1C) 130.9(4)

Li(3)-Li(4)-P(1C)	62.2(3)	O(1K)-Li(6)-Li(5)	43.9(3)
O(1J)-Li(4)-P(1D)	95.6(3)	P(1G)-Li(6)-Li(5)	150.0(4)
P(1F)-Li(4)-P(1D)	111.4(4)	P(1E)#3-Li(6)-Li(5)	55.5(2)
Li(3)-Li(4)-P(1D)	62.0(3)	P(1F)-Li(6)-Li(5)	105.3(3)
P(1C)-Li(4)-P(1D)	98.1(3)	O(1K)-Li(6)-Li(7)	152.1(4)
O(1K)-Li(5)-P(1D)	110.2(4)	P(1G)-Li(6)-Li(7)	55.7(2)
O(1K)-Li(5)-P(1E)	118.8(4)	P(1E)#3-Li(6)-Li(7)	118.0(3)
P(1D)-Li(5)-P(1E)	110.5(3)	P(1F)-Li(6)-Li(7)	53.9(2)
O(1K)-Li(5)-P(1E)#3	89.4(3)	Li(5)-Li(6)-Li(7)	152.8(4)
P(1D)-Li(5)-P(1E)#3	120.2(4)	O(1L)-Li(7)-Li(8)	53.2(3)
P(1E)-Li(5)-P(1E)#3	106.9(3)	O(1L)-Li(7)-P(1F)	136.9(4)
O(1K)-Li(5)-Li(6)	42.9(3)	Li(8)-Li(7)-P(1F)	163.7(5)
P(1D)-Li(5)-Li(6)	102.3(3)	O(1L)-Li(7)-P(1A)#4	97.4(3)
P(1E)-Li(5)-Li(6)	147.1(4)	Li(8)-Li(7)-P(1A)#4	60.0(3)
P(1E)#3-Li(5)-Li(6)	55.9(2)	P(1F)-Li(7)-P(1A)#4	121.0(3)
O(1K)-Li(5)-Li(5)#3	113.2(5)	O(1L)-Li(7)-P(1G)	89.2(3)
P(1D)-Li(5)-Li(5)#3	135.8(5)	Li(8)-Li(7)-P(1G)	59.7(3)
P(1E)-Li(5)-Li(5)#3	53.7(3)	P(1F)-Li(7)-P(1G)	104.7(3)
P(1E)#3-Li(5)-Li(5)#3	53.2(3)	P(1A)#4-Li(7)-P(1G)	95.3(3)
Li(6)-Li(5)-Li(5)#3	103.3(4)	O(1L)-Li(7)-C(1F)	103.2(4)
O(1K)-Li(6)-P(1G)	118.6(4)	Li(8)-Li(7)-C(1F)	155.1(5)
O(1K)-Li(6)-P(1E)#3	89.9(3)	P(1F)-Li(7)-C(1F)	40.27(18)
P(1G)-Li(6)-P(1E)#3	110.5(3)	P(1A)#4-Li(7)-C(1F)	124.0(4)
O(1K)-Li(6)-P(1F)	110.3(4)	P(1G)-Li(7)-C(1F)	135.8(4)
P(1G)-Li(6)-P(1F)	104.2(3)	O(1L)-Li(7)-Li(6)	108.1(4)
P(1E)#3-Li(6)-P(1F)	124.1(3)	Li(8)-Li(7)-Li(6)	111.3(4)

P(1F)-Li(7)-Li(6)	56.0(2)
P(1A)#4-Li(7)-Li(6)	138.6(4)
P(1G)-Li(7)-Li(6)	54.2(2)
C(1F)-Li(7)-Li(6)	81.7(3)
O(1L)-Li(8)-P(1H)	119.5(4)
O(1L)-Li(8)-Li(7)	50.5(3)
P(1H)-Li(8)-Li(7)	165.4(5)
O(1L)-Li(8)-P(1G)	89.3(3)
P(1H)-Li(8)-P(1G)	131.7(4)
Li(7)-Li(8)-P(1G)	62.3(3)
O(1L)-Li(8)-P(1A)#4	97.0(4)
P(1H)-Li(8)-P(1A)#4	113.9(3)
Li(7)-Li(8)-P(1A)#4	62.1(3)
P(1G)-Li(8)-P(1A)#4	98.2(3)

Symmetry transformations used to generate equivalent atoms:

#1 x, y-1, z #2 -x+1, -y, -z+1 #3 -x+1, -y+1, -z

#4 x, y+1, z #5 -x, -y, -z #6 -x+1, -y, -z

Table 4. Anisotropic displacement parameters (Å2x 103) for SBY-4-023. The anisotropic displacement factor exponent takes the form:

-2 p2[h2 *a**2 U11 + ... + 2 h k *a** *b** U12]

	U11	U22	U33	U23	U13	U12
P(1A)	45(1)	29(1)	21(1)	2(1)	10(1)	4(1)
C(1A)	41(3)	16(3)	18(3)	-5(2)	12(2)	2(2)
C(2A)	47(4)	20(3)	21(3)	0(3)	14(3)	4(3)
C(3A)	56(4)	34(4)	27(4)	6(3)	19(3)	9(3)
C(4A)	49(4)	62(4)	25(4)	8(3)	8(3)	12(3)
C(5A)	46(4)	61(4)	20(4)	-4(3)	7(3)	-3(3)
C(6A)	41(3)	28(3)	26(4)	-1(3)	10(3)	-6(3)
P(1B)	39(1)	28(1)	25(1)	3(1)	7(1)	-6(1)
C(1B)	42(3)	22(3)	15(3)	1(2)	8(3)	-8(2)
C(2B)	51(4)	53(4)	36(4)	12(3)	21(3)	7(3)
C(3B)	46(4)	126(7)	53(5)	51(4)	33(4)	35(4)
C(4B)	43(5)	181(9)	36(5)	34(5)	-1(4)	-30(5)
C(5B)	69(5)	125(7)	39(5)	-19(5)	10(4)	-65(5)
C(6B)	57(4)	43(4)	28(4)	-8(3)	12(3)	-26(3)

P(1C)	40(1)	24(1)	24(1)	1(1)	12(1)	0(1)
C(1C)	41(3)	22(3)	23(3)	12(2)	14(3)	-4(3)
C(2C)	46(3)	31(4)	33(4)	14(3)	17(3)	1(3)
C(3C)	38(4)	51(4)	51(4)	17(3)	14(3)	2(3)
C(4C)	42(4)	58(5)	38(4)	19(3)	1(3)	-11(3)
C(5C)	49(4)	53(4)	32(4)	7(3)	9(3)	-15(3)
C(6C)	39(3)	34(4)	30(4)	2(3)	15(3)	-6(3)
P(1D)	44(1)	32(1)	24(1)	4(1)	11(1)	5(1)
C(1D)	45(3)	21(3)	24(3)	13(2)	12(3)	7(3)
C(2D)	54(4)	24(3)	21(3)	6(3)	10(3)	1(3)
C(3D)	68(4)	25(4)	29(4)	4(3)	19(3)	6(3)
C(4D)	57(4)	33(4)	40(4)	9(3)	25(3)	11(3)
C(5D)	45(4)	40(4)	25(4)	16(3)	13(3)	4(3)
C(6D)	49(3)	19(3)	22(3)	8(3)	11(3)	5(3)
P(1E)	35(1)	23(1)	24(1)	-1(1)	10(1)	-3(1)
C(1E)	36(3)	28(3)	9(3)	-4(2)	7(3)	0(2)
C(2E)	47(3)	23(3)	23(3)	-2(3)	14(3)	1(3)
C(3E)	44(3)	33(3)	32(4)	-8(3)	19(3)	-11(3)
C(4E)	40(4)	36(4)	36(4)	-9(3)	14(3)	-7(3)
C(5E)	38(3)	41(4)	29(4)	-2(3)	4(3)	3(3)
C(6E)	36(3)	32(3)	17(3)	2(3)	7(3)	-5(2)
P(1F)	42(1)	17(1)	29(1)	1(1)	10(1)	0(1)
C(1F)	50(3)	8(3)	24(3)	0(2)	15(3)	0(3)
C(2F)	47(3)	19(3)	32(4)	1(3)	12(3)	0(3)
C(3F)	53(4)	19(3)	44(4)	3(3)	20(3)	-2(3)
C(4F)	38(4)	26(4)	58(4)	2(3)	12(3)	-3(3)

C(5F)	47(3)	29(4)	38(4)	2(3)	11(3)	-8(3)
C(6F)	46(3)	22(3)	28(3)	2(3)	14(3)	-3(3)
P(1G)	37(1)	23(1)	20(1)	2(1)	10(1)	-1(1)
C(1G)	37(3)	10(3)	18(3)	-9(2)	2(2)	-3(2)
C(2G)	40(3)	22(3)	27(3)	4(3)	8(3)	2(3)
C(3G)	45(4)	37(4)	51(4)	11(3)	22(3)	0(3)
C(4G)	41(4)	33(4)	64(5)	2(3)	24(3)	8(3)
C(5G)	33(3)	25(3)	52(4)	-2(3)	6(3)	5(3)
C(6G)	39(3)	23(3)	25(3)	-3(3)	5(3)	-2(3)
P(1H)	39(1)	19(1)	28(1)	0(1)	10(1)	0(1)
C(1H)	44(3)	10(3)	22(3)	0(2)	10(2)	3(2)
C(2H)	45(3)	18(3)	33(3)	3(3)	15(3)	-2(3)
C(3H)	43(3)	25(3)	37(4)	7(3)	-1(3)	4(3)
C(4H)	39(4)	24(3)	57(4)	8(3)	12(3)	-3(3)
C(5H)	49(4)	34(4)	40(4)	15(3)	20(3)	3(3)
C(6H)	40(3)	21(3)	29(3)	6(3)	9(3)	4(3)
O(1I)	32(2)	24(2)	21(2)	-5(2)	5(2)	-2(2)
C(1I)	45(3)	33(4)	20(3)	-5(3)	0(3)	-8(3)
C(2I)	40(3)	46(4)	36(4)	2(3)	-1(3)	-14(3)
C(3I)	38(3)	44(4)	35(4)	8(3)	8(3)	1(3)
C(4I)	40(3)	25(3)	30(4)	-3(3)	16(3)	0(3)
O(1J)	40(2)	17(2)	28(2)	1(2)	7(2)	-6(2)
C(1J)	38(3)	27(3)	43(4)	5(3)	16(3)	-7(3)
C(2J)	39(4)	33(4)	50(4)	3(3)	4(3)	-4(3)
C(3J)	49(4)	37(4)	38(4)	-3(3)	8(3)	-1(3)
C(4J)	59(4)	49(4)	23(3)	-5(3)	8(3)	-15(3)

O(1K)	31(2)	25(2)	23(2)	6(2)	11(2)	0(2)
C(1K)	41(3)	31(3)	23(3)	15(3)	14(3)	-3(3)
C(2K)	38(3)	37(4)	28(4)	6(3)	12(3)	-3(3)
C(3K)	33(3)	20(3)	33(4)	0(3)	7(3)	4(3)
C(4K)	34(3)	25(3)	23(3)	3(3)	3(3)	4(3)
O(1L)	34(2)	26(2)	18(2)	-3(2)	5(2)	0(2)
C(1L)	36(3)	29(3)	30(3)	-3(3)	1(2)	-4(3)
C(2L)	35(7)	34(10)	45(7)	-13(6)	15(5)	-4(8)
C(3L)	49(6)	29(8)	31(6)	-4(5)	16(5)	-3(6)
C(4L)	49(7)	39(12)	20(5)	-6(7)	12(5)	-2(7)
C(2L')	38(9)	39(14)	44(8)	-10(9)	13(6)	-10(10)
C(3L')	43(9)	35(9)	38(7)	-10(7)	20(6)	-9(8)
C(4L')	24(9)	24(10)	15(6)	5(7)	6(6)	8(6)
C(1M)	96(5)	50(5)	61(5)	-11(4)	19(4)	16(4)
C(2M)	92(6)	44(4)	70(5)	1(4)	37(4)	-1(4)
C(3M)	116(6)	46(5)	62(5)	17(4)	34(4)	22(5)
C(4M)	103(6)	43(5)	78(5)	-1(4)	3(5)	19(5)
C(5M)	81(6)	39(5)	119(6)	5(5)	35(5)	20(4)
C(6M)	117(6)	44(5)	70(5)	5(4)	52(5)	14(5)
C(1N)	89(5)	32(4)	65(6)	10(4)	23(4)	14(4)
C(2N)	104(5)	30(4)	52(5)	1(4)	8(4)	20(4)
C(3N)	85(5)	30(4)	75(6)	-2(4)	4(4)	19(4)
C(1O)	103(6)	68(6)	37(5)	-9(4)	15(5)	-28(4)
C(2O)	121(7)	56(5)	51(5)	1(4)	19(5)	-15(5)
C(3O)	104(6)	55(5)	46(5)	-7(4)	9(4)	-13(4)
Li(1)	37(6)	32(6)	33(6)	8(5)	9(5)	-2(4)

Li(2)	38(6)	24(5)	24(6)	6(4)	7(5)	-1(4)
Li(3)	37(6)	30(6)	35(6)	-4(5)	6(5)	1(5)
Li(4)	55(7)	38(6)	32(6)	2(5)	17(5)	8(5)
Li(5)	37(6)	32(6)	39(6)	-10(5)	12(5)	-2(5)
Li(6)	39(6)	25(5)	19(5)	-5(4)	4(4)	-5(4)
Li(7)	48(6)	29(6)	23(6)	1(4)	14(5)	-8(5)
Li(8)	50(6)	30(6)	26(6)	-3(5)	8(5)	2(5)

Table 5. Hydrogen coordinates and isotropic displacement parameters for SBY-4-023.

	x	y	z	U(eq)
H(1P)	0.485(3)	-0.215(3)	0.370(2)	0.037
H(2A)	0.572783	-0.300792	0.477636	0.034
H(3A)	0.692625	-0.350598	0.567461	0.045
H(4A)	0.864075	-0.291099	0.590957	0.054
H(5A)	0.912346	-0.180874	0.521263	0.051
H(6A)	0.793795	-0.131780	0.431074	0.037
H(2P)	0.548(3)	0.185(3)	0.493(2)	0.037
H(2B)	0.774416	0.008790	0.482734	0.054
H(3B)	0.949339	0.031314	0.534743	0.085
H(4B)	1.003871	0.165508	0.596465	0.106
H(5B)	0.885064	0.272241	0.601637	0.095
H(6B)	0.713364	0.250171	0.553214	0.052

H(3P)	0.444(3)	0.328(3)	0.362(2)	0.034
H(2C)	0.250649	0.341106	0.303736	0.043
H(3C)	0.090253	0.314440	0.231849	0.055
H(4C)	0.078463	0.223743	0.136069	0.057
H(5C)	0.225842	0.154739	0.115001	0.054
H(6C)	0.385360	0.178999	0.186770	0.040
H(4P)	0.486(3)	0.272(3)	0.121(2)	0.039
H(2D)	0.581307	0.194194	0.046115	0.039
H(3D)	0.708625	0.143956	-0.008431	0.047
H(4D)	0.873953	0.211329	0.009555	0.049
H(5D)	0.912781	0.333617	0.085231	0.043
H(6D)	0.786028	0.384313	0.141443	0.035
H(5P)	0.456(3)	0.320(3)	-0.024(2)	0.032
H(2E)	0.293054	0.242177	-0.001946	0.036
H(3E)	0.119061	0.212977	0.000469	0.042
H(4E)	-0.006873	0.316283	-0.037992	0.044
H(5E)	0.043994	0.451779	-0.080850	0.044
H(6E)	0.217328	0.480804	-0.086241	0.034
H(6P)	0.574(3)	0.591(3)	0.340(2)	0.035
H(2F)	0.756765	0.559947	0.202549	0.039
H(3F)	0.935865	0.581743	0.221979	0.045
H(4F)	1.027286	0.620602	0.329305	0.048
H(5F)	0.938971	0.642263	0.417532	0.046
H(6F)	0.758578	0.622255	0.398639	0.038
H(7P)	0.440(3)	0.812(3)	0.123(2)	0.032
H(2G)	0.366113	0.693642	0.280401	0.036

H(3G)	0.197860	0.673209	0.297653	0.051
H(4G)	0.058051	0.734863	0.226115	0.053
H(5G)	0.090368	0.821667	0.136732	0.044
H(6G)	0.258920	0.845678	0.120395	0.035
H(8P)	0.573(3)	1.082(3)	0.188(2)	0.034
H(2H)	0.789853	1.066297	0.359347	0.037
H(3H)	0.967734	1.096475	0.367257	0.044
H(4H)	1.032418	1.139493	0.272041	0.047
H(5H)	0.919531	1.144642	0.169201	0.047
H(6H)	0.742594	1.115634	0.159629	0.035
H(1I1)	0.365297	-0.082638	0.295314	0.041
H(1I2)	0.345519	0.008662	0.254202	0.041
H(2I1)	0.214992	-0.073625	0.335147	0.050
H(2I2)	0.179361	-0.030777	0.261716	0.050
H(3I1)	0.207699	0.113562	0.304679	0.047
H(3I2)	0.161174	0.064756	0.363611	0.047
H(4I1)	0.342480	0.144289	0.389998	0.036
H(4I2)	0.318430	0.056933	0.430751	0.036
H(1J1)	0.808388	0.389421	0.261213	0.042
H(1J2)	0.845493	0.288126	0.272166	0.042
H(2J1)	0.877967	0.430882	0.369635	0.050
H(2J2)	0.961849	0.359834	0.355570	0.050
H(3J1)	0.890101	0.247841	0.410133	0.050
H(3J2)	0.869404	0.332983	0.454888	0.050
H(4J1)	0.715795	0.228492	0.389360	0.053
H(4J2)	0.698774	0.330769	0.409052	0.053

H(1K1)	0.334831	0.514279	0.202667	0.037
H(1K2)	0.360248	0.422110	0.168045	0.037
H(2K1)	0.170665	0.467082	0.149426	0.040
H(2K2)	0.212117	0.425502	0.085804	0.040
H(3K1)	0.154315	0.563491	0.044368	0.034
H(3K2)	0.195877	0.613358	0.116357	0.034
H(4K1)	0.314665	0.560191	0.020397	0.033
H(4K2)	0.334602	0.646996	0.069736	0.033
H(1L1)	0.841552	0.791494	0.313907	0.039
H(1L2)	0.805121	0.892843	0.317197	0.039
H(2L1)	0.887795	0.936861	0.233313	0.044
H(2L2)	0.962425	0.856187	0.261377	0.044
H(3L1)	0.871958	0.755471	0.180335	0.042
H(3L2)	0.869916	0.845754	0.137279	0.042
H(4L1)	0.703481	0.876833	0.150174	0.043
H(4L2)	0.694353	0.769234	0.145051	0.043
H(2L3)	0.909742	0.938823	0.251402	0.048
H(2L4)	0.947045	0.838349	0.243345	0.048
H(3L3)	0.861138	0.853046	0.136085	0.045
H(3L4)	0.784773	0.926310	0.157024	0.045
H(4L3)	0.676027	0.798542	0.138867	0.025
H(4L4)	0.768291	0.735463	0.174514	0.025
H(1M)	0.406349	0.562880	0.529177	0.082
H(2M)	0.461185	0.558161	0.426619	0.079
H(3M)	0.342822	0.524429	0.328593	0.087
H(4M)	0.167049	0.498376	0.330739	0.092

H(5M)	0.110874	0.502128	0.432577	0.093
H(6M)	0.229657	0.529064	0.532796	0.086
H(1N)	-0.132273	0.015556	0.061439	0.072
H(2N)	0.041384	0.011383	0.116491	0.075
H(3N)	0.171839	-0.011595	0.055942	0.077
H(1O)	0.418786	0.023669	0.091202	0.084
H(2O)	0.575090	-0.048854	0.105079	0.091
H(3O)	0.660032	-0.070050	0.015972	0.084

Table 6. Torsion angles [°] for SBY-4-023.

Li(8)#1-P(1A)-C(1A)-C(6A)	30.9(6)
Li(1)-P(1A)-C(1A)-C(6A)	-93.4(4)
Li(7)#1-P(1A)-C(1A)-C(6A)	84.4(4)
Li(8)#1-P(1A)-C(1A)-C(2A)	-148.2(4)
Li(1)-P(1A)-C(1A)-C(2A)	87.6(4)
Li(7)#1-P(1A)-C(1A)-C(2A)	-94.7(4)
C(6A)-C(1A)-C(2A)-C(3A)	1.1(7)
P(1A)-C(1A)-C(2A)-C(3A)	-179.8(4)
C(1A)-C(2A)-C(3A)-C(4A)	-0.2(8)
C(2A)-C(3A)-C(4A)-C(5A)	-0.4(8)
C(3A)-C(4A)-C(5A)-C(6A)	0.1(8)
C(4A)-C(5A)-C(6A)-C(1A)	0.9(8)
C(2A)-C(1A)-C(6A)-C(5A)	-1.4(7)

P(1A)-C(1A)-C(6A)-C(5A)	179.5(4)
Li(2)-P(1B)-C(1B)-C(6B)	105.0(5)
Li(1)-P(1B)-C(1B)-C(6B)	-163.0(4)
Li(1)#2-P(1B)-C(1B)-C(6B)	-83.9(5)
Li(2)-P(1B)-C(1B)-C(2B)	-78.9(5)
Li(1)-P(1B)-C(1B)-C(2B)	13.1(6)
Li(1)#2-P(1B)-C(1B)-C(2B)	92.2(5)
C(6B)-C(1B)-C(2B)-C(3B)	-1.0(8)
P(1B)-C(1B)-C(2B)-C(3B)	-177.4(4)
C(1B)-C(2B)-C(3B)-C(4B)	0.5(9)
C(2B)-C(3B)-C(4B)-C(5B)	-0.6(11)
C(3B)-C(4B)-C(5B)-C(6B)	1.4(12)
C(4B)-C(5B)-C(6B)-C(1B)	-2.0(11)
C(2B)-C(1B)-C(6B)-C(5B)	1.8(8)
P(1B)-C(1B)-C(6B)-C(5B)	178.1(5)
Li(2)-P(1C)-C(1C)-C(2C)	120.3(5)
Li(4)-P(1C)-C(1C)-C(2C)	-98.8(5)
Li(3)-P(1C)-C(1C)-C(2C)	-163.5(4)
Li(2)-P(1C)-C(1C)-C(6C)	-58.3(5)
Li(4)-P(1C)-C(1C)-C(6C)	82.6(5)
Li(3)-P(1C)-C(1C)-C(6C)	17.9(5)
C(6C)-C(1C)-C(2C)-C(3C)	0.3(7)
P(1C)-C(1C)-C(2C)-C(3C)	-178.3(4)
C(1C)-C(2C)-C(3C)-C(4C)	-1.1(8)
C(2C)-C(3C)-C(4C)-C(5C)	1.4(9)
C(3C)-C(4C)-C(5C)-C(6C)	-0.9(9)

C(4C)-C(5C)-C(6C)-C(1C)	0.1(8)
C(2C)-C(1C)-C(6C)-C(5C)	0.2(7)
P(1C)-C(1C)-C(6C)-C(5C)	178.9(4)
Li(5)-P(1D)-C(1D)-C(6D)	89.2(5)
Li(4)-P(1D)-C(1D)-C(6D)	-39.0(6)
Li(3)-P(1D)-C(1D)-C(6D)	-90.6(5)
Li(5)-P(1D)-C(1D)-C(2D)	-92.1(5)
Li(4)-P(1D)-C(1D)-C(2D)	139.7(5)
Li(3)-P(1D)-C(1D)-C(2D)	88.2(5)
C(6D)-C(1D)-C(2D)-C(3D)	0.2(7)
P(1D)-C(1D)-C(2D)-C(3D)	-178.5(4)
C(1D)-C(2D)-C(3D)-C(4D)	-0.3(8)
C(2D)-C(3D)-C(4D)-C(5D)	0.0(9)
C(3D)-C(4D)-C(5D)-C(6D)	0.3(8)
C(4D)-C(5D)-C(6D)-C(1D)	-0.4(8)
C(2D)-C(1D)-C(6D)-C(5D)	0.1(7)
P(1D)-C(1D)-C(6D)-C(5D)	178.9(4)
Li(5)-P(1E)-C(1E)-C(6E)	94.8(5)
Li(5)#3-P(1E)-C(1E)-C(6E)	16.8(6)
Li(6)#3-P(1E)-C(1E)-C(6E)	-78.6(5)
Li(5)-P(1E)-C(1E)-C(2E)	-84.2(5)
Li(5)#3-P(1E)-C(1E)-C(2E)	-162.2(4)
Li(6)#3-P(1E)-C(1E)-C(2E)	102.4(5)
C(6E)-C(1E)-C(2E)-C(3E)	1.7(7)
P(1E)-C(1E)-C(2E)-C(3E)	-179.3(4)
C(1E)-C(2E)-C(3E)-C(4E)	-1.4(8)

C(2E)-C(3E)-C(4E)-C(5E)	0.2(8)
C(3E)-C(4E)-C(5E)-C(6E)	0.7(8)
C(2E)-C(1E)-C(6E)-C(5E)	-0.8(7)
P(1E)-C(1E)-C(6E)-C(5E)	-179.9(4)
C(4E)-C(5E)-C(6E)-C(1E)	-0.3(8)
Li(4)-P(1F)-C(1F)-C(2F)	74.8(5)
Li(7)-P(1F)-C(1F)-C(2F)	-99.1(4)
Li(6)-P(1F)-C(1F)-C(2F)	-39.4(5)
Li(4)-P(1F)-C(1F)-C(6F)	-105.4(5)
Li(7)-P(1F)-C(1F)-C(6F)	80.6(5)
Li(6)-P(1F)-C(1F)-C(6F)	140.3(4)
Li(4)-P(1F)-C(1F)-Li(7)	174.0(3)
Li(6)-P(1F)-C(1F)-Li(7)	59.7(3)
C(6F)-C(1F)-C(2F)-C(3F)	3.3(7)
P(1F)-C(1F)-C(2F)-C(3F)	-176.9(4)
Li(7)-C(1F)-C(2F)-C(3F)	110.4(5)
C(1F)-C(2F)-C(3F)-C(4F)	-0.9(8)
C(2F)-C(3F)-C(4F)-C(5F)	-1.3(8)
C(3F)-C(4F)-C(5F)-C(6F)	0.9(8)
C(4F)-C(5F)-C(6F)-C(1F)	1.7(8)
C(2F)-C(1F)-C(6F)-C(5F)	-3.7(7)
P(1F)-C(1F)-C(6F)-C(5F)	176.6(4)
Li(7)-C(1F)-C(6F)-C(5F)	-118.1(5)
Li(8)-P(1G)-C(1G)-C(6G)	101.0(5)
Li(6)-P(1G)-C(1G)-C(6G)	-117.1(4)
Li(7)-P(1G)-C(1G)-C(6G)	168.6(4)

Li(8)-P(1G)-C(1G)-C(2G) -80.0(5)

Li(6)-P(1G)-C(1G)-C(2G) 61.8(4)

Li(7)-P(1G)-C(1G)-C(2G) -12.5(5)

C(6G)-C(1G)-C(2G)-C(3G) 1.6(7)

P(1G)-C(1G)-C(2G)-C(3G) -177.5(4)

C(1G)-C(2G)-C(3G)-C(4G) 0.1(8)

C(2G)-C(3G)-C(4G)-C(5G) -0.9(9)

C(3G)-C(4G)-C(5G)-C(6G) 0.1(8)

C(4G)-C(5G)-C(6G)-C(1G) 1.7(8)

C(2G)-C(1G)-C(6G)-C(5G) -2.4(7)

P(1G)-C(1G)-C(6G)-C(5G) 176.6(4)

Li(8)-P(1H)-C(1H)-C(2H) -77.2(5)

Li(3)#4-P(1H)-C(1H)-C(2H) 102.9(4)

Li(2)#4-P(1H)-C(1H)-C(2H) 43.3(5)

Li(8)-P(1H)-C(1H)-C(6H) 102.8(5)

Li(3)#4-P(1H)-C(1H)-C(6H) -77.1(5)

Li(2)#4-P(1H)-C(1H)-C(6H) -136.7(4)

Li(8)-P(1H)-C(1H)-Li(3)#4 179.9(3)

Li(2)#4-P(1H)-C(1H)-Li(3)#4 -59.6(3)

C(6H)-C(1H)-C(2H)-C(3H) -0.9(7)

P(1H)-C(1H)-C(2H)-C(3H) 179.1(4)

Li(3)#4-C(1H)-C(2H)-C(3H) -108.5(5)

C(1H)-C(2H)-C(3H)-C(4H) 1.2(8)

C(2H)-C(3H)-C(4H)-C(5H) -1.4(8)

C(3H)-C(4H)-C(5H)-C(6H) 1.6(8)

C(4H)-C(5H)-C(6H)-C(1H) -1.4(8)

C(2H)-C(1H)-C(6H)-C(5H) 1.0(7)

P(1H)-C(1H)-C(6H)-C(5H) -179.0(4)

Li(3)#4-C(1H)-C(6H)-C(5H) 119.3(5)

C(4I)-O(1I)-C(1I)-C(2I) -17.7(5)

Li(1)-O(1I)-C(1I)-C(2I) 106.1(5)

Li(2)-O(1I)-C(1I)-C(2I) -139.9(4)

O(1I)-C(1I)-C(2I)-C(3I) 34.6(5)

C(1I)-C(2I)-C(3I)-C(4I) -38.2(6)

C(1I)-O(1I)-C(4I)-C(3I) -6.6(5)

Li(1)-O(1I)-C(4I)-C(3I) -134.8(4)

Li(2)-O(1I)-C(4I)-C(3I) 124.8(4)

C(2I)-C(3I)-C(4I)-O(1I) 27.8(5)

C(4J)-O(1J)-C(1J)-C(2J) -22.6(5)

Li(3)-O(1J)-C(1J)-C(2J) -156.5(4)

Li(4)-O(1J)-C(1J)-C(2J) 116.0(5)

O(1J)-C(1J)-C(2J)-C(3J) 35.1(5)

C(1J)-C(2J)-C(3J)-C(4J) -34.1(6)

C(1J)-O(1J)-C(4J)-C(3J) 0.8(5)

Li(3)-O(1J)-C(4J)-C(3J) 136.5(4)

Li(4)-O(1J)-C(4J)-C(3J) -135.5(5)

C(2J)-C(3J)-C(4J)-O(1J) 20.8(6)

C(4K)-O(1K)-C(1K)-C(2K) 20.3(5)

Li(6)-O(1K)-C(1K)-C(2K) 145.1(4)

Li(5)-O(1K)-C(1K)-C(2K) -105.0(5)

O(1K)-C(1K)-C(2K)-C(3K) -36.3(5)

C(1K)-C(2K)-C(3K)-C(4K) 38.6(5)

C(1K)-O(1K)-C(4K)-C(3K)	4.5(5)
Li(6)-O(1K)-C(4K)-C(3K)	-126.1(4)
Li(5)-O(1K)-C(4K)-C(3K)	132.8(4)
C(2K)-C(3K)-C(4K)-O(1K)	-26.9(5)
C(4L)-O(1L)-C(1L)-C(2L)	6.0(18)
Li(7)-O(1L)-C(1L)-C(2L)	154.1(17)
Li(8)-O(1L)-C(1L)-C(2L)	-119.3(17)
C(4L')-O(1L)-C(1L)-C(2L')	26(2)
Li(7)-O(1L)-C(1L)-C(2L')	157(2)
Li(8)-O(1L)-C(1L)-C(2L')	-116(2)
O(1L)-C(1L)-C(2L)-C(3L)	-28(3)
C(1L)-C(2L)-C(3L)-C(4L)	38(3)
C(1L)-O(1L)-C(4L)-C(3L)	18.6(18)
Li(7)-O(1L)-C(4L)-C(3L)	-126.4(12)
Li(8)-O(1L)-C(4L)-C(3L)	145.3(13)
C(2L)-C(3L)-C(4L)-O(1L)	-36(2)
O(1L)-C(1L)-C(2L')-C(3L')	1(4)
C(1L)-C(2L')-C(3L')-C(4L')	-26(4)
C(1L)-O(1L)-C(4L')-C(3L')	-41.5(19)
Li(7)-O(1L)-C(4L')-C(3L')	-174.2(13)
Li(8)-O(1L)-C(4L')-C(3L')	95.3(15)
C(2L')-C(3L')-C(4L')-O(1L)	41(3)
C(6M)-C(1M)-C(2M)-C(3M)	0.8(10)
C(1M)-C(2M)-C(3M)-C(4M)	1.0(11)
C(2M)-C(3M)-C(4M)-C(5M)	-1.2(11)
C(3M)-C(4M)-C(5M)-C(6M)	-0.5(11)

C(4M)-C(5M)-C(6M)-C(1M)	2.3(11)
C(2M)-C(1M)-C(6M)-C(5M)	-2.4(10)
C(3N)#5-C(1N)-C(2N)-C(3N)	-2.9(11)
C(1N)-C(2N)-C(3N)-C(1N)#5	2.9(11)
C(3O)#6-C(1O)-C(2O)-C(3O)	1.5(13)
C(1O)-C(2O)-C(3O)-C(1O)#6	-1.5(13)

Symmetry transformations used to generate equivalent atoms:

#1 x, y-1, z #2 -x+1, -y, -z+1 #3 -x+1, -y+1, -z

#4 x, y+1, z #5 -x, -y, -z #6 -x+1, -y, -z